Head and Neck Tumors

Moni A. Kuriakose, Swagnik Chakrabarti, Sok Ching Cheong, Luiz P. Kowalski, Tiago Novaes Pinheiro, and Camile S. Farah

Contents

Introduction 629

Developmental Lesions of the Head and Neck 629
Dermoid Cyst 631
Epidermoid Cyst 633
Thyroglossal Duct Cyst 634
Branchial Cleft Cyst/Lymphoepithelial Cyst 637

M. A. Kuriakose
Department of Head and Neck Surgery/Plastic and Reconstructive Surgery, Roswell Park Cancer Institute, Buffalo, NY, USA
e-mail: Moni.Kuriakose@RoswellPark.org

S. Chakrabarti
Head and Neck Oncology Services, Tata Memorial Hospital, Mumbai, India
e-mail: dr.swagnik@gmail.com

S. C. Cheong
Cancer Research Malaysia, CARIF Oral Cancer Research Team, Subang Jaya, Malaysia
e-mail: sokching.cheong@cancerresearch.my

L. P. Kowalski
Head and Neck Surgery and Otorhinolaryngology Department, A.C. Camargo Cancer Center, São Paulo, Brazil
e-mail: lp_kowalski@uol.com.br

T. Novaes Pinheiro
Anatomic Pathology Service, Amazonas State University, Manaus, Brazil
e-mail: tpinheiro@uea.edu.br

C. S. Farah (✉)
UWA Dental School and Oral Health Centre of Western Australia, Faculty of Health and Medical Sciences, University of Western Australia, Perth, WA, Australia
e-mail: camile.farah@uwa.edu.au

C. S. Farah et al. (eds.), *Contemporary Oral Medicine*,
https://doi.org/10.1007/978-3-319-72303-7_20

Vascular Malformations 639
Lymphangioma Including Cystic Hygroma 648

Benign Tumors of the Head and Neck 651
Fibroma/Traumatic Fibroma 651
Myofibroma 653
Lipoma 655
Neuroma Including Multiple Endocrine Neoplasia Type 2B (MEN2B) 658
Neurilemoma/Schwannoma 663
Neurofibroma Including Neurofibromatosis 665
Granular Cell Tumor 668
Rhabdomyoma 670
Hemangioma 671
Sinonasal Papilloma 674

Malignant Epithelial Tumors of the Head and Neck 675
Oropharyngeal Cancer 679
Hypopharyngeal Cancer 692
Laryngeal Cancer 696
Nasopharyngeal Cancer 702
Tumors of the Nasal Cavity and Paranasal Sinuses (Skull Base Tumors) 705
Thyroid Cancer 712

Malignant Soft Tissue Tumors of the Head and Neck 721
Fibrosarcoma 726
Liposarcoma 729
Malignant Peripheral Nerve Sheath Tumor 731
Kaposi Sarcoma 732
Angiosarcoma 734
Leiomyosarcoma 735
Rhabdomyosarcoma 736

Tumors of the Temporomandibular Joints 737

Molecular Aspects of Head and Neck Squamous Cell Carcinoma 740
Genome-Wide Studies 743
Copy Number Alterations 744
Mutations 746
Gene Expression 748
Targeting Key Signaling Pathways 748
Immune Markers and Immunotherapy 749

Conclusions and Future Directions 751

Cross-References 751

References 751

Abstract

The head and neck region is a complex part of the human body. The diagnosis of soft tissue lesions of the head and neck comprises a wide variety of pathologic entities. These lesions may originate from developmental problems or from benign or malignant neoplastic transformation of normal tissue. Developmental problems arise from disturbances of organogenesis, histogenesis, or functional maturation of the involved structures. Therefore, these lesions can appear at any time during life, usually caused by the interaction of factors such as the environment and genetics.

This chapter highlights and discusses the most significant features for the diagnosis of epithelial and mesenchymal soft tissue tumors of the head and neck region, in addition to tumors of the temporomandibular joint. Tumors are divided into developmental tumors/tumorlike lesions, benign tumors, and malignant tumors and may

have non-odontogenic, reactive, or neoplastic etiology.

Keywords

Head and neck tumors · Head and neck malignancies · Benign tumors · Neck masses · Oropharyngeal cancer · Nasopharyngeal cancer · Hypopharyngeal cancer · Laryngeal cancer · Human papilloma virus · Nasopharyngeal carcinoma · Tumors of the nasal cavity · Tumors of paranasal sinuses · Thyroid cancer · Treatment guidelines · Tumors of the temporomandibular joint · Temporomandibular joint neoplasms

Introduction

Tumors and tumorlike lesions of the head and neck are commonly encountered in contemporary oral medicine practice. Presentation of a mass in the head or neck should be evaluated with care and examined in detail. These masses may present as lumps with no associated symptoms noted incidentally by the patient, or may present as painful lesion attracting the patient's attention. On presentation to the clinician, a comprehensive head and neck cancer examination should be undertaken in addition to a detailed risk assessment. Detailed information from the patient about their history, risk factors, habits, mass location, mass characteristics, mass growth pattern, and signs and symptoms are all useful pieces of information for establishing an accurate diagnosis. In addition to visual examination and palpation of the lesion, imaging studies and diagnostic studies are often undertaken to better ascertain the exact nature of a tumor in the head and neck region. Indeed many tumors of the laryngopharyngeal sites are not easily assessed clinically, and diagnostic imaging is often the first modality used to better understand the extent of the mass in question. A detailed understanding of the complex anatomy of the head and neck region is required for any clinician attempting to manage such conditions. The intricate and complicated structures of the head and neck region also require care and finesse when diagnostic investigations are undertaken, such as fine needle aspiration, core biopsy, image-guided biopsy, and incisional or excisional biopsy.

The varying tissues and structures of this complex region of the human body also predispose to a varying array of pathologies ranging from developmental lesions to neoplastic ones. Tissues include mucosal epithelium, lymphoid tissues, salivary glands, thyroid tissue, and sinonasal structures. These varying pathologies also call for differing treatment approaches which include surgery, radiation therapy, and chemotherapy. More recently, this has included immunotherapy particularly for head and neck squamous cell carcinomas. As our understanding of the molecular basis of these diseases increases, so will the success in managing these devastating cancers.

In this chapter, developmental tumors, benign and malignant epithelial tumors, soft tissue tumors, and tumors of the thyroid gland and temporomandibular joint are explored in detail expected of a contemporary oral medicine practitioner, particularly as this relates to their involvement in multidisciplinary head and neck teams and tumor boards. The content of this chapter is not exhaustive, and certain tumors are covered in other dedicated chapters such as ▶ "Oral Mucosal Malignancies," ▶ "Salivary Gland Disorders and Diseases," ▶ "Odontogenic Pathology," and ▶ "Non-odontogenic Bone Pathology." In this chapter, we focus on those parts of the anatomy not typically directly dealt with by the oral medicine specialist but for which they must have a comprehensive knowledge base. In addition, tumors not covered elsewhere in this book are also included here for completeness, with some minor overlap. It is expected that the oral medicine clinician will avail themselves of more comprehensive texts on the topics covered here for a more detailed appreciation of the complexity and scope of head and neck tumors (WHO Classification of Head and Neck Tumours 2017).

Developmental Lesions of the Head and Neck

The most significant transformation of the human body takes place during intrauterine life. The head and neck region has a significant role in

all stages of in utero development, which makes it a key point for the diagnosis of developmental diseases. After birth, the developmental transformations are grouped in infancy, adulthood, and old age, each one related to its particular common diseases. This section will focus only on cysts and tumors that may rise in the head and neck region, but consideration should be given to the fact that some lesions are part of systemic developmental disorders, such as syndromes, sequences, and syntropy.

In order to fully understand the etiology of these lesions, a review of the basic nosology of these disorders is necessary. Problems during organogenesis lead to anomalies and malformations. These groups of lesions comprise incomplete formation diseases: such as agenesis, aplasia, hypoplasia, persistency, atresia, and stenosis. Also there are redundant lesions, called supernumerary, and the aberrant ones, known as ectopias, choristomas, and teratomas. Problems in histogenesis may lead to hamartomas or heteroplasias. Finally, problems in functional maturation are known as deformities. Table 1 outlines developmental terms and their definitions and common examples.

Benign developmental tumors/tumorlike lesions of the head and neck comprise choristomas, teratomas, and hamartomas. Although developmental cysts have different explanations relating to their etiology, they are usually related to persistent, ectopic, or heteroplastic epithelium proliferation.

Although developmental lesions may appear at any time during life, 2–3% of these are diagnosed before birth, and this number rises to 4–6% until the fifth year of life. There is no gender predilection, and some lesions may be influenced by or influence hormonal activity, so other key periods of manifestation are puberty and old age.

These lesions usually have a multifactorial origin, but trauma, infections, carcinogenic agents, and spontaneous genetic mutations comprise the major causes of such lesions. These agents are also called dysontogenetic factors or teratogenic agents. Table 2 highlights different dysontogenetic factors and diseases directly related to them.

In order to improve the understanding of these different kinds of lesions, this chapter has grouped the developmental cysts and tumorlike lesions.

Table 1 Correlation of terminology applied to developmental disturbances with their definition and some clinical examples

Developmental problems	Definition	Examples
Agenesis	Absence of organ formation	Teeth, glands
Aplasia	Absence of organ growth	Tooth germ, aplastic bone marrow, limbs
Hypoplasia	Insufficient organ growth	Microdens, hypoplastic heart, lung, kidneys
Persistency	Persistent structure from the developmental process	Thymus, tail, stapedial artery, vomeronasal organ
Atresia	Incomplete formation of a luminal organ	Esophageal, pharyngeal, aural, choanal
Stenosis	Pathologic narrowing of a luminal organ	Salivary duct, arteries, cardiac valves
Supernumerary	Excessive number of a determined organ	Teeth, glands, fingers
Ectopia	Formation of an organ in a different anatomic place	Teeth, glands, limbs, heart
Choristoma and teratoma	Benign neoplastic proliferation of tissue from different embryonal origins	Osseous, cartilaginous, head and neck teratoma
Hamartoma	Benign neoplastic or neoplastic-like proliferation of a tissue in its natural anatomic position	Odontoma, lymphangioma, hemangioma, lipoma
Heteroplasia	Proliferation of a tissue beyond its natural anatomic position	Foregut cysts, dens in dens, lymphoid, glandular
Deformity	Alteration of anatomic form that may compromise normal function	Radicular dilaceration, congenital club foot, septum deviation, micrognathia

Table 2 Potential dysontogenetic factors and associated diseases

Dysontogenetic factors	Pathogens	Process	Diseases
Physical	Trauma	Production of growth factors, persistence of the agent impairing complete recovery of injuries	Vascular malformations, traumatic fibroma
	Radiation	Free radical formation, genetic damage, thermal tissue damage	Carcinomas, sarcomas, hematolymphoid tumors
Chemical	Heavy metals	Direct – alters the cellular genome	Cancers, osteomalacia, cirrhosis, blood disorders, neurotoxicity, kidney diseases, tooth pigmentation, gingivostomatitis, alopecia
		Indirect – depends on dosage, absorption, transport, distribution, storage, biotransformation, and excretion. It can cause its effects in any phase of exposition	
	Organic compounds		Leukemia, carcinomas
	Halogens		Burns, poisoning, mineralized tissue disorders, cancer
Biological	Viruses	Genetic integration with the cellular genome altering its expression	HPV-carcinomas
			EBV-Burkitt's lymphoma, nasopharyngeal carcinomas
			HHV8-Kaposi sarcoma
			HBV and HCV-hepatic carcinoma
	Bacteria	Immunosuppressive action, bacterial endotoxins, and exotoxins	Congenital defects, deafness, blindness, craniofacial anomalies, neural and brain problems
	Fungi	Carcinogenic mycotoxins	Liver cancer, subcutaneous sarcomas, leukemia, pulmonary tumors

Dermoid Cyst

Epidemiology, Etiology, and Pathology

Dermoid cysts originate from cystic formation resulting from sudden proliferation of ectopic epithelium associated with adnexal structures such as hair follicles and sebaceous and sudoriferous glands. The most accepted theory of the origin of these epithelial remnants is that they probably are derived from the fusion of developmental processes. This presumption is based on the usual clinical location of such lesions, in the midline of the floor of the mouth and the soft palatal pillars. Other theories suggest that these lesions could represent a cystic manifestation of a teratoma. These cysts are not restricted to the head and neck region and are commonly found in the ovary and uterus. In these regions, it is usual to find the muscle and even neural tissue in the surrounding tissues of the cystic cavity. The presence of components of all embryonic tissues in these cases is compatible with the characteristics of a teratoma. Cysts found in the head and neck do not show such complexity.

Considered a rare lesion, it has no gender predilection and is usually diagnosed in intraoral sites. Affected patients are generally young and there are even congenital lesions described. The differential diagnosis of a dermoid cyst includes the epidermoid cyst. Lesions that occur close to the skin are more likely to contain adnexal structures nearby, so there is doubt if the latter form part of the lesion in biopsied specimens or just represent characteristics of the anatomic position, being usually diagnosed as epidermoid cysts. Dermoid and epidermoid cysts represent together about 7% of cysts found in the head and neck region, and only 1.6% are located within the oral cavity.

Clinical Presentation

Intraoral lesions present as a yellowish or normally colored fluctuating nodule, with soft resilient consistency on palpation (Fig. 1).

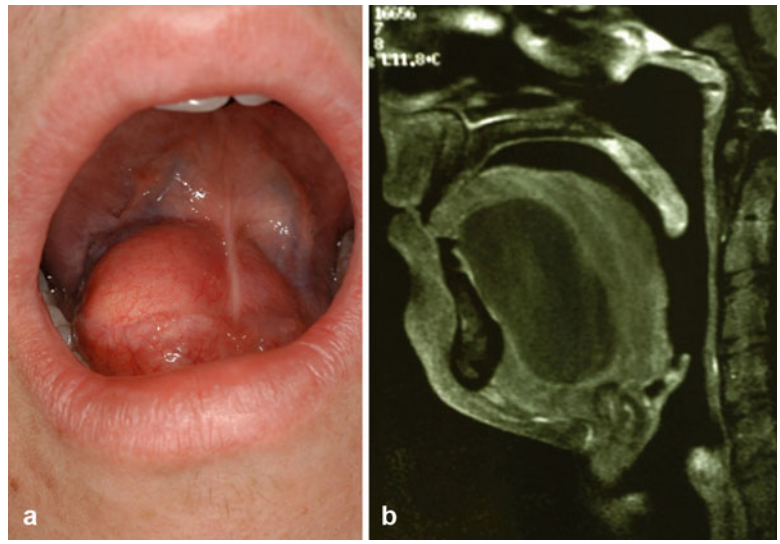

Fig. 1 Dermoid cyst involving the floor of mouth (**a**) and MRI sagittal view (**b**) shows a well-defined large cyst-like lesion positioned medially within the floor of the mouth extending inferolaterally above the hyoid bone

Early clinical identification of these lesions can mimic a ranula or mucocele, mostly due to the coloration which is similar to the adjacent mucosa. Lesions vary in size, most of which measure 2–5 cm, but very large cysts (over 10 cm) have been described.

Investigations

Investigations include ultrasound, computerized tomography (CT), and magnetic resonance imaging (MRI) exams (Fig. 1), in addition to fine needle aspiration cytology (FNAC). Ultrasound examination is low cost and has the advantage that it can be used in real time with other clinical procedures such as FNAC. High-frequency probes (10–15 MHz) and mid-range frequency probes (5–10 MHz) provide better resolution but have less penetration. High-frequency probes are preferred for ultrasound images of superficial lesions (2–4 cm) deep such as dermoid cysts of the head and neck region. The echogenicity of the dermoid cyst is predominantly a hypoechoic circumscribed mass, indistinguishable from other mass lesions such as lipomas. Low-contrast CT imaging usually shows a circumscribed mass with low density, sometimes presenting scattered hyperdense structures, when calcified keratin material is present within the cystic content. High-contrast CT imaging provides a better view of the lesion but is less frequently used due to higher technical complexity. MRI has the best soft tissue quality of imaging, showing soft tissue structures and providing different sonographic appearances with different frequencies, providing a good view of the cystic content and its surrounding structures (Fig. 1) (Rumboldt 2015).

FNAC is useful for surgical planning. Keratin is normally found within the cystic cavity. The quick result from cytopathology also helps differentiate the lesion from a ranula for lesions located close to the midline of the floor of the mouth. This simple procedure may prevent unnecessary dissection of salivary glands which could give rise to a postsurgical mucocele.

Cytopathological examination reveals desquamative epithelial cells, mostly from the keratin layer. Some of these cells also present a clear cytoplasm with hydropic degeneration or signs of karyolysis giving a ghost cell-like appearance.

Gross specimen evaluation of the dermoid cyst usually shows a white-to-brown pasty to granular material. The characteristic keratin odor is usually not affected by tissue fixation. In empty specimens, the cystic internal lining presents as a smooth brilliant surface. Microscopic examination shows a stratified squamous cell orthokeratinized epithelium, without projections to the connective tissue capsule, with five to ten cells thick. The difference with epidermoid,

trichilemmal, and pillar cysts is the marked hypergranulation layer and abrupt transition to the keratin layer. The differential diagnosis with epidermoid cyst is based on the presence of epithelial appendices like glands or hair follicles.

Treatment

Cyst enucleation is the treatment of choice for dermoid cyst. During dissection of the lesion, it can rupture. If this occurs, it is important to perform meticulous cleaning of the surgical site with saline solution to minimize the inflammatory potential of keratin, providing better immediate postsurgical recovery. Recurrence of such lesions is low. If chronic trauma or previous infection has occurred, adherence of the cystic capsule could increase the chance of surgical rupture of the cyst and elevate the chances of recurrence, when part of the lesion is left behind at the surgical site.

Epidermoid Cyst

Epidemiology, Etiology, and Pathology

The epidermoid cyst is considered an infundibular cyst. The infundibular region of the hair follicle represents a major interface zone of mammalian skin epithelium with the environment. A common manifestation, lesions in the head and neck region are usually related to trauma. This cause-effect relationship supports other conditions such as inclusion cysts and pillar cysts. Epidermoid cyst has a male gender predilection, mostly on areas related to razoring of the beard. These lesions are usually mislabeled sebaceous cysts, since its cystic content is mostly filled with keratin. The microscopic characteristics of epidermoid and dermoid cysts are similar, although epidermoid cysts are usually more superficial and more often related to the skin than oral mucosa. The most essential difference of the epidermoid cyst to the dermoid cyst is the hypergranular layer that is usually absent in dermoid cysts and the absence of adnexal structures in the cystic capsule.

Clinical Presentation

Epidermoid cysts manifest as well-circumscribed fluctuating nodules, resilient on palpation (Fig. 2). Due to its superficial position, secondary infection is common, also related to patients' attempt to squeeze the lesion. In these cases, pain, hyperemia, and edema will be noted. Lesions that suffer repetitive drainage attempts also show peripheral fibrosis and inflammatory reactions to keratin and require the removal of at least part of the skin related to the lesion. Similar to the dermoid cyst, it has a particular odor related to keratin.

Investigations

The clinical manifestations of the epidermoid cyst are quite typical, making the presumptive diagnosis highly convergent with histopathological exam. Most cases are located subcutaneously, which makes direct access through the skin very practical. Only unusual site manifestations demand more meticulous investigations. Although less common, it is possible to reach lesions from an intraoral surgical access site. This may be required for esthetic reasons or after deep skin inclusions due to trauma. In this more complex clinical manifestation, the same methods used in dermoid cyst investigation can be applied here.

Ultrasound imaging of epidermoid cysts is similar to dermoid cysts, presenting with a well-circumscribed hypoechoic appearance. Secondary inflammation can contribute to liquid accumulation in the cystic cavity. These cases are reported to show hypoechoic mixed with round anechoic regions giving the cyst a "sack-of-marbles" appearance. Dystrophic calcifications in the keratin close to the epithelium can generate hyperechoic areas. For more complex cases, MRI and CT scans can provide more detail for surgical planning (Fig. 2).

Treatment

Cyst enucleation is the treatment of choice for epidermoid cysts (Fig. 3). During dissection of the lesion, it may rupture. If this occurs, it is important to perform a meticulous cleaning of the surgical site with saline solution to reduce the inflammatory potential of keratin, providing better immediate postsurgical recovery. Recurrence of such lesions is low. If chronic trauma, previous infection, or other changes have occurred, adherence of the cystic capsule could

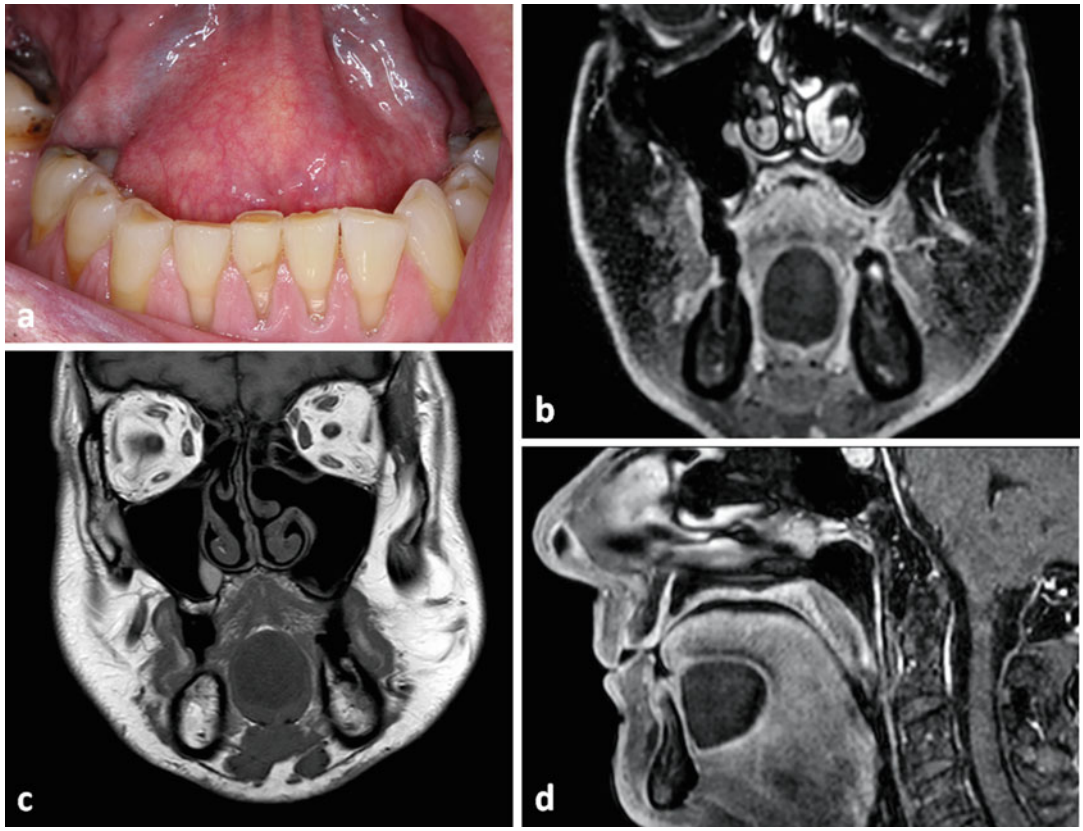

Fig. 2 Epidermoid cyst presenting as a soft tissue fluctuant mass in the anterior floor of mouth with no symptoms (**a**). MRI T1 coronal (**b**) and post-gadolinium coronal (**c**) and sagittal (**d**) views show a well-defined ovoid lesion within the floor of the mouth splaying the geniohyoid and genioglossus muscles and which measures 27 mm craniocaudal × 22 mm transverse × 28 mm AP (**b**). This is T1 hypointense, T2 mildly hyperintense, does not enhance with the administration of contrast (**c** + **d**) and does demonstrate diffusion restriction. It suppresses on fat suppression techniques

increase the chance of surgical rupture of the cyst and elevate the chances for recurrence.

Thyroglossal Duct Cyst

Epidemiology, Etiology, and Pathology

The tongue, the hyoid bone, and the thyroid and the parathyroid glands have their embryologic origin in the fusion of third, fourth, and fifth branchial arches. During the first 10–12 weeks of pregnancy, organogenesis of the thyroid and parathyroid glands begins inside the oral cavity, along with the posterior third of the developing tongue. During histodifferentiation, these glands descend through the thyroglossal duct and end their maturation over the newly formed hyoid bone. The duct has a tortuous path similar to major salivary ducts and blood vessels and is situated mostly in the para-medial region, starting on the tongue surface and ending up in the hyoid bone.

Usually, the cells of the thyroglossal duct enter apoptosis and the duct begins an involution phase. The usual anatomic vestige of its presence is the foramen cecum on the tongue. The thyroglossal cyst origins from remnant epithelial ductal cells that persist after its involution. These developmental problems can also affect the thyroid gland. In some cases, the duct involutes before completion of the gland descent, leading to ectopic positioning. The most extreme cases

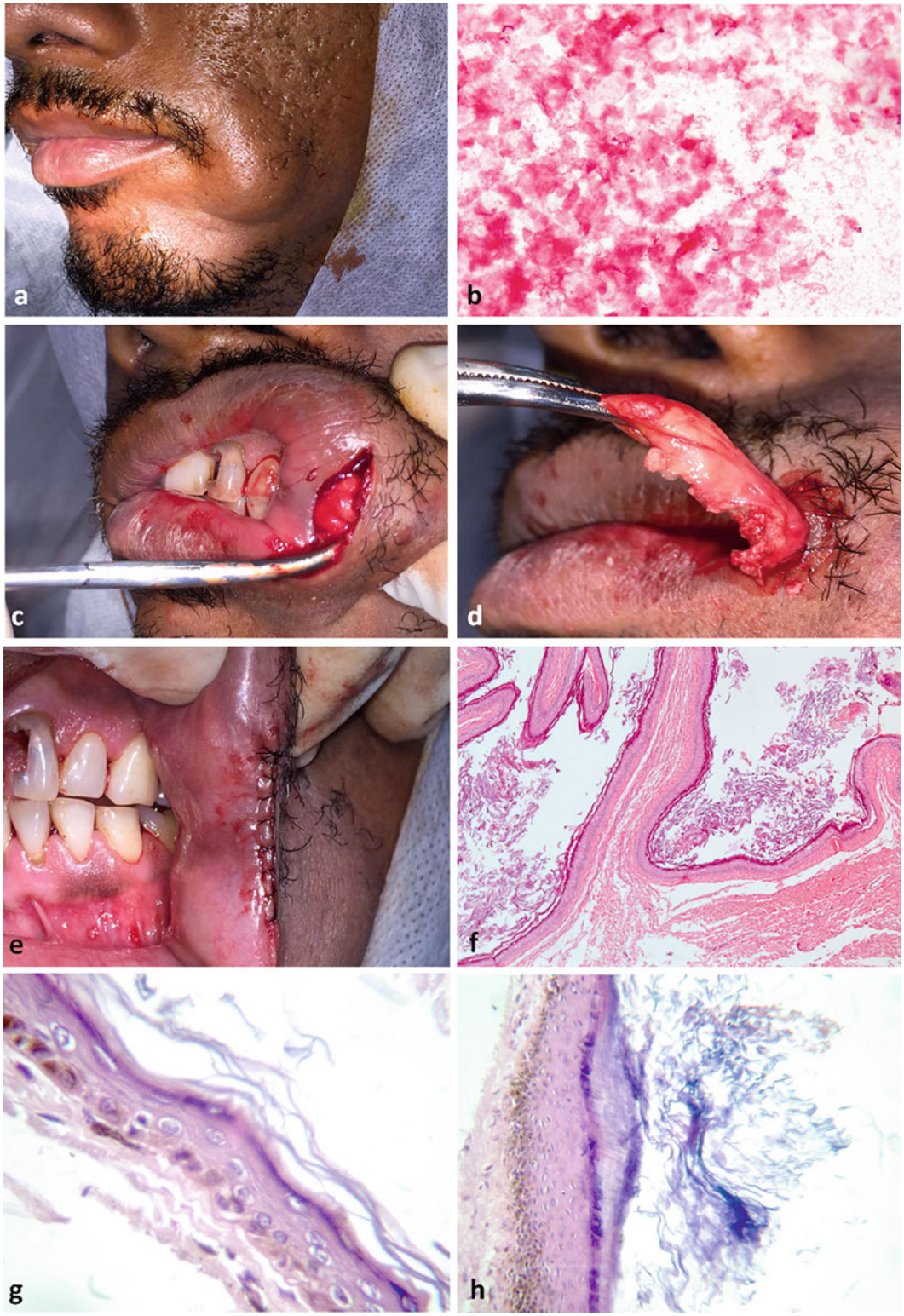

Fig. 3 (continued)

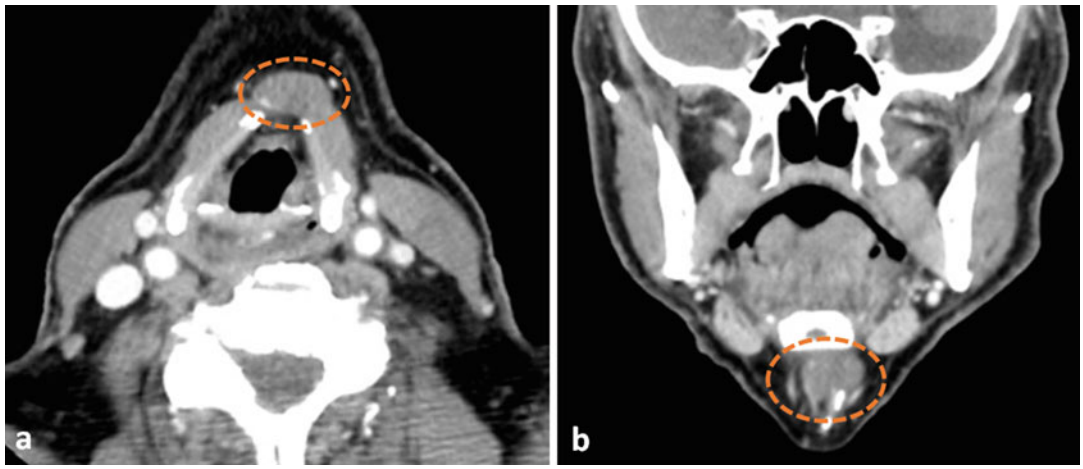

Fig. 4 Thyroglossal duct cyst. Axial (**a**) and coronal (**b**) CT shows a 19 mm ovoid lesion in the position of an infrahyoid thyroglossal duct cyst (dashed orange oval)

show the so-called lingual thyroid, when the gland, or part of it, fully develops on the tongue surface or in some part of the ductal pathway through the neck.

The lesions have a broad spectrum of age incidence, varying from congenital lesions to lesions in older patients. There is a small predilection of male-to-female incidence, according to most studies. These lesions are the most common middle neck mass (Adelchi et al. 2014). Although unusual, malignant transformation of the lesion to a thyroglossal duct carcinoma and the combination of thyroglossal duct cyst with thyroid carcinoma have been reported.

Clinical Presentation

Since the pathway of the duct is long, the lesions can appear at any part of its trajectory (Fig. 4). Most lesions present as a painless nodule located in the midline that are most visible during deglutition, with variable anteroposterior location from the base of the tongue to the hyoid bone. Intraoral lesions develop inside the muscle in the base of the tongue. In these cases, it is normal for the patient to expect symptoms such as dysphagia and dyslalia. Sometimes more than one cyst is present not necessarily close to each other. The usual presentation is a non-tender, mobile neck mass, which is painful on swallowing. Secondary infection is also possible, enhancing the painful sensation and interfering with surrounding tissues, sometimes giving the impression of a non-fluctuating mass on palpation.

Investigations

Most primary investigations comprise imaging procedures. Clinical access of the lesion is one of the major problems. FNAC is an option for

Fig. 3 Epidermoid cyst. Clinical aspect of a fluctuating nodule on the cheek. FNAC was performed at the first visit. During the procedure, a characteristic odor was noticed (**a**). Microscopic findings of the FNAC revealing cornified epithelial cells without evident nuclei forming agglomerates of orthokeratin. The cytopathological diagnosis was suggestive of dermoid/epidermoid cyst (**b**). Surgical excision in the lip commissure was undertaken for esthetic reasons, and access to the cyst (**c**). During enucleation of the cyst, the cystic capsule ruptured revealing its yellow granular content (**d**). Sutures were placed after cleaning the surgical site with abundant irrigation with saline solution (**e**). Cystic cavity filled with keratin with thin epithelial lining of five to eight layers of stratified squamous epithelium with hypergranulosis and absence of epithelial projections and sudoriparous or sebaceous glands in the capsule confirming the diagnosis of epidermoid cyst (**f**). Differential diagnosis of the pillar inclusion cyst, revealing melanosis at the parabasal layers, areas of epithelial thickening with a marked granular layer. In this cyst, it is possible to see adnexal glands due to the proximity to the skin (**g**, **h**) (Hematoxylin and eosin stain)

preoperative diagnosis of thyroglossal duct cyst. Ultrasound guidance for this type of procedure prevents unsatisfactory sampling and transfixation damage of important anatomical structures, such as nerves and major blood vessels. The lesion usually has an anechoic echogenicity.

The cytomorphologic features of thyroglossal duct cyst include colloid (thick and fragmented, thin and watery, or mucinous), macrophages, lymphocytes, and predominantly neutrophils. The epithelium is ciliated columnar, metaplastic squamous, or of mature squamous type. Thyroid epithelium is rarely present. Identification of possible ectopic thyroid tissue can be also verified through scintillography.

Microscopic examination confirms cytomorphologic investigations. Cysts located adjacent to the tongue base are lined with stratified squamous epithelium, while those adjacent to the thyroid gland are lined with cells resembling the thyroidal acinar epithelium. More than half of all thyroglossal duct cyst walls contain ectopic rests of thyroid tissue. Hormonal alterations should also be investigated. Patients with ectopic thyroid tissue may have no other functional glands or present with hypofunctional problems.

Treatment

Enucleation with the Sistrunk technique is the treatment of choice for most cases. This technique dissects the region of the possible remnant of the duct and removes it along with the cyst, including part of the hyoid bone. Although this procedure reduces the chance of recurrence, due to the inconstant, irregular, and thin macroscopic appearance of the ductal remnants, recurrence is still possible.

Branchial Cleft Cyst/ Lymphoepithelial Cyst

Epidemiology, Etiology, and Pathology

The branchial cleft cyst and the lymphoepithelial cyst share the same probable etiology despite different clinical locations (Figs. 5, 6, and 7). The most accepted hypothesis for their etiology is based on epithelial rests from the clefts of the branchial arches, entrapped and persistent after fusion of the branchial arches. These cysts are usually lined by pavemented squamous cell epithelium and found on the surrounding capsular connective tissue, with lymphoid structures, not always well arranged but sometimes exhibiting germinative centers and maturation zones. Another etiological hypothesis for the lymphoepithelial cyst suggests the reactive proliferation of the epithelium from the tonsillar crypts, which may enclose a cystic cavity (Fitzpatrick and Gordon 2013).

These lesions have no gender predilection reported in most epidemiological studies. The most common of the two is the branchial cleft cyst, but both lesions are considered rare manifestations in the head and neck. Lesions are usually diagnosed in young patients, but there is a broad spectrum of age incidence, varying from congenital lesions to lesions in older patients. The branchial cleft cyst is usually diagnosed in the para-medial region of the neck and even within major salivary glands such as the parotid. Lymphoepithelial cysts are found close to intraoral areas of lymphoid tissue from the Waldeyer's ring, which also comprise branchial cleft-derived regions. Therefore, the posterior border of the tongue and the soft palate pillars are the main intraoral sites of occurrence. These lesions can also develop inside major salivary glands such as the parotid, given it also has an ectomesenchymal origin (Luna and Pineda-Daboin 2006).

Clinical Presentation

Branchial cleft cysts are usually painless, fluctuating, flexible nodules on palpation, located in the para-medial line of the neck (Fitzpatrick and Gordon 2013) (Fig. 5). Movements of deglutition can help their detection on physical examination. The median size of these lesions varies from 1 to 3 cm. Larger lesions may give the impression of a double chin, suggesting other cysts such as the thyroglossal duct cyst or dermoid cysts. Sometimes these lesions can be associated with further defects of branchial arch fusion, such as the anatomic continuity of the cyst with a fistula or a

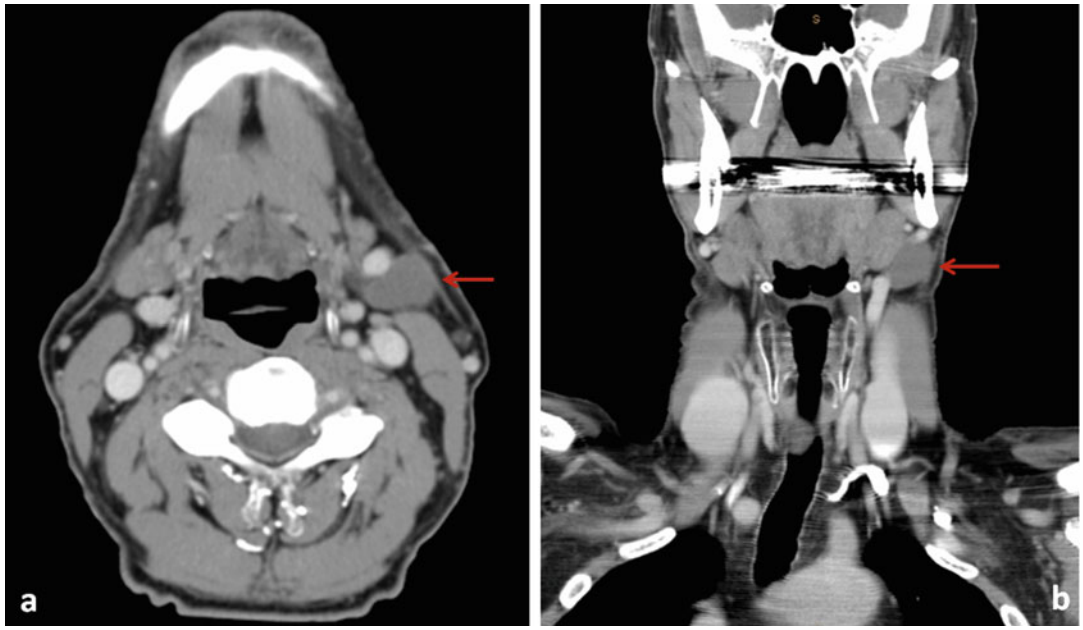

Fig. 5 Post-contrast CT showing a second branchial cleft cyst presenting as a fluid-filled lobular mass on the lateral aspect of the left neck, posterolateral to the submandibular salivary gland, lateral to the carotid space, and anterior to the sternocleidomastoid muscle (red arrows). (Images courtesy of Dr Chady Sader, Western ENT, Perth WA, Australia)

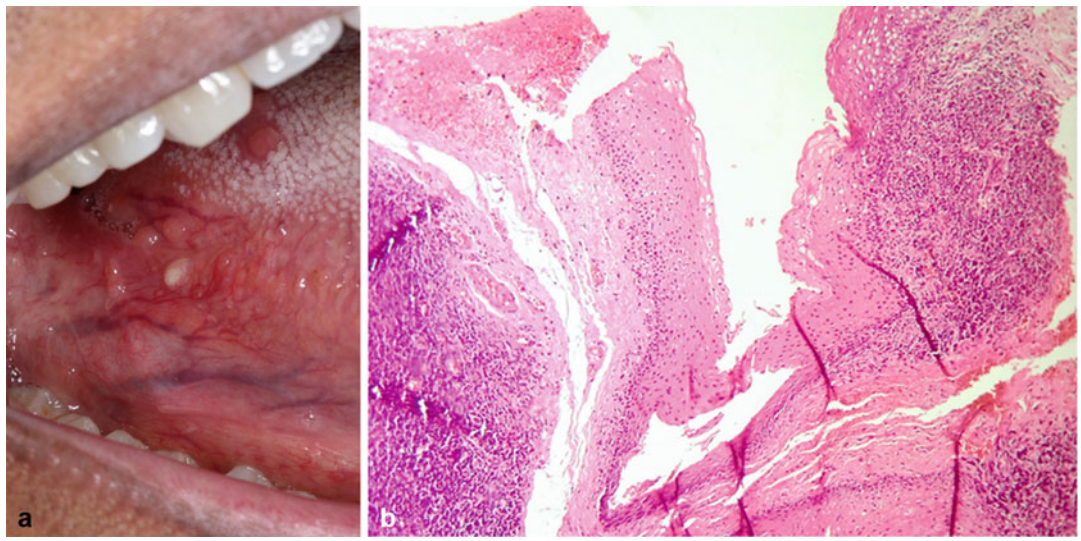

Fig. 6 Lymphoepithelial cyst at the posterior border of the tongue, presenting as a painless firm yellow nodule (**a**). Microscopic view of the cyst (**b**) revealing a deep lingual crypt that entrapped the mucosal epithelium forming a parakeratin and serofibrinous exudate-filled cavity. The epithelial lining is hyperplastic stratified pavementous squamous epithelium. The most characteristic feature of lymphoepithelial and branchial cysts is the presence of organized and disorganized foci of lymphocytic infiltrate, sometimes assuming a follicular pattern, localized close to the cystic epithelium (Hematoxylin and eosin stain)

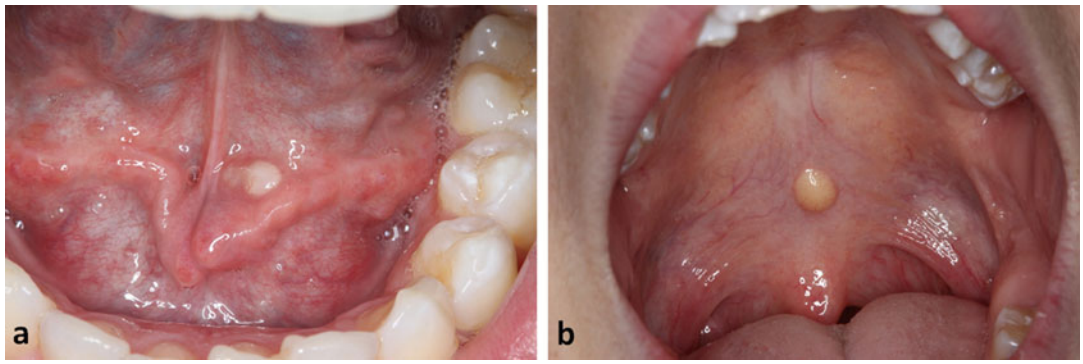

Fig. 7 Lymphoepithelial cysts involving the floor of the mouth (**a**) and palatal mucosa (**b**)

sinus tract. In such cases, secondary infection could alter normal clinical presentation, adding pain and swelling and decreasing the lesion's fluctuation on palpation.

Lymphoepithelial cysts are usually smaller submucosal yellowish, resilient nodules, ranging from 0.5 to 2 cm, located on the posterior border of the tongue and in the soft palate pillars (Figs. 6 and 7). Clinical differential diagnosis comprises salivary duct cysts, mucous extravasation cysts, lipomas, and dermoid cysts. Accessory lingual tonsils also have been related to lymphoepithelial cysts at the posterior border of the tongue. Usually superficial, these lesions can be easily emptied of their contents during puncture.

Investigations

Fine needle aspiration cytology is a good starting point for diagnosing branchial cleft cysts. This procedure has better results when it is performed along with ultrasound guidance. Cytopathologic smears usually comprise squamous epithelial cells, lymphocytes, and histiocytes along with keratinous eosinophilic content. The most common differential diagnoses of branchial cleft cysts are dermoid cysts and thyroglossal duct cysts. The most important differential diagnosis is cystic metastasis of a squamous cell carcinoma, which often originates from the oropharynx and is positive for HPV 16/18 and p16. Immunohistochemistry for cytokeratins may be useful to demonstrate islands of invasive squamous cell carcinoma in the wall of the cystic lesion, as well as staining for p16 and in situ hybridization for HPV 16/18, which is positive in cystic metastasis but not in branchial cyst (Zidar 2016). On ultrasound examination, the branchial cleft cyst presents as a subcutaneous hypoechoic fluctuating mass. Hypercontrast computerized tomographic images reveal a hyperdense nodule. On MRI T2, they present with an intense signal.

Oral lymphoepithelial cysts are usually easier to access and do not demand further imaging (Figs. 6 and 7). Lesions developing inside major salivary gland tissue may require ultrasound, CT, or MRI imaging.

Treatment

Both branchial cleft cysts and lymphoepithelial cysts have low recurrence rates once enucleated or excised. Treatment of branchial cleft cysts can be more complex if the cyst is in continuity with a fistula or a sinus tract.

Vascular Malformations

Epidemiology, Etiology, and Pathology

Vascular malformations comprise a set of different types of lesions all related to vascular non-neoplastic development. There are some controversial perspectives to their classification, as it is difficult to determine if the process is neoplastic or not on clinical examination alone. In fact, this group of lesions is poorly understood. The diagnosis of these lesions demands periodical follow-up prior to any intervention in order to

observe progression and decide on whether the lesion is self-limiting or nonneoplastic.

Vascular malformations are appropriately named by their predominant vessel type. The International Society for the Study of Vascular Anomalies (ISSVA) convenes the official system for classification of congenital disorders of vascular development. Table 3 represents the latest ISSVA classification of vascular malformations approved at the 20th ISSVA Workshop in 2014 and subsequently revised (ISSVA Classification of Vascular Anomalies 2018).

Vascular malfunctions have variable etiological factors such as genetic mutations or molecular changes related to syndromes, trauma, blood flow, and vascular wall resistance and may form part of other systemic diseases. These lesions can develop in any part of the body, and the most common intraoral sites are the tongue and lips. With a wide range of age manifestations,

Table 3 ISSVA classification of vascular malformations approved at the 2014 ISSVA workshop (ISSVA Classification of Vascular Anomalies 2018)

Simple	Combined	Of major named vessels	Associated with other anomalies
Capillary malformations	CM + VM= CVM capillary venous malformation	Affect: Lymphatics Veins Arteries	Klippel-Trenaunay syndrome: CM + VM +/− LM + limb overgrowth
			Parkes Weber syndrome: CM + AVF + limb overgrowth
Lymphatic malformations	CM + LM = CLM capillary lymphatic malformation	Anomalies of: Origin Course Number Length Diameter (aplasia, hypoplasia, stenosis, ectasia/aneurysm) Valves Communication (arteriovenous fistula) Persistence (of embryonal vessel)	Servelle-Martorell syndrome: limb VM + bone undergrowth
Venous malformations	LM + VM = LVM lymphatic venous malformation		Sturge-Weber syndrome: facial + leptomeningeal CM + eye anomalies
			+/− bone and/or soft tissue overgrowth
Arteriovenous malformations	CM + LM + VM = CLVM capillary lymphatic venous malformation		Limb CM + congenital nonprogressive limb hypertrophy
Arteriovenous fistula	CM + AVM = CAVM capillary arteriovenous malformation		Maffucci syndrome: VM +/− spindle cell hemangioma + enchondroma
	CM + LM + AVM = CLAVM capillary lymphatic arteriovenous malformation		Macrocephaly: CM (M-CM/MCAP)
	CM + VM + AVM = CVAVM capillary venous arteriovenous malformation		Microcephaly: CM (MICCAP)
			CLOVES syndrome: LM + VM + CM +/− AVM + lipomatous overgrowth
	CM + LM + VM + AVM = CLVAVM capillary lymphatic venous arteriovenous malformation		Proteus syndrome: CM, VM and/or LM + asymmetrical somatic overgrowth
			Bannayan-Riley-Ruvalcaba syndrome: AVM + VM +macrocephaly, lipomatous overgrowth

AVF arteriovenous fistula, *AVM* arteriovenous malformation, *CAT* cutaneovisceral angiomatosis with thrombocytopenia, *CAVM* capillary arteriovenous malformation, *CCM* cerebral cavernous malformation, *CLAVM* capillary lymphatic arteriovenous malformation, *CLOVES* congenital lipomatous overgrowth, vascular malformations, epidermal nevi, skeletal/scoliosis and spinal abnormalities, *CLM* capillary lymphatic malformation, *CLVAVM* capillary lymphatic venous arteriovenous malformation, *CLVM* capillary lymphatic venous malformation, *CM* capillary malformation, *CM-AVM* capillary malformation-arteriovenous malformation, *CMTC* cutis marmorata telangiectatica congenita, *CNS* central nervous system, *CVAVM* capillary venous arteriovenous malformation, *CVM* capillary venous malformation, *DIC* disseminated intravascular coagulopathy, *GLA* generalized lymphatic anomaly, *GSD* Gorham-Stout disease, *GVM* glomuvenous malformation, *HHT* hereditary hemorrhagic telangiectasia

Table 4 Most common vascular malformations of the head and neck region according to blood flow pattern

Slow flow	High flow
Sturge-Weber syndrome	Arteriovenous malformations
Venous malformations	Arteriovenous fistula
Capillary malformations	Capillary arteriovenous malformation
Capillary venous malformation	Capillary lymphatic venous arteriovenous malformation
Capillary lymphatic malformation	
Lymphatic venous malformation	
Capillary lymphatic venous malformation	

congenital lesions are usually labeled "birthmarks." Intraosseous lesions are not as readily detected, usually incidentally found during other imaging procedures and routine examinations, but can cause asymmetry and even bone expansion.

This group of lesions comprises aneurysms, vascular stenosis, and tumorlike vascular lesions, such as hamartomatous proliferations. It is postulated that vascular malformations do not contain hyperplastic cells but consist of progressively enlarging aberrant and ectatic vessels composed of a particular vascular architecture such as veins, lymphatic vessels, venules, capillaries, arteries, or mixed vessel types (Buckmiller et al. 2010). These lesions can also be classified according to blood flow as either slow flow or high flow. Table 4 shows the most common vascular malformations of the head and neck region according to their blood flow pattern. Congenital vascular malformations are often visible vascular lesions known to affect 4–10% of newborn children (Friedman et al. 2013).

Clinical Presentation

Clinically vascular malformations vary according to the extension of the lesion and location and neighboring tissue displacement. The so-called port-wine stain is one of the most common vascular malformations, found on the skin, in the oral mucosa, and even in the sclera (Fig. 8). They can be isolated or multiple and can be part of other systemic diseases. Sturge-Weber syndrome (SWS, encephalofacial angiomatosis, craniofacial angiomatosis, OMIM 185300) is characterized by intracranial vascular abnormality and leptomeningeal angiomatosis, usually involving the occipital and posterior parietal lobes, associated with facial cutaneous vascular malformations (port-wine stains), seizures, and glaucoma (Friedman et al. 2013) (Fig. 8).

Slow-flow vascular malformations are usually detected at birth. Venous malformations vary in color depending on depth, from normal coloration to deep purple (Fig. 9). The major differential diagnosis for these lesions is the hemangioma but differs from it due to the continuous growth to significant proportions during puberty, under hormonal influence.

High-flow vascular malformations usually appear before the third decade of life, appearing during childhood as a bluish coloration, sometimes resembling port-wine stains. Arteriovenous malformations (AVM) also commonly present at birth but commence with significant clinical changes during puberty (Figs. 10 and 11). Swelling, pain, and bleeding are the most reported events. The lesion is not fluctuant on palpation; sometimes the affected area becomes thickened and even pulsatile. Combined lesions with capillary, venous, and lymphatic vessels behave as high flow due to arterial supply. Lesions should be distinguished from those of conditions such as hereditary hemorrhagic telangiectasia (Fig. 12).

Investigations

The correct diagnosis of vascular malformations has an important role in appropriate treatment planning. The choice of a surgical removal, vascular sclerosis, embolization, or immunotherapy is linked to the classification of the lesion, if they can present with similar clinical features. Investigations commence with imaging, but microscopic evaluation provides the best impression of the vascular alterations present in the lesion.

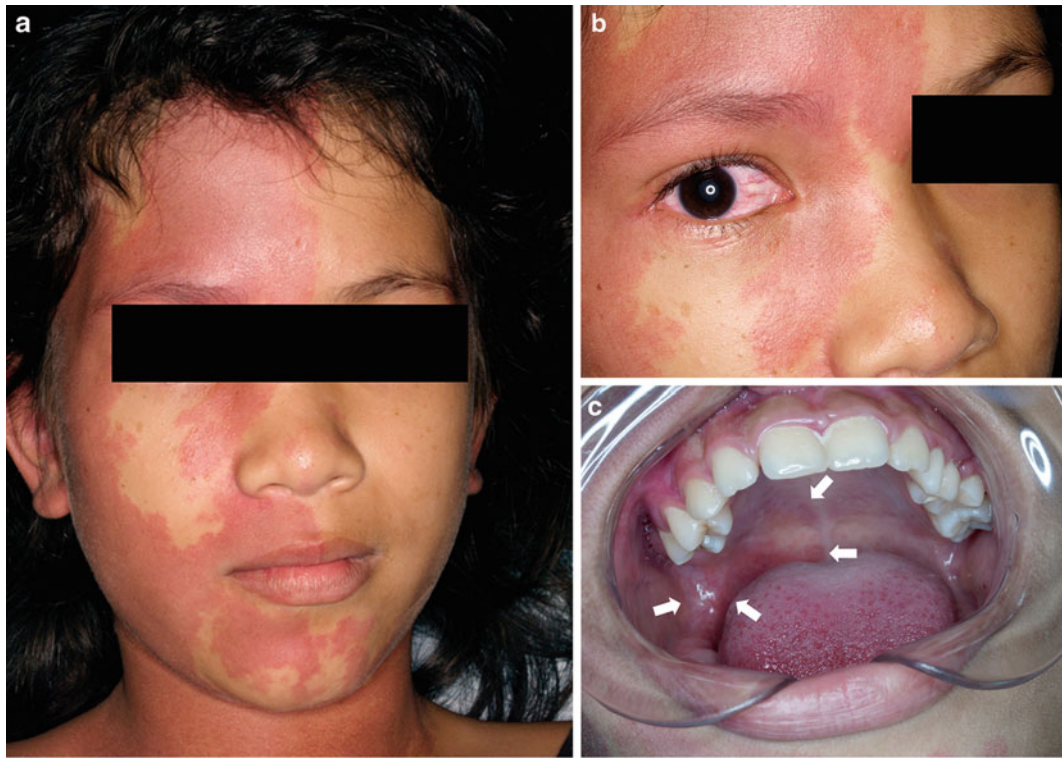

Fig. 8 Sturge-Weber syndrome. Clinical presentation of port-wine stain affecting the head and neck, respecting the midline (**a**). The right sclera (**b**) and oral mucosa (**c**) also present with port-wine stain angiomatosis (white arrows)

Sometimes biopsy procedures represent a high risk for the patient, so whenever microscopic evaluation is possible, correct characterization of the lesion is essential.

Hypercontrast CT examination along with MRI is the best imaging tool for the diagnosis and treatment planning of vascular malformations. Venous malformations have a propensity to occur in muscle groups but can also involve skin and mucosa. Areas frequently involved in the head and neck are masseter, temporalis, tongue musculature, and oral and airway mucosa. MRI remains the diagnostic modality of choice to assess the extent and plan treatment for these lesions. Regarding high-flow lesions such as AVM, MRI with T2-weighted processing will typically reveal a hyperintense, irregular lesion with numerous flow voids. A magnetic resonance arteriogram (MRA) and a computed tomography arteriogram (CTA) can give excellent images of the AVM (Ziyeh et al. 2005) (Figs. 11 and 13).

Microscopic features such as the presence of arteries or arterioles as an integral part of the lesion are determined not only by morphology of the blood vessel but also by identification of specific structures with the aid of specific stains such as elastic tissue stains (Figs. 9 and 11). Further differences can be evaluated through immunohistochemical examination such as S-100, to study the various tissue components present in these lesions. The first important differential diagnosis is to determine whether the lesion is a hemangioma or vascular malformation. Nerve bundles are consistently present in vascular malformations and absent in hemangiomas, serving as a diagnostic clue to differentiate between the lesions and also confirming the hamartomatous nature of these lesions (Adegboyega and Qiu 2005).

Investigation of a series of genetic mutations is essential to diagnose syndromic conditions and other systemic diseases. Simple and combined vascular malformations may have altered genetic expression. Table 5 shows the known causal gene

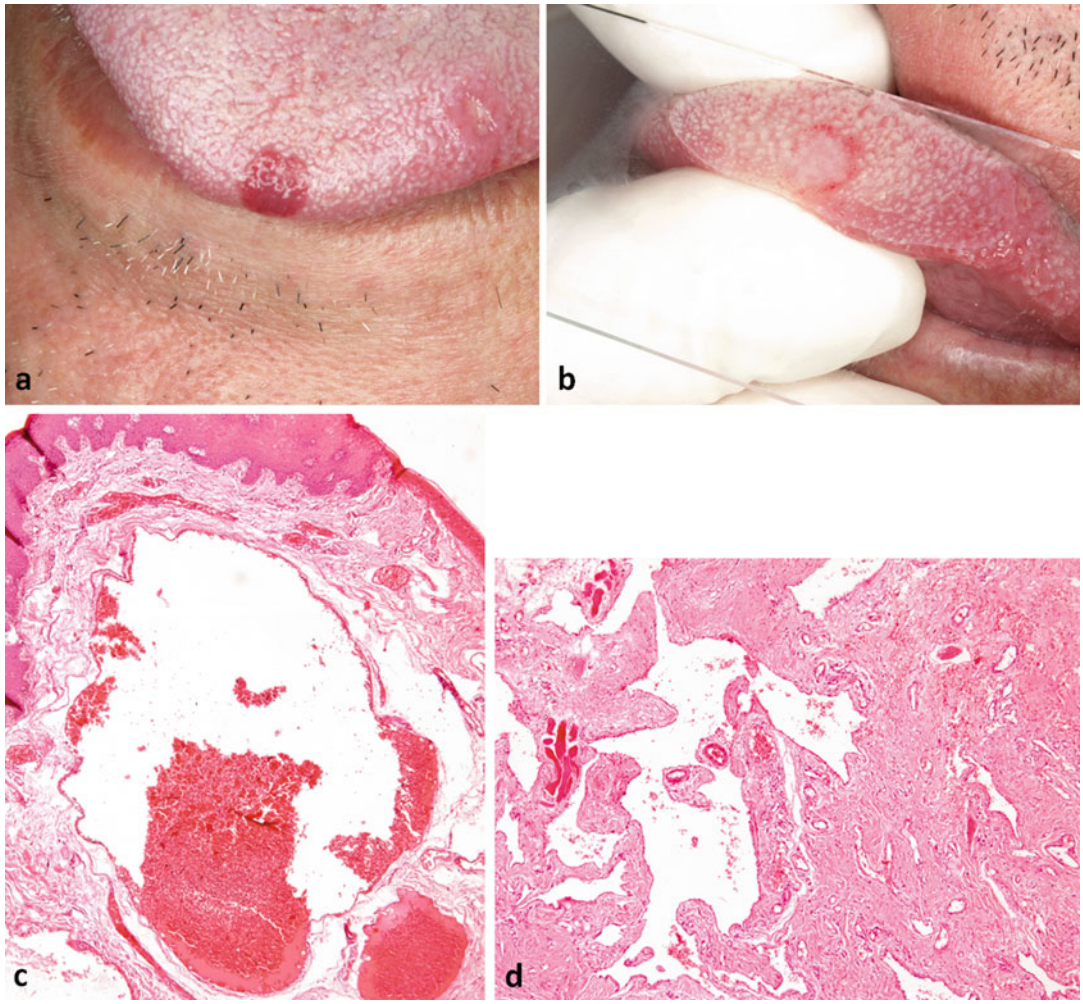

Fig. 9 Vascular malformation at the apex of the tongue presenting clinically as a red patch (**a**). Diascopy (blanching procedure) reveals whitish appearance after compression (**b**). Low power magnification of venous-capillary malformation showing multiple blood vessels of variable width (**c** + **d**) (Hematoxylin and eosin stain)

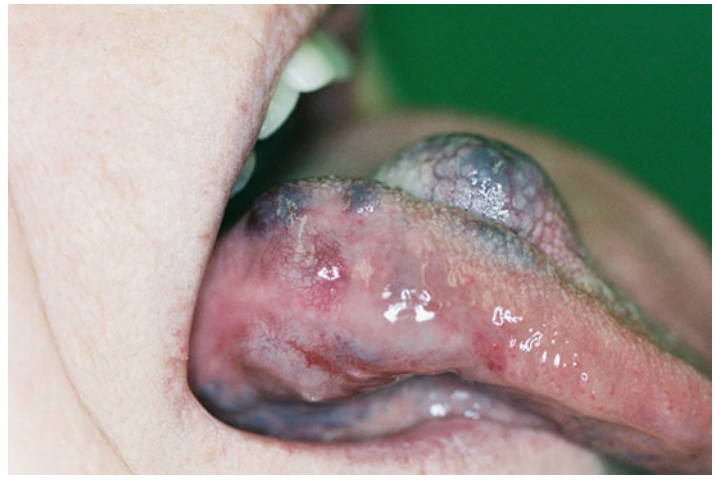

Fig. 10 Arteriovenous malformation involving right dorsal and lateral tongue in an elderly female

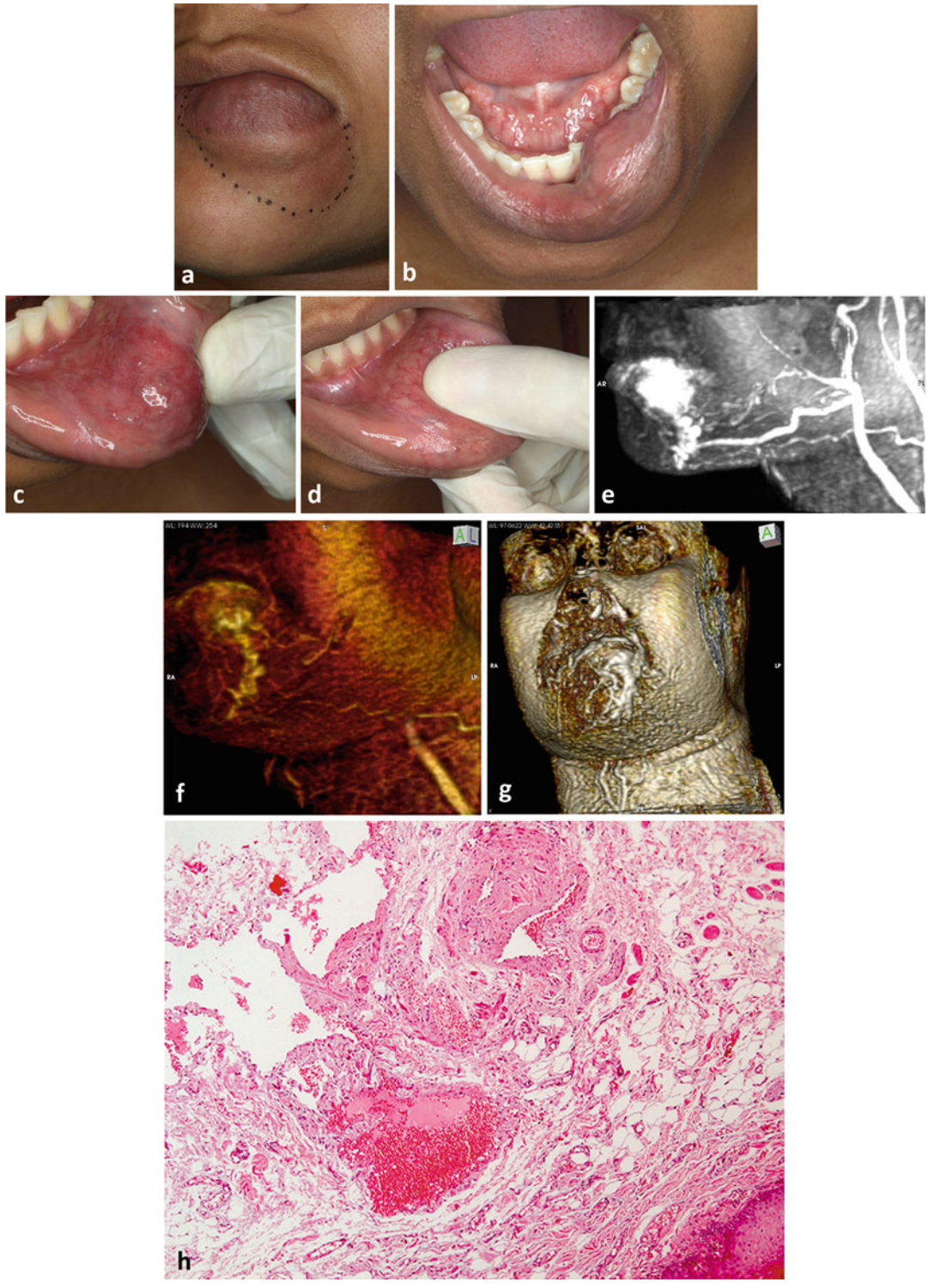

Fig. 11 (continued)

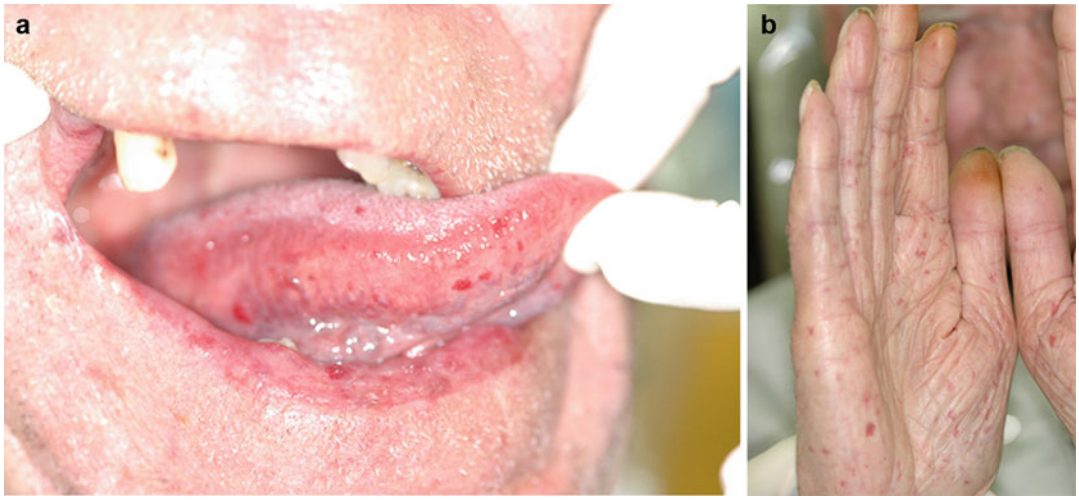

Fig. 12 Patient with hereditary hemorrhagic telangiectasia presenting with multiple red colored lesions on the oral mucosa (**a**) and skin (**b**). (Images courtesy of Dr Sue-Ching Yeoh, Sydney Oral Medicine, Sydney NSW, Australia)

mutations correlated with various vascular malfunctions according to 2014 ISSVA classification.

Intraosseous vascular malformations can present variable imaging patterns. Lesions can present with poorly defined borders or a well-circumscribed halo, ranging from unilocular to multilocular and from unicystic bubble-shaped formations to a honeycomb appearance (Fig. 13). Bone expansion can also produce subperiosteal ossification assuming patterns resembling malignancies or reactive lesions. Differential diagnosis includes odontogenic cysts or tumors. It is difficult to establish immediate correlation of the lesion with the major vessels of the affected region. If the patient does not show asymmetry, pain, or bone expansion, it is extremely uncommon for the clinician to consider vascular malformations as a differential diagnosis.

Treatment

Multiple treatment options exist for vascular malformations, including conservative measures such as head-of-bed elevation and compression for venous malformations, laser therapy, sclerotherapy, embolization, and surgery. Decisions regarding which treatment course to follow vary widely with various specialties and institutions. Because of the wide variety of management options and patient presentations, it is strongly recommended that patients with vascular malformations undergo treatment at a multidisciplinary center for treating vascular anomalies (Buckmiller et al. 2010). Treatment effectiveness of vascular malformations and its prognosis is linked with the correct diagnosis of the lesion.

Conservative measures are only effective for venous malformations. These vascular malformations have a tendency to expand instead

Fig. 11 High-flow arteriovenous malformation. The patient presents with a pinkish non-fluctuating nodule extending from the midline of the lower lip to the left labial commissure (**a** + **b**). The mucosal aspect of the lesion (**c**) and clinical compression exam (**d**) reveals the pulsating behavior of the lesion indicating its flow pattern. MRA exam reveals the arterial origin from the facial artery and the appearance of an arteriovenous fistula forming a plexiform arrangement with dilated vessels and the effluent mental vein (**e**–**g**). Microscopic aspect of the arteriovenous malformation (**h**), revealing the close relationship of arteries with thick walls and narrow lumen, and veins with dilated blood-filled lumen and thin vascular walls. The lesion infiltrates the surrounding tissue. In this specimen, adipose tissue is seen with striated skeletal muscle as well as neural fibers in the original connective tissue from the affected area (Hematoxylin and eosin stain)

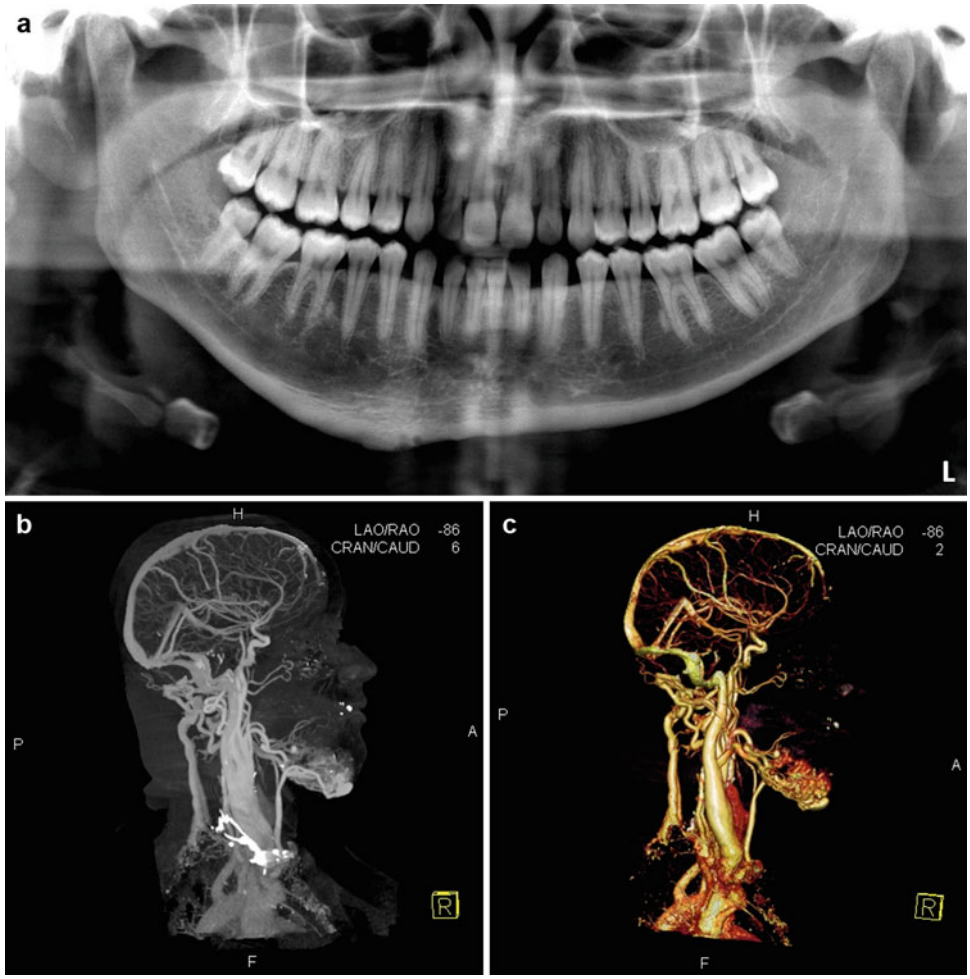

Fig. 13 Orthopantomogram showing deformity of the anterior right mandible demonstrating asymmetry and expansion of the inferior border (**a**). Maximum intensity projection (**b**) and 3D CT angiography (**c**) of same patient show feeding vessels to the right mandible and demonstrate arteriovenous malformation

of proliferate; the resistance of the vascular wall and blood pressure in the area are the main causes of this undesirable development. Therefore, head-of-bed elevation is an important measure to prevent increase of local blood pressure while the patient is in bed. Compression is a good adjunctive conservative measure, effective in body extremities such as limbs, with aids of compressive sleeves, socks, and gloves, but not readily amenable in the head and neck region.

Systemic diseases such as syndromes will present with specific alterations that call for professional management. In cases of Sturge-Weber syndrome, for instance, gingival overgrowth, periodontal disease, and dental extractions will require patient hospitalization prior to performing these procedures. Blood loss control during these procedures is better achieved with aids of a 1.064 nm 10 W Nd:YAG laser, which allows deeper coagulation compared to 10,600 nm wavelength CO_2 laser (Bradley 1997). Electrocautery, presurgical embolization, and splinting of the region are also widely applied in these situations, but reported complications such as postoperative bleeding, infection, and scar formation are more frequent.

Laser therapy is the treatment modality most widely applied for vascular malformations,

Table 5 Known causal gene mutations correlated with the different conditions according to 2014 ISSVA classification (ISSVA Classification of Vascular Anomalies 2018)

Condition	Gene
Capillary malformation of CM-AVM	*RASA1*
Telangiectasia	*ENG*, *ACVRL1*, *SMAD4*
Common and familial venous malformation	*TIE2* and *TIE2* somatic
Glomuvenous malformation	*Glomulin*
Cerebral cavernous malformation types 1–3	*KRIT1*, *Malcavernin,* and *PDCD10*
Arteriovenous malformations and arteriovenous fistulas	*ENG*, *ACVRL1*, *SMAD4*, and *RASA1*
Parkes Weber syndrome	*RASA1*
Sturge-Weber syndrome	*GNAQ*
Macrocephaly syndrome	*PIK3CA*
Microcephaly syndrome	*STAMBP*
CLOVES syndrome	*PIK3CA*
Proteus syndrome	*AKT1*
Bannayan-Riley-Ruvalcaba syndrome	*PTEN*

Table 6 Most common sclerozing agents along with complication and effectiveness rates based on Horbach et al. (2016)

Sclerozing agent	Number of patients	Reported complications	Effectiveness rates (weighted mean)
Pingyangmycin	698	2%	79–100% (98%)
Absolute ethanol	306	18%	84–100% (92%)
OK-432 (Picibanil)	205	6%	50–100% (71%)
Ethanolamine oleate	188	3%	88–100% (98%)
Bleomycin	82	6%	68–100% (82%)
Polidocanol	39	3%	100%
Doxycycline	22	0%	100%
Sodium tetradecyl sulfate	12	0%	83%

promoting thermocoagulation. Capillary malformations present good esthetic results with lasers, while superficial venous malformations have better results than deep and infiltrative lesions. Pulsed dye lasers ranging from 580 to 575 nm CO_2 lasers and Nd:YAG laser tunable to 1064 nm applying 30–70 W/cm^2 per session combined with simultaneous cooling offer good treatment outcomes (Zheng et al. 2010). Arteriovenous malformations are the exception for this treatment modality as these cases demand embolotherapy combined with surgical excision.

A recent systematic review of the literature has identified the most common sclerozing agents used for treating vascular malfunctions and evaluated their performance (Horbach et al. 2016). Table 6 summarizes the most common sclerozing agents along with their complication rates and effectiveness rates. The complications related to the use of these substances can be systemic or at the site of application including hemoglobinuria, infection, nausea, swelling, pain, ulceration, necrosis, and cellulitis.

Surgical excision offers the best chance for cure of vascular malformations. Excision of extensive lesions remains a challenge, as these lesions are rarely well defined and intraoperative bleeding can make identification and preservation of important structures difficult. Preoperative sclerotherapy can be beneficial not only to decrease bleeding, which improves visibility and eases dissection, but also to decrease blood loss and operative time (Buckmiller et al. 2010). High-flow lesions demand MRA or CTA prior to the procedure, as well as adjunctive embolization. Regardless of approach, attention must be made to eradicate the nidus. If the nidus

is left untreated, recruitment and collateralization of new vessels, along with early recurrence, are common (Friedman et al. 2013).

Embolization is usually achieved with cyanoacrylate, onyx, or absolute alcohol injection. Just like in sclerotherapy, alcohol is more often associated with complications such as nerve paralysis, significant swelling, necrosis, ulceration, scaring, and even cardiovascular collapse. Onyx is also very expensive and requires increased fluoroscopy time. Arteriovenous malformations usually recur, and treatment of very extensive lesions is always life-threatening. In bony lesions, the result of embolization is confirmed with new bone formation inside radiolucent spaces during imaging follow-up.

Lymphangioma Including Cystic Hygroma

Epidemiology, Etiology, and Pathology

Lymphangiomas are uncommon, benign, hamartomatous proliferation of lymphatic vessels. Given the benign nature of these anomalies and their wide-ranging manifestations, the preferred all-encompassing term is lymphatic malformations (LM), also applied by the ISSVA. Traditionally, vascular malformations involving the lymphatic vessels were known by a variety of terms including cystic hygroma, lymphangioma, and hemolymphangioma (Fig. 14) (Wall et al. 2016). They can potentially develop in any part of the body, and most of the lesions are identified during childhood.

Usually lesions consist of collections of ectatic lymph vessels that form endothelial lined cystic spaces, classified as macrocystic (single or multiple cysts >2 cm^3), microcystic (single or multiple cysts >2 cm^3), or mixed (Friedman et al. 2013). They can also be classified as simple, cavernous, or cystic, according to the diameter and number of lymphatic vessels in the lesion.

The etiology of these lesions is still an area of constant investigation. Lymphangiogenic growth factors (such as VEGF-C and transcription factor Prox-1) have been reported to be involved in the process through upregulation of VEGFR-3 (Itakura et al. 2009; Pavlov et al. 2009).

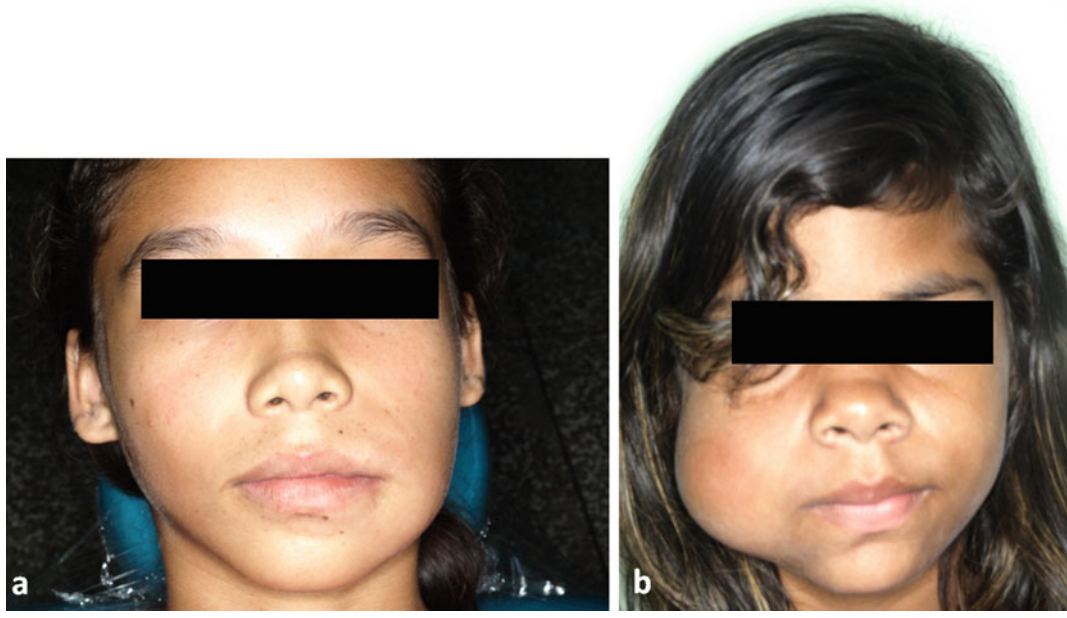

Fig. 14 Facial asymmetry caused by lymphangiomas (**a** + **b**). Note the difference of a microcystic lymphangioma in (**a**) with more diffuse asymmetry and a macrocystic/cystic hygroma with more localized appearance (**b**)

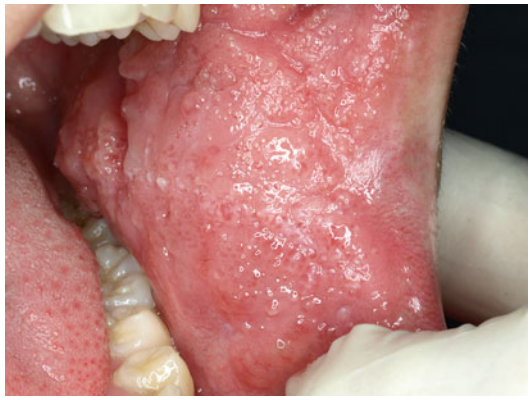

Fig. 15 Intraoral view of a microcystic lymphangioma showing multiple vesicles

Clinical Presentation

Small individual intraoral lymphangiomas are difficult to differentiate from mucoceles and ranulas (de Carvalho et al. 2015). Oral lymphangiomas are usually superficial lesions formed by a cluster of transparent vesicles resembling the appearance of tapioca pudding or frog eggs (Fig. 15). These lesions show slow growth, normal to red-purple coloration, and size varying from 1 to 5 cm in diameter. Differential diagnoses include hemangiomas, dermoid cysts, thyroglossal duct cysts, angiogranulomas, and granular cell tumors. Diagnosis is usually made in childhood, and if not obvious from birth, it may become apparent with infections such as upper respiratory infection or otitis media, which can cause swelling of the malformation caused by increased lymph flow. Lesions typically grow slowly but may rapidly swell with infections or with hormonal changes such as puberty (Buckmiller et al. 2010).

On palpation, lesions usually feel fluid filled and are non-compressible, which can help in distinguishing them from venous malformations. Mucosal and skin surfaces can be affected with vesicle formation, which represents small external fluid-filled cysts. Vesicle formation causes problems with bleeding, weeping of lymph fluid, and pain. Microcystic lymphatic malformations present as soft non-compressible masses with an overlying ill-defined area of clear, yellow, or red (secondary to intracystic bleeding) vesicles. The external component of these lesions continues to involve an increased amount of area with age.

Large lymphatic malformations involving the head and neck identified in utero have the potential to create airway obstruction upon delivery. The morbidity of such cases is usually related to the size and location of the lesions; therefore it is important to assess the extent of the lesion. In patients with more diffuse lesions, the airway must be examined. Macrocystic lymphatic malformations present as a lump beneath normal or slightly bluish skin. These are soft but not compressible (Fig. 14). The mass can undergo sudden enlargement secondary to intracystic bleeding or infection. When affecting the tongue, large lesions may cause airway obstruction and impair feeding and speech. Over time, cystic lymphatic lesions can develop bleeding, infection, and cutaneous vesicles. Recurrent infections and chronic wounds are common with superficial lesions.

Secondary bony overgrowth can cause craniofacial disfigurement. These can be asymptomatic or lead to pathologic fractures. When lymphatic malformations involve the cervicofacial skeleton or the surrounding soft tissues, they can lead to osseous hypertrophy resulting in maxillary or mandibular deformities, malocclusion, or open bite (Friedman et al. 2013).

Investigations

Lymphatic malformations are frequently diagnosed on prenatal ultrasound and may require special preparations for delivery if perinatal airway compromise is suspected. The best imaging modalities for lymphatic malformations are ultrasonography, MRI, and contrast lymphography. Ultrasound is valuable in differentiating lymphatic malformations from other vascular lesions that contain blood flow (e.g., hemangioma). Ultrasound is further able to characterize the size and extent of superficially localized lesions.

MRI remains the visualization method of choice for delineating the extent of the malformation, planning intervention, predicting outcome (macrocystic vs microcystic), and verifying diagnosis. MRI offers an additional advantage of axial imaging that can further identify the extent of

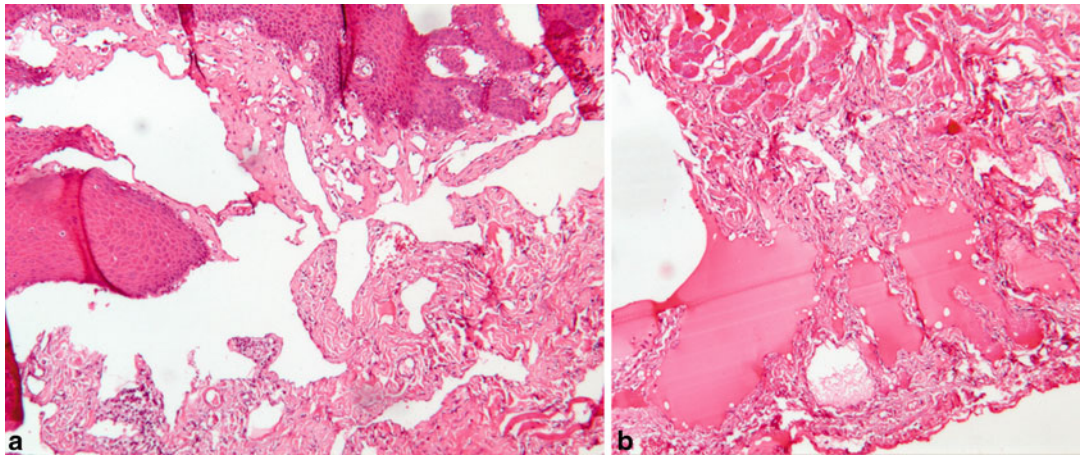

Fig. 16 Cavernous microcystic lymphangioma of the oral submucosa. Numerous vascular spaces with thin endothelial walls (**a**), sometimes filled with plasma/lymph amorphous eosinophilic material (**b**) (Hematoxylin and eosin stain)

large diffuse lesions and highlight the precise relationship between malformations and adjacent anatomical structures (Wall et al. 2016). For the fetus whose airway may be in jeopardy, it is important to try to differentiate, by prenatal MRI, between the soft and usually non-compressive lymphatic malformation from the firm and often airway compressing teratoma (Steigman et al. 2009).

If these lesions are biopsied, they show numerous vascular spaces with thin endothelial walls sometimes filled with plasma/lymph amorphous eosinophilic material (Fig. 16).

Treatment

There are sporadic reports of spontaneous resolution of a small percentage of lymphatic malformations, although this is quite rare (Buckmiller et al. 2010). It has been proposed that the lesions that are most likely to resolve are small, macrocystic, and within the posterior triangle of the neck. Infected and inflamed lesions can show some regression after antibiotics and anti-inflammatory therapy with corticosteroids (Friedman et al. 2013).

Indications for definitive treatment of lymphatic malformations include esthetic considerations and functional compromise. Treatments include surgery, sclerotherapy, and laser therapy. Often, a combination of therapies is utilized. The timing of treatment depends on several variables including extent of functional deficit and cosmetic deformity as well as the possible negative impact of progression of the lesion. Life-threatening lymphatic malformations require early intervention (Friedman et al. 2013).

The preferred approach to sclerotherapy utilizes ultrasound guidance with cyst aspiration followed by injection of a sclerozing agent. Ethanol and sotradecol have traditionally been used to treat lymphatic malformations with good results preferentially in macrocystic lesions. Multiple treatment sessions may be required, and there are sometimes weight-limited dose concerns with these toxic agents in small children. Complications can include skin breakdown, prolonged swelling, pain, and airway compromise. Lymphatic malformations tend to recur and can do so several years after reporting a cure with sclerotherapy, so the literature must be analyzed carefully. Other sclerosants have been reported in an attempt to find an effective treatment while maximizing safety. These include doxycycline, OK-432, and bleomycin. Concerns still remain regarding complications with each treatment. Doxycycline can cause neural damage, OK-432 can be associated with sepsis, shock, myalgia, and bleomycin still carries a warning of pulmonary fibrosis, although this is related to total lifetime dose and doses received for treatment of lymphatic malformation usually do not approach

that level. All of these sclerozants can still cause severe swelling with airway compromise, skin breakdown, and other toxic side effects. It must be emphasized that treatment outcomes are based on multiple treatments, sometimes in excess of five to ten treatments, and long-term follow-up data is lacking (Buckmiller et al. 2010).

Surgery is important not only for removing and hopefully eliminating the malformation but also for correcting the secondary deformities caused by the malformation. Surgical resection is typically required for the treatment of microcystic lesions. These lesions can encase major structures, and great care must be taken to avoid significant vascular and nerve damage. It is often stated that large microcystic lesions in the neck can be the most challenging benign lesions to safely resect. Some lesions can be well vascularized and transfusion may be required. Recurrence is reported from 15% to 50% after surgical resection. Recurrence is associated with incomplete resection, which is often due to the need to preserve critical structures that the cyst is adherent to, such as nerve tissue. Resection and particularly recurrences are associated with fat hypertrophy possibly due to excess lymph fluid and leaking that exits post resection (Wall et al. 2016).

Benign Tumors of the Head and Neck

Benign neoplastic proliferations of soft tissues of the head and neck are slow-growing masses, usually painless, that promote asymmetry. Although most benign soft tissue tumors are asymptomatic and present in the form of a painless nodule or mass, schwannomas and neurofibromas may be tender and painful. Some of these lesions can also form characteristic parts of syndromes. With few exceptions, benign soft tissue tumors are diseases of young and middle-aged adults. Most of these lesions are considered uncommon findings in clinical practice but represent one of the most common benign neoplasms diagnosed in oral and maxillofacial pathology services.

The average size of benign soft tissue tumors at a superficial location is seldom more than 2 cm. Deep tumors, however, may grow to several inches before being detected. Most small and superficial benign soft tissue tumors are diagnosed after surgical excision. Complete excision of such tumors should be considered diagnostic as well as therapeutic. These lesions can be well circumscribed by a fibrous capsule or present an infiltrative pattern demanding careful dissection from the surrounding structures in order to prevent unnecessary surgical sequelae.

Fibroma/Traumatic Fibroma

Epidemiology, Etiology, and Pathology

Fibroma is the most frequent soft tissue tumor of the oral cavity (Castellanos and Diaz-Guzman 2008). These lesions are characterized by collagen rich, hypovascularized connective tissue, lined by the oral mucosa. The true neoplastic nature of these lesions has always been questioned, since it can also be a reactive excess of collagen deposition by an inflammatory process, caused by chronic trauma or irritation (traumatic fibroma/fibroepithelial polyp). Low mitotic activity of the fibroblasts is also a characteristic of these lesions. The presence of inflammation is minimal except in scattered submucosal areas. It has a 2:1 male-to-female gender predilection and can appear at any part of the oral mucosa, although most lesions are found in the vestibular mucosa or areas related to masticatory function. Although fibromas can occur at any time of life, patients usually notice these tissue growths during the fourth to sixth decades.

The main difference of a fibroma from a traumatic fibroma and fibroepithelial polyp is the cause-effect clinical correlation and the intensity of the inflammatory process. While traumatic fibromas and fibroepithelial polyps exhibit areas of intense chronic inflammation, even ulcerated mucosa and epithelial hyperplasia, fibromas appear more mature and almost free from inflammation. In addition, a mature angiogranuloma is microscopically indistinguishable from a fibroma.

Clinical Presentation

These present as sessile or pedunculated, normal colored, soft-to-tender nodules, with slow

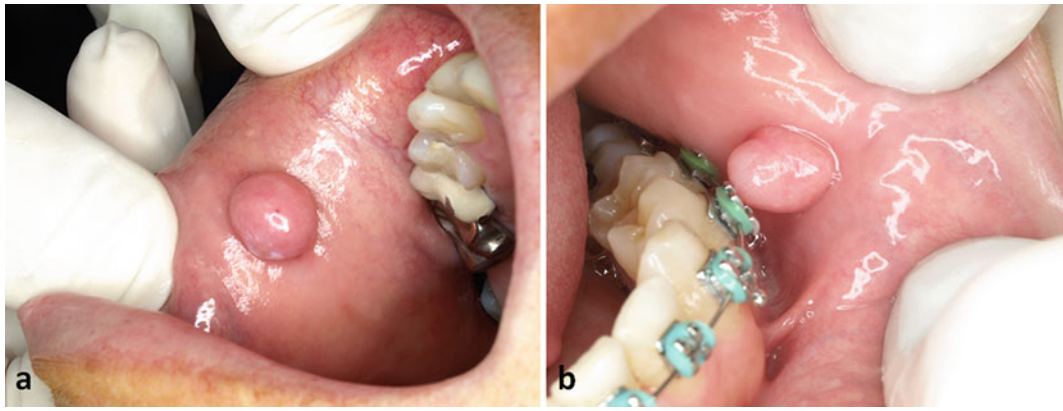

Fig. 17 Fibroma/traumatic fibroma presenting as a pedunculated, normal colored, soft nodule, with slow progression. In this case, there is hyperkeratinization appearing as white patches at the inferior aspect of the nodule due to local irritation (**a**). Cause-effect relationship of a traumatic fibroma, with the patient reporting frequent incidental biting since beginning orthodontic treatment (**b**)

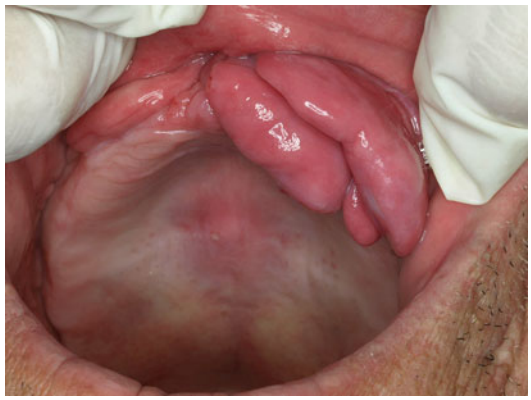

Fig. 18 Large traumatic fibromas caused by overworn upper complete denture in the vestibular sulcus

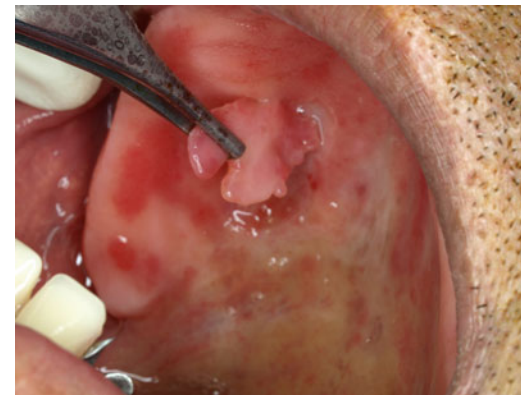

Fig. 19 Leaflike traumatic fibroma related to overworn, uncleaned, complete upper denture

progression (Fig. 17). Lesions can present with hyperkeratinization appearing white if local irritation is present. Fibromas are small lesions, with an average size of 7–8 mm, but can be larger (1–2 cm). Traumatic fibromas and fibroepithelial polyps can progress to more extensive lesions, mostly when related to old, ill-fitting complete prosthesis (Figs. 18 and 19) (van der Waal 2016).

Investigations

Microscopic investigations of this lesion show large areas of atrophic squamous cell epithelium almost without any projections into the underlying connective tissue. The connective tissue is collagenized with fibroblasts that can be fusiform, elongated, round or oval, and sometimes stellate shaped (Fig. 20) (Villa et al. 2016). Chronically inflamed areas are more likely to show epithelial hyperplasia, with typical features of acanthosis, hydropic degeneration, and pseudoepitheliomatous hyperplasia (Fig. 21).

Treatment

Conservative surgical excision is the treatment of choice for these lesions. Recurrence is low if no further irritation or trauma persists in the affected region. Lesions related to prostheses require new, perfectly fitting replacements. Prosthetic hygiene

is also necessary, so the clinician should educate and train the patient on how to take good care of prostheses.

Myofibroma

Epidemiology, Etiology, and Pathology

Myofibroma is a rare benign mesenchymal tumor mostly found in the head and neck region and characterized by the proliferation of fibroblasts, myofibroblasts, or both. Sometimes it manifests as a multifocal lesion called myofibromatosis. Myofibromatosis affects infants and young adults almost exclusively and is known as infantile myofibroma. There are various types of fibroblastic/myofibroblastic lesions, with different behaviors presenting as benign, intermediate with malignant potential, or malignant lesions. Myofibroma is part of the spectrum of these lesions that may also include nasopharyngeal angiofibroma, fibrosarcoma, nodular fasciitis, fibromyxoma, and fibrous hamartoma.

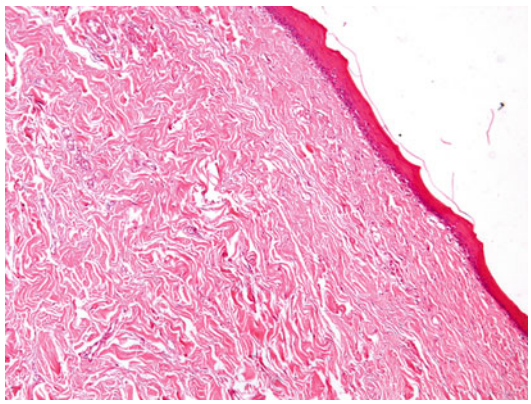

Fig. 20 Collagen rich, hypovascularized connective tissue, lined by thin oral mucosa, without epithelial projections and without a significant inflammatory process (Hematoxylin and eosin stain)

Clinical Presentation

Clinically, myofibromas present as single or multiple, hard, reddish-purple nodules in the skin, muscles, bones, viscera, or central nervous system (Fig. 22). Localized fibromatosis is the most common presentation, seen mainly in the soft tissues of the head and neck. Infantile fibromatosis should be included in the differential diagnosis of multiple bony, soft tissue, and central nervous system lesions in a child, along with Langerhans cell histiocytosis, multiple metastases from neuroblastoma, or sarcomas. Definitive diagnosis is established by means of biopsy (Hourani et al. 2015). Ulceration is a tumor characteristic that may be suggestive of a more aggressive biologic potential and should increase the clinician's suspicion for malignancy. Microscopic evaluation of the lesion with appropriate use of immunohistochemical stains can provide the correct diagnosis.

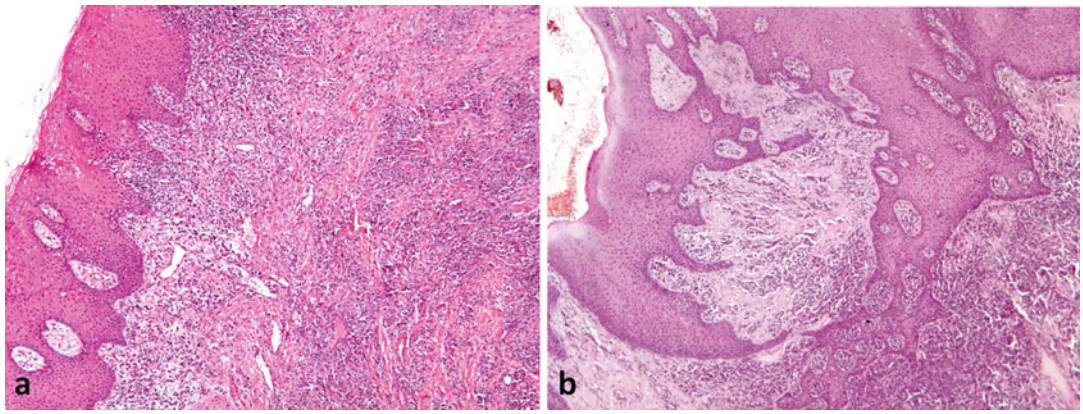

Fig. 21 Chronically inflamed areas of traumatic fibroma (**a**) and fibroepithelial polyp (**b**) show epithelial hyperplasia, with typical features of acanthosis, hydropic degeneration, and pseudoepitheliomatous hyperplasia. The connective tissue presents with an intense diffusely spread lymphocytic exudate (Hematoxylin and eosin stain)

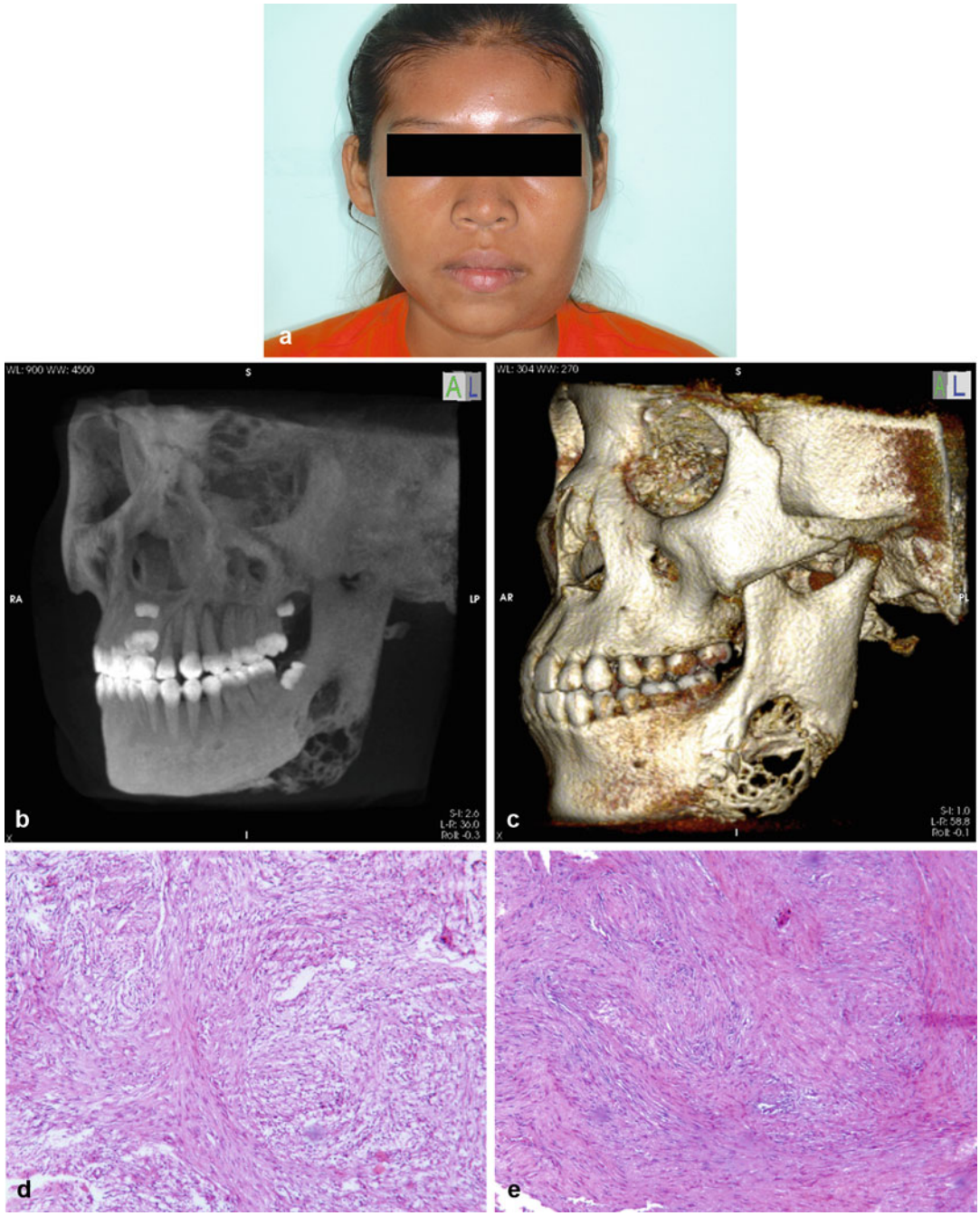

Fig. 22 Myofibroma. Rapid growing solitary lesion involving the left mandible (**a**). Lytic expansile pattern of growth in the posterior mandible noted on CT reconstruction (**b** + **c**). Proliferation of fusiform cells arranged in interlaced bundles (**d**) and fascicles (**e**) (Hematoxylin and eosin stain)

Investigations

The most appropriate imaging exam to identify myofibromas is MRI, which reveals an ill-defined soft tissue mass best viewed with post-contrast enhancement on T1 scans with fat suppression. Computerized tomographic scanning of lesions

involving bone structures reveals an expansive lytic behavior sometimes resembling malignancy but also mimicking odontogenic tumors such as myxoma and ameloblastoma (Fig. 22) (Nabavizadeh et al. 2017). On ultrasound, myofibroma presents as a hyperechoic mass with an anechoic or hypoechoic center traversed by thick septa and surrounded by a thick hypoechoic rim with rare flow on power Doppler (Koujok et al. 2005).

The histopathological examination of myofibroma usually reveals biphasic plexiform paucicellular regions and spindle cell and vascular regions (Fig. 22). Immunohistochemical panels show positive marking for muscle markers such as SMA, muscle-specific actin, HHF35, and vimentin and negativity to neural markers such as CD56, GFAP, and S100.

Treatment

Solitary lesions are amenable to conservative surgical resection. In the generalized form, lesions often regress spontaneously over 6–18 months. In multicentric life-threatening forms, chemotherapy with vinblastine and methotrexate promotes tumor regression (Hourani et al. 2015).

Lipoma

Epidemiology, Etiology, and Pathology

Lipomas are characterized by well-circumscribed benign neoplastic proliferations of adipose tissue and are usually found as long-standing soft nodular asymptomatic swellings covered by normal mucosa or skin. The size of the lesions does not follow the adipose tissue variation, increasing even when patients go through weight loss. Lipomas are more common in men and are one of the most frequent benign mesenchymal tumors, with 15–20% of them seen in the head and neck (Harnsberger and Osborn 2006; Harnsberger et al. 2006). There is a bimodal peak of presentation in children and during the fifth/sixth decades of life, often seen in overweight individuals. Intraoral lesions on the other hand are less frequent than lesions of the head and neck, representing only 1–4% of these tumors. These represent 0.1–5% of all benign tumors of the oral cavity (Fregnani et al. 2003). Lesions can be solitary manifestations or multiple. Patients with multiple lesions in the body should be investigated for syndromes and rare obesity disorders. A retrospective study of 46 cases of lipomas of the oral cavity found the mean age of patients was 52 years, ranging from 8 to 80 years, with 57.8% of female prevalence. The most common site was the buccal mucosa (45.7%), followed by the tongue and lips (13% each) and floor of the mouth (10.9%) (Fregnani et al. 2003). The size of lesions varied from 0.3 to 5 cm, with an average of 2 cm.

Clinical Presentation

Head and neck lipomas are usually found in the posterior neck subcutaneous tissue and in the scalp (Fig. 23). Lesions have soft-to-tender consistency on palpation and present mostly as a loose mobile fluctuating nodule with normal skin coloration.

Oral cavity lipomas are slowly enlarging, with a soft, smooth surface mass of submucosal tissues. When superficial, there is a yellow surface

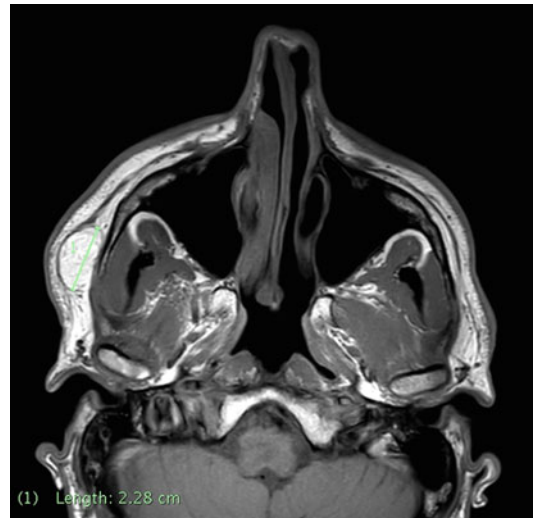

Fig. 23 Axial T1 MRI showing 23 mm lipoma superficial to the right zygomatic arch and the adjacent superior portion of the masseter muscle, immediately deep to the superficial muscular aponeurotic system (SMAS) and temporalis fascia and closely related to the superficial parotid tissue and the zygomaticus major muscle

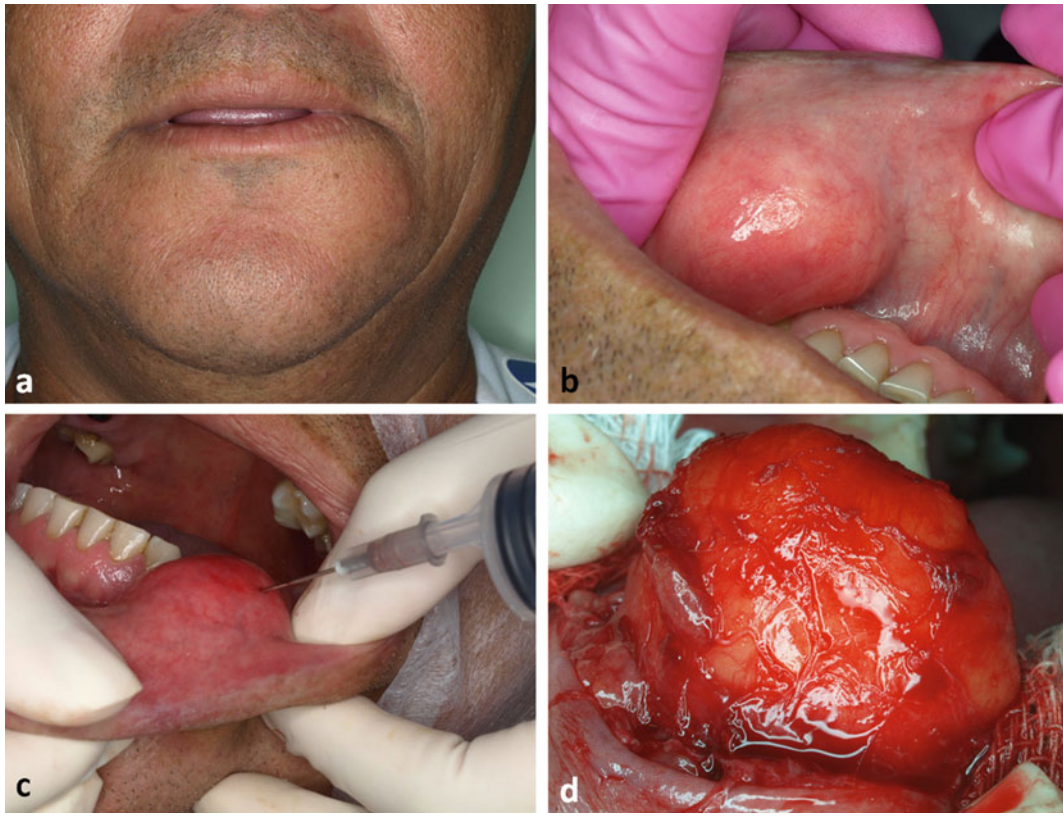

Fig. 24 Lipoma. Patient presenting with extraoral asymmetry involving the left lower lip (**a**). On palpation, a soft well-circumscribed fluctuating nodule was noticed (**b**). FNAC was performed at the first visit (**c**), which showed material with a wet appearance with formation of lobules after fixation spay was applied. The surgical presentation of the dissected lesion, with a thin fibrous capsule and yellow coloration (**d**)

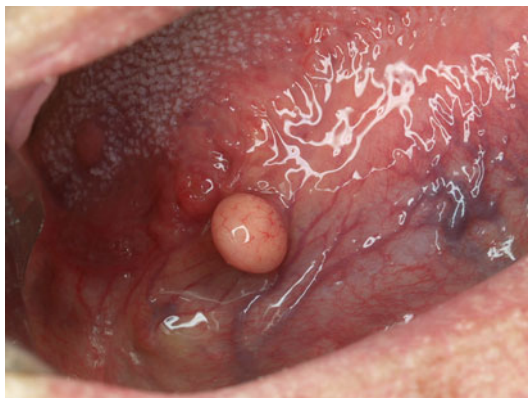

Fig. 25 Lipoma. A small lesion on the posterior border of the tongue that resembles a lymphoepithelial cyst. These lesions float when placed in formalin solution

coloration. Lesions may be pedunculated or sessile, and occasional cases show surface bosselation (Figs. 24, 25, and 26). Puncture of these lesions for FNAC reveals a wet, shiny, transparent or hyaline, gelatinous material. When fixation solution is sprayed over the surface of the slide, it forms a small goticular pattern (Fig. 27).

Although lipomas are well circumscribed, intramuscular lesions require careful dissection and reconstitution of the muscular plane after surgical removal. Grossly, lipomas are of variable size. They tend to appear as smooth or lobulated, often well demarcated or encapsulated, with a yellow color. One distinctive behavior of lipomas is that they float when immersed in formalin solution.

The main differential diagnosis of lipoma includes fibroma, which is composed of fibrous

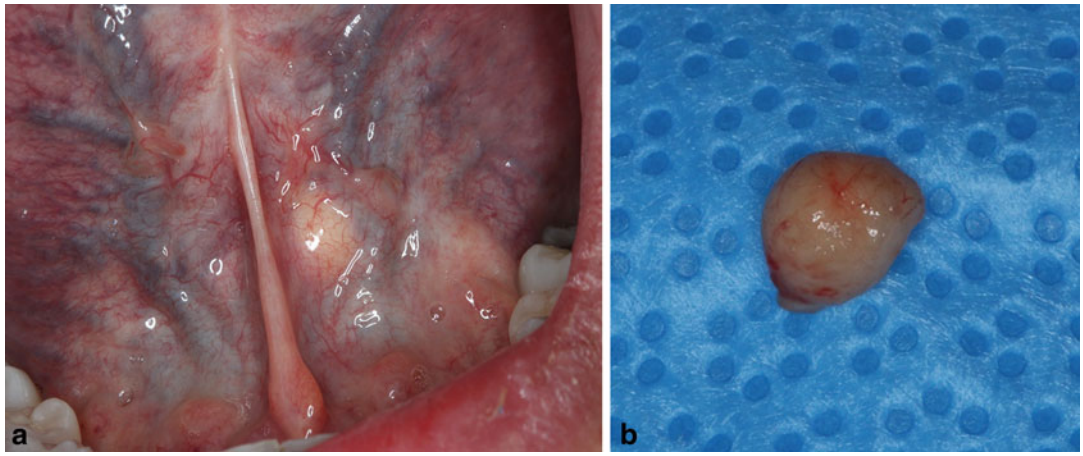

Fig. 26 Lipoma in the floor of the mouth (**a**) appearing as a yellow colored mass under the mucosal surface. Lump was completely excised (**b**)

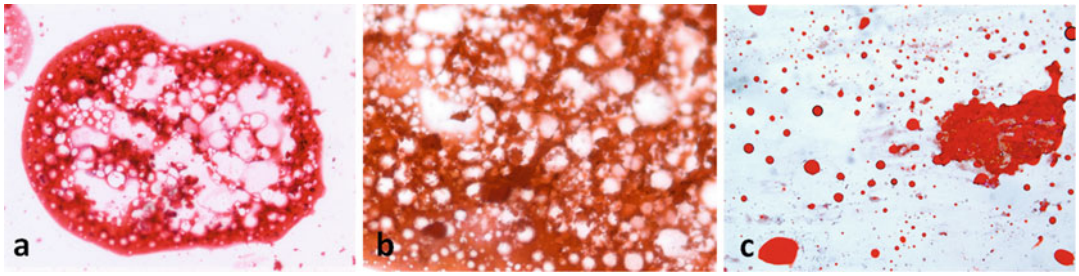

Fig. 27 Microscopic features of FNAC cytologic smear from a lipoma. Hematoxylin and eosin stain (**a**), Papanicolaou stain (**b**), and Sudan red stain (**c**). A globular pattern of the adipocytes is noted, not all of which show preservation of the cytoplasmic membrane. The fat lobules are best visualized with Sudan red stain

tissue and is much more firm than lipoma. Other differential diagnoses include tumors such as granular cell tumor, liposarcoma, neurofibroma, tumor pleomorphic adenoma, traumatic fibroma, mucocele, and other salivary gland tumors (Fig. 28). Histopathological examination is therefore essential for diagnostic conclusion in cases of lipoma.

Investigations

Lipomas demonstrate characteristic low attenuation on CT and signal intensity similar to that of fat on all MRI sequences with minimal internal architecture and mass effect with displacement of the surrounding structures (Fig. 23). The margins may not be easily distinguishable from normal fat. There is no contrast enhancement on CT examinations (Nagornaya and Bhatia 2013).

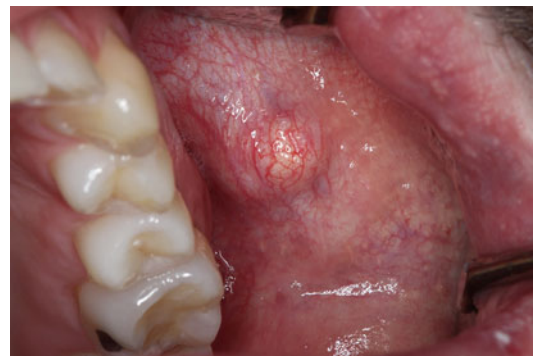

Fig. 28 Lump in the buccal sulcus suggestive of a lipoma but proven histopathologically to be a salivary plasmacytoid myoepithelioma

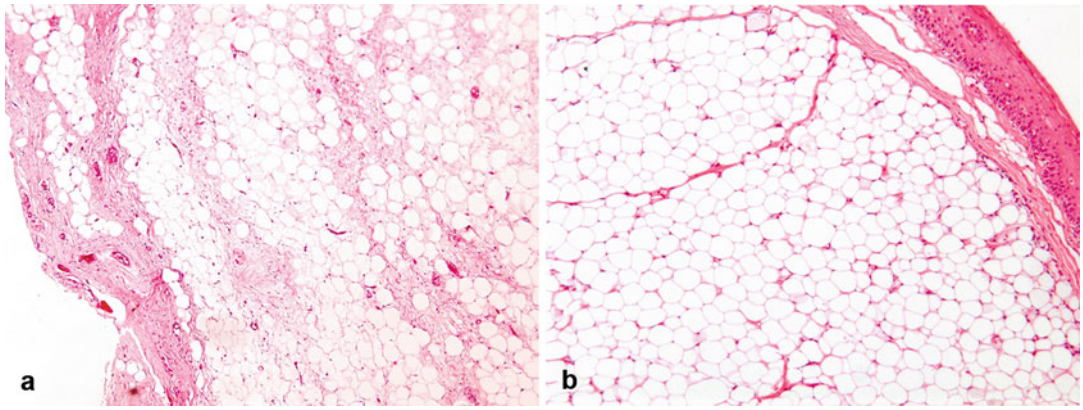

Fig. 29 Microscopic characteristics of lipoma. In (**a**) the lesion was dissected and a thin fibrous capsule circumscribes the well-organized adipose tissue, with loose connective tissue forming bands through the lesion. If the amount of adipose tissue and connective tissue is similar, the lesion is termed a fibrolipoma. In (**b**), the lipoma was submucosal and was excised along with the surrounding tissue. There is still a thin fibrous capsule circumscribing the adipose tissue from the mucosal epithelium (Hematoxylin and eosin stain)

Three different microscopic variations of lipomas are noted including typical lipomas, fibrolipomas, and spindle cell lipomas. Typical lipomas are by far the most common feature, exhibiting a delicate connective tissue capsule circumscribing lobules of hexagonal cells with transparent cytoplasm, with peripherally placed nucleus, resembling normal adipose tissue (Fig. 29). Larger lesions show connective tissue vascularized septa. Fibrolipomas are similar to lipomas by gross examination but microscopically present proportional amounts of connective tissue mixed with agglomerates of adipocytes, mature adipose tissue interspersed by broad bands, or fascicles of dense connective tissue; the capsule is less evident than typical lipomas or even absent. The histologic features of spindle cell lipoma comprise spindle cells, mature adipose tissue, collagen bundles, and myxoid interstitial matrix. Histochemical and immunohistochemical study of the lesion highlights numerous mast cells and immunohistochemical expression of CD34 and vimentin in the spindle cells (Fregnani et al. 2003).

Other microscopic features described in the literature include angiolipomas where there is a well-vascularized lesion, pleomorphic lipomas when the lesion presents pleomorphic lipoblasts and adipocytes, intramuscular/infiltrating lipomas, and salivary gland lipomas according to the site of lipomatous proliferation.

Fine needle aspiration cytopathologic smears are good investigative tools for treatment planning, and when the clinical suspicion of lipoma is present, enough smears should be obtained to perform hematoxylin and eosin or Papanicolau and Sudan red stains (Fig. 27).

Several syndromes include lipomas or lipomatosis as their most significant features including Bannayan-Riley-Ruvalcaba syndrome, multiple symmetric lipomatosis, encephalocraniocutaneous lipomatosis, Proteus syndrome, Cowden syndrome, phosphatase and tensin homolog, and familial partial lipodystrophy type 2 (Fregnani et al. 2003).

Treatment

Surgical excision is the main treatment for lipoma, and recurrence is not likely to occur. For large and difficult-to-access lesions, it is of paramount importance to perform adequate imaging, diagnostic biopsy, and careful assessment before surgery is planned.

Neuroma Including Multiple Endocrine Neoplasia Type 2B (MEN2B)

Epidemiology, Etiology, and Pathology

Neuroma is an abnormal proliferation of hyperplastic axons well delimited by fibrous perineurium.

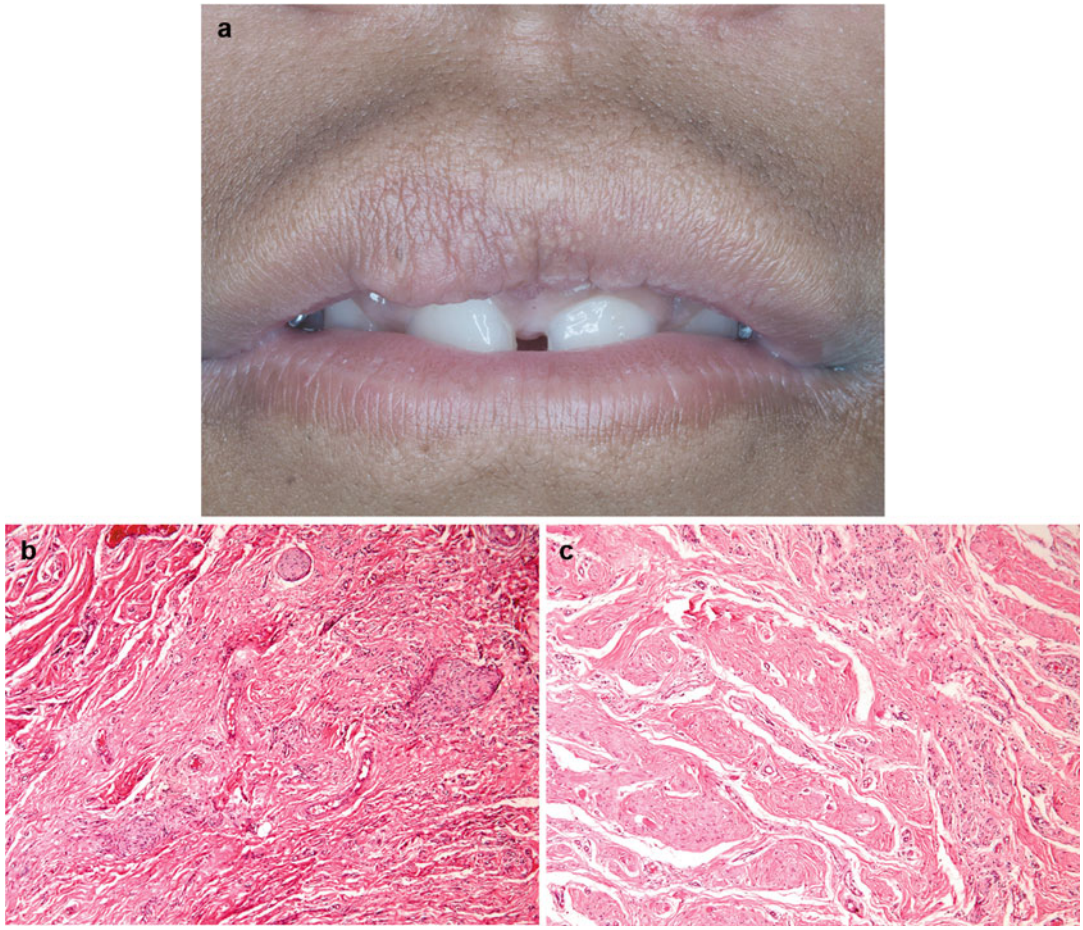

Fig. 30 Traumatic neuroma. Clinical features of a traumatic neuroma after laceration of the right upper lip which healed without professional intervention, causing asymmetry and esthetic concern for the patient (**a**). Microscopically there is mild chronic inflammation (**b**), accentuated fibrosis, and disorganized axons with fibrous perineurium (**c**) (Hematoxylin and eosin stain)

Different pathologic entities use the term neuroma, such as traumatic/amputation neuroma, encapsulated palisaded (solitary circumscribed) neuroma, and mucosal neuroma in multiple endocrine neoplasia type 2B (MEN 2B).

A traumatic neuroma (Fig. 30) is a hyperplastic lesion caused by trauma or surgery that involves the peripheral nerves and is not considered to be a true neoplasm. Traumatic neuromas, also called amputation neuromas, are reactive proliferations of neural tissue that occur after transection or damage to a nerve bundle. These lesions can start after any surgical treatment, such as procedures that need tissue dissection such as biopsy, after tooth extraction, due to local chronic masticatory trauma caused by a total prosthesis to the mental nerve of patients with advanced stage alveolar ridge resorption. The most common sites for a traumatic neuroma in the head and neck are the inferior alveolar nerve, lingual nerve, and great auricular nerve.

Neuroma was first described by Reed et al. in 1972 as a palisaded, encapsulated, solitary, benign cutaneous tumor. It was classified as a primary hyperplasia of nerve fibers (axons and their sheath cells) with equal frequency in both sexes and limited anatomic distribution to areas bordering mucocutaneous junctions, predominantly on the

face, with rare exceptions (Reed et al. 1972). The alternate designation solitary circumscribed neuroma was proposed based on the fact that most lesions were not fully encapsulated and showed only focal palisading (Fletcher 1989). A review of 55 cases of palisaded encapsulated neuromas found that tumors were located on the palate (31), maxillary or palatal gingiva (8) (including one example on an edentulous maxillary alveolar ridge), tongue (4), mandibular gingiva (3), upper lip vermillion border (3), mucosal part of the lower lip (3), lower lip vermillion border (2), and buccal mucosa (1). Patient age ranged from 20 to 73 years, with 70.3% being men and 29.7% women (Koutlas and Scheithauer 2010).

Multiple endocrine neoplasia type 2 is a syndrome of inherited susceptibility to tumors of endocrine cell types including the thyroid "C" cells, the adrenal medulla, and the parathyroid glands. In some disease subtypes, developmental abnormalities may also be present. MEN2 is caused by inherited mutations of the gene that encodes the RET receptor tyrosine kinase which leads to its unregulated activation and is transmitted in an autosomal dominant fashion. Subtypes of MEN2 are MEN2A, MEN2B, and FMTC (familial medullary thyroid carcinoma) (Castinetti et al. 2018). Because of its low point prevalence (0.9–1.65 per million) and incidence (1.4–2.6 per million live births per year), MEN2B (OMIM #162300) remains poorly described in the literature.

Clinical Presentation

Traumatic neuromas present clinically as nodules or masses, less than 2 cm in diameter that can be related to altered sensation on palpation, such as local pain, numbness, or shock (Fig. 30). The mucosa will present normal coloration. Sometimes patients do not remember the cause of trauma, for instance, lesions on the anterior border of the tongue are very common due to masticatory accidental biting. Long-lasting lesions do not show any sign of inflammation. Sometimes reactive fibrous hyperplasia or vascular malformations can be associated with the lesion. Lesions are not well circumscribed or encapsulated, so if the damaged nerve bundle is not visible during the biopsy procedure, it can be difficult to determine the exact extension of the lesion. Differential diagnosis comprises traumatic fibromas, granular cell tumor, schwannoma, and neurofibroma.

Clinically palisaded encapsulated neuromas (Fig. 31) are usually small, rarely ulcerated nodules, the size of which never exceeds 1.0 cm in greatest dimension. Lesion duration can vary from months up to 20 years, but asymptomatic lesion may be reported by the patient as unknown duration. Symptoms are unusual findings, but some patients report pain upon "drinking hot beverages" or "after irritation" (Koutlas and Scheithauer 2010).

MEN2B has a characteristic phenotype with medullary thyroid carcinoma (MTC) and pheochromocytoma. The face may have a wide-eyed expression with thickening and eversion of the upper eyelid margins and visible tarsal plates. Neuromas may be present on the eyelids and conjunctiva, and prominent thickened corneal nerves that extend to the pupillary area may be seen on slit lamp examination. The eyebrows are large and prominent. The face is elongated with prominent "blubbery" lips, and submucosal nodules present on the vermilion border, often laterally. Oral manifestations, which are often the first clue to the syndrome in infancy or early childhood, include mucosal neuromas on the anterior dorsal surface of the tongue. Mucosal neuromas of the tongue are almost pathognomonic in the presence of medullary thyroid carcinoma. Other oral features include palatal and pharyngeal neuromas, a high-arched palate, and a prominent jaw (Morrison and Nevin 1996). MEN2A accounts for about 75% of all MEN2 cases and expresses MTC, pheochromocytoma, and parathyroid gland hyperplasia. FMTC is another variant which accounts for about 20% of MEN2 cases and has a particularly benign course of MTC and a low incidence of other clinical manifestations. MEN2B accounts for only 5% of MEN2 cases; however, its clinical course is the most aggressive. The American Thyroid Association has recommended preventive thyroidectomy before the age of 1 in cases of MEN2B. Patients with MEN2B usually present with very early-onset MTC, a 50% lifetime risk of pheochromocytoma,

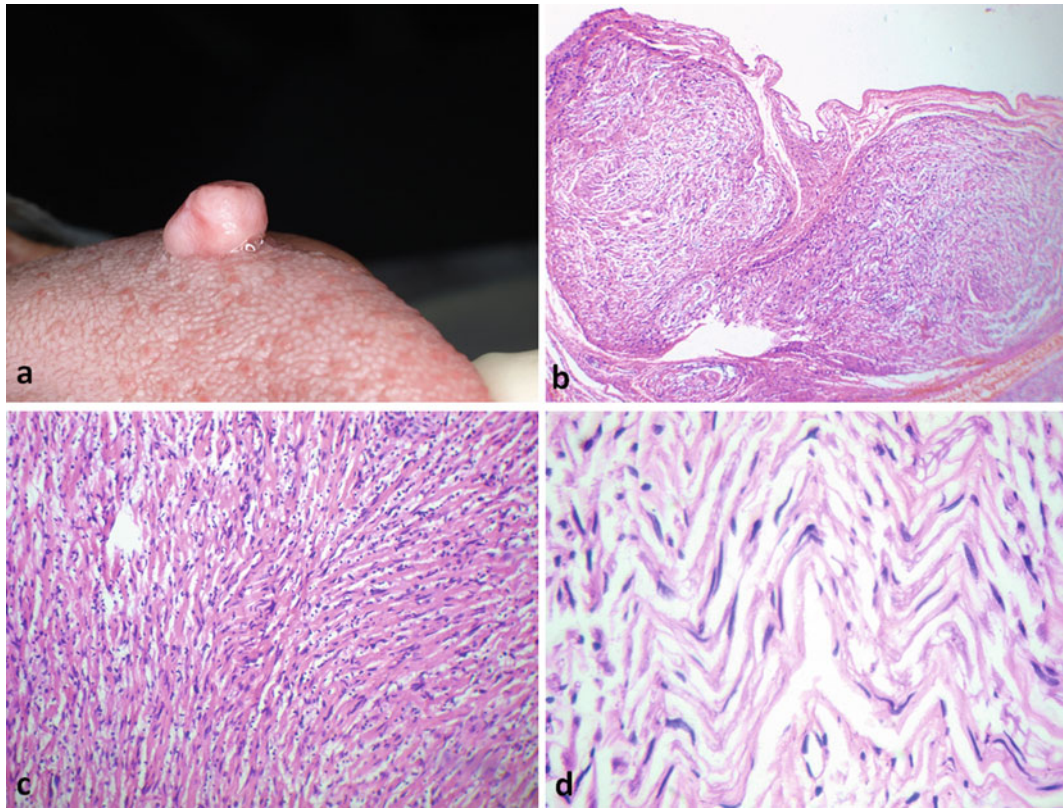

Fig. 31 Palisaded encapsulated neuroma. Firm pedunculated nodule on the anterior border of the tongue (**a**). Nodular arrangement of well-circumscribed neural tissue of the palisaded encapsulated neuroma (**b**). Interlaced fascicles of fusiform Schwann cells with elongated prominent nuclei, in an oriented formation (**c**). Higher magnification showing wavy fusiform nuclei (**d**) (Hematoxylin and eosin stain)

and universal extra-endocrine features, mainly bowel problems due to diffuse intestinal ganglioneuromatosis (constipation, feeding difficulties in infancy, megacolon) and alacrima, both of which can be the earliest presenting features, in addition to mucosal neuromas and a marfanoid body habitus, both of which may not become clinically apparent until several years of age (Castinetti et al. 2018).

Investigations

Microscopic differential diagnosis of the different types of neuromas includes other benign neurogenic tumors such as schwannoma and neurofibroma. Key points of morphologic observations include perineural encapsulation, presence of mast cells, pattern of Schwann cell proliferation, presence of Verocay bodies, axons, and stromal arrangement (Figs. 30, 31, and 32). Inflammation has been mentioned as an important morphologic feature for diagnosis of traumatic neuromas, but long-lasting traumatic neuromas can present with almost an absence of inflammatory cells. Palisaded encapsulated neuromas, mucosal MEN2B neuromas, as well as other benign neurogenic tumors can also present with secondary inflammation caused by secondary trauma or infection (Woodruff 1993; Koutlas and Scheithauer 2010; Lee et al. 2017). Table 7 compares the most important features in the differential diagnosis of neuromas.

MEN2B is caused by a germline missense mutation in the RET proto-oncogene. The *RET* gene which is located on chromosome 10q11.2 encodes a receptor tyrosine kinase. It is expressed in neuroendocrine cells including thyroid C cells,

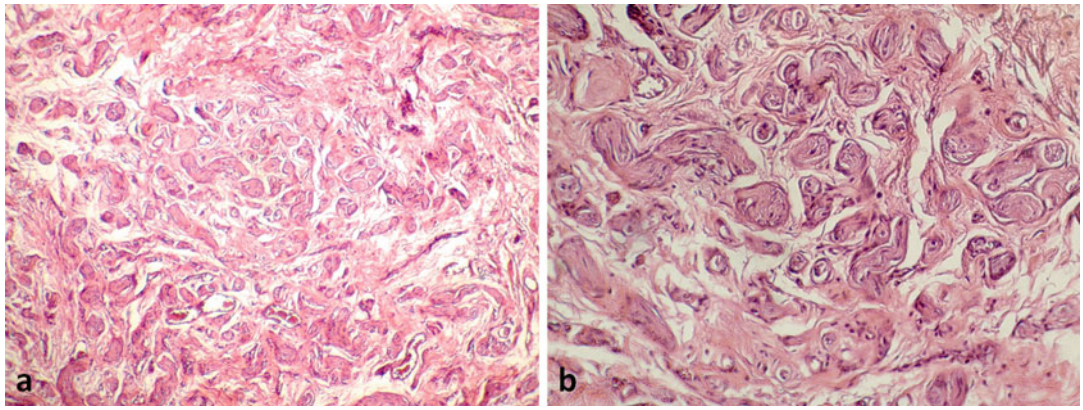

Fig. 32 MEN 2B neuroma showing abnormal hyperplastic axons well delimited by fibrous perineurium, without inflammation or cause-effect correlation (**a**). Higher magnification showing multiple well-delimited anaxonic bundles with perineural cells in the surrounding fibrous stroma (**b**) (Hematoxylin and eosin stain)

Table 7 Important features in differential diagnosis of neuromas

Characteristics	Traumatic neuroma	Palisaded encapsulated neuroma	MEN2B mucosal neuroma	Neurofibroma	Schwannoma
Perineural encapsulation	Absent	Variable	Complete	Absent	Complete
Schwann cell proliferation	Microfascicular compartmentalized and haphazard	Cellular microfascicles coursing in various directions, superficial fascicles blend with connective tissue	Microfascicular compartmentalized and haphazard	Hypocellular sheets	Antoni A and Antoni B patterns
Imumuno-histochemical profile	S100 (+), EMA (+ in perineurium), NFP (+)	S100 (+), EMA (variable), NFP (+)	S100 (+), EMA (+ in perineurium), NFP (+)	S100 (+), EMA (−), factor XIIIa (+), NFP (−)	S100 (+), EMA (+), factor XIIIa (−), NFP (−)
Verocay bodies	Absent	Uncommon	Absent	Absent	Present in Antoni A
Axons	Regenerated, parallel and proportional to proliferating Schwann cells	Multiple with haphazard arrangement	Clusters of separate tortuous bundles	Residual	In the periphery of the tumor
Stroma	Mucoid to fibrocollagenous depending on the "age" of the lesions	Limited collagenous with occasional myxoid areas in the periphery	Loose connective tissue	Mucoid/ myxoid	Collagenous in Antoni A, myxoid in Antoni B
Mast cells	Few eventual	Few eventual	Few eventual	Present	Present in Antoni B

urogenital system cells, adrenal glands, and parasympathetic and sympathetic ganglia. More than 90% of MEN2B cases are caused by a single point mutation of M918T at 918 codon on exon 16 of the *RET* gene.

Treatment

The treatment of traumatic neuromas and circumscribed/encapsulated palisaded neuromas is surgical excision with low recurrence rates (Woodruff 1993). Mucosal neuromas of MEN2B have insignificant repercussion on the quality of life of these patients. In such cases, all attention must be focused on prevention or treatment of MTC and pheochromocytoma which are life-threatening.

Neurilemoma/Schwannoma

Epidemiology, Etiology, and Pathology

Schwannomas are the most common benign neurogenic neoplasms and have propensity to affect sensory nerves more than motor nerves. They are a neoplastic proliferation comprised exclusively of cells that have ultrastructural characteristics closely resembling Schwann cells and have the antigenic phenotype of Schwann cells (WHO Classification of Head and Neck Tumours 2017). Some 25–45% of schwannomas are located in the head, and these often present as diagnostic and management challenges, mainly arising on the tongue, followed by the palate, mouth floor, buccal mucosa, gingiva, lips, and vestibule. It shows no gender predisposition, being more likely to affect middle-aged adults (Das Gupta et al. 1969; Colreavy et al. 2000).

Clinical Presentation

The majority of head and neck schwannomas are non-vestibular and extracranial. Clinically, schwannomas are benign, usually solitary, encapsulated masses of long duration at the time of presentation and rarely show a rapid growth course (Fig. 33). Usually schwannomas are painless and not ulcerated but, depending on location and whether a major nerve is involved, could initially manifest with facial hypoesthesia, paresthesia, or pain (Fig. 34). Obstructive symptoms may occur if the tumor gains enough size to compress the upper aerodigestive tract (Liu et al. 2011).

Bilateral schwannomas are usually related to neurofibromatosis type 2 syndrome (NF2). The etiology of NF2 centers on unregulated growth of neural crest-derived tissues, including Schwann cells. This manifests as lesions involving cutaneous structures and the central and peripheral nervous system. The hallmark of NF2 is hearing loss secondary to bilateral vestibular schwannomas. Neurofibromatosis 2 (NF2) is associated with a rare, potentially treatable type of deafness. Hearing loss usually begins in the third decade and is most often an adult disease. NF2 is the result of inactivation of a classical tumor suppressor gene, NF2, on chromosome 22. Mutations in NF2 are causative, and molecular genetic testing of at-risk family members facilitates early diagnosis and treatment (Gallo et al. 1977; Kluwe et al. 2003).

Investigations

Ultrasound images of schwannoma are characterized by a round or elliptical cross section with a clear border with the internal echo reflective of histology. Patterns may be homogeneous to heterogeneous and cystic change may be seen. Ultrasound has greater diagnostic utility when the diameter of the nerve of origin is large and is connected to a well-delineated nerve.

Computed tomography usually shows well-defined homologous lesions. When a heterogeneous lesion is observed on CT, malignant change may be suspected (Cohen et al. 1986). MRI with contrast is the primary diagnostic test used for schwannomas. These lesions are hypointense on T1-weighted images with post-contrast enhancement with gadolinium. Schwannomas are iso- to hypointense on T2-weighted imaging. MRI is superior to CT at depicting schwannomas, as it is not degraded by dental artifact that plagues CT in the intraoral region. MRI also allows mass size to be accurately measured and mass localization in relation to other structures. Characteristically, these tumors usually appear to be smooth and well

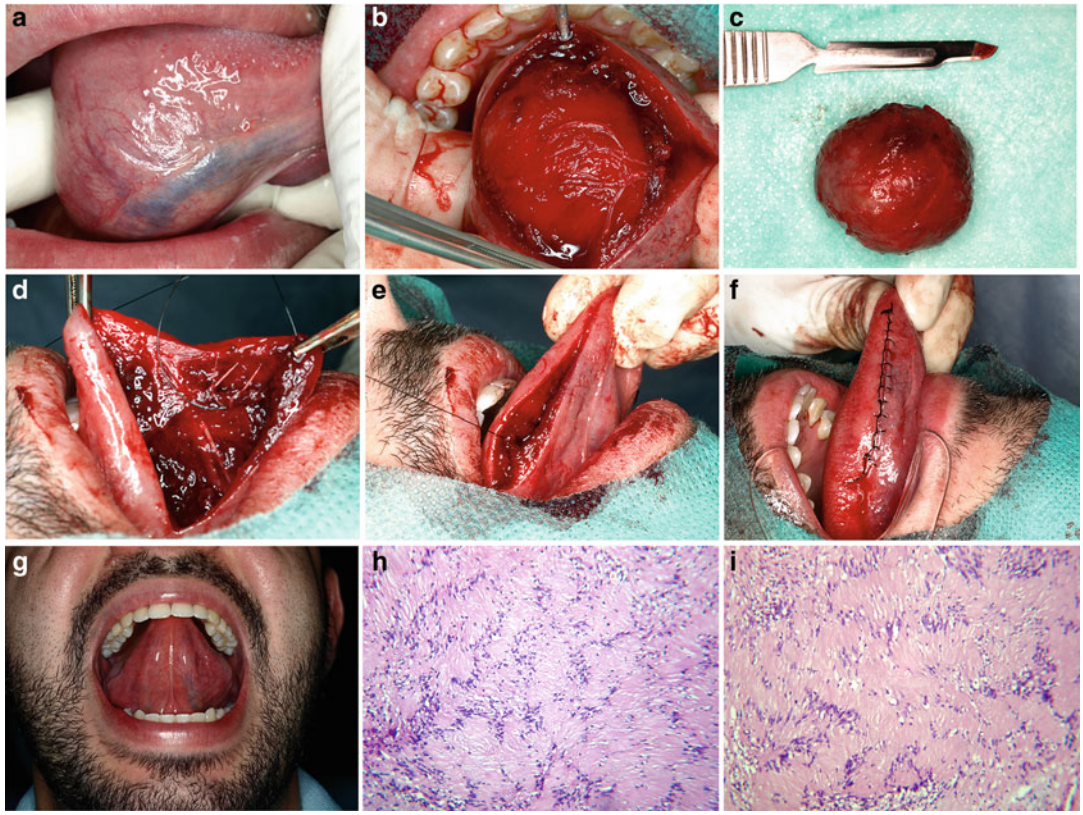

Fig. 33 Neurilemoma/schwannoma. Large firm nodule involving the right tongue. The patient complained about difficulty with speech but no pain or paresthesia (**a**). Surgical access to the lesion choosing the border of the tongue as election point because it is less vascularized (**b**). Gross specimen, a 5-cm-wide nodule (**c**). Surgical site after excision (**d**). Internal suture (**e**) aims to eliminate pathologic spaces and external continuous sutures (**f**) close the wound. Postsurgical follow-up at 3 weeks, the patient was referred to a speech pathologist and recovered from the dyslalia (**g**). Antoni A pattern of schwannoma showing Verocay bodies, eosinophilic hyalinized matrix delimited by fusiform palisading Schwann cells (**h**). In contrast, Antoni B pattern of schwannoma is characterized by storiform arrangement of fusiform cells with pleomorphic nuclei. This pattern varies between areas of more cellularized and vacuolated cells with myxoid areas (**i**) (Hematoxylin and eosin stain)

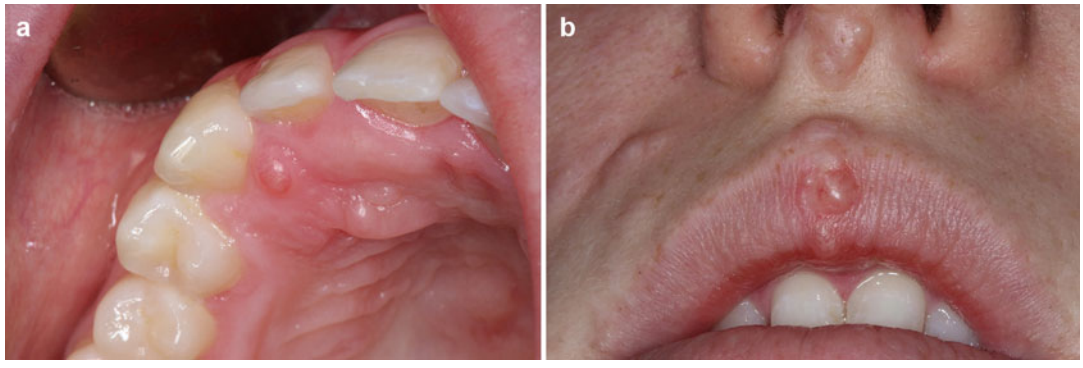

Fig. 34 Palatal oral schwannoma (**a**) with plexiform cutaneous schwannomas (**b**) in the same patient

demarcated and do not invade surrounding structures.

Fine needle aspiration cytology (FNAC) can be performed for tumors located in the superficial part of the neck, although the histological diagnosis and its clearance should be confirmed on paraffin-embedded sections. Smears are expected to contain blood, degenerate cells, and spindle cells. The diagnostic accuracy of FNAC depends strongly on specimen quality and the experience of the cytopathologist.

Histologically, all schwannomas are encapsulated, and beneath the capsules, there are two main patterns observed, called Antoni A and Antoni B types (Fig. 33). The Antoni type A is highly cellular and is composed of elongated Schwann cells, exhibiting areas of organized spindle-shaped cells in a palisading arrangement around acellular, eosinophilic areas, forming Verocay bodies. The Antoni type B is also composed of elongated Schwann cells, but cells are arranged in a less dense myxoid manner and are more disorganized compared to Antoni type A (Fig. 33) (Table 7). Cystic change becomes more prominent as the tumor enlarges and is associated with mucinous degeneration, hemorrhage, necrosis, and microcyst formation.

Treatment

Complete resection is curative in cases of schwannomas and is not likely to recur. Malignant transformation has not been reported. Depending on the location of the lesion, and possible risk to a major nerve or other vital structures, it is possible to opt for close follow-up observation (Lee et al. 2017). For tumors arising from major cranial nerves, excision of the tumor with the division of the nerve of origin renders lifelong morbidity to the patients. On the other hand, other nerve-preserving excision methods, e.g., intracapsular enucleation, do not guarantee intact nerve function after surgery. Because of the substantial chance of nerve palsy after surgery, obtaining an accurate preoperative diagnosis, and preferably with the identification of the nerve of origin, is crucial to the management of the disease.

Neurofibroma Including Neurofibromatosis

Epidemiology, Etiology, and Pathology

Neurofibroma is a benign peripheral nerve sheath tumor composed of a variable mixture of Schwann, perineural-like, and fibroblastic cells, as well as ones with features intermediate between these various cells, contained in a collagenous or myxoid matrix. Neurofibromas may present either as solitary lesions or as part of the generalized syndrome of neurofibromatosis. Approximately, 25% of all neurofibromas are found in the head and neck region, and 6.5% occur in the oral cavity as solitary or multiple lesions associated with neurofibromatosis type 1 (Marocchio et al. 2007).

Neurofibromatosis type 1 (NF1) was described in 1882 by von Recklinghausen who gave the disease its first full description, including recognition that the tumors arose from the fibrous tissue surrounding small nerves, leading to his designation of these tumors as "neurofibromas." The disease also known as von Recklinghausen disease is one of the most common dominantly inherited genetic disorders affecting about 1 in 3000 newborns. NF1 is an autosomal dominant condition caused by mutations of a gene cloned on chromosome 17q11.2. The gene acts as a tumor suppressor gene, and its mutation leads to the development of benign and malignant tumors. More than 500 different mutations of the NF1 gene have been identified which result in disease phenotype.

Clinical Presentation

Solitary neurofibromas are normal colored sessile or pedunculated lesions, a smooth, firm swelling on palpation, usually painless with an unpredictable growth pattern leading to local asymmetry (Fig. 35). Other possible clinical signs less commonly found comprise paresthesia and pain, mostly attributed to nerve compression produced by the lesion. These lesions range from small 1 to 2 cm to disfiguring proportions. Intraosseous lesions are considered to be extremely rare and are described as well-circumscribed non-encapsulated usually on the periphery of a nerve. In the maxilla, there are

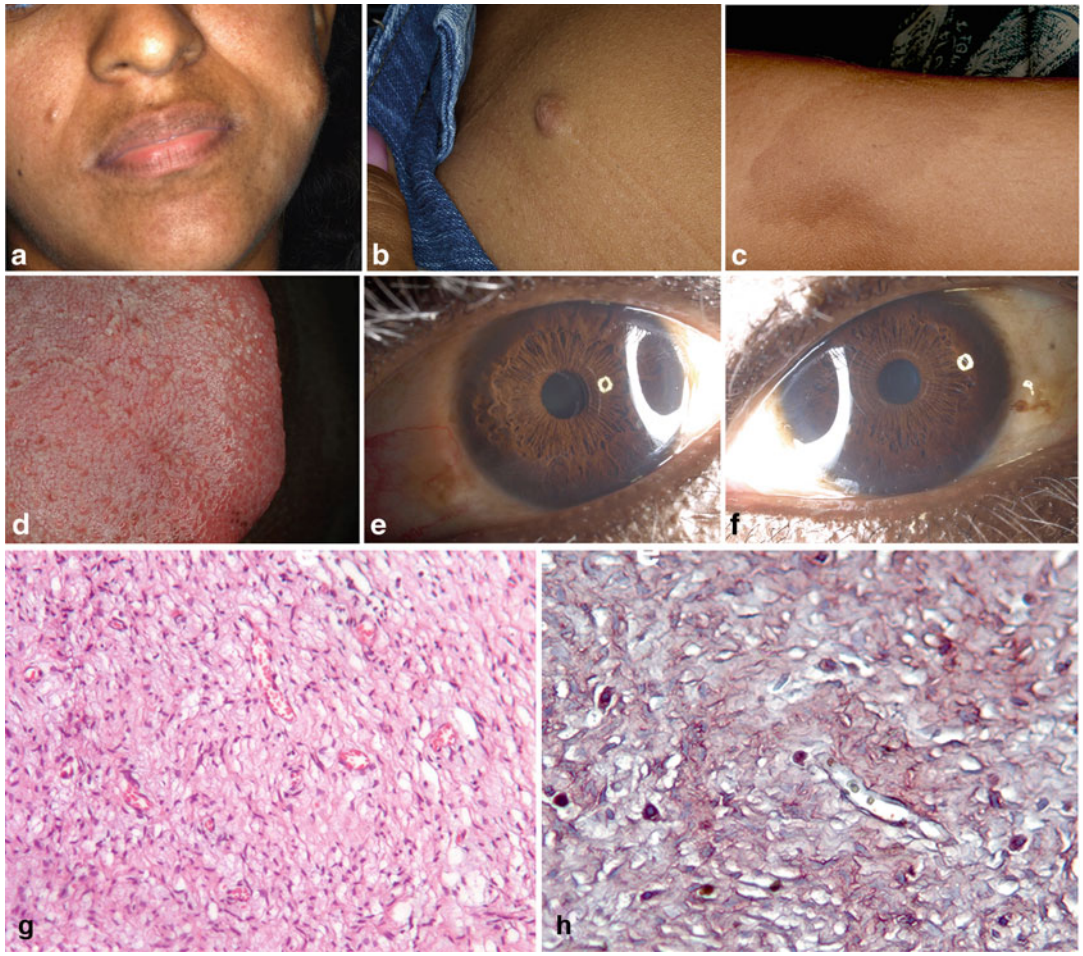

Fig. 35 Neurofibromatosis type I. Soft nodular subcutaneous lesions of neurofibromatosis (**a** + **b**). Café au lait spot on the arm (**c**). Enlarged fungiform papillae (**d**). Lisch nodules are seen in the iris of both eyes (**e** + **f**). Nodular neurofibroma revealing interlaced bundles of fusiform cells with pleomorphic nuclei varying from fusiform to round, ovoid, or stellate (**g**) (Hematoxylin and eosin stain). Toluidine blue stain reveals numerous mast cells within the tumor (**h**)

reports of lesions affecting the nasal sinus, and in the mandible, lesions are usually related to the mandibular nerve. Gross specimen evaluation of the mass shows a whitish to light brown color with a soft, friable consistency. Clinical differential diagnosis comprises other nerve sheath benign neurogenic tumors such as neuromas and schwannomas.

NF1 is typically characterized by multiple café au lait spots, multiple cutaneous neurofibromas, axillary and inguinal freckling, and Lisch nodules (Fig. 35). The underlying predisposition to tumor formation can manifest in a number of other serious conditions including malignant peripheral nerve sheath tumor, plexiform neurofibromas, and central nervous system gliomas (Hirsch and Moskowitz 2013).

Cutaneous neurofibromas develop in 99% of NF1 patients but do not undergo malignant change. They are soft and fleshy, ranging in color from blue to tan. They can be sessile or pedunculated and range in size from less than 1 mm to large and disfiguring masses. Subcutaneous neurofibromas frequently cause pain and neurological symptoms and are occasionally visible just beneath the skin. These are palpable firm

and tender nodules. Plexiform neurofibromas are found in 50–60% of patients and can cause significant neurological deficits and disfigurement. Most plexiform neurofibromas are internal and not suspected clinically. They represent discrete tumors that arise in nerves within organs or tissues beneath the dermis, frequently clustering around proximal nerve roots. They vary in size and can extend along significant lengths of nerves (Chen 2012).

The average life expectancy of individuals with NF1 is reduced by approximately 15 years (Rasmussen et al. 2001). The appearance of malignant peripheral nerve sheath tumors (MPNSTs) and vasculopathy is the important cause of early death in patients with NF1, but the most common cause of death in patients with NF1 is malignancy. MPNSTs usually arise from pre-existing subcutaneous neurofibromas or plexiform neurofibromas but can develop de novo (Tucker et al. 2005). These are the most frequent malignant neoplasms associated with NF1. These tumors are very aggressive and are often fatal. MPNSTs are difficult to diagnose because they develop in patients who are generally habituated to develop other lumps and skin changes. Warning signs associated with the development of MPNST in a patient with pre-existing neurofibroma include persistent or nocturnal pain, rapid increase in size, asymmetric growth, new neurological deficit, or change to a more firm texture and consistency. The lifetime risk of developing an MPNST in a patient with NF1 is 5–13%. MPNSTs that develop in children and adolescents are rare but tend to be low grade. In contrast, MPNSTs that develop in patients in their 20s and 30s tend to be high-grade tumors.

Clinical diagnosis of NF1 is based on the criteria set forth by a National Institutes of Health Consensus Conference in 1987 and is still accepted for routine clinical use. The diagnostic criteria are met in a patient with the presence of at least two major disease features out of the following:

- A first-degree relative with NF1, six or more cafe´ au lait patches >5 mm in greatest diameter in prepubertal individuals, and >15 mm in greatest diameter in postpubertal individuals (Fig. 35)
- Axillary or groin freckling, two or more neurofibromas, or one plexiform neurofibroma
- Two or more Lisch nodules in the iris (Fig. 35)
- Optic pathway glioma
- A distinctive osseous lesion, including bony dysplasia of the sphenoid wing, or pseudoarthrosis of the long bones (Fig. 36)

Investigations

Neurofibromas may appear as soft tissue opacities on standard radiographs. On ultrasonography, these lesions appear as well-demarcated fusiform, hypoechogenic structures, in close relation to the native nerve. On CT, the lesions have low density. MRI is the imaging technique of choice for detection and characterization of tumors of peripheral nerves. On MRI, neurogenic tumors are of low to intermediate signal intensity on T1-weighted images and of variably increased signal intensity on T2-weighted MR images (Baert 2008).

Neurofibromas have a variable morphological pattern on histopathological examination. They are composed of fusiform cells in a mucoid/myxoid matrix. The tumor is composed of an irregular pattern of proliferative fibers and mucoid masses, with a variable mixture of Schwann, perineural-like, and fibroblastic cells (Fig. 35). Two major variants are described, a well-circumscribed nodular variant and the plexiform variant which produces poorly circumscribed tumors. The later carries risk of malignant transformation. Neurofibromas form tortuous cords along the segments and branches of a nerve with a tendency to develop centripetally along a nerve course. Inflammation is found in 44% of specimens (Marocchio et al. 2007), which is important when differentiating these from other neurogenic tumors such as traumatic neuromas. Other comparative morphologic characteristics of the tumor are displayed on Table 7.

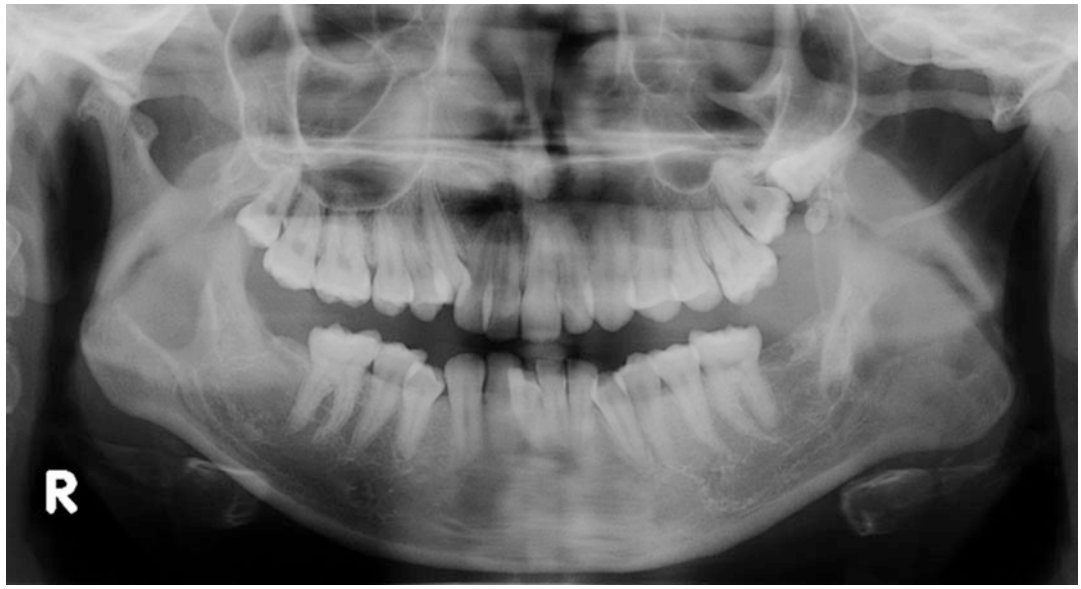

Fig. 36 Neurofibromatosis 1 in a 25-year-old female. The left condylar head is significantly hypoplastic, and there is elongation of the left condylar neck and flattening of the right condylar head with osteophyte formation. There is deformity of the left sigmoid notch. There is thinning of the mandibular rami. There appears to be discontinuity of the infraorbital rim and hypoplasia of the paranasal sinuses. There is enlargement of the mandibular foramina. These changes are consistent with features of neurofibromatosis type 1. Other findings not described

Treatment

The gold standard treatment for neurofibromas is surgical excision. Easy-to-access lesions such as on the skin do not demand further precautions, but some head and neck lesions can show some complications related to anatomy, sacrifice of cranial nerves that can result in functional problems such as permanent anesthesia or loss of motor function, and even significant deformity. The clinical behavior of neurofibromas is characterized by a benign course with a low frequency of recurrence after surgical excision.

Other therapies such as photodynamic therapy have been proposed for large and difficult-to-access lesions, with promising results, but still lack long-term research of its effectiveness (Hamdoon et al. 2012).

Neurofibromatosis type 1 raises the need for periodic clinical follow-up of patients in order to prevent malignant neoplasms. The survival rate of most patients with NF1 exceeds 50 years. Once diagnosed with NF1, it is important to provide genetic counseling to the patient and their relatives.

Granular Cell Tumor

Epidemiology, Etiology, and Pathology

Granular cell tumor (GCT) was described in 1926 by Abrikossoff, and the etiology of this disease is controversial and much discussed in the literature. Schwann cells, fibroblasts, histiocytes, myoblasts, and undifferentiated mesenchymal cells have been identified in the histogenesis of GCT. It is a rare benign neoplasm of soft tissues, characterized by poorly demarcated proliferation of round or spindle plump cells with granular cytoplasm. The granular appearance is a result of increased accumulation of lysosomes in the cytosol of the cells.

Considered a rare lesion, the most common sites for this lesion are in the head and neck region accounting for 50% of cases, although it can appear in any area of the body. In the oral cavity, the most affected site is the tongue, but other sites such as the hard palate, buccal mucosa, lips, uvula, parotid gland, and gingiva have been reported. The peak age of incidence of GCT is 40–60 years, but it can affect all ages. Most reports describe a female-to-male ratio of 2:1,

and higher incidence in black populations has been noticed.

Clinical Features

GCT presents as a firm, polypoid, or sessile tumor that forms a "lump" on the surface of the affected site (Fig. 37). It is superficial, poorly circumscribed, and slow-growing involving the subcutaneous or submucosal tissues. Most lesions are small, do not exceed 3 cm in diameter, and are covered by mucosa that can be normal colored, yellow colored, or with pale to leukoplakic appearance. On palpation, the tumor often appears demarcated but not encapsulated.

The differential diagnosis for these lesions comprises other benign soft tissue neoplasms such as fibromas, lipomas, neurofibromas, neuromas, and schwannomas. Reactive lesions such as traumatic fibroma can also resemble GCT, but the inflammatory process usually adds symptoms such as pain and discomfort as well as cause-effect correlation.

Investigations

Microscopic analysis shows a lesion mainly consisting of large polygonal or elongated cells with clear, granular cytoplasm and an oval or round nucleus with loose chromatin (Fig. 37). Periodic acid-Schiff (PAS)-stain-positive granules are detected in the cytoplasm. The tumor cells are strongly positive for S-100, vimentin, and CD68 and are negative for GFAP and NFP. Intraoral lesions present frequently with pseudoepitheliomatous epithelial hyperplasia in the overlying mucosa; therefore, care should be taken to avoid an erroneous diagnosis of squamous cell carcinoma (Ferreira et al. 2017).

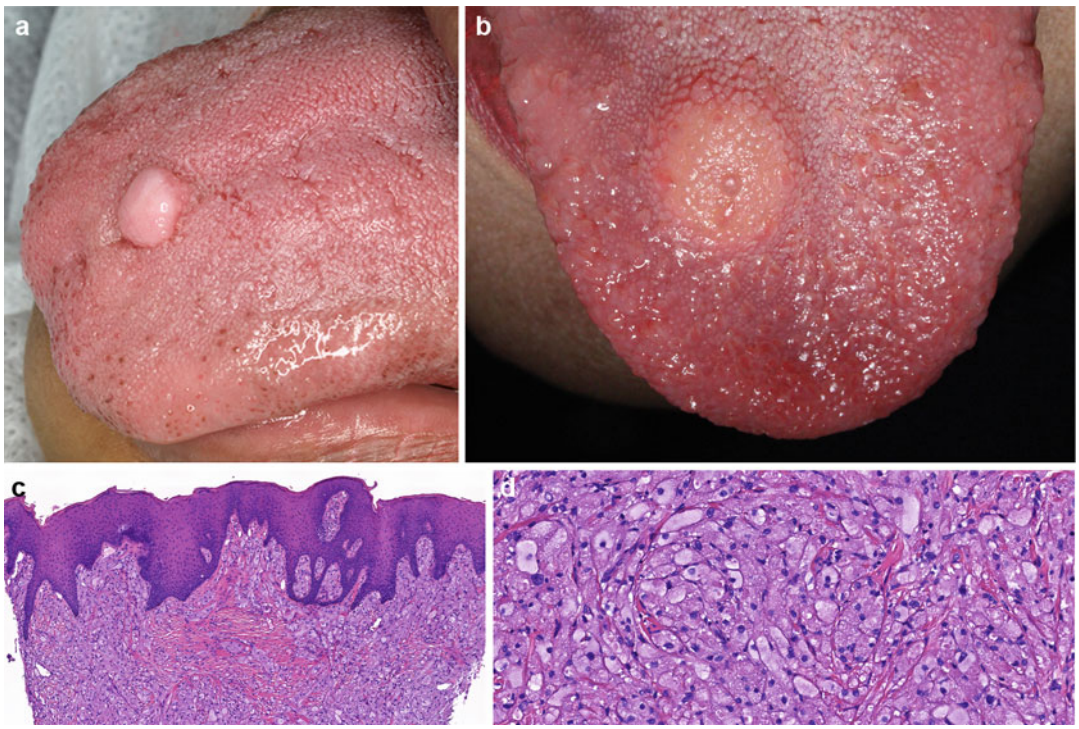

Fig. 37 Granular cell tumor. Sessile nodule forming a lump of pale coloration on the dorsum of the tongue (**a**), and raised hard lump with yellow coloration on dorsal tongue in a separate patient (**b**). Microscopic features of granular cell tumor of the tongue show epithelial hyperplasia of the mucosa (**c**) and a poorly circumscribed lesion consisting of large polygonal or elongated cells with clear, granular cytoplasm and an oval or round nucleus with loose chromatin (**d**) (Hematoxylin and eosin stain)

Multiple GCT may be familial and associated with syndromes such as LEOPARD, NF1, or Noonan, all related to the Ras/MAP kinase pathway probably caused by mutation in *PTPN11*. Rare examples of malignant GCT characterized by pleomorphism, mitotic activity, and necrosis have also been described (van der Wal 2016).

Treatment

Surgical excision with a safe margin of tissue is the treatment of choice for GCT, although this is not always possible because the tumor lacks a capsule, as histologically demonstrated by an undefined cellular margin. Recurrence is low, although it has been reported in incompletely removed lesions and in patients with multiple GCT.

Rhabdomyoma

Epidemiology, Etiology, and Pathology

Rhabdomyoma is a rare benign proliferation of mesenchymal cells with skeletal striated muscle differentiation (Fig. 38). It is estimated that rhabdomyomas represent less than 2% of soft tissue tumors and are considerably less common than its malignant counterpart the rhabdomyosarcoma. Rhabdomyoma is classified into cardiac and extracardiac, based on anatomic location. It can manifest as a local or multifocal lesion. Among the different types of rhabdomyomas, the cardiac rhabdomyoma occurs almost exclusively in the heart of infants and young children, is the most prevalent, and is related to tuberous sclerosis. Extracardiac rhabdomyomas are subdivided into fetal, adult, and genital. Extracardiac rhabdomyomas are true neoplasms, with a reciprocal translocation between chromosomes 15 and 17 (Gibas and Miettinen 1992). Because rhabdomyomas are more commonly found in the neck and preauricular region, it is speculated that the etiology of these neoplastic cells is based on branchial musculature of the third and fourth branchial arches. The median age is 60 years with 3:1 male-female predominance.

Clinical Features

In the head and neck region, only the fetal and adult forms are likely to occur; the genital form is exclusive to the female gender affecting the vagina and vulva of middle-aged women. Although usually solitary, adult-type rhabdomyoma can occasionally be multinodular and rarely multifocal. Multifocal adult-type rhabdomyoma usually presents as slow-growing lumps in the parapharyngeal region. Large or multilobulated lesions may be first identified due to complaints of progressive dysphagia, hoarseness, and snoring.

Investigations

Contrast-enhanced CT and MRI are the best imaging examinations to identify rhabdomyomas.

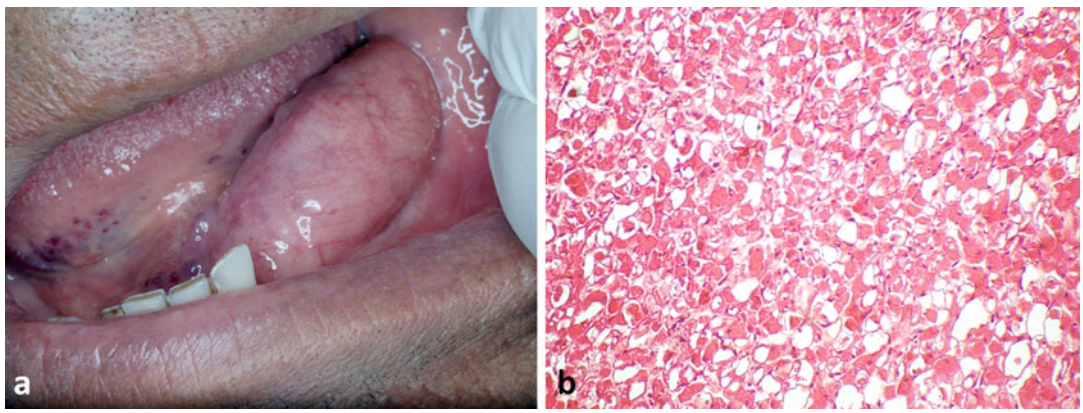

Fig. 38 Rhabdomyoma. Large normal colored mass in the floor of the mouth (**a**). Intermediate magnification showing a uniform tumor formed by polyhedral granular cells with focal vacuolization (**b**) (Hematoxylin and eosin stain)

Usually the tumors develop close to other skeletal muscles, as a well-circumscribed mass with homogenously similar intensity. Aspiration of these tumors contains diluted blood without agglutination; therefore schwannoma is included as the primary differential diagnosis (Lu et al. 2017). Radiologically rhabdomyoma presents as a well-circumscribed mass without invasion of surrounding soft tissues. In addition, the characteristically increased 18 F-fluoro-2-deoxy-D-glucose (18 F-FDG) uptake on positron-emission tomographic CT is vitally useful for the detection of multifocal adult rhabdomyoma, especially in the case of very small lesions, which are easily missed with traditional examination (de Trey et al. 2013).

Adult-type rhabdomyoma is the most common subtype of extracardiac rhabdomyoma, characterized by mature skeletal muscle differentiation forming homogeneous masses of polygonal cells sometimes with more than one nucleus, with eosinophilic granular cytoplasm resulting in a "spider web" appearance (Fig. 38). In contrast, fetal-type rhabdomyoma exhibits immature muscle differentiation, characterized by bland spindle cells associated with fetal myotubules haphazardly arranged in abundant myxoid stroma (Fig. 38). Microscopic differential diagnosis of rhabdomyoma comprises granular cell tumor, hibernoma, oncocytoma, paraganglioma, or crystal-storing histiocytosis. The lesion is PAS positive, and immunohistochemical panels show positivity for desmin, MSA, SMA, and myoglobin and negativity for S100, EMA, and cytokeratin.

Treatment

Surgical resection of the tumor performed through a transcervical approach and transoral incision under general anesthesia applies to most lesions due to its regular site manifestation. Rhabdomyomas are removed easily with blunt dissection. These tumors appear as a soft, tissue-encapsulated mass with a smooth shiny surface. Cut sections present with a pink and smooth texture that is similar to muscle tissue. Rhabdomyomas are not likely to recur if removed completely; however, when small lesions are located in vital structures, the risk-to-benefit ratio of complete excision should be carefully weighed.

Hemangioma

Epidemiology, Etiology, and Pathology

Hemangiomas are true neoplasms of blood vessels formed by endothelial proliferation assuming variable width. The lesion is usually present at birth and can regress spontaneously. They are distinct from vascular malformations due to a higher mitotic activity. Reactive lesions such as angiogranuloma, which are ulcerated and have a clear cause-effect relationship, have similar mitotic activity and microscopic appearance and frequently cause discussions as to whether it represents a true hemangioma, also named lobular capillary hemangioma.

The origin of hemangiomas, although still under debate, has been narrowed to embryonic placental angioblasts or intrinsic endothelial progenitor cells with the ability to clonally duplicate in a precise environment of cytokines and estrogen concentration (Yu et al. 2004). It is even possible that both theories regarding the origin of hemangiomas coexist. Hemangiomas likely arise from progenitor cells with directional preponderance to become placental-like tissue in specific organs such as skin and liver (Barnes et al. 2007).

The role of molecular signaling involved in vascularization is better understood in hemangioma development. Increased levels of common molecular contributions to endothelial cell migration and new vessel development have been discovered during the proliferative phase of hemangioma growth such as vascular endothelial growth factor (VEGF), basic fibroblast growth factor (b-FGF), insulin-like growth factor (IGF), and matrix metalloprotease-9 (MMP-9). Similarly, and as would be expected, the levels of angiogenic markers also wane during the involution phase of hemangiomas (Buckmiller et al. 2010).

Hemangiomas proliferate during the first 9–12 months of life and subsequently involute at a variable course over many years. The tumor has a female predominance, occurring commonly in the head and neck region but rarely in the oral cavity. These lesions are subdivided into two categories based on their clinical behavior and histology. The more common infantile hemangioma (IH) develops shortly after birth and follows the

expected course of proliferation with prolonged involution. Infantile hemangiomas are vascular tumors comprised of rapidly dividing endothelial cells affecting up to 10% of the population with a greater incidence in Caucasians and premature and low-birth-weight infants. Approximately 60% occur in the head and neck region. Congenital hemangioma is rare, is present at birth, and does not follow the natural growth phase of its infantile counterpart.

Clinical Features

These lesions present a smooth reddish purple, sessile, polypoid, or pedunculated masses, often with increasing size and occasional bleeding (Fig. 39). Most infantile hemangiomas are not apparent at birth or may appear to be a small "scratch" or "bruise." Infantile hemangiomas become evident shortly after birth as well-demarcated, red, vertically expansive lesions. They can be overlooked during the first month of life as they are difficult to differentiate from other common skin blushes seen in the newborn. During this period, they are flat, pink, and sometimes more pale or bluish than their surrounding tissue. Slower but continuous growth occurs up to 9 months in most patients. Rapid expansion can lead to adjacent skin and soft tissue ischemia, necrosis, and ulceration. The bright red discoloration is persistent until the onset of involution when resurfacing is observed as variable graying of the overlying skin. No two hemangiomas are the same, and the rate of growth is variable in the proliferative phase. Involution may occur as early as 6 months of age in isolated lesions or much later when deep or segmentally distributed hemangiomas are present.

Infantile hemangiomas are usually superficial lesions, but their depth can vary, altering its clinical presentation. Depth can be expressed as superficial, deep, or mixed/compound which indicates the amount of tissue involvement. Superficial IH will typically have a deep red appearance on the skin or mucosa. Deep IH often will be visualized to have a bluish hue under the normal-appearing skin. Compound IH possess attributes of both (Friedman et al. 2013).

Investigations

Since most hemangiomas are superficial lesions and respond to objective tests such as diascopy, there is limited use for imaging exams, only applied for differential diagnosis or in deep or difficult-to-access lesions. For that matter, ultrasound and MRI are helpful tools. These can be used to distinguish between IH and vascular malformations if the diagnosis is in question. Color Doppler ultrasound will demonstrate either fast-flow or slow-flow lesions. The best diagnostic radiologic clue for IH is the presence of a high-flow soft tissue mass. On ultrasound, hyperechoic and/or hypoechoic lesions can be seen with

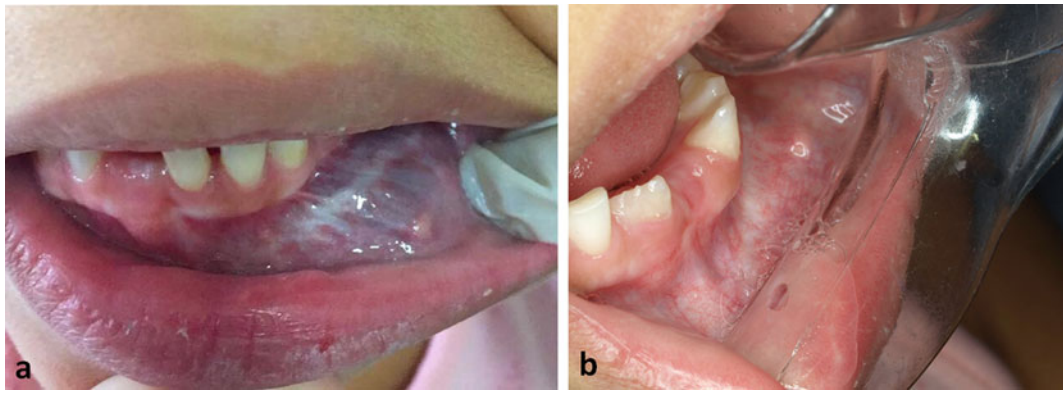

Fig. 39 Infantile hemangioma in a 4-year-old female, presenting as a growing blue sessile mass, first noticed during her first year of life (**a**). Patient received sclerotherapy with four periodical local infiltrations of monoethanolamine oleate, with complete remission of the lesion after 8 months from initial diagnosis (**b**)

variable presence of vessels. MRI for IH typically shows a well-defined, non-infiltrating lesion. Intermediate signal intensity is seen on T1-weighted images and increased signal intensity of T2-weighted sequences. After gadolinium injection, strong enhancement is observed.

MRI is especially important in the evaluation of patients with large facial hemangiomas to rule out neurocutaneous PHACES syndrome [OMIM #606519]. This syndrome is characterized by **p**osterior cranial fossa anomalies (P), facial **h**emangiomas (H), and one or more major cervical and **a**rterial cerebral vascular (A), **c**ardiovascular (C), **e**ye (E), and **s**ternal or supraumbilical (S) anomalies/defects (Heyer et al. 2008).

Microscopically hemangiomas are classified according to the lumina of the capillary vessels that are predominant in the lesion. Capillary hemangiomas consist of multilobular arrangements of proliferating endothelial cells and capillaries of various shapes and sizes surrounded by pericytes (Fig. 40). The capillary type appears more cellularly rich, but mitotic activity is similar to the cavernous type. The lumina may be subtle or dilated, especially in IH. Cavernous hemangiomas are named due to the similarity to the capillaries found in the penial cavernous body and show larger dilated vascular spaces lined by endothelial cells (Fig. 40).

The most difficult microscopic differential diagnosis of hemangiomas is the angiogranuloma. Good clinical information is essential to avoid confusion between these lesions without molecular investigation; loss of integrity of skin/mucosal lining also favors the diagnosis of angiogranuloma. Other important differential diagnoses of vascular tumors include congenital hemangiomas, tufted angiomas, and a variety of hemangioendotheliomas. Final diagnosis of this lesion can demand the use of an immunohistochemical panel.

Immunohistochemical panels for the diagnosis of hemangiomas show CD34, CD31, and ERG positive. Infantile hemangiomas have a specific marker (GLUT1) which is negative for angiogranuloma and congenital hemangioma (2017).

Treatment

The treatment of hemangiomas comprises a variety of modalities that are best suited for each case. Infantile hemangiomas include observational follow-up, since up to 50% of lesions completely resolve by 5 years of age, 70% by 7 years, and 90% by 9 years. Bleeding, ulceration, functional risk, and esthetic concerns usually require professional intervention. Historically corticosteroid therapy was used in IHs. This therapy can be systemic or local infiltration. Systemic administration has important side effects in children,

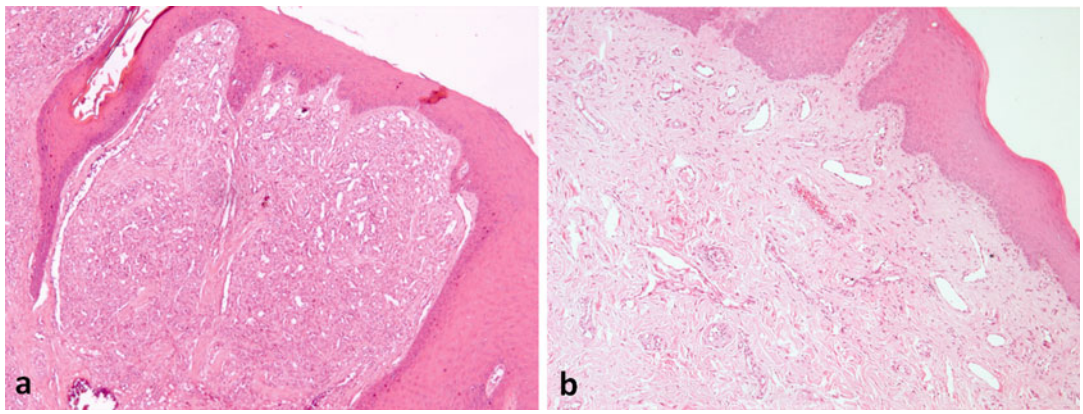

Fig. 40 Low magnification of infantile hemangioma presenting as a cellular well-circumscribed lesion with endothelial cells in a lobular arrangement (**a**). Mature lesion of hemangioma with flattened endothelial cells and more evident vascular spaces in a more fibrous stroma (**b**) (Hematoxylin and eosin stain)

mostly related to long-term use. Steroids are effective in retarding the growth phase of IH, but if discontinued, the lesion returns to its normal growth.

Flash lamp dye laser therapy has also produced good results, promoting regression in the size of the lesions. This treatment modality offers the best results in superficial lesions. Such lesions require future excision of residual scar. Adjunctive antibiotic ointment before and after flash lamp dye laser therapy improves healing and prevents infection of ulcerated lesions.

In the past decade, propranolol has become first-line treatment for IH (Leaute-Labreze et al. 2008). Since the serendipitous discovery of the favorable results of beta-blockers in these lesions, many studies have shown good outcomes, initially with small case series, but lately larger sample size studies have reinforced its safe use with 96.9% effectiveness and low complications (3.8%). Complications include sleep disturbance, diarrhea, and bronchospasm. In one study, only 22.6% of cases had incomplete involution of IH and needed further assistance with other adjunctive therapies including timolol maleate or pulsed dye laser (Zhang et al. 2017). The mechanism of action of propranolol on reducing or curing hemangiomas remains unclear although the most likely mechanism is the pharmacologic stimulation of programmed endothelial cell death (apoptosis). A dose of 1–2 mg/kg/day for the treatment of infantile hemangiomas is currently being applied. The treatment may last for up to 6 months, demands close monitoring, and is terminated when the infant reaches 1 year of age.

Sinonasal Papilloma

Epidemiology, Etiology, and Pathology

Sinonasal papillomas are surface mucosal lesions of the sinonasal tract related to HPV infection, as well as exposure to solvents, smoking, and alcohol consumption. They manifest in three different forms: inverted type, oncocytic type, and exophytic type. This differentiation is based on the pattern of proliferation that these lesions can produce. The inverted papilloma is the most frequent type with estimated prevalence of 0.74–2.3 new cases per 100,000 population, affecting patients ranging from 6 to 84 years, 2.5–3 times as common in males as in females. The oncocytic papilloma has no gender predilection, and most patients are over 50 years of age. This type lacks correlation with HPV infection, which is distinct from the other two types. Sinonasal exophytic papilloma is most related to HPV infection with up to 63.5% of cases, affecting two to ten times more males than females, typically in patients aged 20–50 years. Malignant transformation and/or other malignant lesions arising from sinonasal papillomas are exceptions worth careful attention (Maitra et al. 2001).

Clinical Presentation

Patients with sinonasal papillomas first present with non-specific symptoms such as nasal obstruction, polyps, epistaxis, rhinorrhea, hyposmia, and headache. Unilateral nasal obstruction and the presence of an asymptomatic mass can also represent sinus papilloma progression. Exophytic sinonasal papillomas usually arise on the lower anterior nasal septum and present warty appearance.

Investigations

Because of its non-specific symptoms, delay in diagnosis is sometimes reported, as unsuccessful treatments of "recurrent sinusitis" or "chronic rhinitis." Diagnostic imaging is important for diagnosis with CT and MRI offering the best information about the site of origin of the tumor. Endoscopy is also a valuable complementary exam for lesions affecting the nasal cavity.

Inverted growth is the hallmark of the inverted sinonasal papilloma, forming islands or nests of stratified squamous epithelium and/or columnar respiratory cells. The basement membrane is intact, with eventual mitotic figures only in the basal layer. Dysplastic features may cause concern about malignant transformation. The American Joint Committee on Cancer (AJCC) staging system is commonly used for staging these lesions. The oncocytic type presents both exophytic and endophytic growth patterns, and the oncocytic appearance of the epithelium is due to

the hyperchromatic nuclei and the abundant granular eosinophilic cytoplasm. Cilia in various stages of regression are occasionally found in the superficial layers. Finally, the exophytic type resembles the endophytic epithelial lining changing only the direction of growth. Keratinization of the epithelial surface is possible, mostly in lesions exposed to trauma or drying effects of the air, and malignant transformation is less likely to occur. The main differential diagnosis of this lesion is the cutaneous squamous cell papilloma, which is more keratinized and does not present signs of respiratory epithelium and submucous glands in the specimen.

HPV is detected more frequently in exophytic papillomas than in endophytic ones, with a weighted prevalence of 65.3% (Lawson et al. 2008). Types 6/11 are found in most cases. HPV has been detected with variable frequency in inverted sinonasal papilloma, with a mean rate of 16% (Lawson et al. 2008). A preponderance of HPV 6/11 has been reported as compared to HPV 16/18, with a ratio of low-risk to high-risk HPV types of 2.8:1 (Lawson et al. 2008). The frequency of HPV detection increases in inverted papillomas with dysplasia and in lesions with malignant progression to carcinoma, with a shift toward a higher frequency of high-risk subtypes (Lawson et al. 2008).

Inverted papillomas present monoclonal proliferations, as shown by X chromosome analysis. However, the chromosomal loss of heterozygosities (LOHs) at arms 3p, 9p21, 11q13, 13q11, and 17p13 have not been detected (Califano et al. 2000). The main differential diagnosis of the inverted type is with sinonasal cylindrical cell carcinoma and squamous cell carcinoma, which can be distinguished by the presence of significant nuclear pleomorphism, atypical mitoses, and stromal invasion. Respiratory epithelial adenomatoid hamartoma can be separated from inverted sinonasal papilloma because it contains numerous gland-like structures lined by respiratory epithelium, surrounded by thick hyalinized basement membrane, which is not present in sinonasal papilloma.

The epithelial cells of oncocytic papillomas stain for the mitochondrial enzyme cytochrome C oxidase (Levine et al. 1987) and for cytokeratins (Maitra et al. 2001). Oncocytic papilloma may be confused with low-grade sinonasal adenocarcinoma, which often shows a papillary growth pattern but presents an epithelial growth characterized by a single-layered, non-oncocytic epithelium with some degree of atypia, occasional mitotic figures, and invasive growth. Due to the presence of several microcysts within the epithelial layer, oncocytic papilloma may also be confused with rhinosporidiosis. In this infectious disease, however, organisms are found both in the epithelium and the stroma, and the epithelium does not show oncocytic changes (Franchi 2016).

Treatment

Complete surgical excision is the treatment of choice, and these lesions are not likely to recur, but surgical access to the lesions can be difficult and incomplete removal may lead to recurrence. If high-risk HPV infection and/or dysplasia is detected, clean surgical margins should be pursued during surgical excision (Levine et al. 1987; Karligkiotis et al. 2014).

Malignant Epithelial Tumors of the Head and Neck

Laryngopharyngeal cancers constitute about 40% of all head and neck cancers. The pharynx is divided into three subsites: the nasopharynx which extends from the posterior choana to the level of free border of the soft palate, the oropharynx which consists of the soft palate, tonsils, lateral pharyngeal wall, and the base of the tongue. It extends from the level of the soft palate to the level along the superior surface of the hyoid bone. The hypopharynx is the region of the pharynx from the plane along the superior level of the hyoid bone to the plane along the inferior border of the cricoid bone. This region consists of the pyriform sinuses, the postcricoid region, and the posterior pharyngeal wall.

The larynx is subdivided into the supraglottis, glottis, and subglottis. The supraglottis extends from the superior level of the hyoid bone to the laryngeal ventricles and consists of the epiglottis,

aryepiglottic folds, arytenoids, and false cord. The glottis includes the vocal cords and extends from the ventricles inferiorly by 1 cm. The subglottis extends from the level of the glottis to the inferior level of the cricoid cartilage (Fig. 41).

In contrast to cancers of the oral cavity which mostly draw early attention due to a visible lesion, tumors originating in the oropharynx and hypopharynx usually present late due to their location in apparently hidden areas and non-specific symptoms masquerading as many benign conditions.

Apart from the routine blood investigations, which include complete blood count, renal function, and coagulation profile, tissue diagnosis and imaging are required for treatment planning. Diagnostic evaluation for HPV status is mandatory (Table 8).

A biopsy from the primary lesion is needed to establish the primary diagnosis. A deep biopsy (to include the basement membrane) from the most "representative" part of the lesion should be taken. Large ulcers tend to have a necrotic center, and biopsy from the necrotic area should be avoided. In cases of infiltrative disease which spreads submucosally, a wedge biopsy is required to target the most indurated area. Such lesions are common in the base of tongue (BOT) region (Fig. 42).

Imaging is complementary to clinical examination in treatment planning. While endoscopic evaluation maps the mucosal extent of the disease, involvement of the soft tissues, bone, and cartilage can be determined by imaging. Pretreatment staging is done based on both clinical and radiological findings. Contrast-enhanced CT of both the head and neck and chest are the most commonly employed imaging modalities. MRI with contrast is an alternate approach. If an organ preservation strategy using chemotherapy and radiotherapy is planned, PET/CT may be considered for response evaluation (Fig. 43). The advantages of each are depicted in Table 9 and are outlined in more detail in the chapter on ▶ "Diagnostic Imaging Principles and Applications in Head and Neck Pathology." The imaging modality of choice varies with the subsite and the disease extent.

The same modality used to image the primary lesion is used to image the neck. Metastatic neck nodes on imaging appear enlarged and rounded and show necrosis, extracapsular spread, and invasion of adjacent structures. Necrosis is the most reliable criteria for metastasis. The sensitivity and specificity of CT for assessing neck nodal metastasis vary from 55% to 95% and 39–96%,

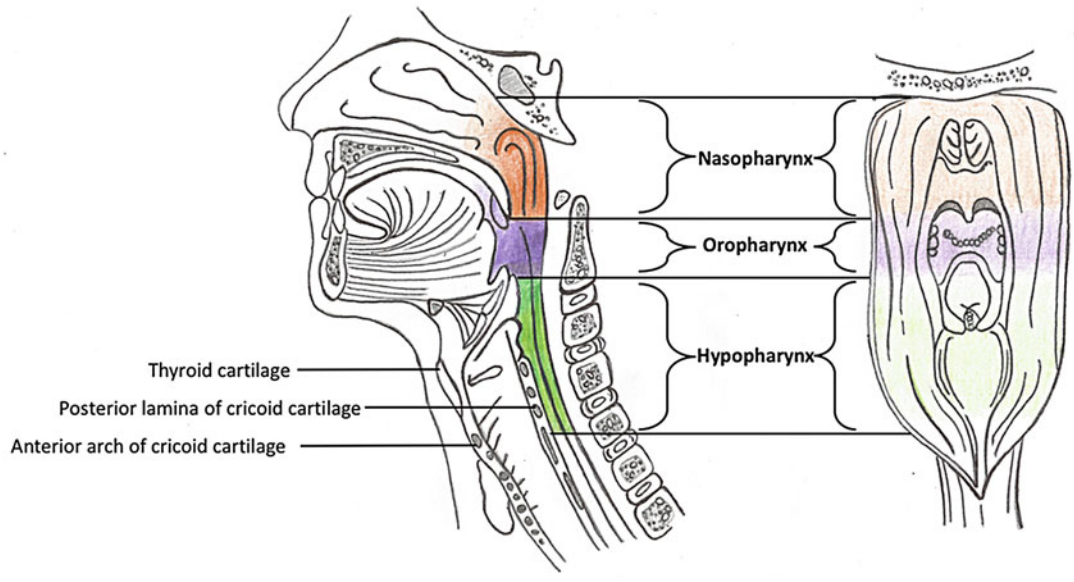

Fig. 41 Anatomy of the pharynx including the laryngopharyngeal subsites

Table 8 Principles, merits, and demerits of validated laboratory methods of HPV detection

PCR for HPV detection
Principle
HPV DNA or RNA sequence is amplified several orders of magnitude through several rounds of denaturing, annealing, and DNA replication using a DNA polymerase
Merits
Highly sensitive cost-effective method for HPV detection
Demerits
Low specificity
Does not differentiate between HPV that is present in neoplastic cells and surrounding nonneoplastic epithelium
Does not distinguish between episomal and integrated HPV DNA
Technically cumbersome to perform
HPV-16 DNA in situ hybridization
Principle
Only molecular method allowing reliable detection and identification of HPV in topographical relationship to pathological lesions
Whole HPV detection occurs within the nuclei of infected cell
Merits
Detection of clinically significant HPV infection within tumor specimen
Evidence of active oncogenic transcription
High specificity (100%)
Demerits
Poor sensitivity (80–85%) due to inability to detect HPV oncogenic strains other than HPV-16
Technically difficult to perform
p16 immunohistochemistry
Principle
Overexpression of p16 is a result of inactivation of pRb by the HR-HPV E7 oncoprotein and consequent release of pRb-mediated negative regulation of p16
Surrogate marker
Merits
High sensitivity
Accessible to most laboratories
Demerits
Surrogate marker
Lacks specificity due to non-HPV-related causes of p16 overexpression resulting in high false positives
Lack of standardization and interpretation of results

respectively, while those for MRI are 64–92% and 40–81%, respectively (de Bondt et al. 2007).

Distant metastasis (DM) from head and neck squamous cell carcinomas most commonly spread to the lungs followed by the liver and bone (Mamelle et al. 1994). Factors associated with distant metastatic disease include histologic tumor type, T stage, N stage, extranodal tumor spread, and number and level of neck nodes. FDG-PET in head and neck SCC alters TNM stage in 43% and management in 13.7% of cases (Lonneux et al. 2010). The National Comprehensive Cancer Network (NCCN) guidelines recommend FDG-PET/CT for the initial work-up of patients with stage III and IV head and neck cancers. Taking into consideration the lack of availability and cost of FDG-PET/CT, a multi-slice CT (MSCT) of the chest is an equally good alternative in advanced cancers as the most common sites for DM are the lungs and mediastinal nodes (Fig. 44).

Treatment protocols are determined primarily by the oncologic outcome followed by the functional and cosmetic outcome. Cost-effectiveness,

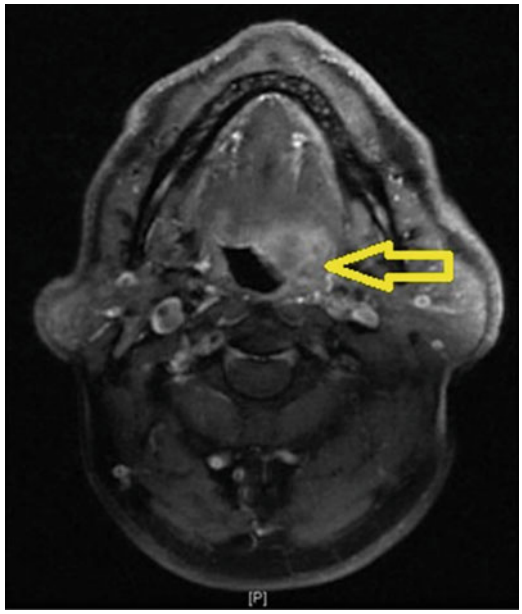

Fig. 42 Contrast-enhanced T1 MRI image showing an infiltrative tumor over the left base of tongue (arrow)

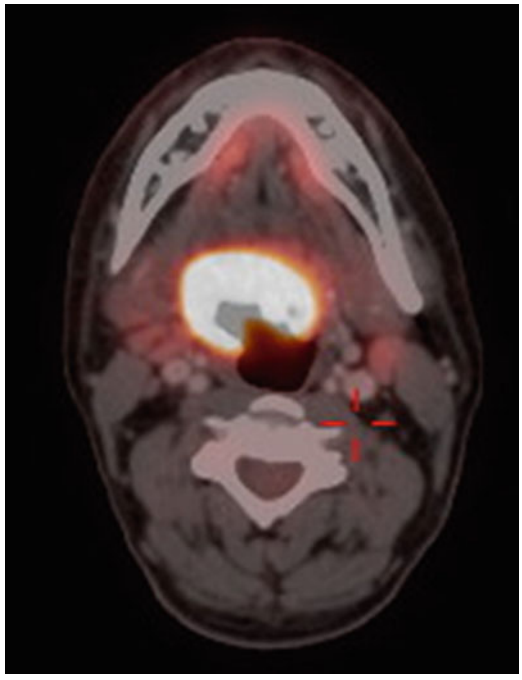

Fig. 43 PET/CT fusion axial image showing an enhancing lesion involving the right base of tongue suggestive of neoplastic etiology

Table 9 Commonly used imaging modalities

Advantages of CT
Imaging modality of choice for assessing bone erosion
Easy availability
Less time-consuming
Less costly
Advantages of MRI
Better soft tissue delineation
Better delineation of perineural invasion
No radiation exposure
No iodinated contrast
Quality of image not affected by dental artifacts

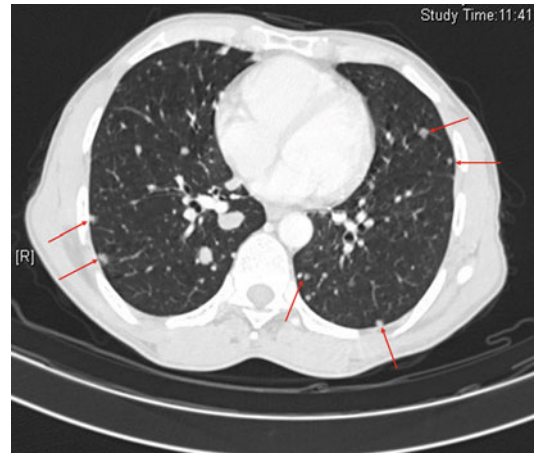

Fig. 44 Contrast-enhanced CT thorax axial sections showing multiple metastatic lung nodules (some shown by red arrows)

patient preferences, and quality of life (QoL) should also be taken into account. Early-stage cancers (stages I and II) are usually treated with single modality (surgery or radiation), while advanced stages (stages III and IV) are treated with multimodality treatment which includes surgery, radiation, and/or chemotherapy.

Posttreatment surveillance (Table 10) is an elaborate part of patient management. Identifying early recurrence improves the oncologic outcome. Functional and cosmetic issues can also be addressed through surveillance which improves the QoL for cancer survivors. There is no fixed protocol for frequency and duration of follow-up, but several guidelines exist such as the NCCN guidelines. Patient compliance, place of stay,

Table 10 Posttreatment surveillance

3 monthly follow-up for 2 years, 6 monthly follow-up for next 5 years, yearly follow-up thereafter
Post-treatment baseline imaging within 6 months of treatment completion
Yearly chest imaging especially in smokers
Thyroid function tests six monthly in patients receiving radiation to the head and neck
Voice and swallowing evaluation and appropriate rehabilitation
Habit cessation counseling and rehabilitation
Nutritional evaluation and rehabilitation
Psychiatric evaluation if required

nature of work, and commitment of caregivers decide how frequently the patient is followed up. Generally, patients are followed three monthly for the first 2 years, six monthly for the next 5 years, and yearly thereafter. All patients undergo a routine head and neck clinical examination to detect early recurrences or second primary cancers. Patients of oropharyngeal, hypopharyngeal, and laryngeal cancers should also undergo a flexible endoscopy with air insufflation (for pyriform sinus and postcricoid cancers) or rigid endoscopic examination. First posttreatment imaging (MSCT or contrast-enhanced MRI) should be done within 6 months of treatment completion. For patients undergoing nonsurgical treatment, contrast-enhanced FDG-PET/CT is recommended for response assessment. PET/CT should not be carried out before 8 weeks and preferably after 12 weeks posttreatment completion to allow for the inflammatory response to subside. If residual disease, recurrence, or a synchronous second primary is suspected within 8 weeks, a MSCT or MRI is recommended. Yearly imaging of the chest is recommended especially in patients with a history of smoking. All patients undergoing radiation to the head and neck need to undergo a thyroid function test six monthly. As radiation adversely affects the constrictors, swallowing functions should be evaluated during follow-up. Voice evaluation is required in patients undergoing total laryngectomy. On each follow-up, patients need to undergo detailed nutritional assessment as they are prone to nutritional deprivation as a result of impaired swallowing. Shoulder function should be assessed in patients undergoing neck dissection and encouraged for active shoulder exercises. Tobacco cessation and alcohol counseling should be carried out with patients continuing these habits. Patients suffering from depression and psychosocial and end-of-life issues require proper psychiatric consultation and social support.

Oropharyngeal Cancer

Epidemiology, Etiology, and Pathology

Squamous cell carcinoma (SCC) constitutes more than 90% of malignant tumors of the oropharynx. Oropharyngeal tumors are now distinctly divided into two subtypes, namely, HPV-positive SCC and HPV-negative SCC. HPV-negative tumors tend to behave like their counterparts in the oral cavity and appear to be associated with increased risk of exposure to tobacco and alcohol.

Human papillomavirus (HPV) infection is now clearly associated with a subset of head and neck cancers. Among all subsites of head and neck SCC (HNSCC), HPV prevalence is the highest in oropharyngeal cancers where 40–80% are positive for the virus, and the number continues to increase (D'Souza et al. 2007; Adelstein et al. 2009; Dayyani et al. 2010; Chaturvedi et al. 2011). HPV is an epitheliotropic small double-stranded DNA virus with more than 200 identified subtypes (Oguejiofor et al. 2013). Of these, about 15 types are thought to have high-risk oncogenic potential. HPV strains 16, 18, 31, 33, and 35 are associated with oropharyngeal SCC (OPSCC) with strain HPV-16 being responsible for more than 90% of HPV-induced cancers (Marur et al. 2010).

HPV has a predilection for the basal cells of the epithelium. Initially the viral genome remains as an episome expressing early replicative protein E2. Subsequently integration into the host genome occurs following which E2 protein is suppressed and E6 and E7 proteins become activated. The main aim of E6 is to abrogate p53 function to facilitate its own replication and results in allowing genetic mutations in the absence of p53 function. E6 inhibits p53 directly

as well as via E6-associated protein (ubiquitin ligase). The function of E7 is degradation of the *Rb* gene complex resulting in activation of E2F protein and subsequent progression of the cell cycle beyond the G1S checkpoint. Apart from the oncogenic proteins E6 and E7, E5 plays a significant role in oncogenesis by enhancing the transforming activity of E6 and E7, upregulating epidermal growth factor receptor (EGFR), and inhibiting major histocompatibility complex (MHC). More detailed discussion about HPV-associated tumors and molecular understanding of head and neck squamous cell carcinoma can be found in a later section of this chapter.

The oropharynx is also rich in minor salivary glands and lymphoid tissue and is the site for salivary gland neoplasms and hematolymphoid malignancies. Oropharyngeal salivary gland tumors constitute about 1.1–3.3% of all minor salivary gland tumors (Spiro et al. 1973; Eveson and Cawson 1985; Ellis et al. 1991). Nearly half of these salivary neoplasms are malignant adenoid cystic carcinoma (ACC) and mucoepidermoid carcinoma (MEC) (Eveson and Cawson 1985).

Adenoid cystic carcinomas are relatively common, and 42.5% of these occur in the minor salivary glands (Gnepp 2001). About 20% of these minor salivary gland ACCs occur in the oral cavity and oropharynx (Gnepp 2001). They usually present as a slow-growing submucosal mass with ulceration in advanced cases. The most common histologic subtype is the cribriform variant although tubular and solid patterns can also be seen (Waldron et al. 1988). The cribriform variant carries a favorable prognosis as compared to other variants. Perineural invasion is common and symptoms like pain raise the suspicion of such spread. These tumors commonly spread through the hematogenous route with the lungs being the most common site for metastatic disease. Neck nodal metastasis occurs in 10–15% of patients. Surgery remains the main treatment for ACCs with neck dissection being reserved for clinically metastatic neck disease. As these tumors are relatively radiosensitive, adjuvant radiation is warranted in most cases. Imaging of the chest is mandatory in the initial work-up and on a yearly basis in the follow-up period. As metastatic lesions usually have an indolent behavior, treatment of the primary lesion is undertaken even in the presence of metastatic disease.

Mucoepidermoid carcinomas are most common minor salivary gland malignancies and account for 9–23% of all salivary gland tumors (Eveson and Cawson 1985; Waldron et al. 1988; Ellis et al. 1991). In the oropharynx, they have a propensity to involve the palate. Treatment is essentially surgical resection with neck dissection being indicated in high-grade, high-stage tumors and those with evidence of neck nodal metastasis. Adjuvant radiation is indicated in high-grade, high-stage tumors, positive/close resection margins, perineural invasion, and lymphovascular spread.

Hematolymphoid malignancies, most commonly non-Hodgkin's lymphoma, present with an exophytic mass, submucosal bulge, or an ulcerated lesion commonly involving the palatine tonsils or the base of tongue. Rarely, mucosal melanomas can present in the oropharynx as a blackish, gray, or reddish pigmented (rarely amelanotic) lesion. These are very aggressive tumors, and the mainstay of treatment is surgery with multimodality adjuvant therapy.

An increasing number of oropharyngeal cancers are associated with HPV. HPV has emerged as a mutagen for head and neck cancers with the oropharynx being the most common site and being associated with about 60–70% of oropharyngeal cancers (D'Souza et al. 2007). The prevalence of HPV-associated oropharyngeal cancers is low in the Asia-Pacific region in comparison to Western developed countries.

Presence of HPV is now considered a distinct clinical, pathological, and prognostic entity in the etiology of head and neck cancers, especially those of the oropharynx. Epidemiological studies have shown that the incidence of HPV-induced oropharyngeal cancers is increasing worldwide over the last decades, while the overall incidence of head-neck SCC has declined in the developed countries (Benson et al. 2014). Although HPV-positive OPSCC presents at a relatively advanced stage as compared to HPV-negative OPSCC, they have a significantly better prognosis with 60–80% reduced risk of death as compared to the HPV-negative

Table 11 Treatment outcome of HPV-positive and HPV-negative tumors in multiinstitutional trials

Study	Author (year)	N	Primary end point	Follow-up	HPV +ve vs −ve tumors
ECOG 2399	Fakhry et al. (2008)	96	Tumor progression	2 years	2-year survival (95% vs 62%)
RTOG 0129	Ang et al. (2010)	323	Overall survival	4.8 years	3-year survival (82.4% vs 57.1%)
			Progression-free survival		
TROG 02.02	Rischin (2010)	185	Overall survival	5 years	2-year survival (91% vs 74%)
			Failure-free survival		
DHANCA 6 and 7	Lassen (2011)	794	Overall survival	5 years	(62% vs 47%) conventional RT
			Disease-free survival		(52% vs 48%) accelerated RT
TAX 324	Posner (2011)	111	Disease-specific survival	5 years	5-year survival (82% vs 35%)
			Overall survival		

counterpart (Gildener-Leapman et al. 2014). Multiple multiinstitutional trials have shown better prognosis of HPV-positive OPSCCs (Table 11). Compared to matched staged HPV-negative tumors, patients with HPV-positive tumors have better overall survival (Ang et al. 2010), and while this is not completely understood, these could be attributed to several factors including the fact that HPV-positive tumors respond better to chemotherapy and radiotherapy (perhaps due to the presence of non-mutated tumor suppressor genes, TP53 and RB), have higher immunogenic response to viral-specific tumor antigens, have lower risk of developing secondary tumors (perhaps due to less field cancerization), are less likely to express biomarkers of poor prognosis such as the epidermal growth factor receptor (EGFR), and are found in younger patients with fewer comorbidities and good performance status (Westra et al. 2008; Adelstein et al. 2009; Hong et al. 2010). Based on the evidence of better prognosis of HPV-positive OPSCC, the American Joint Committee on Cancer (AJCC) has staged HPV-positive OPSCC as an entity separate from HPV-negative OPSCC in the most recent AJCC 8th Edition Cancer Staging System (Lydiatt et al. 2017).

Clinical Presentation

Clinically, HPV-positive OPSCC is seen in younger subjects with less exposure to tobacco and alcohol. White men with higher socioeconomic status are more commonly affected (2017). Increased lifetime number of oral and genital sexual partners, younger age at the time of first sexual intercourse, infrequent use of condoms, and history of previous sexually transmitted infection has found to be associated with HPV-induced OPSCC (Heck et al. 2010). Patients with HPV-positive OPSCC commonly present with small primary tumors with large cystic lymph nodes (Fakhry et al. 2008). Tonsils, followed by the base of tongue, are the most common sites for primary OPSCC tumors (2017). Patients presenting with HPV-negative OPSCC typically present with sore throat or difficulty swallowing (2017).

Symptoms vary as per the subsite of origin (Table 12). The base of tongue, tonsillar fossa, and pyriform sinus are rich in lymphatics, and cancers of these subsites commonly present with metastatic neck nodes as the initial sign. Any patient presenting with neck nodal metastatic squamous cell carcinoma (SCC) without any obviously visible primary lesion should be meticulously evaluated for a hidden lesion in these subsites. Cancers arising from the base of tongue (BOT) usually present late. Early symptoms of a sore throat, feeling of a lump in the throat, and slight discomfort on swallowing are non-specific and often ignored by the patient as well as by the primary care physician. In most cases, metastatic neck nodes draw attention to the primary lesion. Late symptoms include dysphagia, referred otalgia, change in quality of speech (hot potato voice), and hemoptysis. Early tonsillar cancers

Table 12 Common symptoms of oropharyngeal, hypopharyngeal, and laryngeal cancers

Symptoms of oropharyngeal cancers
Throat discomfort
Metastatic neck nodes (most commonly level II nodes)
Dysphagia
Odynophagia
Referred otalgia
Hot potato voice
Symptoms of hypopharyngeal cancers
Metastatic neck nodes (levels II–IV)
Dysphagia
Pain
Earache
Change in voice
Aspiration
Dyspnea
Symptoms of laryngeal cancers
Dyspnea
Hoarseness of voice
Metastatic cervical neck nodes (levels II and III)

remain hidden within the tonsil or the tonsillar bed and are rarely diagnosed at this stage, and metastatic level II neck nodes are the earliest presenting symptoms. Advanced tumors present with bleeding, pain, voice change, and trismus (due to masticatory muscle involvement).

Investigations

Carcinomas of the oropharynx, hypopharynx, and nasopharynx are notorious for their presentation with metastatic neck nodes without any obviously discernible primary lesion. In these circumstances, a fine needle aspiration biopsy (FNAB) from the clinically suspicious neck nodes helps in establishing the tissue diagnosis as well as identifying the putative site of the primary tumor. It is an effective, minimally invasive, and cost-effective diagnostic tool with negligible risk of complications such as tumor seeding along the needle tract, bleeding, infection, and fistula formation. FNAB usually yields representative cellular samples both for routine histological staining and immunohistochemistry (IHC). With an experienced histopathologist, FNAB achieves a diagnostic sensitivity of 83–97% and a specificity of 91–100% for metastatic lesions (Gourin and Johnson 2000; Layfield 2007). However, for large cystic nodes (commonly seen in HPV-positive cancers), the sensitivity of FNAB drops to 33–50% (Pisharodi 1997) due to high false-negative results. Ultrasound-guided FNAB is useful in this scenario to guide the needle to the wall of the node for obtaining cellular material. A p16 IHC, HPV DNA ISH, and Epstein-Barr-encoded RNA on ISH can help to localize the site of primary tumor.

The presence of HPV can be detected by HPV in situ hybridization which detects the presence of HPV genetic material in tissue sections of the tumor and could simultaneously detect several high-risk HPV genotypes including HPV-16 and HPV-18. In addition, the expression of p16 which increases in HPV-positive tumors is a surrogate marker and can be detected by immunohistochemistry which can be performed routinely in most pathology laboratories. HPV detection in tumor cells can also be undertaken by polymerase chain reaction (PCR) for detection of HPV DNA (or reverse transcription PCR for detection of HPV mRNA). HPV classification is made when the sample is positive for HPV ISH and p16 immunohistochemistry (Westra 2009; Robinson et al. 2010). The principles, merits, and demerits of each are outlined in Table 8.

Imaging for early oropharynx cancers is a diagnostic challenge as abundant lymphoid tissue fills the oropharynx which enhances on contrast administration. An additional challenge with CT is distortion of image quality due to dental artifact (Figs. 45 and 46). Tongue and swallowing movements can hamper the quality of MRI images; however, for better delineation of tumor from adjacent soft tissues, MRI remains the investigation of choice for oropharyngeal cancers (Figs. 47 and 48). Staging of oropharyngeal tumors is outlined in Table 13. Lymph node compartments are separated into levels and sublevels as shown in Fig. 49.

Treatment

The current preferred therapy for oropharyngeal cancer is radiation or concurrent chemoradiation (depending on the stage of disease), and while these could result in good patient outcomes, they nevertheless are often linked with worrying side effects, such as damage to the larynx and throat

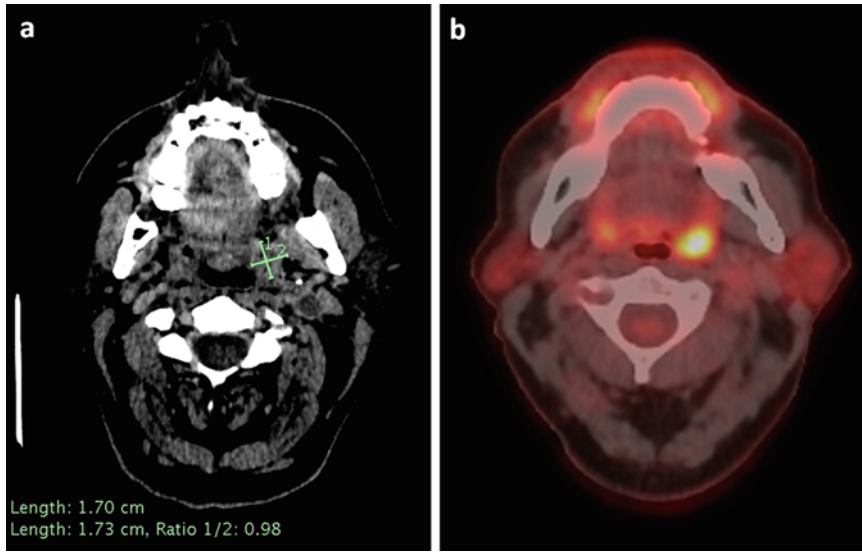

Fig. 45 T1N2b squamous cell carcinoma of the palatine tonsil. CT (**a**) shows a heterogeneously enhancing centrally necrotic mass within the superior aspect of the left palatine tonsil, measuring up to 17 mm consistent with a left tonsillar SCC. Multiple centrally necrotic/cystic left cervical lymph nodes were present including a predominantly cystic 32 mm left level II node. On PET/CT (**b**) there is intense asymmetric activity at the left palatine tonsil corresponding to the lesion seen on CT

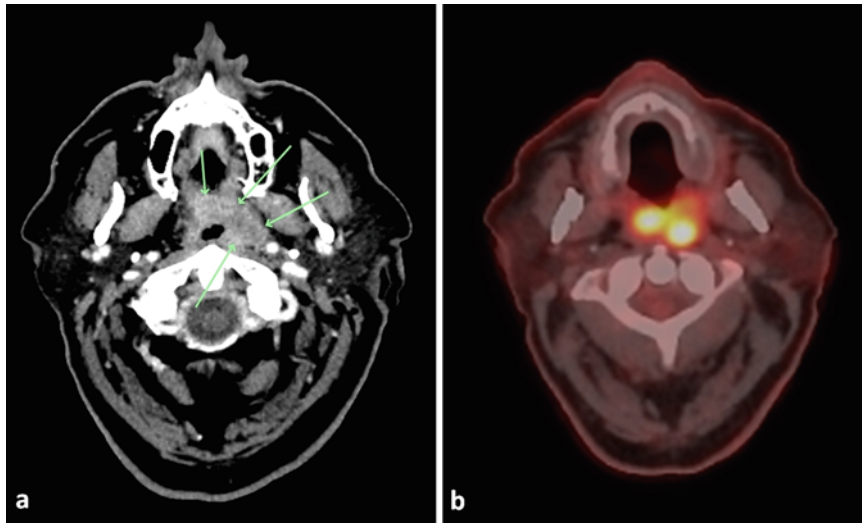

Fig. 46 Squamous cell carcinoma of the palatine tonsil. CT (**a**) shows an expansile enhancing mass lesion centered in the left palatine tonsil. The lesion has an unusual morphology, and it involves the entire left palatine tonsil and extends superiorly to the junction of the upper oropharynx with the lower nasopharynx. Anteriorly at the upper pole region, it crosses the midline and involves the posterior aspect of the soft palate and the uvula, and further inferiorly it involves the anterior tonsillar pillar and fills the glossotonsillar sulcus. It approximately measures 44 mm craniocaudal × 35 mm transverse oblique × 26 mm AP oblique. PET/CT (**b**) shows intense uptake centered on the left palatine tonsil with quite extensive involvement of the soft palate extending across the midline to the right side and superiorly to the junction of the oropharynx with the nasopharynx

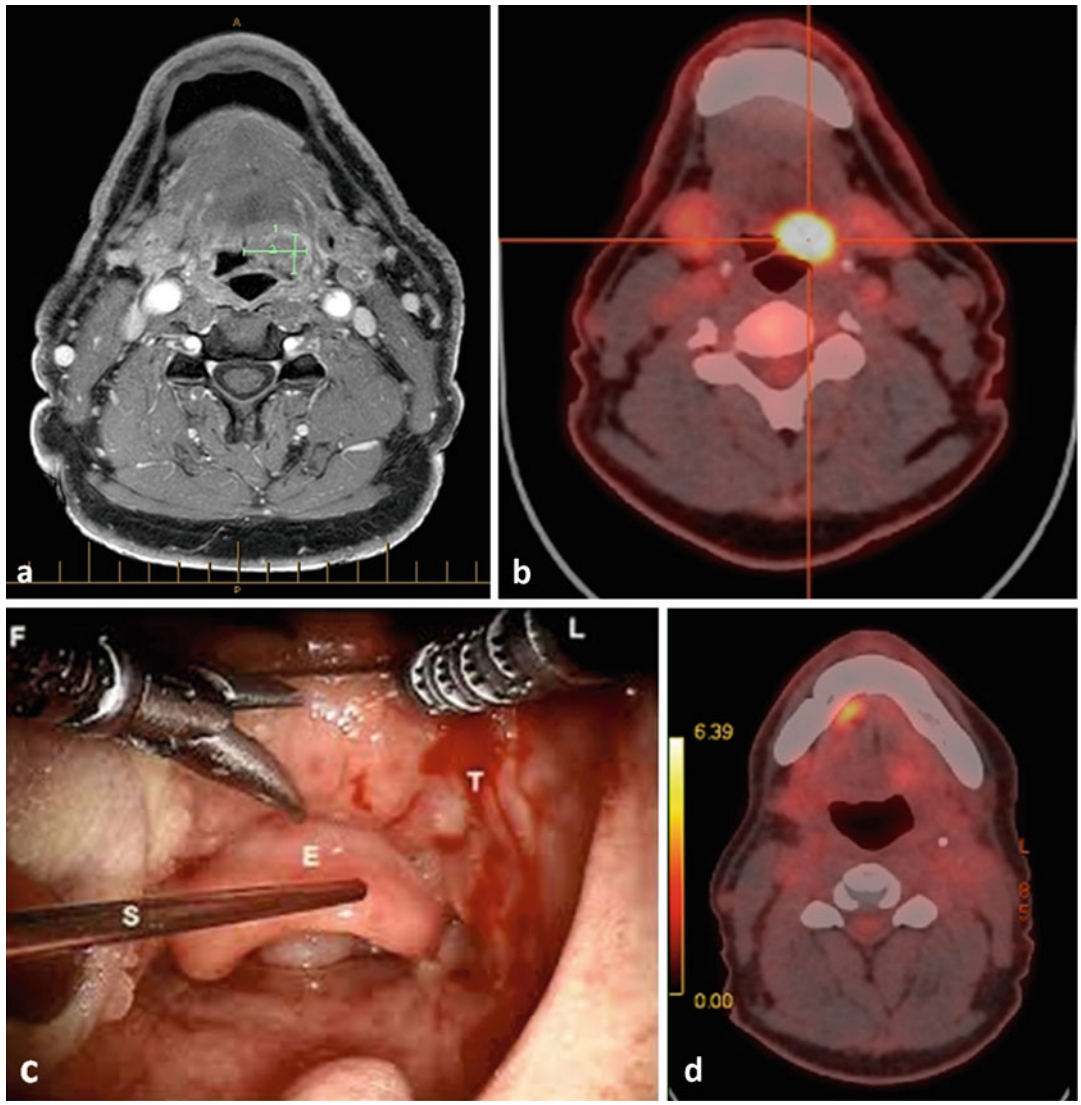

Fig. 47 Base of tongue squamous cell carcinoma. MRI (**a**) shows a well-defined, left-sided tongue base mass measuring 26 mm in its superoinferior dimension with a mediolateral width of 21 mm and a depth of 13 mm. The lesion fills the left vallecula and has a peripheral enhancing margin merging with the normal oropharyngeal and tongue base mucosa. There is no overt invasion of the remainder of the tongue base, the oral tongue, or the oropharynx. The tumor extends to the midline including the median glossoepiglottic fold. The tumor is of identical signal to lymphoid tissue. PET/CT before surgery (**b**). Patient received TORS (**c**), neck dissection, and postoperative radiation, with excellent functional outcomes and disease-free at 54 months posttreatment (**d**) (Images courtesy of Dr Chady Sader, Western ENT, Perth WA, Australia)

which could affect speech and swallowing, respectively.

Early Oropharyngeal Cancers

For early-stage oropharyngeal cancers (Fig. 50), the fundamental principle is to maximize the likelihood of cure with a single modality treatment – either surgery or radiation therapy (RT). The preferred treatment modality is RT in most patients as it comprehensively addresses both the primary site and the neck nodes and has excellent functional outcome. A major advantage of RT is

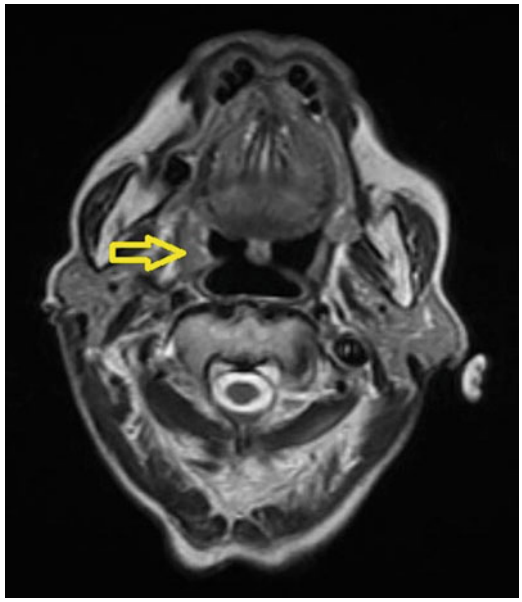

Fig. 48 Contrast-enhanced T1 MRI image showing thickening of the tonsillar fossa (arrow) suggestive of an early tumor

that it addresses the retropharyngeal nodes which carry a high chance of metastasis in oropharyngeal cancers and are not usually addressed in routine neck dissection. With improved radiation techniques such as intensity-modulated radiation therapy (IMRT), there has been significant improvement of function compared with conventional radiation treatment (Garden et al. 2007; Nutting et al. 2011). The major drawback of surgery is the associated morbidity and the high rate of occult neck metastasis which results in addition of adjuvant RT and its toxicities. However, proponents of surgery argue that the overall dose of radiation to the pharynx is less in the adjuvant setting compared to the definitive setting, thus reducing toxicities (Figs. 51 and 52). Minimally invasive surgery in the form of transoral laser surgery (TOLS) or transoral robotic surgery (TORS) is the treatment of choice in patients where it can be carried out with minimal functional morbidity and in appropriately selected salvage cases (Figs. 53 and 54).

Advanced Oropharyngeal Cancers

Concurrent chemoradiation is the preferred treatment modality for stage III and IV oropharyngeal cancers (Fig. 55). RT alone can be considered for low bulk stage III disease (T1, 2 N1). Primary surgery can also be considered for selected low-volume stage III cancers (T3 N0) (Hurtuk et al. 2012). If the margins of resection are negative with no pathological metastatic nodes or other adverse risk factors like perineural invasion (PNI) or lymphovascular spread (LVS), surgery alone may be adequate thus reducing the cost and treatment morbidity. On the contrary for other stage III diseases, patients require adjuvant radiation or even chemoradiation (if positive margins or extracapsular spread) resulting in significant morbidity. For stage IV cancers, concurrent chemoradiation is the treatment modality of choice. In general, it involves concomitant cisplatin chemotherapy with full-dose RT (70 Gy, 35#) to the primary site and the neck. Chemotherapy can be given either in three weekly or weekly doses.

HPV-Associated Oropharyngeal Cancers

HPV-associated oropharyngeal cancers have a relatively better prognosis as compared to HPV-negative counterparts. Selected HPV-positive patients (T1-3, N0-2a) treated by RT alone have low locoregional failure and distant metastasis (O'Sullivan et al. 2013). Based on these results, the concept of de-intensification of treatment in HPV-positive oropharyngeal cancers to reduce the treatment-related morbidities has been proposed (O'Sullivan et al. 2013). While this may be ideal, implementation has not been straightforward as clinical observation suggests that even within HPV-positive patients, there is a significant minority who still respond poorly to treatment and have a poor prognosis (Ang et al. 2010).

Currently there are no clinically relevant markers to distinguish these individuals, making the possibility of selecting patients who may benefit from treatment de-escalation rather challenging. Notwithstanding, based on features of these patients which include heavy smoking (>10 pack-years smoking) and advanced nodal disease (N2b and above), patients who match these criteria have been excluded from treatment de-escalation trials

Table 13 Staging of pharyngeal tumors. TNM clinical classification and staging of pharyngeal malignant tumors (Adapted from Brierley et al. 2017)

Primary tumor (T)	
p16-negative cancers of the oropharynx	
TX	Primary tumor cannot be assessed
T0	No evidence of primary tumor
T1	Tumor 2 cm or less in greatest dimension
T2	Tumor more than 2 cm but not more than 4 cm in greatest dimension
T3	Tumor more than 4 cm in greatest dimension or extension to lingual surface of epiglottis
T4a	Tumor invades any of the following: larynx[a], deep/extrinsic muscle of the tongue (genioglossus, hyoglossus, palatoglossus, and styloglossus), medial pterygoid, hard palate, or mandible
T4b	Tumor invades any of the following: lateral pterygoid muscle, pterygoid plates, lateral nasopharynx, skull base, or encases carotid artery
p16-positive cancers of the oropharynx	
TX	Primary tumor cannot be assessed
T0	No evidence of primary tumor
T1	Tumor 2 cm or less in greatest dimension
T2	Tumor more than 2 cm but not more than 4 cm in greatest dimension
T3	Tumor more than 4 cm in greatest dimension or extension to the lingual surface of the epiglottis
T4	Tumor invades any of the following: larynx[a], deep/extrinsic muscle of the tongue (genioglossus, hyoglossus, palatoglossus, and styloglossus), medial pterygoid, hard palate, mandible[a], lateral pterygoid muscle, pterygoid plates, lateral nasopharynx, skull base, or encases carotid artery
Hypopharynx	
TX	Primary tumor cannot be assessed
T0	No evidence of primary tumor
T1	Tumor limited to one subsite of the hypopharynx (see page 23) and/or 2 cm or less in greatest dimension
T2	Tumor invades more than one subsite of hypopharynx or an adjacent site or measures more than 2 cm but not more than 4 cm in greatest dimension, *without* fixation of the hemilarynx
T3	Tumor more than 4 cm in greatest dimension or with fixation of the hemilarynx or extension to the esophagus
T4a	Tumor invades any of the following: thyroid/cricoid cartilage, hyoid bone, thyroid gland, esophagus, and central compartment soft tissue[b]
T4b	Tumor invades prevertebral fascia, encases carotid artery, or invades mediastinal structures
Nasopharynx	
TX	Primary tumor cannot be assessed
T0	No evidence of primary tumor
T1	Tumor confined to the nasopharynx or extends to the oropharynx and/or the nasal cavity without parapharyngeal involvement
T2	Tumor with extension to parapharyngeal space and/or infiltration of the medial pterygoid, lateral pterygoid, and/or prevertebral muscles
T3	Tumor invades bony structures of skull base cervical vertebra, pterygoid structures, and/or paranasal sinuses
T4a	Tumor with intracranial extension and/or involvement of cranial nerves, hypopharynx, orbit, and parotid gland and/or infiltration beyond the lateral surface of the lateral pterygoid muscle
Regional lymph nodes (N)	
Oropharynx (p16-negative) and hypopharynx	
NX	Regional nodes cannot be assessed
N0	No regional lymph node metastasis
N1	Metastasis in a single ipsilateral lymph node, 3 cm or less in greatest dimension without extranodal extension
N2	Metastasis described as:
N2a	Metastasis in a single ipsilateral lymph node more than 3 cm but not more than 6 cm in greatest dimension without extranodal extension
N2b	Metastasis in multiple ipsilateral lymph nodes, none more than 6 cm in greatest dimension, without extranodal extension

(*continued*)

Table 13 (continued)

N2c	Metastasis in bilateral or contralateral lymph nodes, none more than 6 cm in greatest dimension, without extranodal extension		
N3a	Metastasis in a lymph node more than 6 cm in greatest dimension without extranodal extension		
N3b	Metastasis in a single or multiple lymph nodes with clinical extranodal extension[c]		
Oropharynx (p-16 positive)			
NX	Regional nodes cannot be assessed		
N0	No regional lymph node metastasis		
N1	Unilateral metastasis, in lymph node(s), all 6 cm or less in greatest dimension		
N2	Contralateral or bilateral metastasis in lymph node(s), all 6 cm or less in greatest dimension		
N3	Metastasis in lymph node(s) greater than 6 cm in dimension		
Nasopharynx			
NX	Regional nodes cannot be assessed		
N0	No regional lymph node metastasis		
N1	Unilateral metastasis, in cervical lymph node(s), and/or unilateral or bilateral metastasis in retropharyngeal lymph nodes, 6 cm or less in greatest dimension, above the caudal border of the cricoid cartilage		
N2	Bilateral metastasis in cervical lymph node(s), 6 cm or less in greatest dimension, above the caudal border of the cricoid cartilage		
N3	Metastasis in cervical lymph node(s) greater than 6 cm in dimension and/or extension below the caudal border of the cricoid cartilage		
Distant metastasis (M)			
M0	No distant metastasis		
M1	Distant metastasis		
Staging			
Stage	**TNM classification**		
Oropharynx (p16-negative) and hypopharynx			
0	Tis	N0	M0
I	T1	N0	M0
II	T2	N0	M0
III	T3	N0	M0
	T1, T2, T3	N1	M0
IVA	T1, T2, T3	N2	M0
	T4a	N0, N1, N2	M0
IVB	T4b	Any N	M0
	Any T	N3	M0
IVC	Any T	Any N	M1
Oropharynx (p-16 positive)			
0	Tis	N0	M0
I	T1, T2	N0, N1	M0
II	T1, T2	N2	M0
	T3	N0, N1, N2	M0
III	T1, T2, T3	N3	M0
	T4	Any N	M0
IV	Any T	Any N	M1
Nasopharynx			
0	Tis	N0	M0
I	T1	N0	M0
II	T1	N1	M0
	T2	N0, N1	M0

(*continued*)

Table 13 (continued)

III	T1, T2	N2	M0
	T3	N0, N1, N2	M0
IVA	T4	N0, N1, N2	M0
	Any T	N3	M0
IVB	Any T	Any N	M1

[a]Mucosal extension to the lingual surface of the epiglottis from primary tumors of the base of the tongue and vallecula does not constitute invasion of the larynx

[b]Central compartment soft tissue includes prelaryngeal strap muscles and subcutaneous fat

[c]The presence of skin involvement or soft tissue invasion with deep fixation/tethering to underlying muscle or adjacent structures or clinical signs of nerve involvement is classified as clinical extranodal extension. Midline nodes are considered ipsilateral nodes

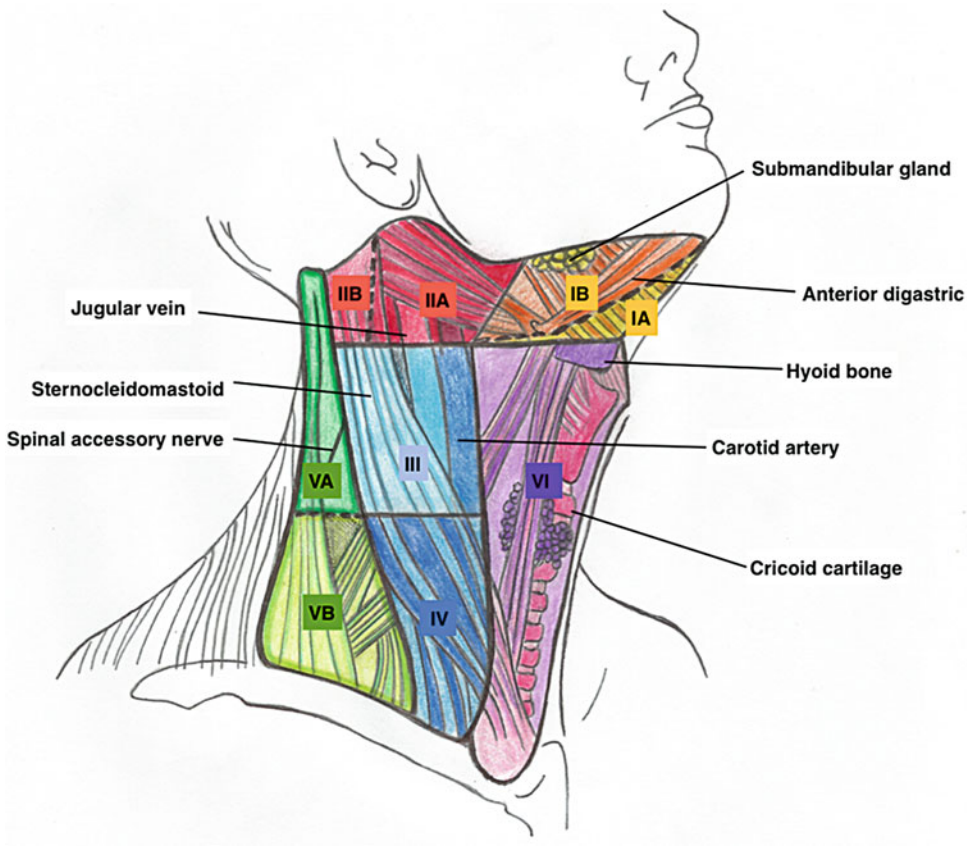

Fig. 49 Lymph node compartments separated into levels and sublevels. The level I node compartment includes the submental and submandibular nodes, above the hyoid bone and anterior to the posterior edge of the submandibular gland. The level II, III, and IV nodes are arrayed along the jugular veins on each side, bordered anteromedially by level VI and laterally by the posterior border of the sternocleidomastoid muscle. The level III nodes are bounded superiorly by the level of the hyoid bone and inferiorly by the cricoid cartilage; levels II and IV are above and below level III, respectively. Levels I, II, and V can be further subdivided as noted IA, IB, IIA, IIB, VA, and VB. The level V nodes are in the posterior triangle, lateral to the lateral edge of the sternocleidomastoid muscle. Level VI contains the thyroid gland, and the adjacent nodes bordered superiorly by the hyoid bone, inferiorly by the innominate (brachiocephalic) artery, and laterally on each side by the carotid sheaths. The inferior extent of level VI is defined as the suprasternal notch. Many authors also include the pretracheal and paratracheal superior mediastinal lymph nodes above the level of the innominate artery (sometimes referred to as level VII) in central neck dissection

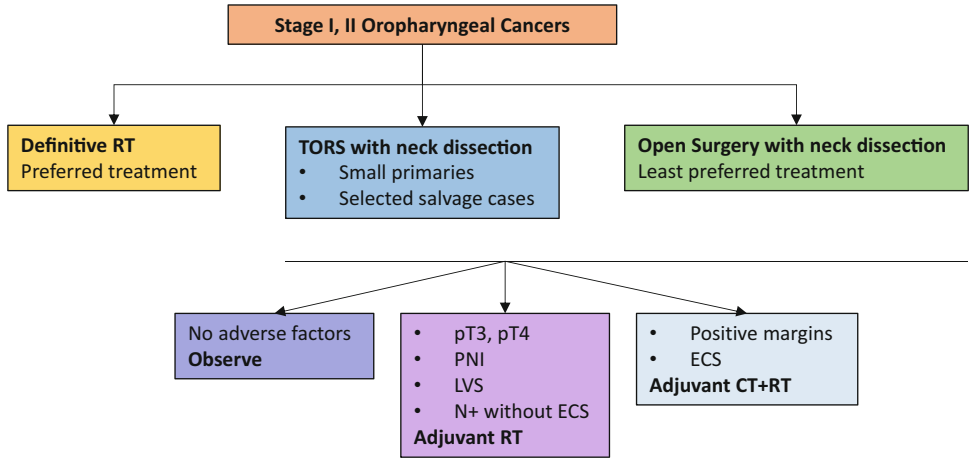

Fig. 50 Treatment algorithm of early oropharyngeal cancers

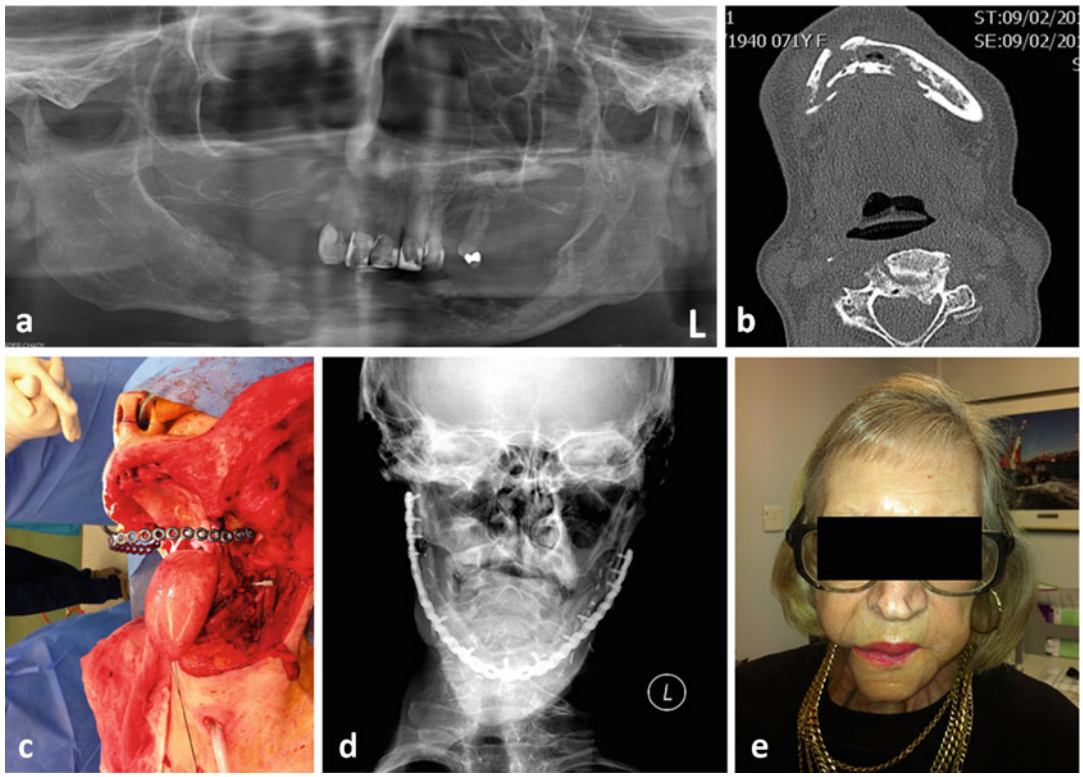

Fig. 51 Extensive osteoradionecrosis in a 71-year-old female post chemoradiation for oropharyngeal squamous cell carcinoma (**a** and **b**). Significant symptoms of pain, trismus, and an orocutaneous fistula were present. The patient underwent oromandibular resection and reconstruction with a free fibula flap (**c** + **d**). The patient had significant functional and quality of life improvement (**e**) (Images courtesy of Dr Chady Sader, Western ENT, Perth WA, Australia)

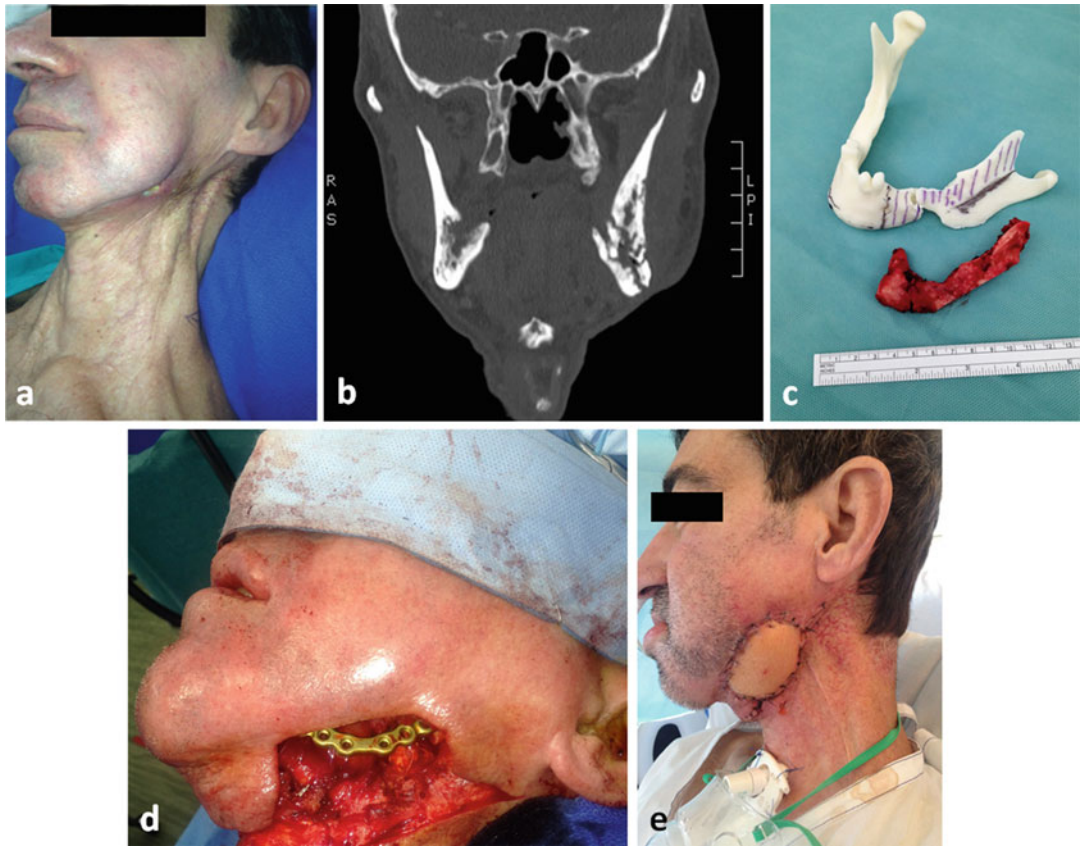

Fig. 52 Clinical (**a**) and CT radiological (**b**) appearance of osteoradionecrosis with a pathological mandibular fracture and orocutaneous fistula in a 50-year-old male who had previously undergone neck dissection and radiation for a left tonsillar squamous cell carcinoma. The 3D computer-generated model of the mandible (**c**) aided the free tissue reconstruction of the jaw (**d**). The skin paddle of the pedicle was used to reconstruct the cutaneous defect of the neck (**e**) (Images courtesy of Dr Chady Sader, Western ENT, Perth WA, Australia)

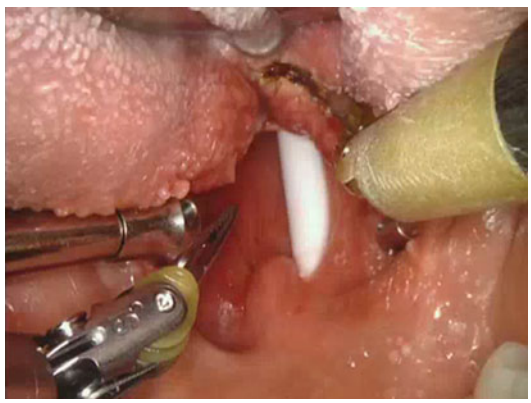

Fig. 53 Oropharyngeal cancer removed with transoral robotic surgery (TORS) (Image courtesy of Dr Chady Sader, Western ENT, Perth WA, Australia)

(Ang et al. 2010; Granata et al. 2012). Patients whose tumors have evident tumor-infiltrating lymphocytes have superior survival suggesting that the immune infiltrate could identify the subset of HPV-positive patients who have poor prognosis (Ward et al. 2014). While such biomarkers could impact on patient selection and have the potential to change clinical practice, the evaluation of tumor-infiltrating lymphocytes is still at an early stage and not yet in mainstream clinical use. Trials for de-escalation of treatment in HPV-positive OPSCC are underway (ADEPT, ECOG 3311, PATHOS).

The role of HPV vaccines in preventing oropharyngeal cancers is an area of active discussion. As the majority of oropharyngeal cancers are caused

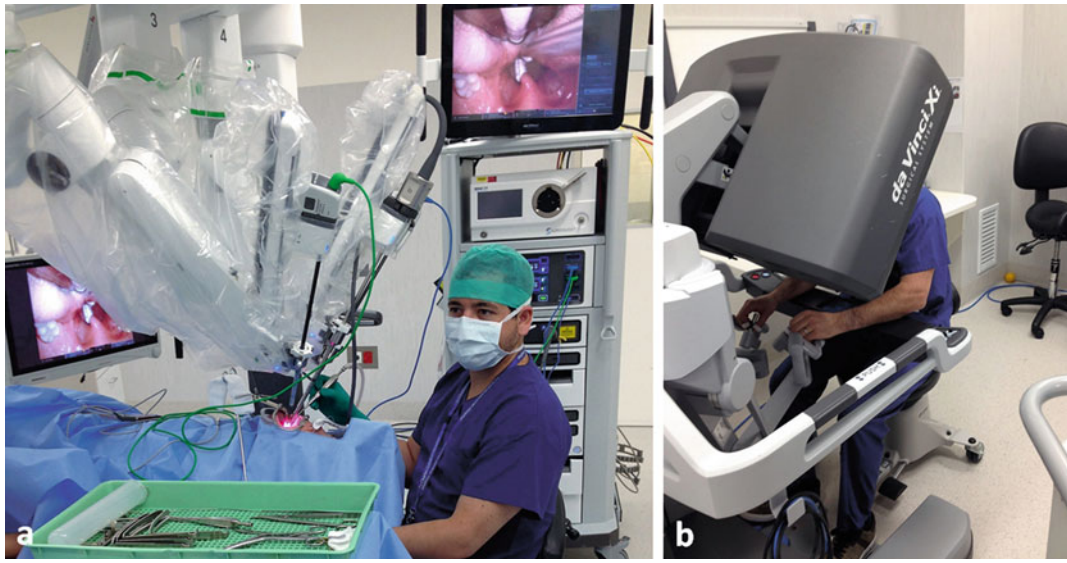

Fig. 54 TORS setup showing the surgical assistant at the bedside (**a**) ensuring patient safety, facilitating any adjustments to the robotic arms, communicating with the surgeon, and ensuring smoke evacuation and suction of blood/secretions. The surgeon is seated in the surgeon's console (**b**) and operating the robot (Images courtesy of Dr Chady Sader, Western ENT, Perth WA, Australia)

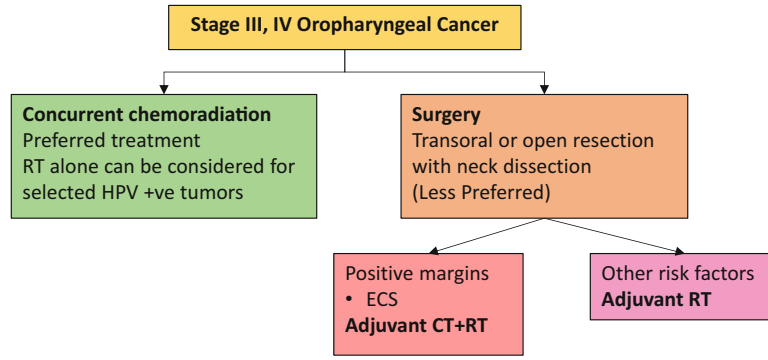

Fig. 55 Treatment algorithm of advanced oropharyngeal cancers

primarily by HPV-16, a particularly dangerous strain of the virus, it is conceivable that the two vaccines that protect against HPV-16 that are currently approved to prevent cervical cancer could also do the same for oropharyngeal cancer. The quadrivalent HPV vaccine types 6, 11, 16, and 18 (Gardasil/Gardisil/Silgard) are effective in preventing anal, cervical, vaginal, and vulvar precancers and cancers, while the bivalent HPV vaccine types 16 and 18 (Cervarix) have been demonstrated to be effective in cervical precancers and cancers (Garland and Smith 2010; Lu et al. 2011). More recently 9-valent HPV vaccine types 6, 11, 16, 18, 31, 33, 45, 52, and 58 (Gardasil 9) have been approved by the US FDA for routine vaccination of adolescents (girls and boys) at age 11 or 12 years and can be started as early as 9 years of age. While it is theoretically possible, studies to determine if HPV vaccine will prevent oropharyngeal cancers are hampered by the need for invasive sampling deep in the tonsillar area where the cancer arises, and therefore, the vaccine is currently not indicated for the prevention of head and neck cancers, but it is likely that population-based observation studies in vaccinated cohorts will reveal a positive benefit in the future (Scudellari 2013).

Hypopharyngeal Cancer

Epidemiology, Etiology, and Pathology

Although 95% of hypopharyngeal cancers are SCCs, rarely lymphomas, sarcomas, and adenocarcinomas can arise from the hypopharynx. While tobacco smoking is the primary etiologic factor of laryngeal cancers, hypopharyngeal cancers are associated with alcohol abuse (Spitz 1994). Ethyl alcohol during metabolism is first converted into acetaldehyde (a carcinogenic by-product) which is further metabolized into acetate (excretory end product) by an enzyme acetaldehyde dehydrogenase. Inability to convert acetaldehyde to acetate due to mutations in acetaldehyde dehydrogenase gene results in accumulation of carcinogenic metabolic intermediate acetaldehyde. The carcinogenic effect of acetaldehyde is exerted by generation of free radicals, direct DNA damage, and upregulation of enzymes of the cytochrome P450 system which results in activation of certain procarcinogens to carcinogens. Additionally, alcohol acts as a solvent for tobacco increasing the cellular permeability of tobacco carcinogens through the mucosa of the upper aerodigestive tract. Alcohol also impairs immunity and causes nutritional deficiencies thus lowering the resistance to cancer. Alcohol is believed to act synergistically to tobacco in the etiology of head and neck cancers.

Dietary risk factors have also been implicated as a risk factor for hypopharyngeal cancers. Plummer-Vinson syndrome is characterized by iron deficiency anemia, hypopharyngeal webs, koilonychias, weight loss, and dysphagia. This syndrome is accompanied by an increased risk of postcricoid SCC. Treatment of iron deficiency anemia has been found to decrease the risk of malignancy.

Clinical Presentation

Pyriform fossa and postcricoid tumors of the hypopharynx initially present with non-specific throat symptoms and metastatic cervical nodes. However, advanced tumors present with dysphagia, hoarseness of voice (due to laryngeal involvement), symptoms of aspiration, pain, earache (referred otalgia), and dyspnea.

Endoscopic evaluation of the upper aerodigestive tract is undertaken to map the extent of the disease as well as to take a biopsy from the primary lesion. Disease mapping includes assessment of the adequacy of the airway, evaluation of the mucosal extent of disease, and mobility of the vocal cords and arytenoids and signs of aspiration. All cases of hypopharyngeal cancers should undergo a rigid esophagoscopy to delineate the lower extent of tumor and for evaluation of a potential second primary lesion in the esophagus.

Investigations

Cross-sectional imaging with CT and MRI plays an indispensable complementary role to endoscopy in the pre-therapeutic work-up of hypopharyngeal cancer and is very valuable for the detection of tumor recurrence after surgery or radiation treatment as well. CT is the preferred imaging method for staging of hypopharyngeal cancer. The primary tumor typically appears as a solid soft tissue nodule or region of superficial thickening with increased enhancement. When it extends beyond the confines of the pharynx, the surrounding fat planes are obliterated. Careful assessment of cervical lymph nodes is essential as up to 75% of patients with hypopharyngeal SCCs have nodal metastases at the time of diagnosis (Fig. 56). MRI has the ability to be superior to CT in local staging and assessing perineural spread; however, relatively long acquisition times and degradation by motion artifact are sometimes challenging. Both CT and MRI are routinely used for detection of subtle cartilage invasion (Fig. 57), but there is still controversy about which modality can most accurately detect cartilage invasion, and both modalities have shortcomings (2003). As is the case with other metabolically active tumors, FDG PET/CT has an increasing role in the diagnosis, staging, and follow-up of hypopharyngeal tumors (Fig. 58). Staging of hypopharyngeal tumors is outlined in Table 13.

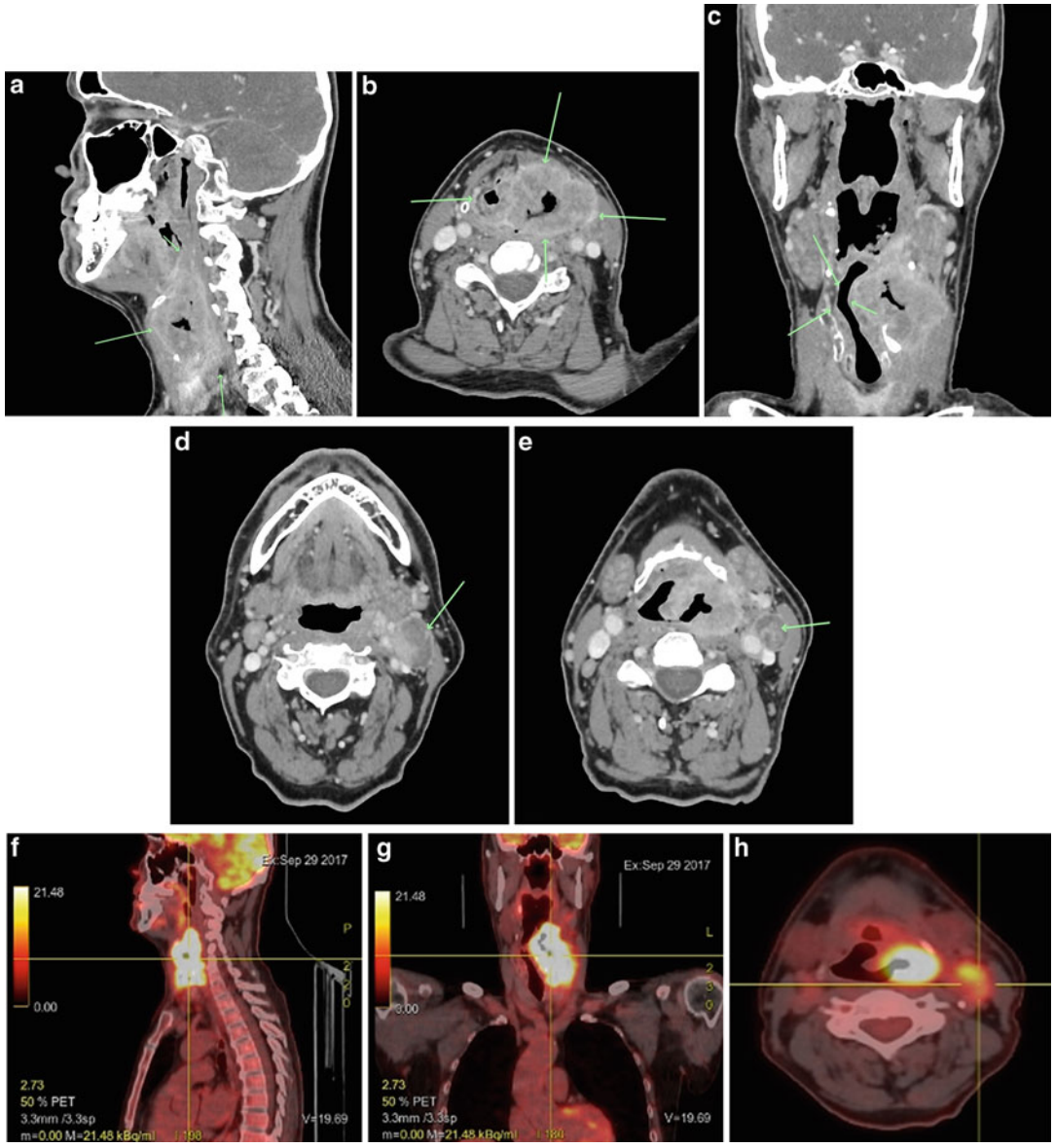

Fig. 56 Hypopharyngeal carcinoma. Post-contrast CT sagittal (**a**), axial (**b**), and coronal (**c**) views show an extremely large heterogeneous and partially necrotic left-sided mass lesion (arrows). This measures approximately 10 cm craniocaudal × 6.8 cm transverse × 4.5 cm AP. Cranially, the lesion is centered in the hypopharynx and aryepiglottic fold on the left extending anterior to involve the pre-epiglottic space but spreads into the left paralaryngeal space markedly narrowing and displacing the supraglottic airway to the right. It crosses posteriorly into the right side of the hypopharynx and involves both left and right false cords. It spreads laterally to erode the posterior aspect of the left thyroid cartilage and extends into the extra-laryngeal space where it infiltrates the undersurface of the strap muscles and extends inferiorly to infiltrate the superior aspect of the left lobe of the thyroid. There is associated extensive left-sided necrotic and obviously metastatic lymphadenopathy within the left IIA, IIIA, and IVA levels (**d** + **e**). PET/CT(F-18 FDG) fusion sagittal (**f**), coronal (**g**), and axial (**h**) views. There is a large invasive left neck mass centered on the hypopharynx which is intensely FDG-avid and appears to cross the midline to the right hypopharynx. There are enlarged left level IIa and III lymph nodes with central photopenia and peripheral intense FDG uptake, consistent with necrotic nodes

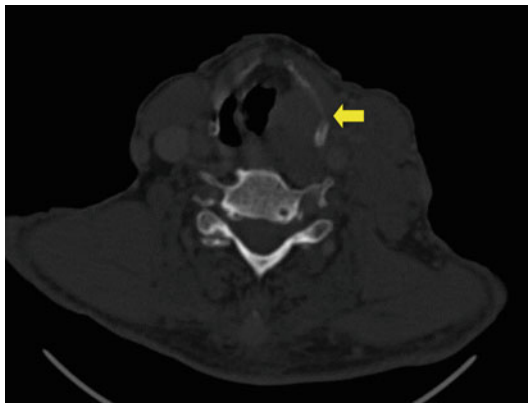

Fig. 57 Contrast-enhanced CT neck (bone window) showing a pyriform fossa tumor showing erosion of the inner lamina of the thyroid cartilage without exolaryngeal spread (arrow)

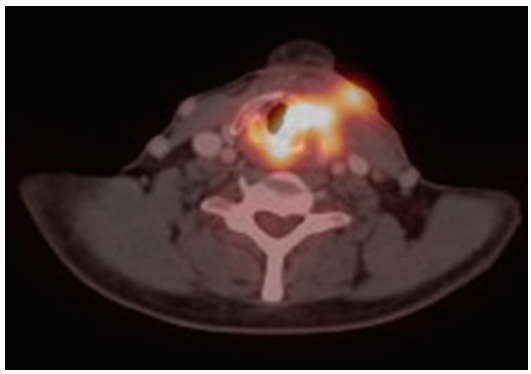

Fig. 58 PET/CT fusion axial image showing an enhancing lesion involving hypopharynx with gross exolaryngeal extension

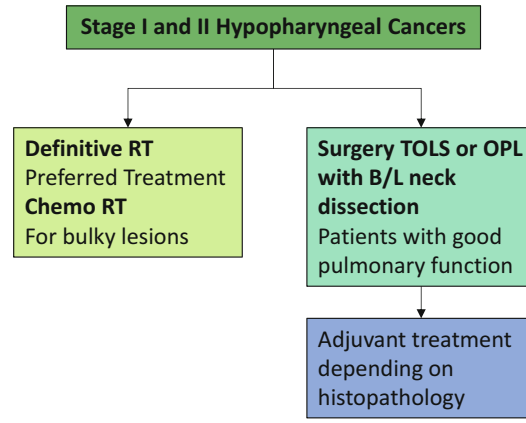

Fig. 59 Treatment algorithm for early hypopharyngeal cancer

Treatment

Early Hypopharyngeal Cancer

Radiotherapy is the preferred treatment modality for early hypopharyngeal cancers as surgery in this region results in high odds of aspiration (Fig. 59). Moreover, due to the high propensity of occult nodal metastasis, surgery frequently upstages the neck resulting in administration of multimodality treatment. Surgical procedures, if planned, are either TOLS or open partial laryngopharyngectomy. The morbidity of TOLS is significantly less than open surgery including the avoidance of a temporary tracheostomy and a shorter hospital stay. However, the neck must be addressed in all patients. If TOLS is the primary treatment modality, neck dissection can be carried out either simultaneously or after an interval of 7–10 days. The advantages of interval neck dissection include a second look into the operated cavity under general anesthesia and for margin revision if required based on the final histopathology, avoid acute edema of the larynx which can occur if bilateral neck dissection is undertaken simultaneously with the primary resection, and address transit lymphatics (not a universally accepted concept). The major drawback of interval neck dissection is the need for a second surgery under general anesthesia.

Advanced Hypopharyngeal Cancers

In advanced lesions which require total laryngectomy with pharyngectomy, induction chemotherapy can be utilized to facilitate organ preservation (Fig. 60). An EORTC phase III RCT has shown that in the group randomized to the nonsurgical arm (induction chemotherapy with cisplatin and fluorouracil followed by radiation in responders), more than half of patients who survived preserved their larynx (Lefebvre et al. 1996, 2012). There was no difference in 5- and 10-year overall or progression-free survival between the surgical (surgery followed by adjuvant treatment) and nonsurgical arms (Lefebvre et al. 1996, 2012).

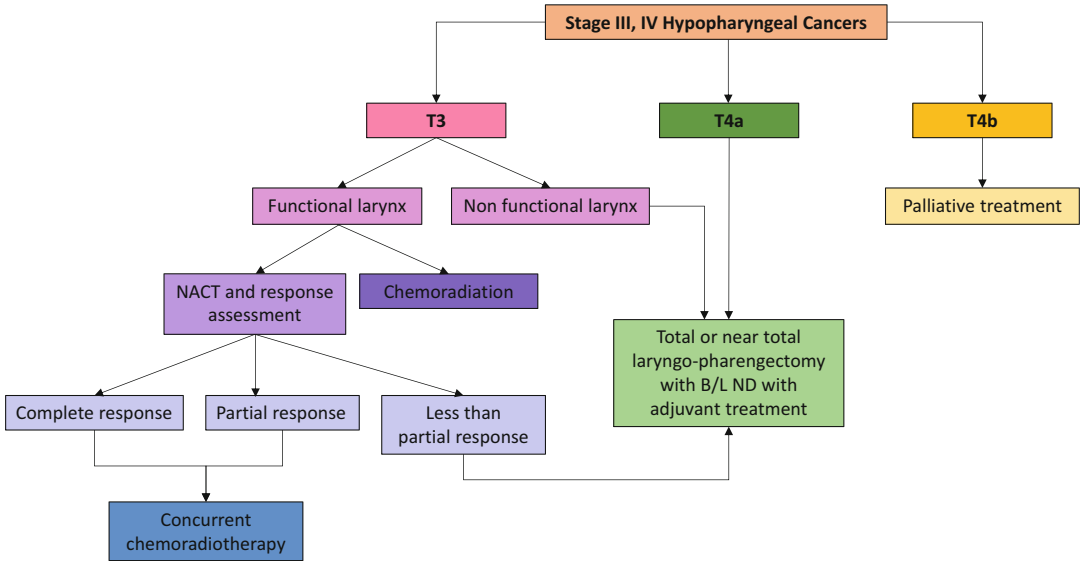

Fig. 60 Treatment algorithm for advanced hypopharyngeal cancers

To further facilitate organ preservation with induction chemotherapy, docetaxel has been used in combination with cisplatin and fluorouracil (5FU) in a triple therapy regimen commonly known as TPF (Taxotere, Platinol, Fluorouracil). Although overall survival was the same in the TPF and PF (cisplatin/5FU) arms, a higher tumor response rate (80% vs 59%) and laryngeal preservation rate (70% vs 57%) was seen in the TPF arm compared to PF arm (Pointreau et al. 2009).

Concurrent chemoradiation remains a treatment option for advanced hypopharyngeal cancers, although there is no conclusive evidence for its role in exclusive hypopharyngeal cancer patients. Data is extrapolated from studies on laryngeal and general head and neck cancers. A meta-analysis of 17,346 patients of head and neck cancers demonstrated an absolute benefit of 6.5% and 2.4% in overall survival with concurrent chemoradiotherapy and induction chemotherapy with radiotherapy, respectively. The benefit of concurrent chemotherapy was predominantly seen in younger patients with no benefit seen in patients >70 years of age (Pignon et al. 2009).

In patients who are not candidates for concurrent chemotherapy (poor performance status, renal insufficiency, or sensorineural hearing loss), hyper-fractioned radiation can be considered. Similar to concurrent chemotherapy, no benefit of hyper-fractioned radiation has been demonstrated in patients >70 years old (Baujat et al. 2010). Alternatively, biological targeting agents can be used in patients not fit for concurrent chemotherapy. In a phase III RCT of advanced head and neck cancer patients comparing radiation alone with radiation plus weekly cetuximab, a 10% overall survival benefit was found in patients treated with concurrent cetuximab (Bonner et al. 2006). Cisplatin potentiates radiation-induced toxicities and causes its own toxicities limiting its doses and thus efficacy, whereas cetuximab on the other hand does not enhance radiation-induced toxicities and thus is better tolerated than concurrent cisplatin.

Advanced hypopharyngeal cancers with nonfunctional larynx or extra-laryngeal spread are candidates for total laryngectomy with partial or circumferential pharyngectomy with appropriate reconstruction followed by adjuvant treatment depending on final histopathology. Patients with positive resection margins or extracapsular nodal spread receive adjuvant chemoradiation, while others receive adjuvant radiation alone.

Laryngeal Cancer

Epidemiology, Etiology, and Pathology

Laryngeal cancers are primarily squamous cell carcinomas with minor salivary gland cancers, sarcomas, neuroendocrine tumors, and hematolymphoid tumors forming a minority of the cases.

Tobacco and alcohol are the two major risk factors of laryngopharyngeal cancers, with tobacco smoking representing the primary etiologic factor for laryngeal cancers. Tobacco is consumed in the smoked and the smokeless form. Tobacco smoke contains about 60 carcinogens of which polycyclic aromatic hydrocarbons constitute the main carcinogen followed by aromatic amines. Smokeless tobacco contains about 16 carcinogens, nitrosamines being the major constituent. Metabolism of tobacco products results in the formation of electrophilic intermediates which bind to normal DNA resulting in the formation of DNA adducts. These adducts are either repaired or undergo apoptosis. Persistence of miscoding leads to mutation of crucial genes regulating the cell cycle (e.g., *RAS*, *MYC*, *p53*, *p16*, *RB*) resulting in carcinogenesis.

Clinical Presentation

Laryngeal cancers as opposed to pharyngeal cancers present relatively early due to symptoms related to airway obstruction and voice change. Supraglottic cancers present initially with neck nodes and dyspnea. Hoarseness of voice appears relatively late. Glottis cancers on the other hand present at early stage with hoarseness of voice. Due to the paucity of lymphatics in the glottic region, neck nodes appear late when the tumor has spread to the adjacent subsites of supraglottis or the pyriform sinus.

Investigations

The pre-epiglottic space is best evaluated in axial and sagittal images (Figs. 61, 62, and 63). The sensitivities of CT and MRI are 100%, with specificity for CT being 93% and MRI being 84–90% (Becker 1998). Radiological invasion of the paraglottic space is best seen in axial and coronal sections (Figs. 64 and 65). The sensitivities for CT and MRI are 93% and 97%, respectively,

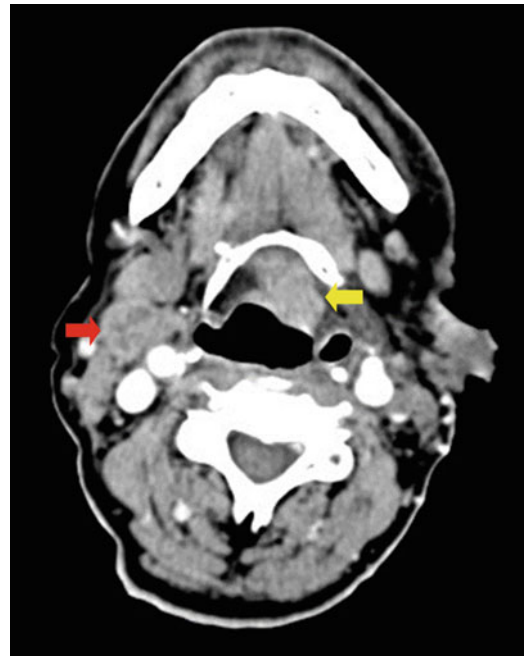

Fig. 61 Contrast-enhanced CT neck axial image showing tumor involvement of the pre-epiglottic space (yellow arrow) and necrotic level II lymph node (red arrow)

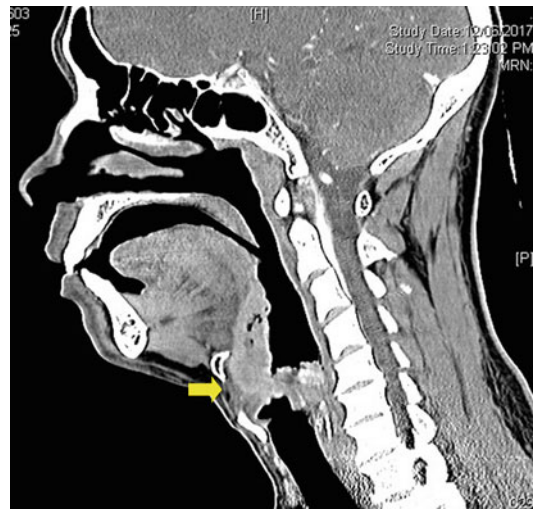

Fig. 62 Contrast-enhanced CT neck sagittal image showing a base of tongue tumor infiltrating into the pre-epiglottic space (yellow arrow)

while the specificity varies between 50% and 76%. Reduced specificity is due to disease overestimation because of peritumoral inflammation (Becker 1998). Overall, contrast-enhanced CT is

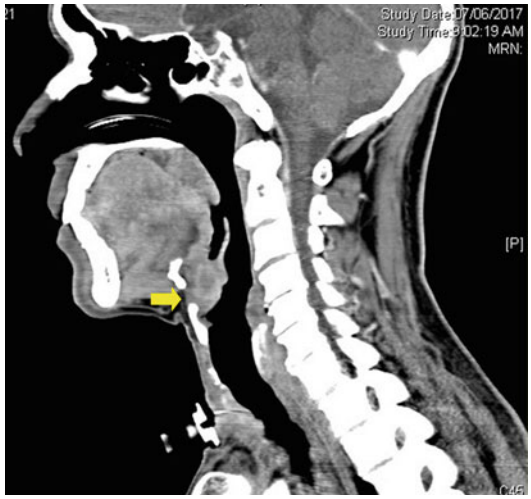

Fig. 63 Contrast-enhanced CT neck sagittal image showing a supraglottic tumor almost completely filling the pre-epiglottic space (yellow arrow)

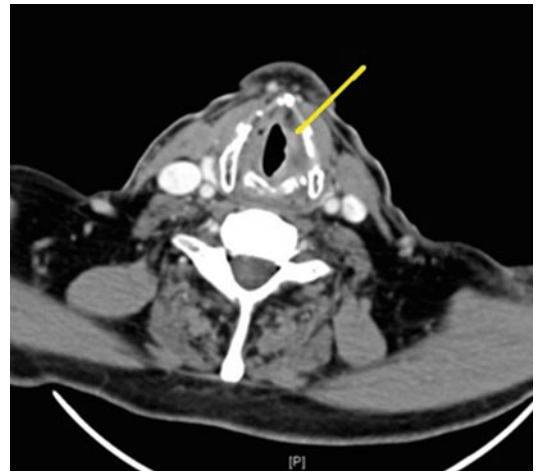

Fig. 65 Contrast-enhanced CT showing a glottic tumor involving the paraglottic space (yellow line)

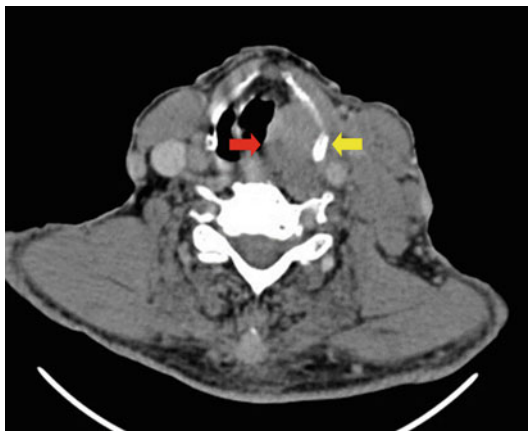

Fig. 64 Contrast-enhanced CT neck (soft tissue window) showing a pyriform fossa tumor with paraglottic extension (red arrow), erosion of the inner lamina of the thyroid cartilage without exolaryngeal spread (yellow arrow)

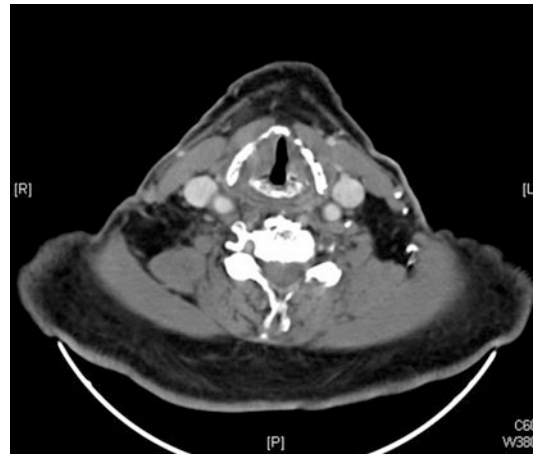

Fig. 66 Contrast-enhanced CT neck showing a laryngeal tumor with sclerosis of the thyroid cartilage indicating early cartilage invasion

the investigation of choice for laryngeal cancers (Fig. 66) with MRI reserved for cases with doubtful erosion on CT and in patients with allergy to iodinated contrast or compromised renal function. Videostroboscopy helps determine the location and size of a tumor, as well as how the tumor has affected the function of the larynx and hypopharynx. Histopathology shows squamous differentiation and invasion on biopsy. Cartilage invasion and extra-laryngeal spread are major determinants in upstaging the disease and management of laryngeal and hypopharyngeal cancers. Radiologically, cartilage invasion can be divided into three stages (Becker et al. 1997): (1) sclerosis, (2) erosion/lysis, and (3) extra-laryngeal tumor spread.

Sclerosis histologically corresponds to early perichondral involvement or microscopic intra-cartilaginous spread. CT is sensitive in detecting sclerosis but specificity varies between cartilages

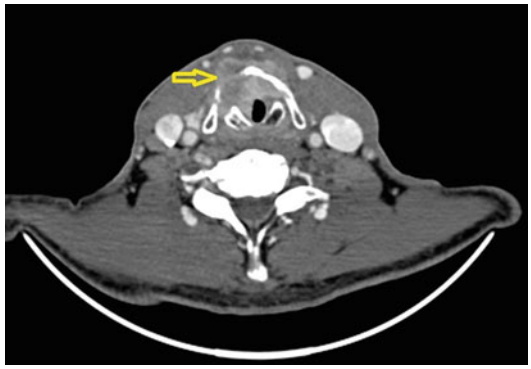

Fig. 67 Contrast-enhanced CT neck showing a supraglottic tumor with cartilage erosion and exolaryngeal spread (yellow arrow)

being lowest for thyroid cartilage (40%) and higher for cricoid (76%) and arytenoid cartilages (79%). Erosion or lysis corresponds to osteolysis without through and through cartilage disruption, with/without new bone formation. Contrast-enhanced CT has a high specificity for erosion detection (93%), but the sensitivity is poor (Fig. 67) (Becker et al. 1997). Extension of the tumor outside the laryngeal framework is termed as extra-laryngeal spread. Similarly, for extra-laryngeal spread multi-slice CT (MSCT) has high specificity (95%) with a poor sensitivity (Becker et al. 1997). MRI has higher sensitivity (89–95%) but lower specificity (74–84%) as compared to CT in detecting cartilage invasion. The negative predictive value of MRI is very high (94–96%) (Mukherji and Bradford 2006). Tumor infiltration of the marrow is best identified in T1 contrast images with fat suppression. Staging of laryngeal tumors is outlined in Table 14.

Treatment

T1 Glottic Cancers

The primary goal of treatment is to maximize cure and minimize treatment-related morbidity. T1a glottic cancers can be treated either by definitive RT or transoral laser surgery (TOLS) (Table 15) (Fig. 68). Both treatment modalities have similar locoregional control and disease-specific survival (Khan et al. 2012; Canis et al. 2015). Although the oncologic outcomes are comparable, larynx preservation is higher in patients treated with TOLS (100%) compared to those treated with definitive RT (93%) (Remmelts et al. 2013).

No prospective study has been performed comparing the oncologic and voice outcomes of TOLS versus definitive RT for T1a glottic cancers. Available data from multiple retrospective series have not found any significant difference in oncologic or voice outcomes between the two treatment modalities although larynx preservation has been found to be better in TOLS patients. In a meta-analysis based on over 7600 patients, there was no difference in local control or laryngectomy-free survival between TOLS and RT (Higgins et al. 2009). Although there was a trend toward improved overall survival in patients treated with TOLS, and improved voice outcome in definitive RT patients, the difference did not reach statistical significance (Higgins et al. 2009). Another meta-analysis of 1729 patients comparing the oncologic and functional outcomes of TOLS and RT found no difference in local control, overall survival, disease-specific survival, or posttreatment voice quality between the two groups; however, larynx preservation was significantly higher in the TOLS group compared to the RT group (Abdurehim et al. 2012). Due to the lack of prospective data, the treatment modality for T1 glottic cancers should be individualized. Young patients with mid-cord lesions and a good endoscopic exposure are preferably treated with TOLS. Patients with lesions involving anterior commissure or involving both cords and patients who are voice professionals are preferably treated with definitive RT. Pros and cons of each treatment option should be discussed with the patient before choosing a treatment modality.

T2 Glottic Cancers

Similar to T1 glottic cancers, the treatment of T2 glottic cancers with mobile cords is TOLS or definitive RT (Fig. 69). The treatment should be individualized depending on institutional expertise and patient preference. Tumors with restricted cord mobility indicate infiltrative disease which responds poorly to RT alone. These patients are preferably treated with chemoradiation. TOLS has a limited role in these lesions as resection is

Table 14 Staging of laryngeal tumors. TNM clinical classification and staging of laryngeal malignant tumors (Adapted from Brierley et al. 2017)

Primary tumor (T)	
Supraglottis	
TX	Primary tumor cannot be assessed
T0	No evidence of primary tumor
Tis	Carcinoma in situ
T1	Tumor limited to one subsite of supraglottis with normal vocal cord mobility
T2	Tumor invades mucosa of more than one adjacent subsite of supraglottis or glottis or region outside the supraglottis (e.g., mucosa of base of the tongue, vallecula, medial wall of the piriform sinus) without fixation of the larynx
T3	Tumor limited to the larynx with vocal cord fixation and/or invades any of the following: postcricoid area, pre-epiglottic space, paraglottic space, and/or inner cortex of the thyroid cartilage
T4a	Tumor invades through the thyroid cartilage and/or invades tissues beyond the larynx, e.g., trachea, soft tissues of the neck including deep/extrinsic muscle of the tongue (genioglossus, hyoglossus, palatoglossus, and styloglossus), strap muscles, thyroid, or esophagus
T4b	Tumor invades prevertebral space, encases the carotid artery, or mediastinal structures
Glottis	
TX	Primary tumor cannot be assessed
T0	No evidence of primary tumor
Tis	Carcinoma in situ
T1	Tumor limited to vocal cord(s) (which may involve anterior or posterior commissure) with normal mobility
T1a	Tumor limited to one vocal cord
T1b	Tumor involves both vocal cords
T2	Tumor extends to supraglottis and/or subglottis, and/or with impaired vocal cord mobility
T3	Tumor limited to the larynx with vocal cord fixation and/or invades paraglottic space and/or the inner cortex of the thyroid cartilage
T4a	Tumor invades through the outer cortex of the thyroid cartilage and/or invades tissues beyond the larynx, e.g., trachea, soft tissues of the neck including deep/extrinsic muscle of the tongue (genioglossus, hyoglossus, palatoglossus, and styloglossus), strap muscles, thyroid, the esophagus
T4b	Tumor invades prevertebral space and encases the carotid artery or mediastinal structures
Subglottis	
TX	Primary tumor cannot be assessed
T0	No evidence of primary tumor
Tis	Carcinoma in situ
T1	Tumor limited to subglottis
T2	Tumor extends to vocal cord(s) with normal or impaired mobility
T3	Tumor limited to the larynx with vocal cord fixation
T4a	Tumor invades the cricoid or thyroid cartilage and/or invades tissues beyond the larynx, e.g., trachea, soft tissues of the neck including deep/extrinsic muscle of the tongue (genioglossus, hyoglossus, palatoglossus, and styloglossus), strap muscle, thyroid, and esophagus
T4b	Tumor invades prevertebral space and encases the carotid artery or mediastinal structures
Regional lymph nodes (N)	
NX	Regional nodes cannot be assessed
N0	No regional lymph node metastasis
N1	Metastasis in a single ipsilateral lymph node, 3 cm or less in greatest dimension without extranodal extension
N2	Metastasis described as:
N2a	Metastasis in a single ipsilateral lymph node, more than 3 cm but not more than 6 cm in greatest dimension without extranodal extension
N2b	Metastasis in multiple ipsilateral lymph nodes, none more than 6 cm in greatest dimension, without extranodal extension

(*continued*)

Table 14 (continued)

N2c	Metastasis in bilateral or contralateral lymph nodes, none more than 6 cm in greatest dimension, without extranodal extension		
N3a	Metastasis in a lymph node more than 6 cm in greatest dimension without extranodal extension		
N3b	Metastasis in a single or multiple lymph nodes with clinical extranodal extension[a]		
Distant metastasis (M)			
M0	No distant metastasis		
M1	Distant metastasis		
Staging			
Stage	**TNM classification**		
0	Tis	N0	M0
I	T1	N0	M0
II	T2	N0	M0
III	T3	N0	M0
	T1, T2, T3	N1	M0
IVA	T1, T2, T3, T4a	N2	M0
	T4a	N0, N1	M0
IVB	T4b	Any N	M0
	Any T	N3	M0
IVC	Any T	Any N	M1

[a]The presence of skin involvement or soft tissue invasion with deep fixation/tethering to underlying muscle or adjacent structures or clinical signs of nerve involvement is classified as clinical extra nodal extension. Midline nodes are considered ipsilateral nodes

Table 15 Benefits of different treatment modalities for early glottis cancers

Advantages of TOLS
Single-stage procedure reduces treatment time
No RT-induced toxicities
Cost-effective
Better larynx preservation rates
Reserves other treatment options like redo surgery and RT for recurrence or second primary
Advantages of RT
No surgical expertise required
Possibly improved voice quality

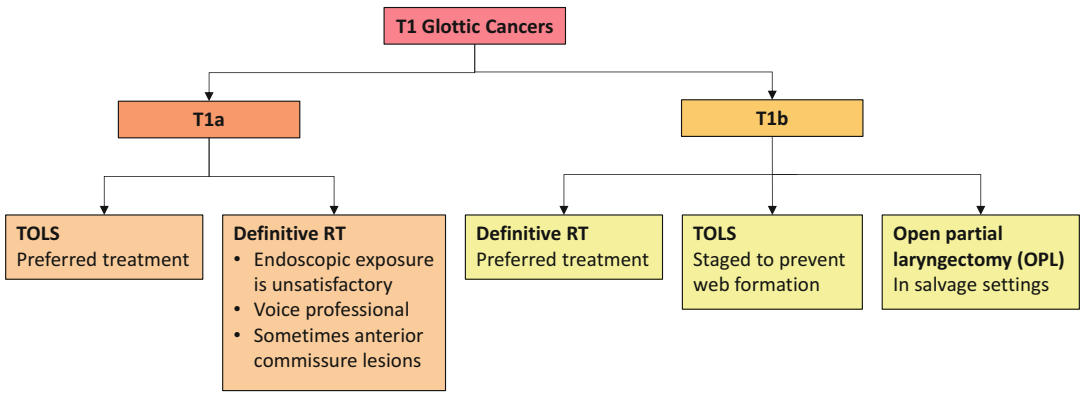

Fig. 68 Treatment algorithm for T1 glottic cancers

extensive (a type III or IV cordectomy) rendering the patient with poor voice quality and significant chances of aspiration.

Early Supraglottic Cancers

Early supraglottic cancers can be treated either with definitive RT or surgery (Fig. 70). In view of the high propensity of occult neck nodal metastasis, surgery when used as the primary treatment modality frequently upstages the neck resulting in administration of adjuvant RT, converting a single modality into a multimodality treatment. Thus, definitive RT remains the treatment of choice for early supraglottic cancers. In patients with bulky tumors, concurrent chemoradiation may be considered as lesions >6 cm^3 do not respond well to RT alone (Mancuso et al. 1999). Surgery, mostly TOLS or open partial laryngectomy, is usually considered in the salvage setting. Five-year local control with surgery (TOLS or open surgery) and radiation are comparable in T1 cancers (90–100% for surgery and 77–100% for radiation), while surgery has slightly better local control for T2 lesions (80–97% for surgery and 62–83% for RT) (Ambrosch 2007).

Advanced Laryngeal Cancers

Patients with advanced laryngeal cancers with a functional larynx and no extra-laryngeal spread are preferably treated on an organ preservation protocol (Fig. 71). Concurrent chemoradiotherapy is the treatment of choice, although recent evidence suggests a higher morbidity and mortality as compared to neoadjuvant chemotherapy followed by radiation. The VA trial published in 1991 was the first RCT comparing neoadjuvant chemotherapy followed by RT with the standard practice of total laryngectomy followed by

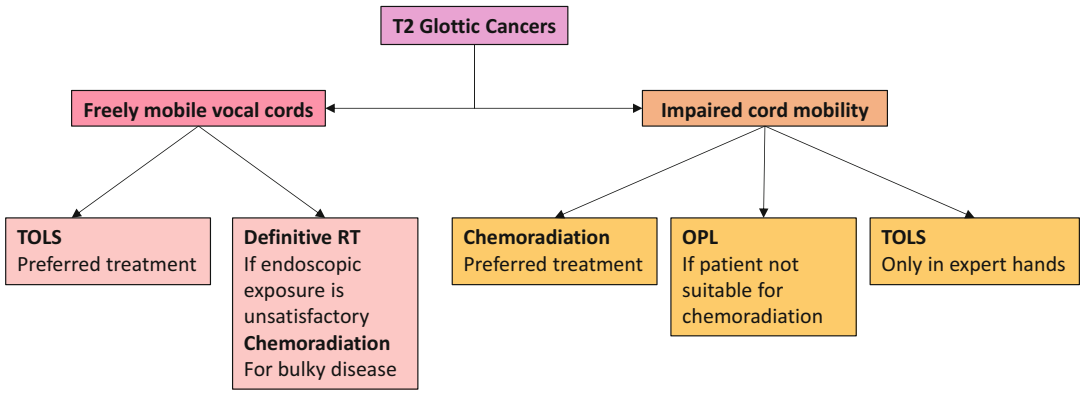

Fig. 69 Treatment algorithm for T2 glottic cancers

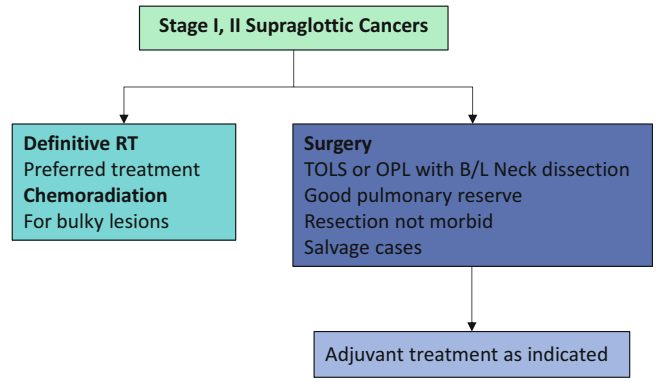

Fig. 70 Treatment algorithm for early supraglottic cancers

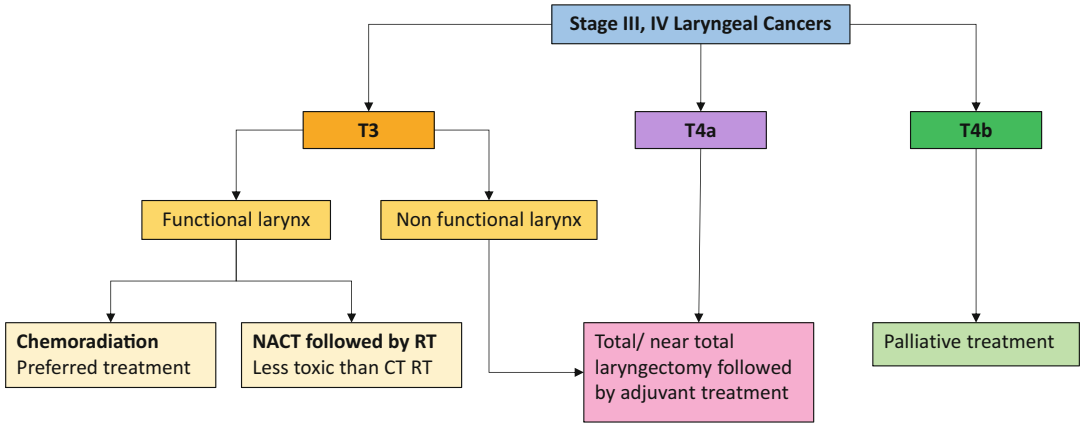

Fig. 71 Treatment algorithm for advanced laryngeal cancer

adjuvant treatment in advanced laryngeal cancers (Department of Veterans Affairs Laryngeal Cancer Study et al. 1991). The estimated 2-year survival was 68% in both groups. In the nonsurgical arm, the larynx could be preserved in 64% of patients. The pattern of recurrence differed significantly with more local recurrences and few distant failures in the nonsurgical arm. Patients with stage IV tumors as compared to stage III tumors, and T4 disease as compared to smaller primaries, had significantly increased rates of salvage laryngectomies.

Concurrent chemoradiotherapy (CT RT) and neoadjuvant chemotherapy (NACT) followed by RT and RT alone have been used as treatment modalities in advanced laryngeal cancers (large-volume T4 lesions excluded) (Forastiere et al. 2003). Follow-up of patients with advanced laryngeal cancers treated with one of these modalities showed that larynx preservation was significantly higher in the CT RT group compared to the two other groups at 3.8 years posttreatment. Ten-year follow-up data revealed no difference in overall survival and laryngectomy-free survival between NACT followed by RT and concurrent chemoradiotherapy CT RT (Forastiere et al. 2013). Although local control and larynx preservation continued to be significantly better in the CT RT arm, there were significantly more noncancer-related deaths in the CT RT arm compared to NACT arm (Forastiere et al. 2013). Least number of salvage surgeries were required in the CT RT patients; however, fistula formation following salvage surgery was most commonly seen in these patients.

Patients with nonfunctional larynx (tracheostomy tube or Ryles tube in situ) and extralaryngeal disease respond poorly to organ preservation and are treated with surgery (total/near-total laryngectomy with neck dissection) followed by appropriate adjuvant treatment (Fig. 72).

Nasopharyngeal Cancer

Epidemiology, Etiology, and Pathology

The nasopharynx forms the superior most part of the pharynx and is a cuboidal cavity located beyond the choanae or the posterior nares. It comprises two lateral walls and a roof which slopes down till the level of the uvula thereby making the soft plate as its floor. Nasopharyngeal carcinoma (NPC) is a squamous cell carcinoma arising from the surface epithelium of this region (Wenig 1999).

NPC is endemic to Southeast Asia (Southern China) and also includes the first-generation emigrated Chinese population in the West. Alaskan Eskimos and Mediterraneans also report incidence of NPC. In the Indian subcontinent, it is more prevalent in the northeastern states which have a substantial mongoloid population. There are rare incidences of NPC in the rest of the world. In terms of age standardized ratio, the highest incidence is in Southern China ranging from 15 to 50 per 100,000.

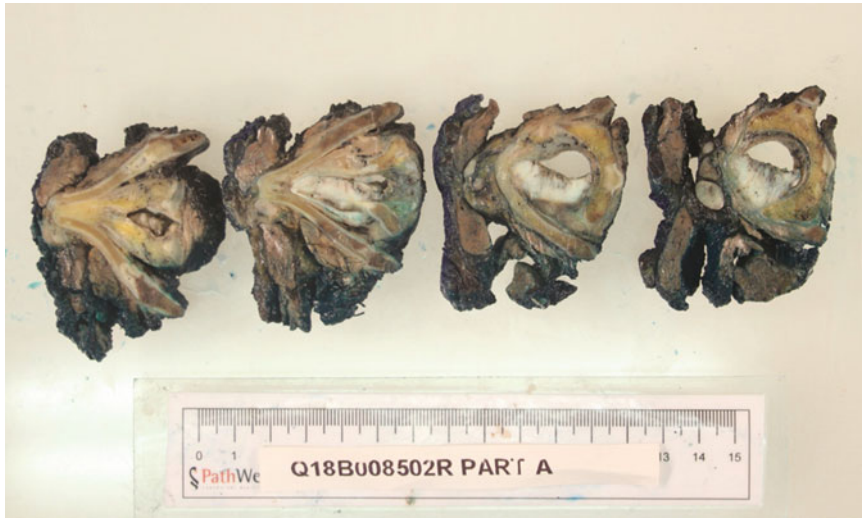

Fig. 72 Macroscopic appearance of the larynx sectioned transversely from superior to inferior (left to right) showing a left glottic squamous cell carcinoma which invades left paraglottic soft tissue and extends into subglottis. The tumor abuts the thyroid cartilage and crosses the midline anteriorly. The tumor does not involve overlying strap muscles or left hemithyroid (Image courtesy of Dr Chris Van Vliet, Pathwest, Perth WA, Australia)

There is a high male preponderance with a male-to-female ratio of 3:1 and an usual age of presentation between 20 and 60 years of age (Marks et al. 1998; Harrison 2014).

NPC has a multifactorial etiology which is markedly different from other sites in the head and neck like tobacco and alcohol. Viral, genetic, and environmental factors contribute to NPC etiology. Salted fish with high content of nitrosamine, poor hygiene, improper ventilation, smoking, and the use of nasal balms have been attributed as environmental factors. There has been an increased genetic susceptibility associated with HLA-A2, B-17, B246, and BW58 genotypes, and reduced risk is associated with A11, B13, and B22 loci. There has been a drop in the incidence of NPC in the last 40 years which suggests the role of environmental factors[2]. The viral etiology is mainly attributed to Epstein-Barr virus (EBV) for the endemic WHO type II/III. EBV is a B-lymphotropic herpes virus. It has a consistent role in the etiopathogenesis which can be seen from the early stages of the disease. EBV is absent in normal nasopharyngeal mucosa. Clonal viral genomes and latent membrane proteins (LMP-1) of EBV have been detected in NPC. Human papilloma virus (HPV) is associated with some NPC arising from oropharyngeal subsites (Marur et al. 2010).

The World Health Organization (WHO) classifies NPC into either keratinizing squamous cell carcinoma (WHO type I), non-keratinizing squamous cell carcinoma (WHO type II), or basaloid squamous cell carcinoma (Chan et al. 2005).

Clinical Presentation

Initially NPC involves the fossa of Rosenmuller in the majority of cases, and as it advances, it involves the nasal cavity, sphenoid sinus, posterior ethmoids, orbit, parapharyngeal space sphenopalatine fossa, foramen lacerum, and middle cranial fossa. Symptoms of NPC include breathing difficulty and nasal blockage, painless neck mass, hearing loss, ear discharge, epistaxis, cranial nerve deficits, proptosis, and trismus. Nine out of ten patients usually present with at least unilateral metastatic neck nodes either in parapharyngeal or the jugular digastric nodal stations (Marks et al. 1998; Chan et al. 2005).

Investigations

The nasopharynx can be clinically examined with a flexible fiber-optic endoscope or a rigid rod endoscope 0-degree or 70°. Neck examination

by palpation is imperative. Imaging can be done by means of contrast-enhanced CT (CECT) which provides excellent information regarding the primary site, nodal burden, and bone invasion, whereas an MRI can be complementary for better soft tissue extent of the tumor, to differentiate between mucus and tumor and perineural spread of the tumor (Sakata et al. 1999) (Figs. 73, 74, and 75). More than 20% of NPC can present with distant metastasis to the bone, lung, and liver in increasing frequency. Hence a PET/CT is recommended in stage III/IV cases (Vikram et al. 1985). Biopsy can be either taken from the primary site using a punch forceps with the help of an endoscope under topical local anesthesia. FNAC from the nodes can also demonstrate NPC cells and can be used for tissue diagnosis. Serological markers like IgA antibody against viral capsid antigen of EBV can be used for screening which has a sensitivity upward of 80%. Plasma EBV DNA using PCR also is used as a serological marker with a sensitivity up to 96% and can be used in early detection (Leung et al. 2006).

Treatment

NPC are distinct in regard to other cancers of the head and neck as they are extremely radiosensitive; therefore, they can be effectively treated with radiotherapy (Harrison 2014). Radiotherapy can cover all the areas of the nasopharynx and the potential sites of its spread without extensive morbidity or toxicity. Single modality treatment is advised in the early stages. In advanced stages, multiple trials have shown the advantage of using

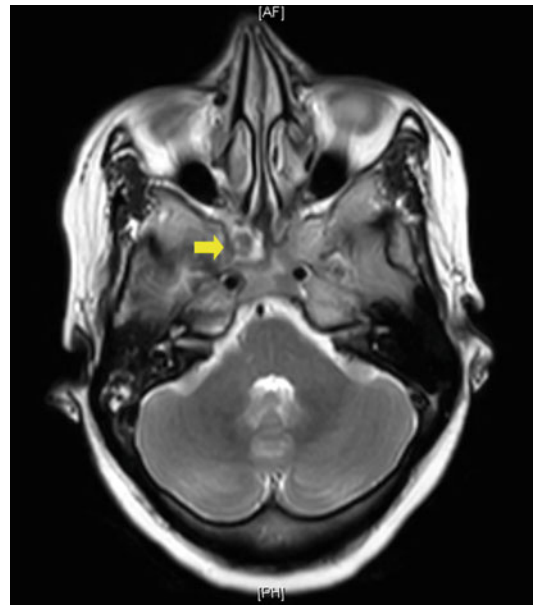

Fig. 73 Shows an axial image of T2 MRI showing a right-side nasopharyngeal carcinoma

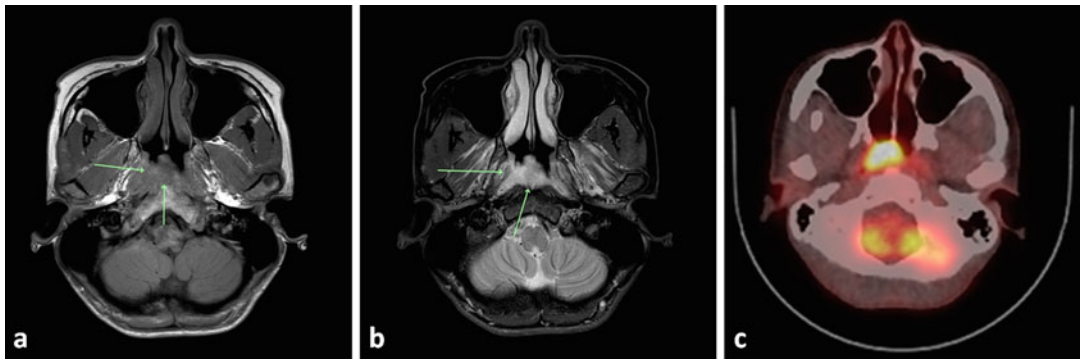

Fig. 74 T1N2M0 nasopharyngeal carcinoma. On MRI there is a polypoid carcinoma in the right central aspect of the nasopharyngeal mucosal space. The tumor demonstrates T1 isointensity (**a**) and T2 hyperintensity (**b**) with mild to moderate enhancement. The lesion measures 26 mm transverse × 9 × 22 mm AP and 8 mm craniocaudal. There is preservation of the normal marrow signal of the clivus with no evidence of central skull base invasion. The lesion is confined within the nasopharyngeal mucosal space with no convincing evidence of submucosal extension. There are no pathological retropharyngeal enlarged lymph nodes and no evidence of perineural tumor spread along the trigeminal nerve. PET/CT (**c**) shows intense abnormal FDG activity related to a soft tissue mass of the posterosuperior right nasopharynx. Activity appears well localized with no bone erosion

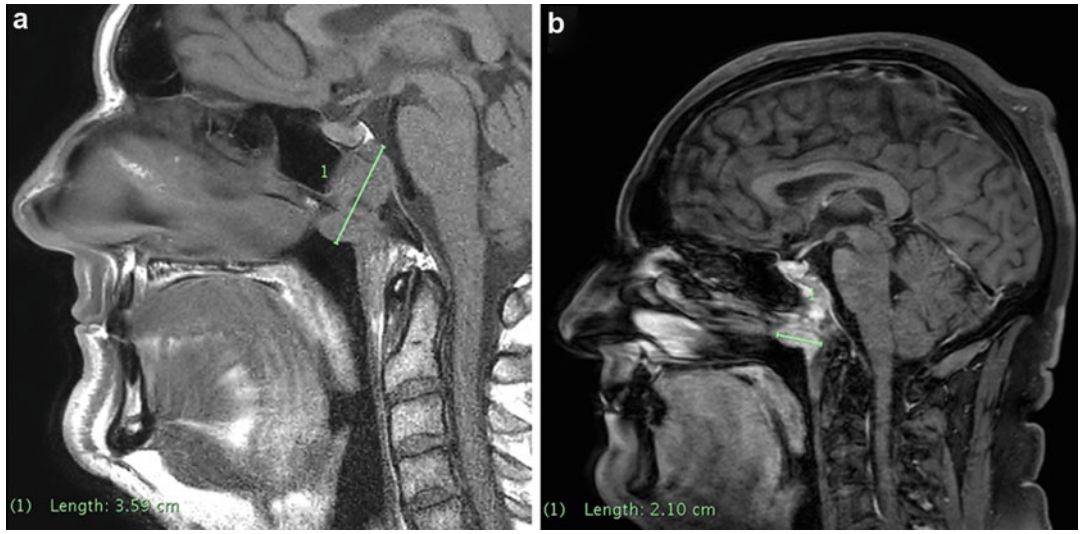

Fig. 75 T4N0M0 nasopharyngeal carcinoma. MRI shows an aggressive strongly enhancing lobular mass within the central skull base, occupying most of the basisphenoid and the anterosuperior aspects of the basiocciput, protruding minimally into the pre-pontine cistern, where it abuts the basilar artery, involving the posteromedial aspects of both sphenoid sinuses and extending in continuity with abnormal soft tissue in the central superior and nasopharynx. The extent of the lesion is up to 36 mm superoinferior × 29 mm transverse × 21 mm anteroposterior (**a**). The lesion is markedly T2 hypointense (**b**) and shows significant diffusion restriction, both features implying a densely cellular tumor consistent with a nasopharyngeal carcinoma

concurrent chemoradiation, with or without altered fractionation. An overview of the management is shown in Fig. 76. In cases of residual disease or recurrent cases, various modalities have been attempted in the salvage setting. These include salvage re-irradiation, nasopharyngectomy, salvage neck dissection, stereotactic radiosurgery, and intracavitary brachytherapy.

Traditionally 2D techniques were used and they are still used at present in certain centers around the world. Two-dimensional techniques can be effectively used for early lesions. Shielding of the brainstem areas and the spinal cord is done to prevent toxicities. Three-dimensional conformal therapy (3DCRT) and IMRT are currently used and have improved dose homogeneity and permit dose escalation to high-risk areas with less toxicities to normal adjacent structures. Brachytherapy and stereotactic radiosurgery boost escalating doses to the primary site alone in early stages of NPC (Harrison 2014).

The NCCN guidelines have recommended repeat of the baseline imaging or PET/CECT after at least 8–12 weeks and 12 weeks, respectively, for response assessment. Routine follow-up should occur 1–3 months in the first year, 2–6 months in second year, and 4–8 months from 3 to 5 years with imaging every 6 months. Routine thyroid function test and speech and swallowing evaluation every 6 months have been recommended. Plasma EBV DNA in endemic patients can be used for surveillance and has been recommended by the NCCN guidelines (Adelstein et al. 2017).

Tumors of the Nasal Cavity and Paranasal Sinuses (Skull Base Tumors)

Etiology, Epidemiology, and Pathology

Tumors of the nasal cavity and paranasal sinuses generally referred to as skull base tumors constitute a heterogeneous group of tumors with varied characteristics. Management of these tumors is relatively challenging owing to the intricate anatomy and the presence of vital structures in the vicinity.

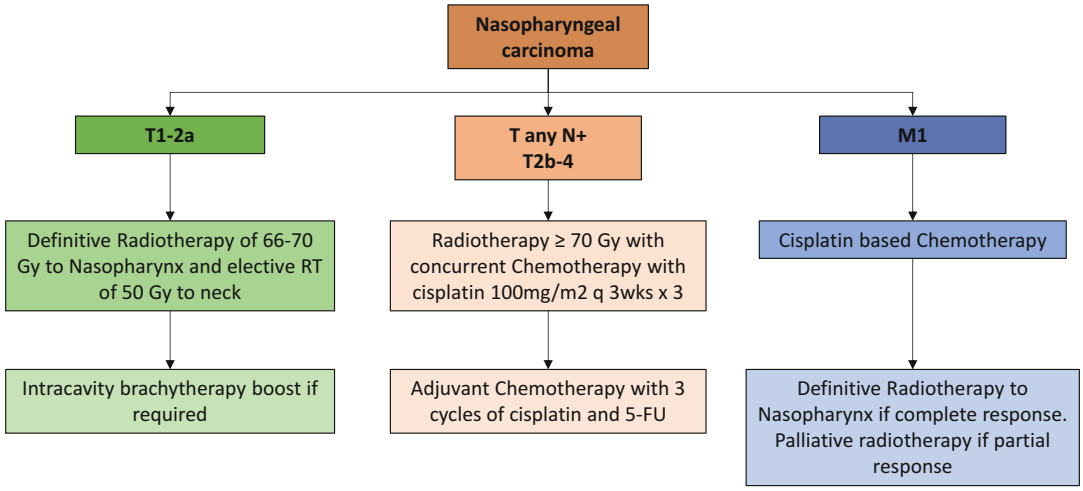

Fig. 76 Overview of management of nasopharyngeal carcinoma

Tumors of the nose and paranasal sinuses (PNS) encompass a wide spectrum of clinicopathologically distinct tumors (Table 16). Benign sinonasal tumors are relatively common as compared to their malignant counterparts. Benign tumors can be classified into soft tissue tumors and fibro-osseous lesions. Sinonasal papillomas (also called Schneiderian papillomas) are benign epithelial neoplasms of the nose and PNS. They are divided into three pathological subtypes – inverted, fungiform, and oncocytic papillomas. Inverted papillomas are the most common. These tumors are more commonly seen in males usually in the fifth and sixth decades of life and mostly originate from the lateral nasal wall. They are mostly unilateral (bilateral in 2–4% cases) and present as a pink nontranslucent polypoidal mass with a convoluted surface protruding from the nasal cavity. Microscopically, they are characterized by an endophytic growth pattern into the underlying stroma but with an intact basement membrane. Common differentials include nasal polyps and mucoceles.

Juvenile angiofibromas (Fig. 77) are highly vascular tumors occurring in young males usually in the second decade of life (Neel et al. 1973; Bremer et al. 1986). They originate in the region of the sphenopalatine foramen and usually present with profuse epistaxis. As the name suggests, these tumors are composed of a fibrous and vascular component and are essentially benign. The vascular component ranges from capillaries to compressed slit-like spaces to ecstatic capillaries. Biopsy is not usually indicated as the clinical and radiological profile is adequate for diagnosis.

Fibrous dysplasias are slow-growing fibro-osseous lesions. They result from a defect in osteoblastic differentiation and maturation that leads to replacement of the bone by fibrous tissue of variable cellularity and immature woven bone. They usually present at a young age. Clinically, fibro-osseous dysplasias are monostotic (80%) or polyostotic (20%). Monostotic lesions affect both genders equally, but polyostotic lesions have a female preponderance. Polyostotic fibrous dysplasia can be associated with McCune-Albright syndrome; the additional clinical features being cafe-au-lait spots, endocrine anomalies, and precocious puberty.

Malignant neoplasms of the nasal cavity and paranasal sinuses are relatively rare and constitute about 2–3% of upper aerodigestive tract cancers (Ali et al. 1986; Osguthorpe 1994). Squamous cell carcinoma is the most common subtype with a male preponderance and a peak incidence in the fifth and sixth decades of life although other age groups can be affected (Robin et al. 1979; Roush 1979; Grau et al. 2001; Myers et al. 2002; Bhattacharyya 2003). Increased incidence of SCC has been reported in nickel-refining workers

Table 16 Common tumors of the nasal cavity and paranasal sinus

Benign tumors	Malignant tumors
Soft tissue tumors	**Epithelial**
Schneiderian papillomas	Squamous cell carcinoma
Inverted	Adenocarcinoma
Fungiform	Adenoid cystic carcinoma
Oncocyte	Sinonasal undifferentiated carcinoma
Juvenile angiofibromas	**Mesenchymal**
Lobular capillary hemangiomas	Sarcomas (with notable exceptions)
Schwannomas	Hemangiopericytoma
Meningiomas	**Neuroendocrine tumors**
	Esthesioneuroblastoma
	Ewing sarcoma
	Melanoma
Fibro-osseous lesions	**Hematolymphoid**
Fibrous dysplasia	Lymphoma
Ossifying fibroma	Metastatic deposits from head, neck, kidney, lung, or breast primaries
Osteoma	

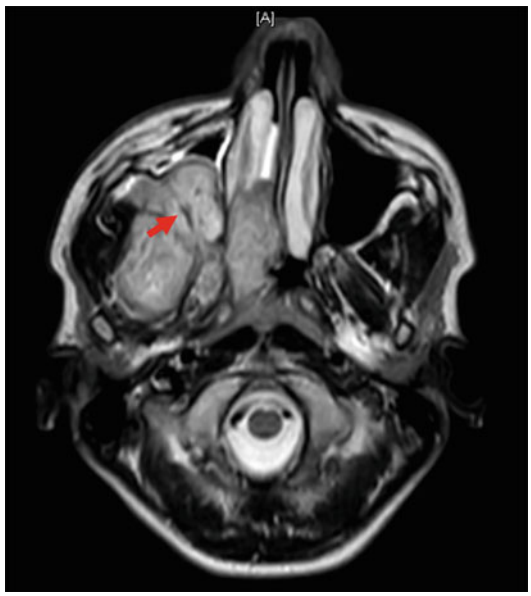

Fig. 77 Holman-Miller sign – anterior bowing of the posterior maxillary sinus wall (red arrow) (pathognomonic of juvenile angiofibroma)

with the risk directly proportional to the duration of exposure and inversely proportional to the age of exposure. Although smoking has traditionally not been associated as a major risk factor for sinonasal SCC (Fig. 78), there is substantial evidence that heavy smoking and snuff use are associated with nasal and PNS SCC. Furthermore, smoking has been found to be a multiplicative risk factor for SCC in nickel-refining workers (Andersen et al. 1996). Squamous cell cancers can occur after radiation exposure to the PNS after a long latent period. Thorotrast (thorium dioxide) is a radiopaque contrast agent injected into the maxillary sinus and was used in the past for imaging of the maxillary sinus. The dye gets retained in the maxillary sinus lifelong and decays into mesothorium which emits radioactivity which reaches its peak in 15 years. Squamous cell carcinoma is found to occur in patients who have undergone thorotrast injection after a period of 10–21 years (Wingo et al. 1998). Similarly SCC has been found in patients in radium dial painting industry after a long latent period of 30–40 years (Holmstrom and Lund 1991; Wingo et al. 1998). It is assumed that radium gets absorbed from the oral mucosa in workers who used to lick the paintbrushes during painting of the watch dials. Inverted papillomas have a 5–26% chance of being associated with a SCC – either synchronous or metachronous (Szabo 1954; Zak and Lawson 1974; Cove 1979; Hofbauer et al. 2002; Mannone et al. 2004; Bradley 2006).

Adenocarcinomas and adenoid cystic carcinomas are other epithelial malignancies arising in

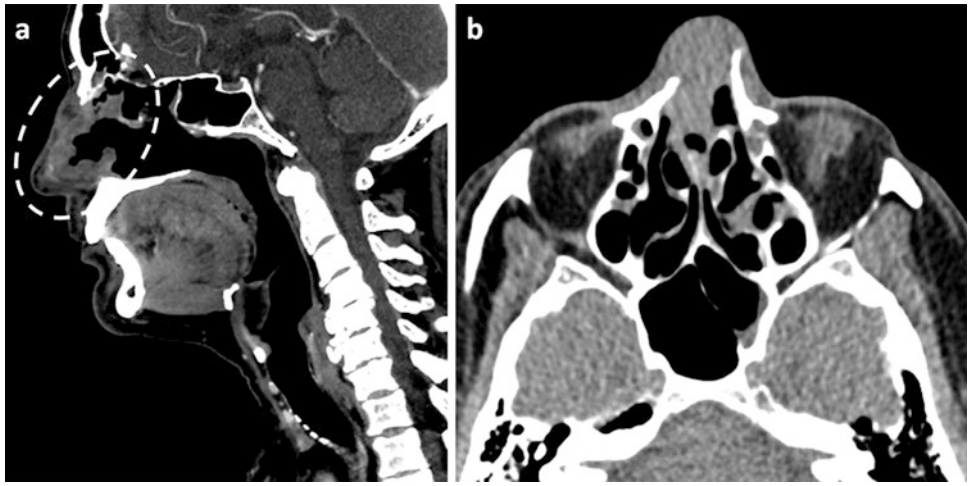

Fig. 78 T2N2M0 sinonasal carcinoma. On CT there is a lobular irregular enhancing mass occupying most of the dorsa of the external nose with sparing of the nasal tip (**a**) and extending into and partially destroying the anterior aspect of the nasal septum (**b**). The mass measures up to 47 mm superoinferior × 38 mm anteroposterior × 22 mm transverse. Anteriorly it extends into the skin over the nasal dorsum and nasal bridge. Inferiorly it extends virtually to the philtrum, and there is erosion of the anterior nasal spine. Superiorly, it causes subtle erosion of both nasal bones. The tumor is slightly bulkier on the right. There is no evidence of extension to the anterior skull base. The posterosuperior margin of the tumor involves the septum about 4 mm below the anterior cribriform plate

the nasal cavity and PNS. They tend to account for 10–15% of the PNS malignancies in the United States and as high as 40% in Europe. This disparity is primarily because of widespread of hardwood in Europe exposure to which has been found to be an etiology for adenocarcinoma (Klintenberg et al. 1984; Hanna 2009). The latency period from the exposure to the tumor development is long (about 40 years). The most common site for adenocarcinoma in the PNS is the ethmoids (Fig. 79). These tumors are pathologically divided into intestinal and subtypes. The intestinal type resemble adenocarcinomas arising in the intestinal tract; the non-intestinal type has a predominant seromucinous appearance.

Adenoid cystic carcinomas constitute about 10–15% of the PNS malignancies. The most common subsites are the maxillary sinus and the ethmoids. Three histologic subtypes have been described – tubular, cribriform, and solid. The peak incidence is in the fifth and sixth decades of life. No known etiologic factors are associated with ACCs.

Esthesioneuroblastomas are malignant neuroendocrine neoplasms arising from the olfactory mucosa. No definite etiologic factor is identified in its causation. It has a slight male preponderance with bimodal peak at the second to third and the sixth to seventh decades of life. They occur most commonly in the cribriform area and can spread early into the anterior cranial fossa through the olfactory fibers. Macroscopically, they present as a reddish gray polypoidal mass that bleeds easily. Microscopically they present as "small round cell tumors" with immunohistochemistry positive for general neuroendocrine tumors (NSE, SNP, S100).

Skull base sarcomas are anatomically and histologically distinct neoplasms arising from the mesenchymal tissue and constitute only 10% of sarcomas and 1% of head and neck tumors (Weber et al. 1986; Kraus et al. 1994; Landis et al. 1999; Jemal et al. 2002). Although most of them share a common embryonal origin, notable exceptions are malignant peripheral nerve sheath tumors and Ewing sarcoma which arise from the neuroendocrine tissue. The skull base and the neck are the commonest sites for head-neck sarcomas. Unlike extremity sarcomas where distant metastasis is a major cause of death, skull base sarcomas are

prone to local recurrence involving vital structures (brain, internal carotid artery, cavernous sinus, orbital apex) which is the leading cause of death in these patients.

Sinonasal mucosal melanomas are extremely rare and account for 1% of all melanomas and 0.6–4% of all tumors of the nasal cavity and the PNS. They tend to occur in elderly individuals (60–70 years) with a slight male preponderance. In the head and neck, the nasal cavity is the most common site (55–79%) followed by the oral cavity. The lateral nasal wall and the inferior turbinate are most common sites for origin of melanomas. Macroscopically, these tumors are brown to black polypoidal lesions that tend to ulcerate. Microscopically, they display morphological diversity with undifferentiated small round cell being most common. Melanin pigment is found in two-thirds of cases. These tumors are positive for vimentin, HMB 45, and S100.

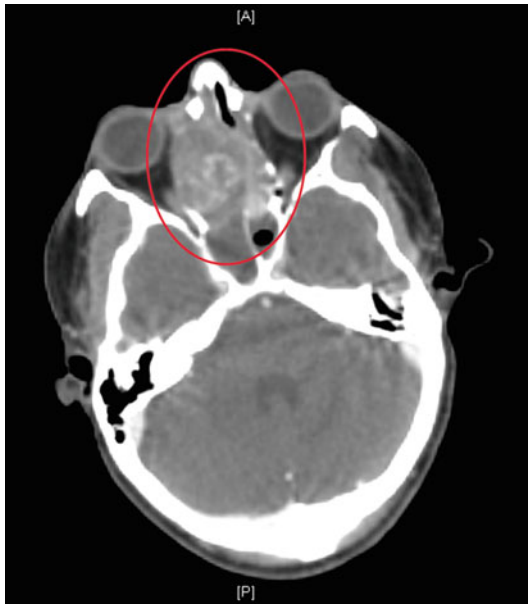

Fig. 79 Contrast-enhanced CT of paranasal sinuses axial image showing a heterogeneously enhancing lesion (oval) involving the ethmoids with erosion of the nasal septum and medial wall of right orbit

Clinical Presentation

Presenting symptoms depend on the biologic behavior and the anatomical location of the tumor. Common symptoms of skull base tumors are outlined in Table 17. Most patients initially present with unilateral nasal obstruction. Recurrent profuse epistaxis especially in young adult may be due to a juvenile angiofibroma, although malignant tumors like esthesioneuroblastoma and sarcomas cannot be ruled out. Anosmia as a presenting symptom can be due to a pathology located at the region of the cribriform plate; a common etiology being esthesioneuroblastoma. Tumors compressing or invading the orbit, the optic nerve, or the cavernous sinus can result in diplopia, proptosis, or loss of vision. Tumors located in the anteromedial aspect of the maxilla can infiltrate or obstruct the lacrimal duct causing epiphora. Tumors of the maxilla with erosion of the bone can result in facial swelling and asymmetry. Involvement of the branches of the trigeminal nerve can result in facial numbness or pain. Nasopharyngeal tumors or those involving the nasopharynx can cause blockage of the Eustachian tube resulting in conductive hearing loss. Malignant tumors can present with metastatic neck nodes, although not very common in nasal and PNS cancers.

Table 17 Common symptoms and signs of skull base tumors

Symptoms	Signs
Unilateral/bilateral nasal obstruction	Nasal mass
Epistaxis	Cranial nerve deficit
Hyposmia/anosmia	Proptosis
Diplopia	Middle ear effusion
Vision loss	Cervical adenopathy
Facial swelling	
Hearing loss	

Investigations

The goals of preoperative imaging are to study the anatomical relationship of the lesion with the normal structures and thus to map the extent of the disease. Furthermore, imaging can provide an insight to the differential diagnosis. Contrast-enhanced CT scan and MRI are complementary in imaging of the skull base. CT scan is the modality of choice for evaluating bony structures, skull base foramina, calcifications, and bony reactions to the tumor. High-resolution images with thin sections (<3 mm) with 1 mm overlap scans are ideal for imaging of the skull base. MRI on the other hand is the preferred modality for soft tissue delineation. Unenhanced axial T1-W images are used for anatomical relationships and to detect highly cellular lesions (e.g., malignant tumors). Water-rich tissues enhance on T2-W images, and these images are very important to differentiate tumors from retained secretions (Figs. 80, 81, and 82) and post-therapy fibrosis. Gadolinium enhancement with fat suppression (short tau inversion recovery, STIR) images is ideal for evaluation of malignant lesions, as the lesions become clearer with contrast and the margins better delineated due to fat suppression. MR angiography has replaced conventional angiography as it is noninvasive and nonionizing. MRI is contraindicated in patients with cardiac pacemakers and ferromagnetic intracranial aneurysm clips. Table 18 depicts the salient radiological findings of common skull base tumors.

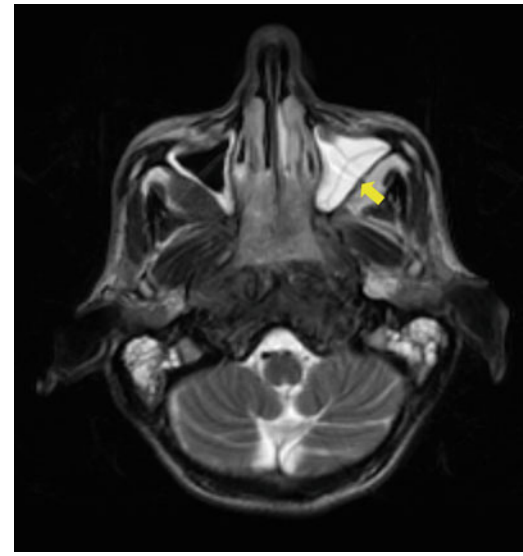

Fig. 80 Axial T2 MRI image of paranasal sinuses showing tumor originating in the nasopharynx with extension into the nasal cavity with retained secretions in the left maxillary sinus (yellow arrow)

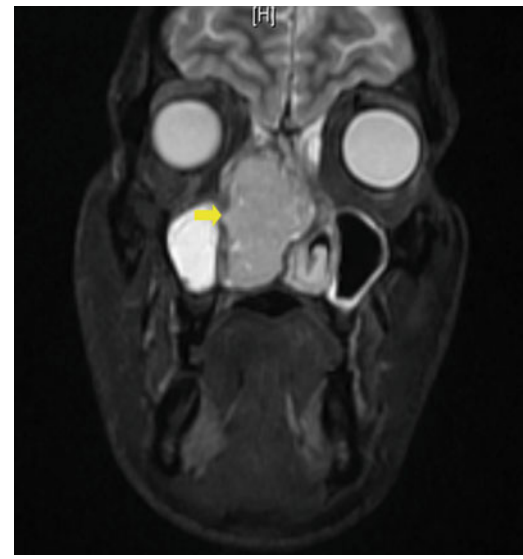

Fig. 81 Coronal T2 MRI image of paranasal sinuses showing tumor in the right nasal cavity with retained secretions in the right maxillary sinus (yellow arrow)

Treatment

Benign tumors of the skull base are essentially treated by surgery. The treatment of most malignant tumors is a multimodality treatment approach which includes surgery, radiotherapy, and chemotherapy. Excepting for hematolymphoid malignancies, surgery plays a key role in the management of skull base malignancies. The basic principles of surgery are gross total resection and maximum preservation of function. Surgical approaches to the skull base are either open or endoscopic (Fig. 83).

The choice of the surgical approach depends on multiple factors: the site of origin, the extent and pathology of the tumor, and the surgical expertise available. The major advantages of endoscopic approaches include direct access to the tumor, no brain retraction and edema, lesser morbidity, and reduced hospital stay. However,

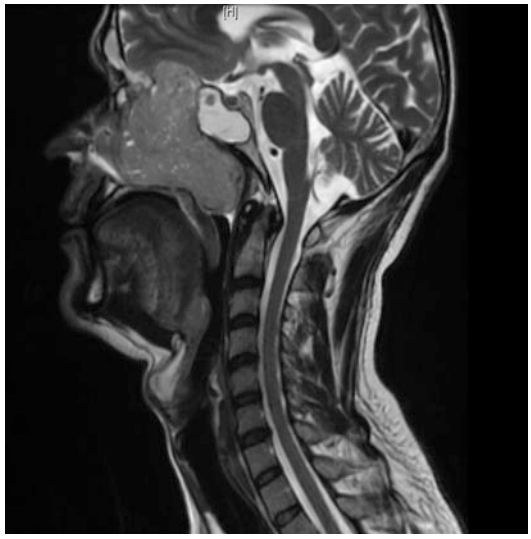

Fig. 82 Sagittal T2 MRI image of paranasal sinuses showing tumor occupying the entire nasal cavity and ethmoid sinuses with gross bone destruction and intracranial extension with retained secretions in the sphenoid sinus

the concept of "en bloc" tumor resection is violated by the endoscopic approaches, and it requires a steep learning curve. The indications and contraindications of endoscopic approaches are depicted in Table 19.

Although no randomized controlled trial has been conducted comparing endoscopic and open surgical approaches to the skull base, data from different studies reveal similar oncologic results with reduced morbidity in patients undergoing endoscopic resection (Howard et al. 2006; Ganly et al. 2011; Abergel et al. 2012; Meccariello et al. 2016). However, proper patient selection and surgical expertise is a key to endoscopic approaches.

Endoscopic resection has several advantages over open surgery which include better cosmesis, better quality of life, less CSF leakage, less cranial morbidity, and better illumination. Radiotherapy is usually used as an adjuvant to surgery. Definitive radiation is usually not used for resectable skull

Table 18 Salient radiological findings of common skull base tumors

Tumor	Salient radiologic findings
Inverted papilloma	Located in the lateral nasal wall/medial wall of the maxillary sinus
	Unilateral
	Bone remodeling/erosion
	Slight contrast enhancement
	Calcifications
Juvenile angiofibroma	Bright contrast enhancement
	Erosion of the upper medial pterygoid plate (early sign)
	Anterior bowing of the posterolateral wall of the maxilla (Holman-Miller sign) (pathognomonic)
Meningioma	Isointense on T1 and T2 images, marked post-contrast enhancement
	"Dural tail" and "CSF cleft" signs on MRI
Meningocele, meningomyelocele	Hypointense on T1 and hyperintense on T2-W images
	CSF leak on cisternography
Squamous cell carcinoma	Bone erosion
	Post-contrast enhancement
Adenoid cystic carcinoma	Nerve thickening with irregular enhancement (perineural invasion)
	Widening of the skull base foramina
Esthesioneuroblastoma	Origin near the cribriform area
	Focal calcifications
	Marked post-contrast enhancement
	Bone destruction
Sarcoma	Marked post-contrast enhancement "onion skin" appearance on CT - Ewing sarcoma
	Chondroid matrix, ringlike calcifications – chondrosarcoma
Chordoma	Origin at the region of the clivus
	Intratumoral calcifications
	Honeycomb appearance

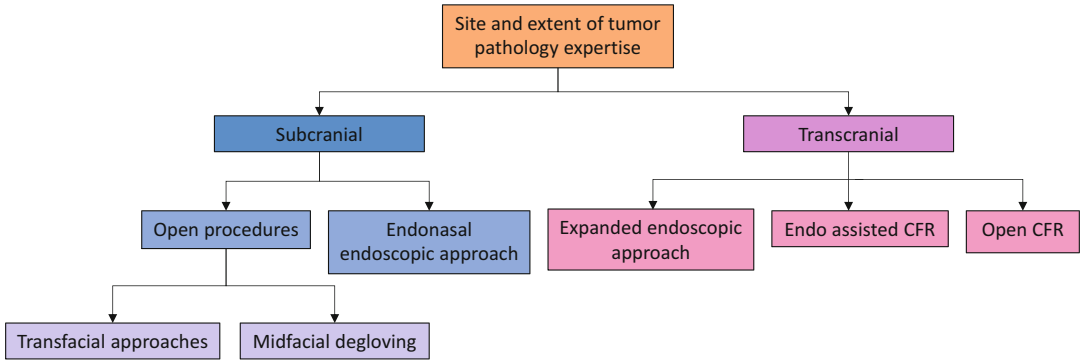

Fig. 83 Treatment algorithm for nasal and paranasal cancers

Table 19 Indications and contraindications for endoscopic approach to skull base tumors

Indications	Contraindications
Tumor confined to the sinonasal cavity or with "limited" dural or brain involvement	Extensive involvement of brain parenchyma
	Involvement of dura lateral to mid pupillary line
Expertise for endoscopic resection	Involvement of the anterior wall of the frontal sinus
	Involvement of orbital contents
	Skin involvement
	Lacrimal apparatus involvement
	Palatal involvement

base cancers for two reasons: poor oncologic outcome as compared to surgery with adjuvant radiation and toxicities (Choussy et al. 2008). Serious visual complications occur in 16–66% of patients with conventional radiation. Unilateral blindness occurs in 20–35% of patients and bilateral blindness in 6–10% of patients. Complications of skull base radiation include blindness, diplopia, painful red eye, brain necrosis, meningitis, hearing loss, memory loss, hypopituitarism, skin fistula, trismus, bone/cartilage necrosis, and saddle nose deformity. The most common cause of ipsilateral blindness is retinopathy and contralateral blindness is optic neuropathy. However, in unresectable tumors, radiotherapy alone has been found to have a modest local control (Jansen et al. 2000).

The objectives of systemic therapy in skull base cancers are to improve tumor control as well as organ preservation. The role of chemotherapy is well established in "small round cell tumors" which include Ewing sarcoma, rhabdomyosarcoma, and hematolymphoid malignancies. Sinonasal undifferentiated carcinoma and neuroendocrine carcinoma are aggressive tumors requiring multimodality therapy, and chemotherapy has a role in their management, although the optimal strategy is not yet determined. Tumor and patient characteristics need to be evaluated before planning the optimal regimen of systemic therapy.

Thyroid Cancer

Epidemiology, Etiology, and Pathology

More than 95% of thyroid tumors are benign. Thyroid carcinoma has an excellent prognosis when detected early and treated appropriately (Howlader et al. 2016). Thyroid cancer represents 1% of all cancers and is the most common endocrine malignancy (Reiners et al. 2004). It is the fifth most common cancer among women in the United States. There has been a significant and steady increase in the incidence of thyroid cancers in the last decade which is partly due to detection bias in developed countries, particularly South Korea. Thyroid malignancies encompass a wide spectrum of diseases ranging from well-differentiated thyroid cancers with excellent

prognosis at one extreme to anaplastic thyroid cancers carrying an equally dismal prognosis at the other (Cabanillas et al. 2016) (Table 20).

Ionizing radiation has long been noted as an etiological factor for thyroid cancer. Its association was first described in the 1950s. Subclinical doses of radiotherapy have shown a dose-response relationship particularly when exposed during young age. Historical treatments of pediatric diseases like acne, impetigo, sinusitis, adenoid enlargements, keloids, and lymphomas with radiotherapy were associated with increased incidence of thyroid cancers in adulthood. The risk ratio (RR) in such individuals ranges from 4.6 to 14.6 times and has a dose-dependent increase in risk till 20 Gy (Favus et al. 1976). Risk of environmental exposure of radiation after the Chernobyl nuclear disaster of 1986 resulted in a significant increase in incidence of thyroid malignancy among individuals who were either fetuses or children till the age of 15 at the time of the radiation exposure. Geographic areas with high background radiation hold increased risk of thyroid carcinoma (Baverstock et al. 1992). Thyroid cancer is more common among females, and hence multiple studies have been carried out to investigate the association of female reproductive history and thyroid cancer; however, no conclusive trends have been found (Negri et al. 1999). The relationship between oral contraceptive use and thyroid cancer has also yielded variable results. Pooled analysis suggests oral contraceptives to be a promoter of thyroid cancer; however, the risk is eliminated once its use is ceased (La Vecchia et al. 1999). Genetic causes for thyroid cancers are well known for medullary thyroid carcinoma (MTC) with 25% of them being associated with MEN2 syndromes (Fig. 84 and Table 21). Five to ten percent of papillary thyroid cancers also have a known genetic predilection and are also associated with syndromes like familial adenomatous polyposis (FAP), Gardner's syndrome, Cowden syndrome, and Carney complex (Richards 2010).

Clinical Presentation

The thyroid gland is an endocrine gland located in the anterior aspect of the neck. It consists of two lobes connected by a thin isthmus which lies over the second to fourth tracheal rings (Harrison 2014). In about 50–75% of patients, an additional pyramidal lobe is present usually on the left side which is a remnant of the thyroglossal duct. The term "goiter" is used to describe any enlargement of the thyroid gland (Figs. 85 and 86). The enlargement can present either in the form of a solitary nodule (50%), multiple nodules, or smooth or diffuse enlargement (Reiners et al. 2004). Endemic goiter is the most common form and is defined when it is prevalent in 10% of the population in a particular geographic area or community.

Investigations

Thyroid function tests (TFT) are the initial investigation for evaluation of a thyroid nodule. Most thyroid cancers are euthyroid at presentation. An elevated or normal thyroid-stimulating hormone

Table 20 Classification of thyroid malignancies

Follicular cell-derived thyroid cancer		**Neuroendocrine C-cell-derived thyroid cancer**
Differentiated thyroid cancer	**Anaplastic thyroid cancer**	**Medullary thyroid carcinoma**
Papillary carcinoma	Rare approx. 1% of thyroid malignancies	1–2% of thyroid malignancies
Most common (85%)		
Follicular carcinoma	Rapidly growing and aggressive	MEN 2 syndrome, RET proto-oncogene mutation
Have higher risk of hematogenous metastasis		Patients with hereditary mutations to undergo prophylactic thyroidectomies
Hurthle cell carcinoma	Early compressive symptoms like hoarseness, dyspnea, and dysphagia	
Poorly differentiated thyroid cancer	Poor prognosis	
Poorer prognosis when compared to other differentiated thyroid cancers		

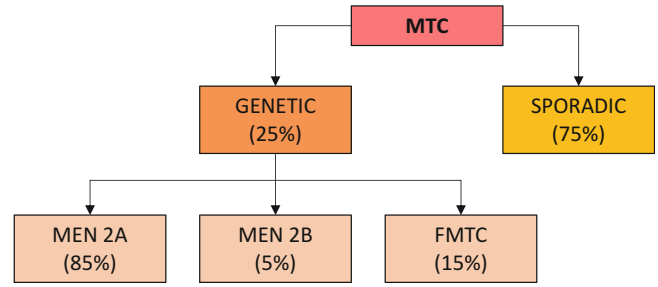

Fig. 84 MEN syndromes and medullary thyroid cancers

Table 21 Multiple endocrine neoplasia syndrome

Syndrome	Inheritance pattern	Clinical findings	Genetics	Remarks
MEN 2A (85%)	Autosomal dominant	MTC (100%)	Most commonly mutation in codon 634 of exon 10 or 11	Age of onset – second to third decade
		Pheochromocytoma (50%)		
		Hyperparathyroidism (10–20%)	Other mutations are in codons 609, 611, 618, 620, and 630	
		Cutaneous lichen amyloidosis		
		Hirchprung disease		
MEN 2B (5%)	Autosomal dominant	MTC (100%)	Most commonly mutation in codons 918 and 883	Age of onset – first to second decade
		Pheochromocytoma (50%)		Most aggressive form of the disease
		Marfanoid habitus (>95%)		
		Mucosal neuromas (>95%)		
Familial MTC (FMTC) (15%)	Autosomal dominant	Four or more members of a kindred without other endocrine tumors	Common mutations are 768, 790, 791, 804, and 891	Age of onset – fourth to fifth decade
				Mildest form of the disease

(TSH) harbors increased risk of malignancy, and further investigations are directed toward the diagnosis of malignancy. Conversely, chances of malignancy are low if TSH is subnormal, and further investigations are directed toward diagnosis of a toxic nodule (Fig. 87). Ultrasound is complementary to TFT in the diagnosis of thyroid malignancies.

High-resolution ultrasound of the thyroid and the neck (7.5–12 MHz) is the next step in the work-up of a thyroid nodule. Ultrasound features suggestive of malignancy are depicted in Table 22 (Figs. 88 and 89). Although ultrasound is a simple, cost-effective, widely available, non-ionizing, and recommended diagnostic tool for evaluation of thyroid nodule, a contrast-enhanced CT scan of the neck and thorax is indicated in certain situations. These include:

(a) Suspected retrosternal extension of the thyroid nodule (clinically lower limit of the nodule is not felt above the thoracic inlet) (Fig. 90)
(b) Suspected infiltration into adjacent structures like the trachea and esophagus (history of hoarseness of voice, aspiration, dyspnea and dysphagia, clinical finding of vocal cord paralysis) (Figs. 91 and 92)
(c) Metastatic nodes at lower neck (level VI, IV, or V) which harbors high chance of mediastinal adenopathy (Fig. 93)

There has been a concern that contrast would interfere with postsurgery radioactive iodine (RAI) therapy making it less effective; however, RAI therapy is usually performed at least 4–6 weeks after surgery, and the contrast agent used for preoperative scanning is eliminated from

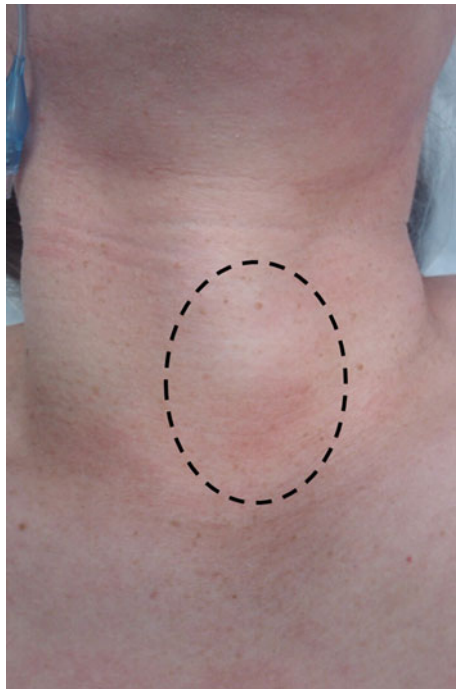

Fig. 85 Benign thyroid nodule of the neck in a female patient (black dashed oval) histopathologically confirmed as colloid nodular goiter (Image courtesy of Dr Chady Sader, Western ENT, Perth WA, Australia)

the body by that time. PET/CT is usually not used in the preoperative work-up of thyroid cancers (Harrison 2014).

Fine needle aspiration cytology (FNAC) is used to investigate thyroid nodules. Ultrasound-guided FNAC improves the diagnostic yield and accuracy but may not be routinely performed due to logistic purposes. Ultrasound guidance is recommended to target the solid portion in a solid-cystic nodule, when nodules are located in the posterior aspect of the thyroid, in case of multinodular goiter to target the most suspicious nodule(s), for repeating nondiagnostic cytology on blind FNAC, and when non-palpable nodules are picked up on other imaging. The indications of FNAC in a thyroid nodule based on sonographic features have been outlined in the American Thyroid Association (ATA) 2015 guidelines (Table 23) (Haugen et al. 2016). In order to maintain uniformity in the reporting of thyroid FNAC, the Bethesda system is used (Table 24) (Crippa et al. 2010).

Work-up of a thyroid nodule with FNAC reported as medullary thyroid carcinoma includes serum calcitonin, urinary or plasma metanephrines, serum calcium, RET mutation analysis, locoregional and distant imaging, and assessment of vocal cord mobility. Staging of thyroid cancer is outlined in Table 25.

Treatment

The management of patients with thyroid nodules is guided by thyroid function test, imaging, and FNAC. The goals of treatment are to:

(a) Improve overall and disease-specific survival.
(b) Reduce the risk of persistent/recurrent/metastatic disease.
(c) Minimize the risk of treatment-related morbidity.

Surgery plays the major role in the management of thyroid malignancies. Adjuvant radioiodine treatment and radiotherapy are indicated in high-risk patients.

The Bethesda reporting system provides a uniform baseline for treatment of thyroid nodules.

Bethesda I

An US-guided FNAC is preferred and, if available, on-site cytologic evaluation is done. Repeatedly nondiagnostic nodules without a high-suspicion sonographic pattern require close observation or surgical excision for histopathologic diagnosis. Diagnostic surgery should be considered if there is high suspicion on US features, growth of the nodule (>20% in two dimensions) is detected during US surveillance, or clinical risk factors for malignancy are present.

Bethesda II

No further diagnostic or therapeutic intervention is required. Dietary iodine supplementation can be given in patients from iodine-deficient areas. There is no role of TSH suppression therapy in these patients.

Bethesda III

Repeat FNA or molecular testing may be used to supplement malignancy risk assessment. If repeat

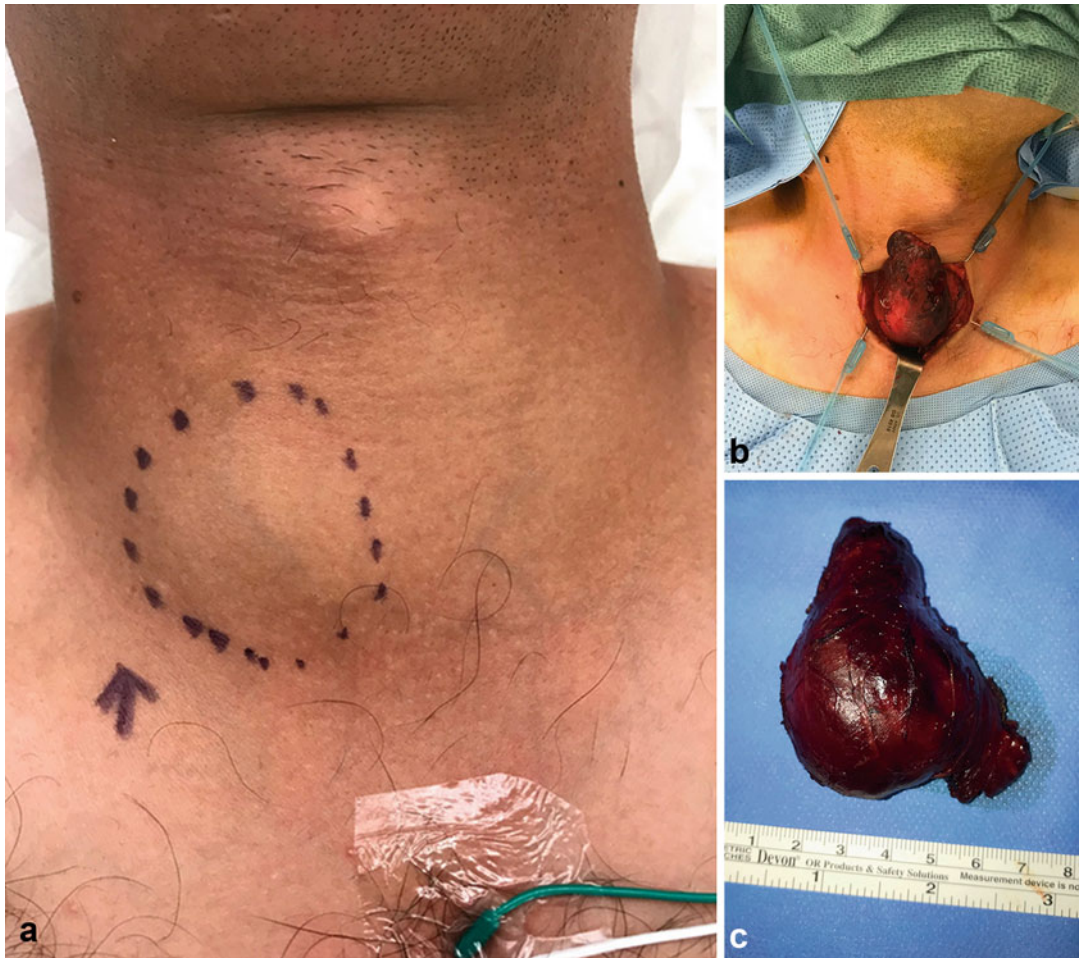

Fig. 86 Large thyroid nodule in male patient (**a**), exposed during surgery (**b**), and final macroscopic specimen (**c**) confirmed histopathologically as benign nodular goiter (Images courtesy of Dr Chady Sader, Western ENT, Perth WA, Australia)

FNA cytology, molecular testing, or both are not performed or inconclusive, either surveillance or diagnostic surgical excision (hemithyroidectomy) may be performed based on clinical risk assessment, sonographic features, and patient preference.

Bethesda IV

Follicular neoplasm encompasses three types of histology: follicular adenoma, follicular carcinoma, and follicular variant of papillary carcinoma. Diagnostic surgical excision is the long-established standard of care for the management of follicular neoplasm. However, after consideration of clinical and sonographic features, molecular testing may be used to supplement malignancy risk assessment data, although there is no robust evidence for molecular testing as an alternative to diagnostic hemithyroidectomy in Bethesda IV lesions. The protocol for management of Bethesda IV tumors is depicted in Fig. 94.

Bethesda V and VI

Treatment of Differentiated Thyroid Cancer

The mainstay of treatment of thyroid cancers is surgery (Haugen et al. 2016). The extent of surgery (hemi- or total thyroidectomy) has been a

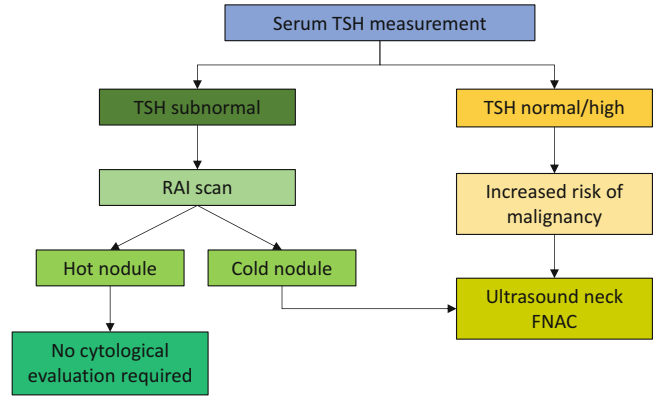

Fig 87 Initial work-up of a thyroid nodule

Table 22 Ultrasound features suggestive of malignancy in a thyroid nodule

Solid nodules
Microcalcifications
Hypoechogenicity
Irregular (infiltrative) margins
Taller than wider shape
Extracapsular extension
Suspicious metastatic neck nodes

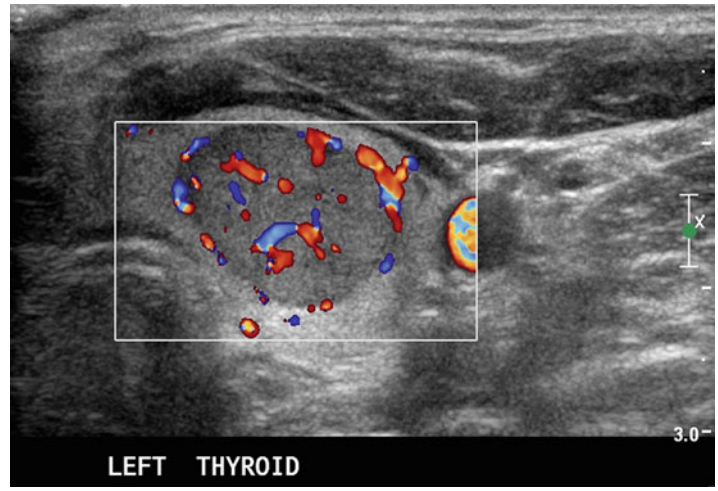

Fig. 88 Ultrasound of thyroid nodule demonstrating intrinsic vascularity suspicious for thyroid carcinoma (Image courtesy of Dr Chady Sader, Western ENT, Perth WA, Australia)

matter of considerable discussion and evolution over the years. The indications of total and hemithyroidectomy for differentiated thyroid cancers are depicted in Fig. 95. Tumors >4 cm, those with extrathyroid extension, and metastatic (nodal or distant) disease at presentation are absolute indications for total thyroidectomy (Fig. 96). Intrathyroid unifocal <1 cm tumors without any nodal or distant metastasis and no family history of thyroid cancer or history of radiation exposure are indications for hemithyroidectomy. Tumors between these two extremes can be managed either with total or hemithyroidectomy; the decision of which needs to be

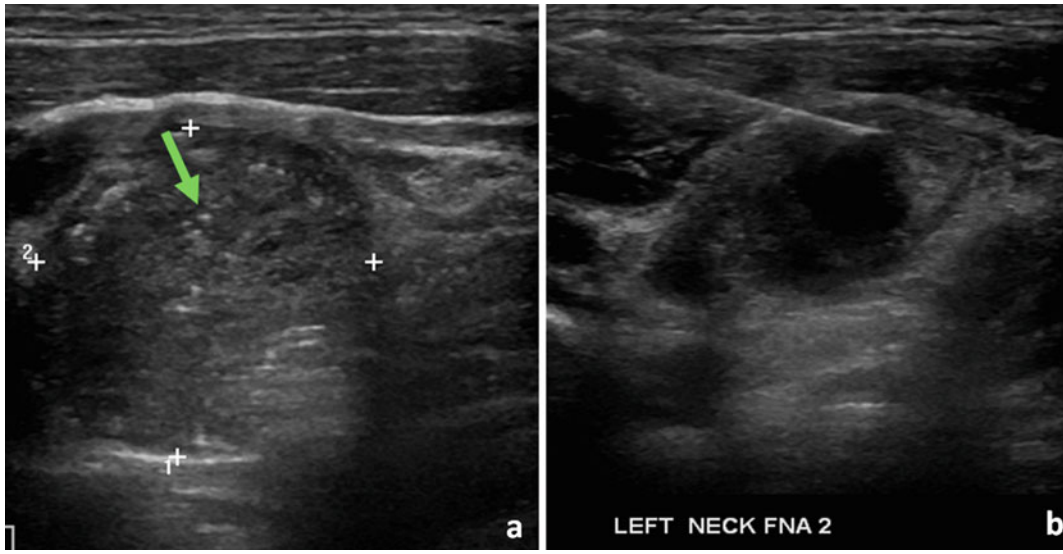

Fig. 89 Papillary thyroid carcinoma. Left thyroid nodule with microcalcifications (**a**) and FNA of a partially cystic left neck node with metastatic lymphadenopathy (**b**) (Images courtesy of Dr Chady Sader, Western ENT, Perth WA, Australia)

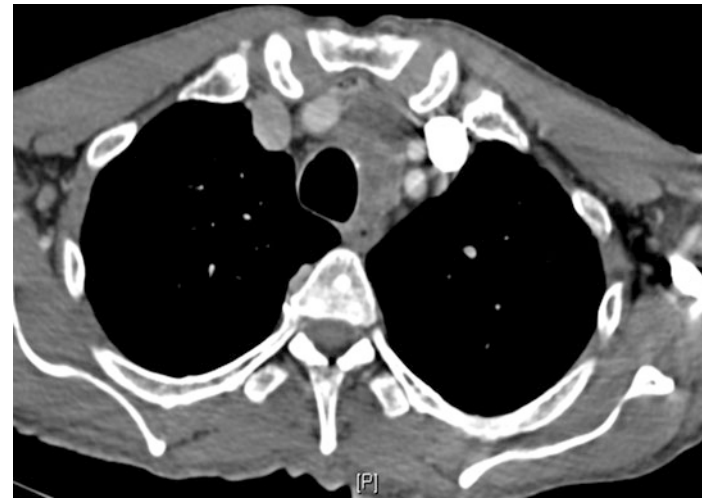

Fig. 90 Contrast-enhanced CT axial section showing retrosternal extension of thyroid tumor

taken unanimously by the physician and the patient. Based on retrospective studies, total thyroidectomy improves survival and decreases recurrence rates as compared to hemithyroidectomy. It also allows routine use of RAI remnant ablation and facilitates detection of remnant or persistent disease during follow-up. The major drawback of total thyroidectomy is the need for lifelong exogenous thyroid hormone therapy. The clinical outcome of hemithyroidectomy is very similar to total thyroidectomy in properly selected patients. Furthermore, follow-up regimen has moved away from diagnostic RAI scanning to serial ultrasound and detection of changing Tg levels. Most physicians are adopting a conservative approach to the relatively indolent cancer, and there is a shifting paradigm from total to hemithyroidectomy. However, careful patient selection is the key factor in the decision-making.

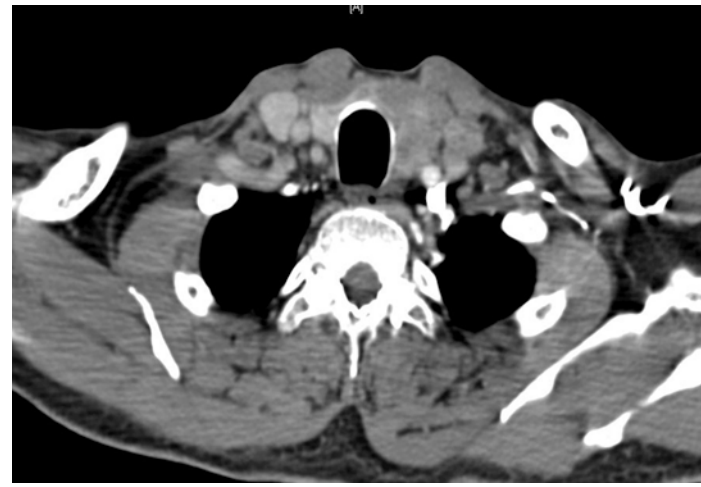

Fig 91 Axial contrast-enhanced CT image of a thyroid tumor of the left lobe with extrathyroidal extension and loss of fat plane with the strap muscles, trachea, and carotid artery

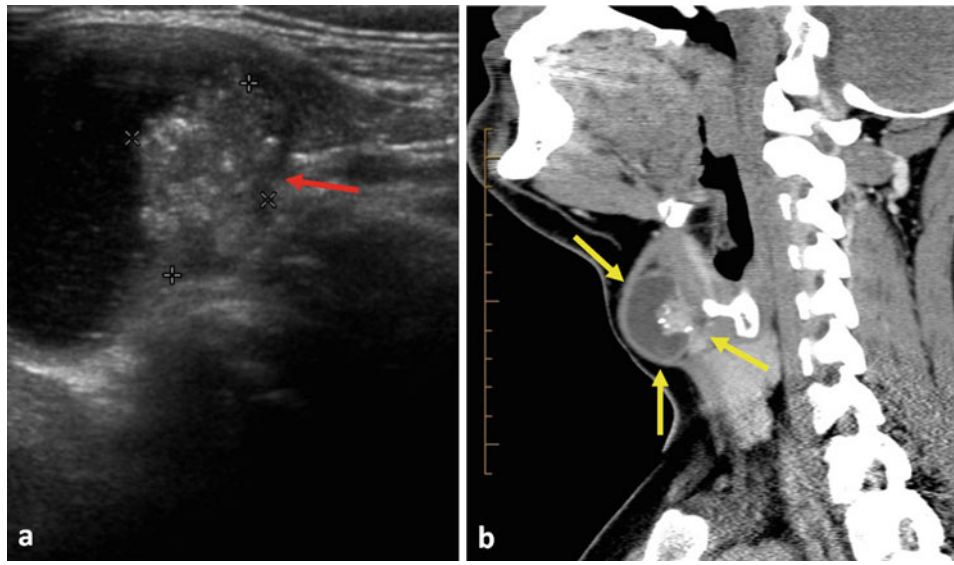

Fig. 92 Papillary carcinoma in a thyroglossal duct cyst. Ultrasound of mass in the superior midline of the anterior neck showing cystic lesion with solid nodule containing microcalcifications (red arrow) (**a**). CT sagittal reconstruction shows midline anterior neck cyst elevating strap muscles with mural solid nodule containing microcalcifications (yellow arrows) (**b**). (Images courtesy of Dr Chady Sader, Western ENT, Perth WA, Australia)

The central compartment of the neck (levels VI and VII) is the first echelon nodal station from thyroid cancers. Therapeutic central compartment clearance is indicated in clinical or radiological evidence of metastatic nodes in central compartment. Prophylactic central compartment clearance is indicated in T3 or T4 primary tumors with N0 neck or in presence of metastatic lateral compartment nodes. Care should be taken to prevent injury to the parathyroids and their blood supply and the recurrent laryngeal nerves during central compartment clearance. If there is devascularization injury to the parathyroids, autotransplantation should be considered. Lateral compartment nodal dissection (levels II–V) is indicated in cases of metastatic lateral

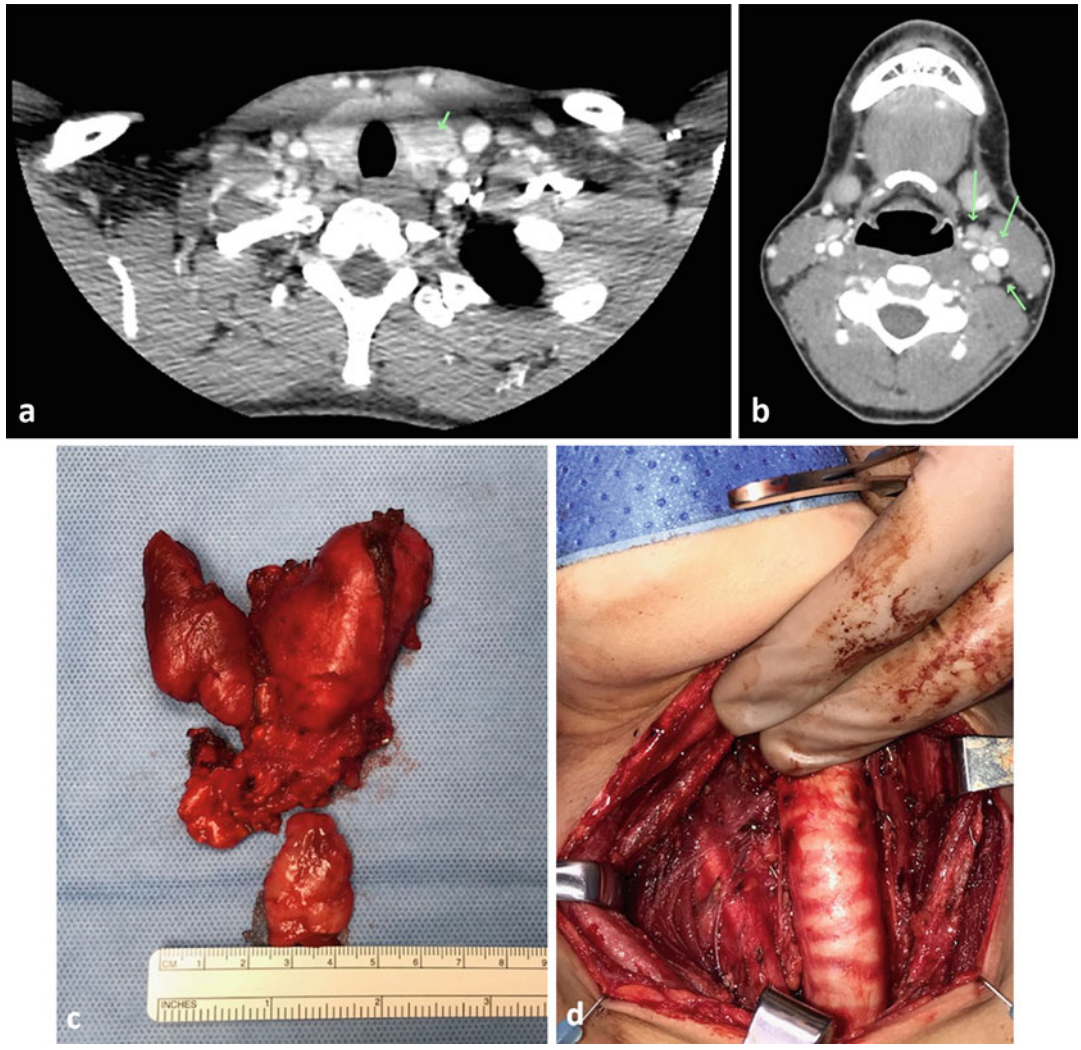

Fig. 93 Papillary thyroid carcinoma in a 21-year-old female. CT shows a large left thyroid mass biopsied and shown to be papillary carcinoma (**a**). This is associated with extensive left level II, III, and IV adenopathy on the left (**b**). Total thyroidectomy and central neck dissection specimen (**c**), and surgical bed demonstrating the trachea, both laryngeal nerves and right common carotid (**d**). (Images courtesy of Dr Chady Sader, Western ENT, Perth WA, Australia)

compartment nodes, in metastatic central compartment nodes, or in tumors located in the region of the upper pole of the thyroid gland.

Postsurgery patients of differentiated thyroid cancer are stratified into low, intermediate, and high risk based on clinical and histopathological criteria (Table 26). Based on these criteria, the need and extent of adjuvant treatment are planned. The details of adjuvant RAI treatment are depicted in Figs. 97, 98, 99, and 100.

Treatment of Medullary Thyroid Cancer

Treatment of choice of medullary thyroid cancer (MTC) is surgery. There is no role for RAI in the management of MTC. Tumors $\geq$1 cm in size or with bilateral thyroid disease are treated with total thyroidectomy with bilateral central compartment clearance. Tumors $<$1 cm can be treated with total thyroidectomy, but central compartment clearance should preferably be considered. The role of adjuvant radiation is not clear (Harrison 2014)

Table 23 Indications of fine needle aspiration cytology in a thyroid nodule (ATA guidelines 2015) (Haugen et al. 2016)

Level of suspicion on ultrasonography	Ultrasound features	Risk of malignancy in percentage	Recommendation by the ATA
High suspicion	Solid hypoechoic nodule or solid hypoechoic component of a partially cystic nodule with one or more of the following features: irregular margins (infiltrative, microlobulated), microcalcifications, taller than wide shape, rim calcifications with small extrusive soft tissue component, and evidence of ETE	>70–90	FNA at ≥1 cm
Intermediate suspicion	Hypoechoic solid nodule with smooth margins without microcalcifications and ETE or taller than wide shape	10–20	FNA at ≥1 cm
Low suspicion	Isoechoic or hyperechoic solid nodule or partially cystic nodule with eccentric solid areas, without microcalcification, irregular margin or ETE, or taller than wide shape	5–10	FNA at ≥1.5 cm
Very low suspicion	Spongiform or partially cystic nodules without any of the sonographic features described in low-intermediate-, or high-suspicion patterns	<3	To consider FNA at ≥2 cm/observation
Benign	Purely cystic nodules (no solid component)	<1	FNA not indicated

Table 24 Bethesda system of reporting of thyroid fine needle aspiration cytology (Crippa et al. 2010)

Bethesda system	Diagnostic category	Estimated risk of malignancy (%)
I	Nondiagnostic/unsatisfactory	1–4
II	Benign	0–3
III	Atypia of undetermined significance/follicular lesion of undetermined significance	5–15
IV	Follicular neoplasm or suspicious for follicular neoplasm	15–30
V	Suspicious of malignancy	60–75
VI	Malignancy	97–99

although it is recommended for tumors with extra-thyroid extension (T4 tumors), gross residual disease where attempts of surgical re-excision have been ruled out, and in metastatic nodes with extra-capsular spread (Adelstein et al. 2017). Prophylactic thyroidectomy is carried out in patients with MEN syndrome as depicted in Figs. 101 and 102.

Differentiated thyroid carcinomas have a good overall survival upward of 90% (Society 2015). The 5-year survival and 10-year survival for both papillary and follicular carcinomas are approximately equal at almost 90% for age group <45 years. Above 45 years of age with increasing age, there is a significant decrease in the overall survival seen up to 50% in the group of 60–69 years at 10 years. Follow-up is usually done every 6 months with serum thyroglobulin, US, RAI scan, and thyroid function test with TSH suppression in cases of high risk (Durante et al. 2013; Haugen et al. 2016). Patients are re-risk stratified as low, intermediate, and high based on the criteria depicted in patients, and further treatment is planned as required. The follow-up protocol for MTC relies on calcitonin levels carried out 2–3 months postsurgery. MTC patients are started on thyroxine supplementation immediately after surgery.

Malignant Soft Tissue Tumors of the Head and Neck

Malignant neoplasms of the soft tissues display a diverse array of lesions and a wide spectrum of clinical activity ranging from relatively slow-growing lesions to aggressive local and regionally destructive lesions with the potential for systemic

Table 25 Staging of thyroid cancer. TNM clinical classification and staging of thyroid malignant tumors (Adapted from Brierley et al. 2017)

Primary tumor (T)[a]			
TX	Primary tumor cannot be assessed		
T0	No evidence of primary tumor		
T1	Tumor 2 cm or less in greatest dimension, limited to the thyroid		
T1a	Tumor 1 cm or less in greatest dimension, limited to the thyroid		
T1b	Tumor more than 1 cm but not more than 2 cm in greatest dimension, limited to the thyroid		
T2	Tumor more than 2 cm but not more than 4 cm in greatest dimension, limited to the thyroid		
T3	Tumor more than 4 cm in greatest dimension, limited to the thyroid or with gross extrathyroidal extension invading only strap muscles (sternohyoid, sternothyroid, or omohyoid muscles)		
T3a	Tumor more than 4 cm in greatest dimension, limited to the thyroid		
T3b	Tumor of any size with gross extrathyroidal extension invading strap muscles (sternohyoid, sternothyroid, or omohyoid muscles)		
T4a	Tumor extends beyond the thyroid capsule and invades any of the following: subcutaneous soft tissues, larynx, trachea, esophagus, and recurrent laryngeal nerve		
T4b	Tumor invades prevertebral fascia and mediastinal vessels or encases the carotid artery		
Regional lymph nodes (N)			
NX	Regional nodes cannot be assessed		
N0	No regional lymph node metastasis		
N1	Regional lymph node metastasis		
N1a	Metastasis in level VI (pretracheal, paratracheal, and prelaryngeal/Delphian lymph nodes) or upper/superior mediastinum		
N1b	Metastasis in other unilateral, bilateral, or contralateral cervical (levels I, II, III, IV, and V) or retropharyngeal		
Distant metastasis (M)			
M0	No distant metastasis		
M1	Distant metastasis		
Staging[b]			
Stage	**TNM classification**		
Papillary and follicular[c] **under 55 years**			
I	Any T	Any N	M0
II	Any T	Any N	M1
Papillary and follicular 55 years and older			
I	T1a, T1b, T2	N0	M0
II	T3	N0	M0
	T1, T2, T3	N1	M0
III	T4a	Any N	M0
IVA	T4b	Any N	M0
IVB	Any T	Any N	M1
Medullary			
I	T1a, T1b	N0	M0
II	T2, T3	N0	M0
III	T1, T2, T3	N1a	M0
IVA	T1, T2, T3	N1b	M0
	T4a	Any N	M0
IVB	T4b	Any N	M0
IVC	Any T	Any N	M1
Anaplastic			
IVA	T1, T2, T3a	N0	M0

(*continued*)

Table 25 (continued)

IVB	T1, T2, T3a	N1	M0
	T3b, T4a, T4b	N0, N1	M0
IVC	Any T	Any N	M1

[a]Including papillary, follicular, poorly differentiated, Hurthle cell, and anaplastic carcinomas
[b]Separate stage groupings are recommended for papillary and follicular (differentiated), medullary, and anaplastic (undifferentiated) carcinomas
[c]Including papillary, follicular, poorly differentiated, Hurthle cell carcinoma

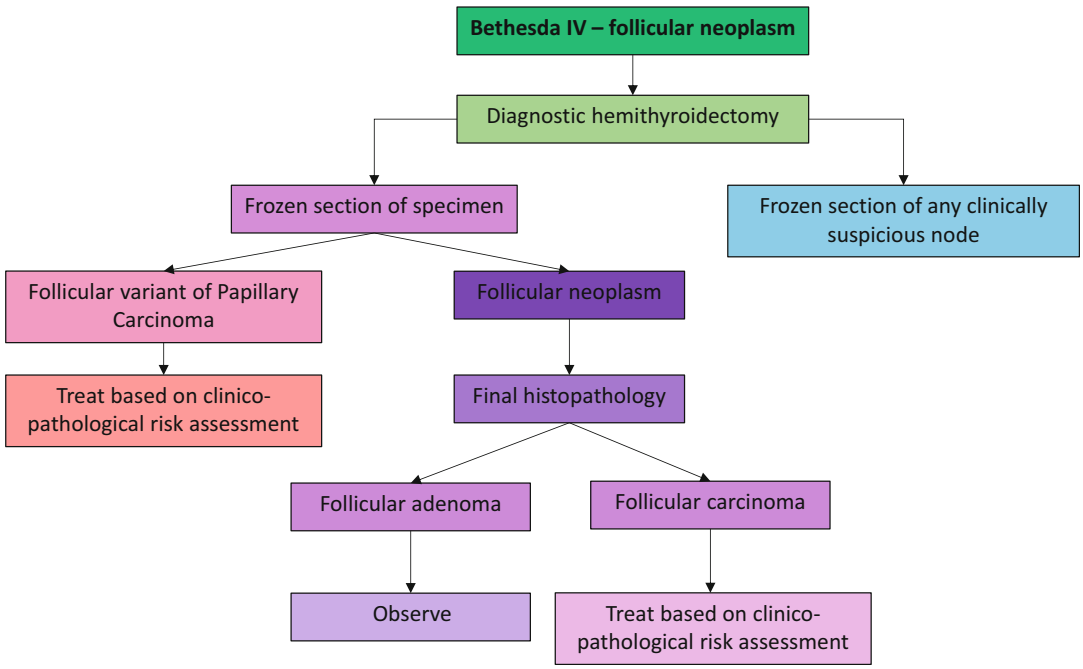

Fig. 94 Management protocol for follicular neoplasm

metastasis (Pellitteri et al. 2003). Sarcomas of the head and neck most commonly present as painless submucosal or subcutaneous masses of uncertain duration.

The success of treating these lesions has a strong correlation between how early and how quickly the diagnosis is made. The resemblance between some of these lesions is not restricted to their clinical behavior, most of which have microscopic features that make immunohistochemical investigation essential for conclusive diagnosis. Before molecular investigations, these lesions were collectively known as sarcomas, not otherwise specified.

Most of these lesions are independent new neoplasms, but 10–20% have a history of malignant transformation from a benign counterpart. Since they can possibly initiate at any part of the body, it is also important to investigate if lesions of the head and neck region are in fact primary tumors or metastatic ones. Occurrence in the head and neck is rare, accounting for less than 1% of all malignant tumors in this site. These lesions may attain a great size before symptoms occur and are often noted on routine dental, head, neck, or pharyngeal examination.

Sarcoma growth and local advancement employ a compressive mechanism, whereby tissue adjacent to the tumor together with a local inflammatory response contributes to the formation of a pseudocapsule composed of normal tissue and both inflammatory and malignant neoplastic cells. Despite the advances in oncology, the treatment

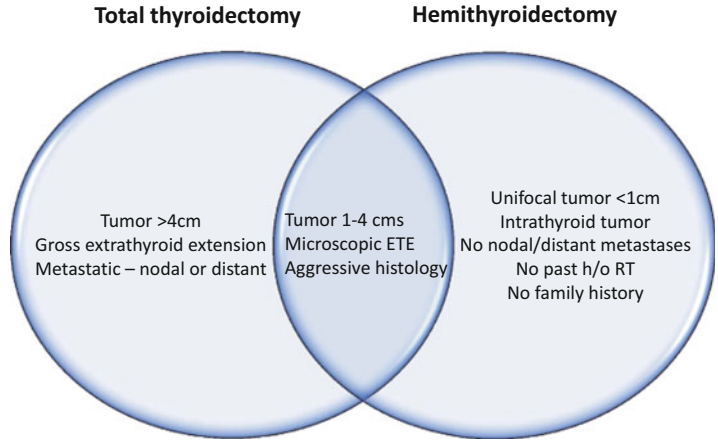

Fig. 95 Extent of surgery in differentiated thyroid cancers

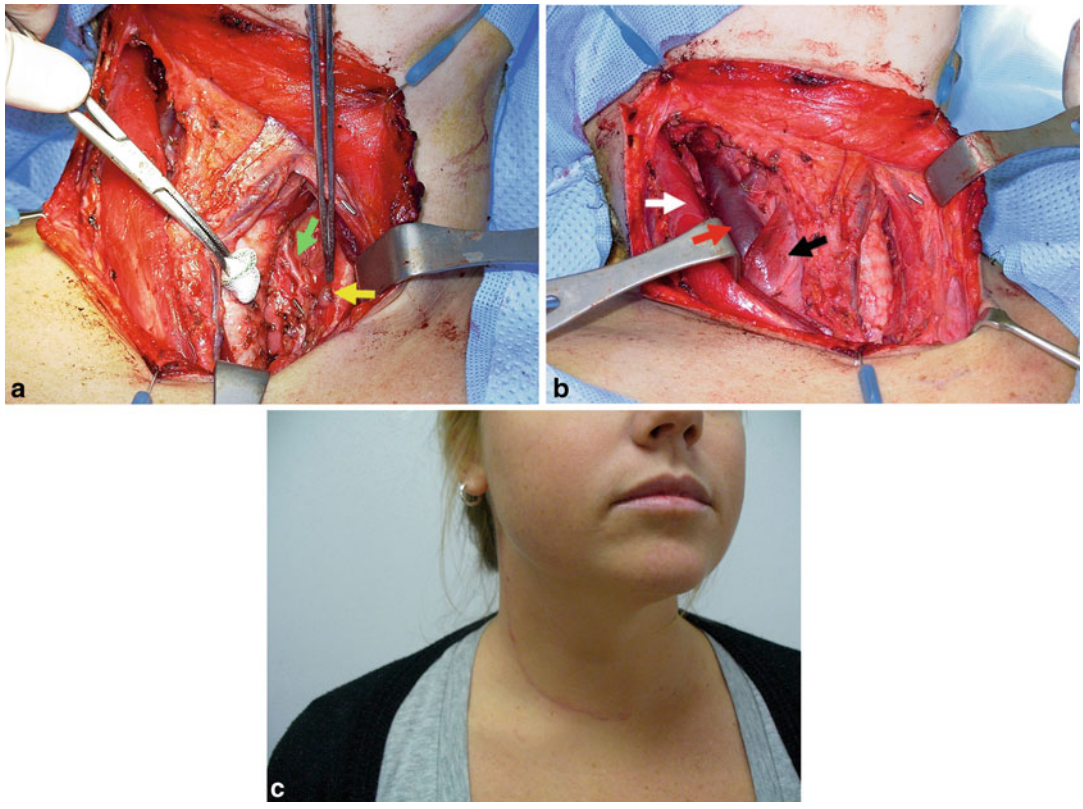

Fig. 96 Papillary thyroid carcinoma surgery in a 19-year-old female. Intraoperative photo (**a**) shows the appearance after thyroidectomy illustrating the trachea (peanut swab), the left recurrent laryngeal nerve (green arrow), and the superior left parathyroid gland (yellow arrow). Intraoperative view at completion of neck dissection (**b**) shows the sternomastoid (white arrow) and omohyoid (black arrow) muscles as well as the internal jugular vein (red arrow). Appearance of postoperative wound (**c**) (Images courtesy of Dr Chady Sader, Western ENT, Perth WA, Australia)

Table 26 ATA risk stratification system with proposed modifications according to ATA guidelines 2015 (Haugen et al. 2016)

ATA low risk	Papillary thyroid cancer (with all of the following):
	No local or distant metastases
	All macroscopic tumor has been resected
	No tumor invasion of locoregional tissues or structures
	The tumor does not have aggressive histology (e.g., tall cell, hobnail, variant, columnar cell carcinoma)
	If ^{131}I is given, there are no RAI-avid metastatic foci outside the thyroid bed on the first posttreatment whole-body RAI scan
	No vascular invasion
	Clinical N0 or ≤5 pathologic N1 micrometastases (<0.2 cm in largest dimension)[a]
	Intrathyroidal, encapsulated follicular variant of papillary thyroid cancer[a]
	Intrathyroidal, well-differentiated follicular thyroid cancer with capsular invasion and no or minimal (<4 foci) vascular invasion[a]
	Intrathyroidal, papillary microcarcinoma, unifocal or multifocal, including BRAFV600E mutated (if known)[a]
ATA intermediate risk	Microscopic invasion of tumor into the perithyroidal soft tissues
	RAI-avid metastatic foci in the neck on the first posttreatment whole-body RAI scan
	Aggressive histology (e.g., tall cell, hobnail, variant, columnar cell carcinoma)
	Papillary thyroid cancer with vascular invasion
	Clinical N1 or >5 pathologic N1 with all involved lymph nodes <3 cm in largest dimension[a]
	Multifocal papillary microcarcinoma with ETE and $BRAF^{V600E}$ mutated (if known)[a]
ATA high risk	Macroscopic invasion of tumor into the perithyroidal soft tissues (gross ETE)
	Incomplete tumor section
	Distant metastases
	Postoperative serum thyroglobulin suggestive of distant metastases
	Pathologic N1 with any metastatic lymph node ≥3 cm in the largest dimension[a]
	Follicular thyroid cancer with extensive vascular invasion (>4 foci of vascular invasion)[a]

[a]Proposed modifications, not present in the original 2009 initial risk stratification system

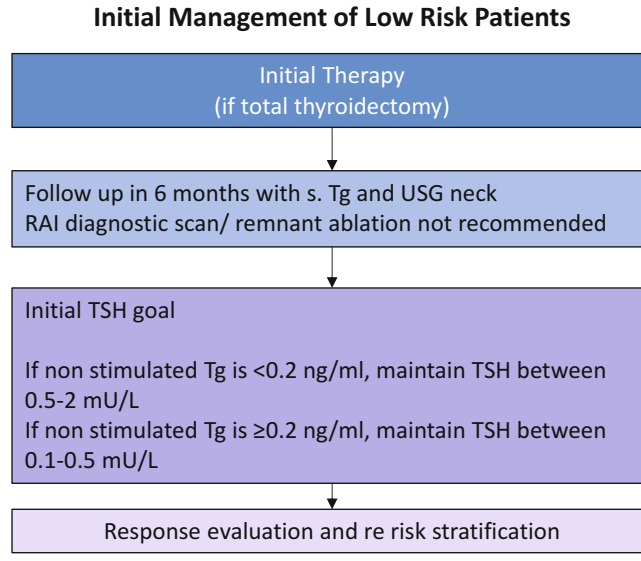

Fig. 97 Postsurgery management of low-risk patients treated with total thyroidectomy

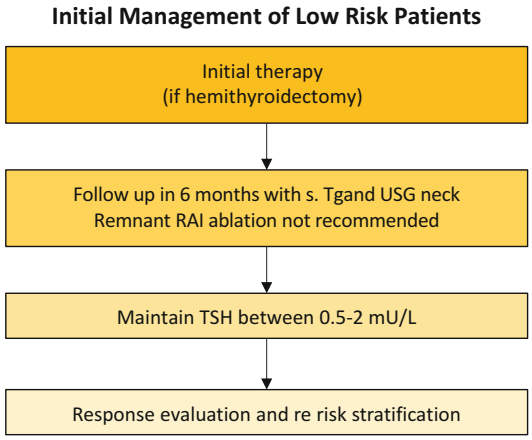

Fig. 98 Postsurgery management of low-risk patients treated with hemithyroidectomy

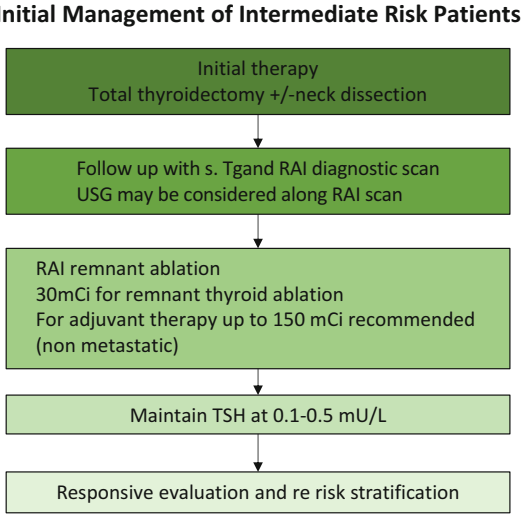

Fig. 99 Postsurgery management of intermediate-risk patients

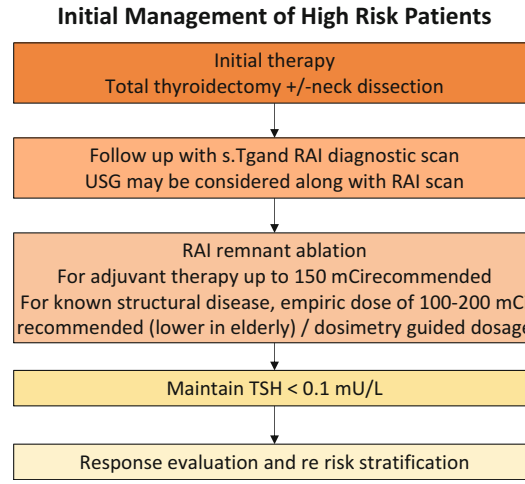

Fig. 100 Postsurgery management of high-risk patients

of these lesions consists of en bloc resection with normal tissue removal a considerable distance away from the identifiable tumor. This is due to the extension of the tumor along anatomic planes formed by the fascia, muscle, and bone.

Surgical treatment of these lesions is therefore frequently devastating, making the treatment itself just as harmful as the neoplasm itself. Size as related to the involvement of critical neurovascular structures, thus limiting en bloc resection, has obvious implications for unfavorably impacting both local control and survival. The rapidity of growth is variable depending on the biologic behavior and grade of the tumor. Symptoms attributable to growth vary according to location; those involving the aerodigestive tract generally become symptomatic earlier in the course of disease as compared with tumors involving the neck.

Tumor grade significantly impacts the biologic and clinical behavior of sarcomas and has implications with respect to treatment, control, and long-term survival. Metastatic potential is higher in higher-grade sarcomas. Lymph node metastasis occurs rarely and almost exclusively in high-grade tumors. Distant metastases occur early with high-grade sarcomas, but unfortunately even low-grade tumors can metastasize.

Fibrosarcoma

Epidemiology, Etiology, and Pathology

Fibrosarcoma is a malignant neoplasm of mesenchymal origin, with possible occurrence in the head and neck region (Fig. 103). Before the era of immunohistochemistry, fibrosarcoma was a very frequent diagnosis and represented one of the most common types of soft tissue sarcoma. With the development of immunohistochemical and molecular techniques, it is now rare for a

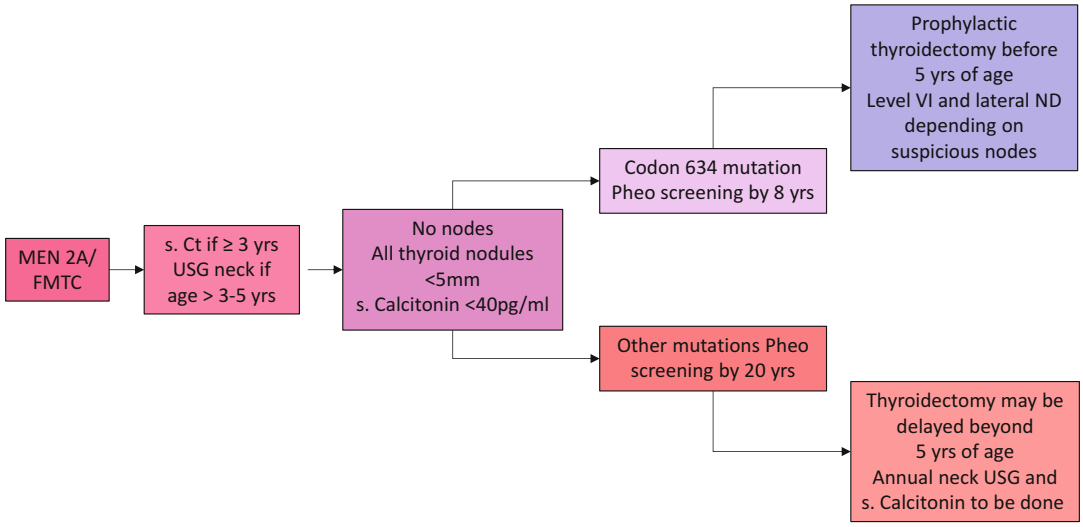

Fig. 101 Prophylactic thyroidectomy in MEN 2A/FMTC patients

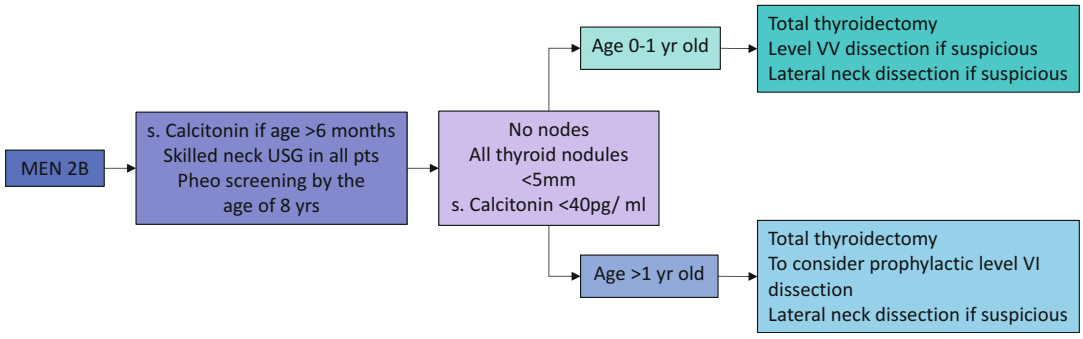

Fig. 102 Prophylactic thyroidectomy in MEN 2B patients

sarcoma to be termed fibrosarcoma, which by its name implies fibroblasts as the cell of origin.

Fibrosarcoma can arise in soft tissues or within the bone. Intraosseous fibrosarcomas may develop endosteally or possibly periosteally, the latter affecting the bone by spread from adjacent soft tissue. The mean age for occurrence of fibrosarcoma is between the second and sixth decades with equal gender distribution.

Clinical Features

Clinically, the lesion can cause pain, swelling, paresthesia, and occasionally loss of teeth and ulceration of the overlying mucosa. The clinical behavior of fibrosarcoma is characterized by a high local recurrence rate and a low incidence of locoregional lymph node and/or distant hematogenous metastases. However, hematogenous metastasis may involve the lungs, mediastinum, abdominal cavity, and bone.

Fibrosarcoma of the oral cavity most often manifests as a clinically innocuous, lobulated, sessile, painless, and nonhemorrhagic submucosal mass of normal coloration. On the other hand, aggressive fibrosarcomas tend to be a rapidly enlarging (Fig. 103), hemorrhagic mass similar in clinical appearance to an ulcerated angiogranuloma, peripheral giant cell granuloma, or peripheral ossifying fibroma.

Investigations

Before therapy, the local extent of the neoplasm and the presence or absence of local and distant metastases must be determined. Evaluation continues with directed imaging to determine the extent of tumor and involvement of critical adjacent structures which may influence biopsy technique. Metastatic surveys should include chest radiography, scintigraphic bone scanning, and abdominal ultrasound and/or computed tomography.

Either CT or MRI represent forms of imaging which may be used individually or in combination. Contrast-enhanced head and neck CT has proven to be a valuable tool for delineating the size of the tumor and infiltration of neighboring tissue. MRI, especially with gadolinium contrast, may be used as a supplement or alternative to CT scanning. It has a distinct soft tissue advantage and is superior in delineating vascular involvement, especially with magnetic resonance angiography (MRA). CT offers an improved evaluation for bony structure involvement of the paranasal sinuses, orbit, and cranial base. Formal cranial angiography may be necessary to eliminate the possibility of carotid or vertebral artery involvement and for the assessment of the feasibility of performing angioinvasive techniques such as embolization and selective intra-arterial chemotherapy. Positron-emission tomography (PET) is of value in the staging of malignancy to determine distant disease.

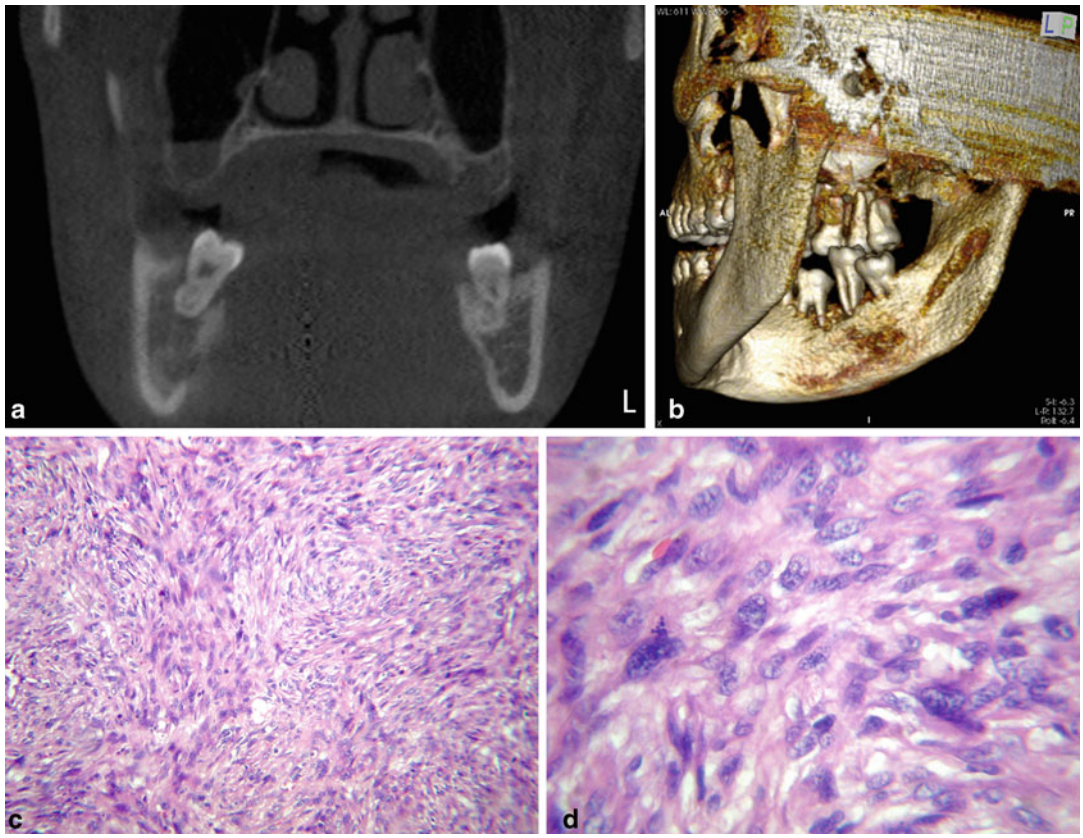

Fig. 103 Fibrosarcoma. CT of large soft tissue mass extending from the floor of the mouth, affecting the right side of the tongue, altering the air spaces, and invading the right mandibular bone (**a**) causing irregular osteolytic destruction affecting dental support (**b**). Intermediate (**c**) and high magnification (**d**) of the lesion characterized by fusiform cells with nuclear atypia, numerous atypical mitotic figures forming whorls, in a storiform pattern (Hematoxylin and eosin stain)

The histological appearance of high-grade fibrosarcoma may be similar to other tumors, such as malignant fibrous histiocytoma, liposarcoma, or synovial sarcoma (Fig. 103). Fibrosarcoma can be graded as low- or high-grade malignancy. Low-grade fibrosarcoma shows spindle cells arranged in fascicles with low to moderate cellularity with a herringbone appearance. There is a mild degree of nuclear pleomorphism and rare mitosis, with a collagenous stroma. High-grade lesions show intense nuclear pleomorphism, greater cellularity, and atypical mitosis. The nuclei can be spindle shaped, oval, or round. Positive immunostaining for vimentin, together with negativity for muscular immune markers, helps to diagnose fibrosarcoma (Soares et al. 2006).

Treatment

Wide local excision remains the treatment of choice, with at least 1 cm of margin confirmed by histopathologic clearance. Unfortunately, it is often difficult to achieve complete resection of the tumor, and high recurrence rates have been observed with surgery alone.

Radiotherapy is mandatory when adequate safety margins cannot be obtained and salvage surgery is not possible. On the other hand, there is a significant number of radiotherapy-induced sarcomas of the head and neck region.

Adjuvant chemotherapy for sarcomas has been applied in tumors of the trunk and extremities, as well as in the head and neck. Although some reports have raised the possibility of some benefit in certain types of sarcomas, the benefit of adjuvant chemotherapy with regard to prolonged survival remains controversial. Chemotherapy is most commonly employed in the setting of attempted control of metastatic disease. Its role in adjuvant therapy aimed at cure is not established (Eeles et al. 1993).

Liposarcoma

Epidemiology, Etiology, and Pathology

Liposarcomas are malignant neoplastic proliferations of mesenchymal cells with adipocyte phenotype (2017). According to its grading and differentiation, the neoplastic cells show variable capability of lipid storage, generally assuming a multivacuolated form. Factors considered to be important in the etiology of liposarcoma include genetics, trauma, and irradiation.

Three biologic categories of liposarcomas are distinguished: well-differentiated/dedifferentiated, myxoid, and pleomorphic. The most common type is the well-differentiated/dedifferentiated type, and the most affected sites in the head and neck region are the pharynx, mouth (usually related to the tongue), larynx, and neck.

Liposarcoma of the head and neck region represents approximately 1% of head and neck sarcomas. Although considered a rare tumor of the head and neck region, liposarcomas usually affect older males, ranging from 40 to 60 years of age (Golledge et al. 1995).

Clinical Features

Despite its malignant nature, the tumor has a slow growth pattern, as a painless submucosal fatty-fibrous texture that can sometimes ulcerate. Depending on the location of the tumor, other symptoms can also be noted such as airway obstruction or dysphagia.

Investigations

The microscopic appearance of the most common type of liposarcoma is characterized by adipocytes of variable size, with hyperchromatic and enlarged nuclei. The surrounding fibrous tissue also presents atypical features. Non-lipogenic areas of dedifferentiation present with pleomorphic cells such as spindle cells, round cells, and giant cells or even fibroblast-like appearance in a myxoid matrix. Immunohistochemical panels include MDM2 and CDK4 positivity in 90% of tumors.

Treatment

Surgical excision is the treatment of choice for liposarcomas. The lesion has a high recurrence rate, up to 50%. There is a direct relationship with tumor site and grading with the prognosis of treatment. Oral liposarcoma is associated with a poor outcome despite the high proportion of low-grade tumors.

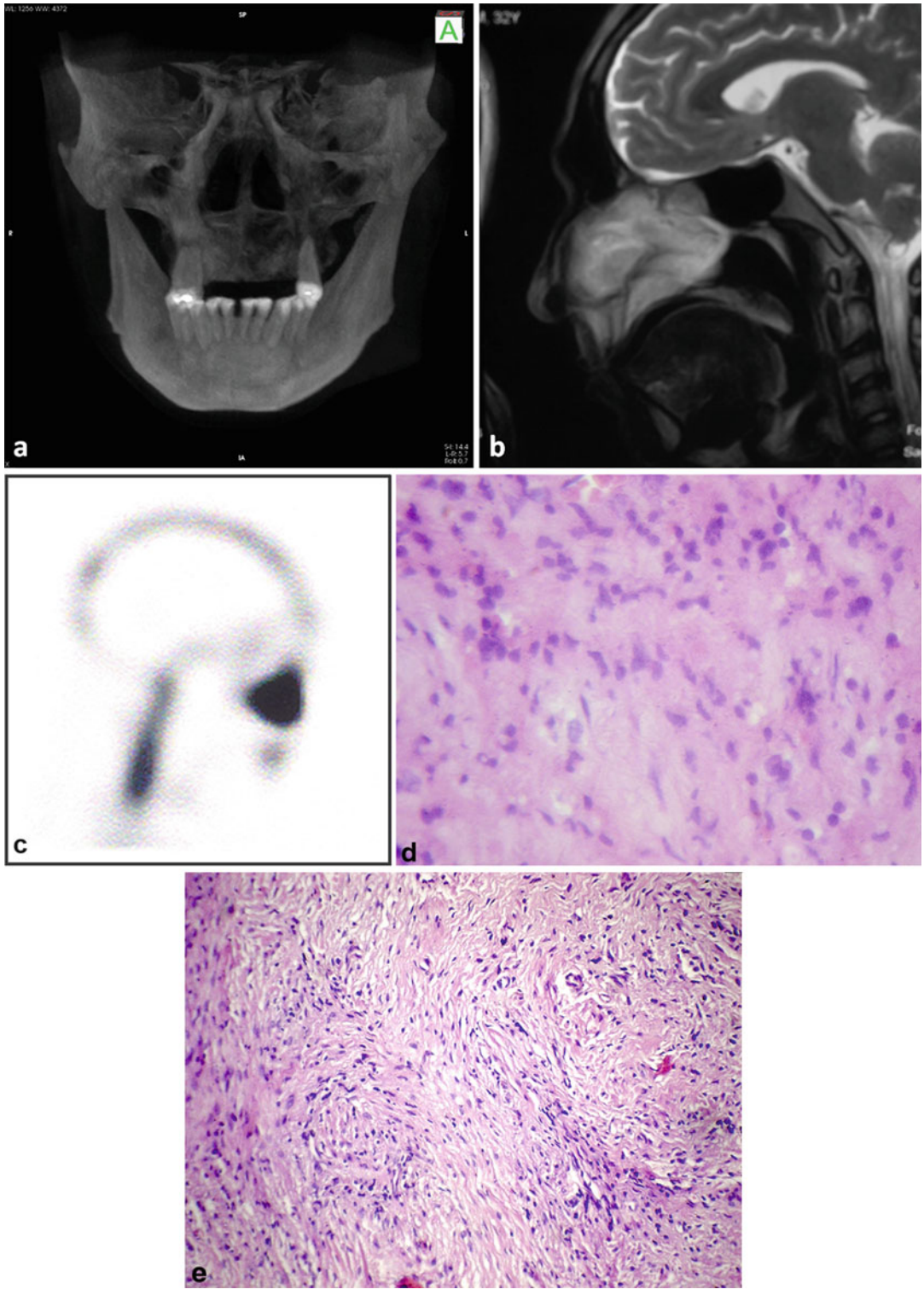

Fig. 104 (continued)

Malignant Peripheral Nerve Sheath Tumor

Epidemiology, Etiology, and Pathology

The malignant peripheral nerve sheath tumor (MPNST) also known as malignant schwannoma, neurofibrosarcoma, and malignant neurilemmoma is characterized by malignant proliferation of the soft tissues by peripheral nerves or benign nerve sheath tumors, with variable differentiation toward one of the cellular components of the nerve sheath, such as Schwann cells, fibroblasts, or perineural cells (Fig. 104) (Anghileri et al. 2006).

About 20% of all MPNSTs develop in the head and neck, representing 5% of all soft tissue sarcomas. As mentioned above, MPNST has a strong correlation with NF type 1 syndrome, affecting up to 25–30% of the patients with this particular syndrome. The peak occurrence of this lesion is during adulthood, during the third and fourth decades of life.

Clinical Features

MPNST can arise de novo or from a pre-existing neurofibroma. The most affected nerves of the head and neck region are the vagal and vestibular nerves. Malignant transformation of a pre-existing schwannoma is possible but considered to be rare. Symptoms include pain associated with a rapid growing mass, which may also compromise motor or sensory neural function (Eeles et al. 1993).

Tumors may present as a white, solid, firm consistency within or attached to a nerve trunk or neurofibroma. Sometimes the development of tumors in intraosseous neural branches can produce local enlargement of the nerve canal with or without bone destruction of the surrounding bone. Pseudocystic spaces originating from hemorrhage or focal necrosis may be observed during surgical incision of the tumor.

Investigations

Microscopic investigation of MPNST reveals an unencapsulated lesion, with highly infiltrative cells with different morphotypes such as epithelioid, pleomorphic, small round cells and spindle-shaped cells. The lesion is composed of interlacing fascicular arrangements, forming variable patterns, with highly cellularized areas of vacuolated cells with a myxoid matrix, alternating to whorls of storiform formations, with palisaded cells, sometimes assuming a rosette formation. The nuclei are large and hyperchromatic, sometimes small, and other times fusiform with eventual atypical mitosis or binucleated cells. The tumors are graded low grade and high grade according to their mitotic index, number of atypical mitosis, pleomorphism, and necrosis (Fig. 104).

Immunohistochemical investigation of the lesion is frequently necessary, as other sarcomas can present similar morphological features. This is essential for small incisional biopsies. The immunohistochemical panel should include S-100, SOX10, and nestin strong positivity, and cytokeratins, EMA, and CD34 may be positive, but their expression has not been described in the epithelioid variant. Genetic investigation of NF1 is also recommended if the patient has no other evident signs. There is loss of NF1 on 17q11 and TP53 on 17q13 (2017).

Treatment

MPNSTs are treated with radical surgical excision. The aggressive behavior of the lesion is frequently associated with large lesions. It is the main cause of death of NF1 patients representing up to 25% of deaths of NF1-affected patients. Therefore, to discover these tumors as early as possible, patients with NF1 syndrome should be followed carefully, because of the likelihood that they may develop MPNSTs. Presentation with either primary or recurrent disease, tumor size,

Fig. 104 Malignant peripheral nerve sheath tumor. CT scan of an irregular osteolytic lesion of the left maxilla (**a**). T2-weighted MRI revealing the extension of the lesion in the maxilla (**b**). Bone scintillography imaging showing increased radiotracer accumulation in the affected area (**c**). Fascicles of atypical fusiform cells with irregular nuclei forming variable patterns with highly cellularized areas of vacuolated cells with a myxoid matrix (**d**), alternating with whorls of storiform formations and palisaded cells (**e**) (Hematoxylin and eosin stain)

and tumor location have major importance with regard to prognosis. Complete tumor resection with negative margins should be the objective of surgery (Minovi et al. 2007).

The recurrence rate is as high as 40%, and adjunctive radiotherapy and chemotherapy are often required, but the lesion usually metastasizes to the lungs and bone. Adjuvant radiation therapy should be delivered to improve local control and may also be beneficial for survival. High-grade and large MPNSTs have particularly aggressive behavior, and thus patients with these tumors should be considered for new adjuvant medical treatments.

Kaposi Sarcoma

Epidemiology, Etiology, and Pathology

Kaposi sarcoma (KS) is an angioproliferative malignant neoplasia of endothelial cells forming an infiltrative capillary-rich lesion that eventually disseminates to multiple cutaneous sites, viscera, and lymph nodes. Kaposi sarcoma was first described by Moritz Kaposi in 1872 as "idiopathic multiple pigmented sarcomas of the skin." Until the HIV pandemic in the 1970s and 1980s, KS was considered a rare and usually nonaggressive lesion. After the pandemic infection with HIV virus, lesion incidence arose as one of the diseases related to acquired immunodeficiency syndrome (AIDS) with aggressive behavior becoming one of the major causes of death among AIDS patients.

Today KS is known to be caused by HHV8 infection of endothelial cells. HHV8 is found in immunocompetent people and is active in immunosuppression. In fact in the beginning of the twenty-first century, it was discovered that Tat protein produced by lymphoid cells infected with HIV promoted the infection of HHV8, contributing to the highly aggressive nature of AIDS-KS by inducing inflammatory cytokines and angiogenesis (Moore and Chang 1995; Gallo 1998; Aoki and Tosato 2004).

Until the AIDS epidemic, this tumor was identified in three different settings: classic KS (a slowly growing tumor particularly prevalent among elderly men of Mediterranean or Jewish ancestry), African-endemic KS, and immunosuppressive drug-related KS. All these forms of KS share a similar histopathology that has been divided into different progressive stages correlating with both clinical appearance and progression of lesions. AIDS-associated KS is the most frequent tumor of human immunodeficiency virus type I (HIV-l) infection and the most aggressive and rapidly growing form of KS in AIDS, with early dissemination in the skin and viscera. In spite of the clear clinical differences, the histopathology of the various KS forms is essentially the same, with characteristic changes related to stage in the development of the KS tumor. Only the AIDS-related type is associated with oral manifestations. As many as 20% of individuals with HIV-1 infection develop oral KS, usually in the fourth to fifth decades of life.

The incidence of KS has dramatically decreased in both the United States and Europe in the era of highly active antiretroviral therapy (HAART). However, KS remains the second most frequent tumor in HIV-infected patients worldwide and has become the most common cancer in sub-Saharan Africa. Since the beginning of the AIDS pandemic, AIDS-related KS has been more prevalent in homosexual and bisexual men.

Clinical Features

The most affected oral location of KS is the hard palate, followed by the gingiva and tongue (Figs. 105-108). Up to 70% of patients with cutaneous AIDS-related KS also have oral lesions. Multiple patches and papules with bluish to purple color are the most common skin and mucosal presentations (Fig. 105). With the progression of the disease, the patched lesions develop to a nodular stage (Fig. 108). Intraoral advanced lesions may present with hemorrhage, pain, ulceration, and secondary infections. Highly aggressive lesions are infiltrative, involving soft tissue and bone (Chen et al. 2014). These lesions may disseminate compromising visceral organs and lymphatic nodes.

Investigations

Early "patch-stage" KS lesions are histologically characterized by the proliferation of small and

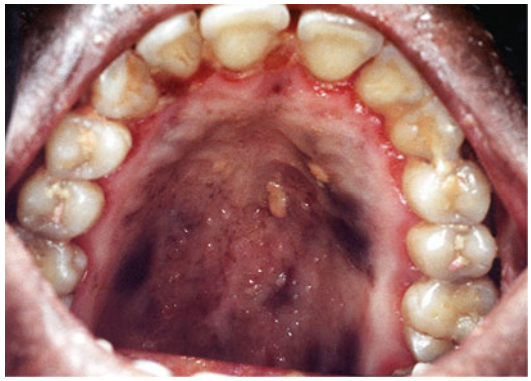

Fig. 105 Multifocal macular AIDS-related Kaposi sarcoma and aggressive periodontal disease in 29 years old Zambian male. (Image courtesy of Dr Tim Hodgson, Eastman Dental Institute, University College London, UK)

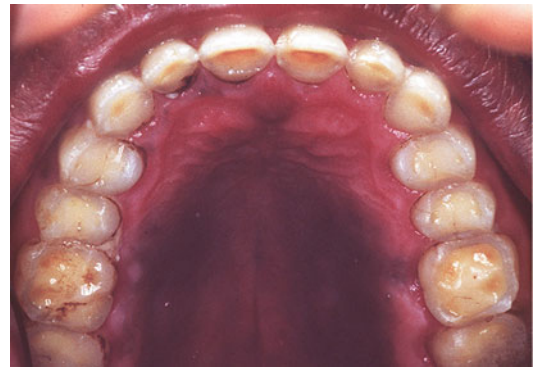

Fig. 107 Extensive diffuse AIDS-related Kaposi sarcoma and tooth wear in a 45 year old Malawian male. (Image courtesy of Dr Tim Hodgson, Eastman Dental Institute, University College London, UK)

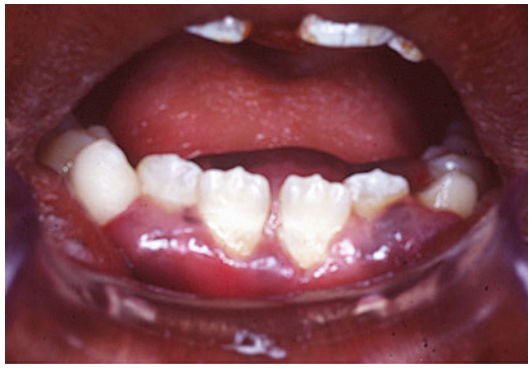

Fig. 106 Gingival AIDS-related Kaposi sarcoma in 9 year old Malawian female. (Image courtesy of Dr Tim Hodgson, Eastman Dental Institute, University College London, UK)

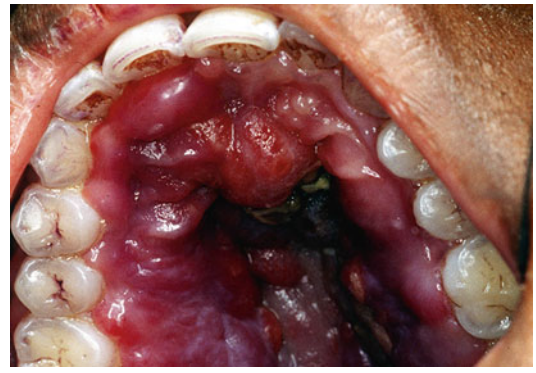

Fig. 108 Nodular palatal AIDS-related Kaposi sarcoma in 28 years old Zambian female. (Image courtesy of Dr Tim Hodgson, Eastman Dental Institute, University College London, UK)

jagged endothelial-lined spaces surrounding normal dermal vessels and irregularly shaped, slit-like vascular spaces dissecting collagen bundles, often parallel to the epithelium, with extravasated erythrocytes and lymphocytes. The more advanced stages of KS consist of the accumulation of spindle-shaped cells, which are considered to be the tumor cells of KS, showing intra- and extracellular hyaline globules and increased mitotic activity.

The histologic differential diagnoses of Kaposi sarcoma include angiosarcoma, fibrosarcoma, arteriovenous malformations, and spindle cell hemangioendothelioma. Clinicopathological features, mainly immunohistochemical studies, help to exclude these differential diagnoses. Immunohistochemical investigation of KS targets HHV8 primarily, but podoplanin (D2-40), LYVE1, VEGFR3, PROX1, CD34, CD31, and ERG are also positive.

Treatment

The behavior and thus the treatment of KS depend on a number of factors such as the form of the disease, the symptoms, the location and extent of the lesion, the immunocompetence of the patient, and the general medical condition of the patient. Local excision, radiation therapy, chemotherapy, and the adjustment of immunosuppressive medications can all be considered (La Ferla et al. 2013).

Local recurrence is common in AIDS-KS patients, but survival is more related to the immunological status of these patients; the mortality rate can reach 20–25%. In patients with iatrogenic KS associated with immunosuppressants for rheumatic disease, tumor regression occurs in response to treatment in about two-thirds of cases. Primary mucosal KS appears to have a similar prognosis to that of the typical cutaneous form presenting on the extremities. Localized nodular KS has the best prognosis, with few deaths directly attributable to KS.

Clinical classification of KS may be the best prognosticator, comparing localized nodular disease, locally aggressive disease, and generalized KS. The association between the aggressive clinical course of classic KS and immunosuppression has previously been suggested. The immunological dysfunction underlying classic KS is unknown and may result from advanced age or chronic infection. Its induction by immunosuppressive therapy and its subsequent regression on removal of immunosuppression provided early clinical recognition of the reversibility of classic KS (Gallo 1998).

Angiosarcoma

Epidemiology, Etiology, and Pathology

Angiosarcoma, also referred to as hemangiosarcoma and lymphangiosarcoma, is a rare malignant tumor of vascular endothelial cells, representing 2% of all sarcomas. They appear during middle age, and their prognosis depends on location, size, and degree of tissue invasion. Angiosarcoma occurs predominantly in the elderly and is confined to the face and the scalp region in more than 50% of cases but has been described in the spleen, bone, liver, and breast. Most angiosarcomas of the head and neck arise in the dermis of the scalp and upper half of the face. Oral and salivary gland angiosarcomas are rare tumors in adults that generally behave more favorably than do angiosarcomas in other locations, regardless of grade.

There are three main types of angiosarcoma of the head and neck: idiopathic angiosarcoma of the head and neck in elderly patients, lymphoedema-associated angiosarcoma (Stewart-Treves syndrome), and postirradiation angiosarcoma. Besides an association with persistent chronic lymphoedema, previous irradiation, and pre-existing vascular malformation, little is known regarding the causative factors of this disease. With respect to pathogenesis, among others, upregulation of the glycopeptide VEGF-D, a vascular endothelial growth factor, seems to be responsible for endothelial cell proliferation.

Clinical Features

Clinically the appearance of an angiosarcoma of the head and neck region can be variable. Early lesions most commonly present as single or multifocal ill-defined, bruise-like erythematous-purplish areas with indurated borders. Sometimes it may resemble hematoma-like lesions, being misinterpreted as benign inflammatory or allergic hyperemias. More advanced lesions can present as dark bluish, sometimes keratotic papules or nodules with ulceration and bleeding, mimicking other malignancies like squamous cell carcinoma, basal cell carcinoma, malignant melanoma, lymphoma, and metastases. Tumors usually extend transdermally for far wider distances than their clinical appearance suggests (Ettl et al. 2008; Trevino-Gonzalez et al. 2009).

Investigations

Microscopically a cutaneous angiosarcoma is typically characterized by numerous, irregular, and anastomosing vascular channels. These are lined by pleomorphic, hyperchromatic endothelial cells with variable mitotic activity (Fig. 109). Immunohistochemical positivity for the endothelial markers CD31 and factor VIII-related antigen as well as for the transcription factor Fli-1 may help to establish diagnosis. The differential diagnosis includes hemangioma, especially tufted, cavernous, and epithelioid hemangioma on the one hand and acantholytic carcinoma on the other hand. Especially in immunocompromised patients, Kaposi sarcoma might be a further differential diagnosis. Lack of cytoplasmic hyaline globules, spindled cells with distinctive cytoplasmic borders, and scattered plasma cells distinguish angiosarcoma from Kaposi sarcoma.

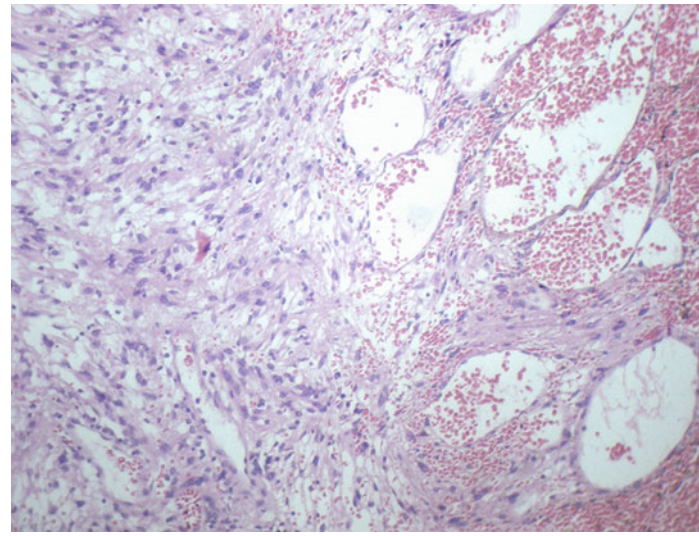

Fig. 109 Angiosarcoma. Vascular spaces delimited by pleomorphic hyperchromatic endothelial cells in a cellular stroma with fusiform and vacuolated cells (Hematoxylin and eosin stain)

Morphologically, oral and salivary gland angiosarcoma differs from that of angiosarcoma elsewhere (Fanburg-Smith et al. 2003). Although the most common angiosarcoma morphology in the oral and salivary gland location is spindled vasoformative and solid, one-third of oral and salivary gland angiosarcomas in the literature are the unusual epithelioid angiosarcoma variant. The epithelioid subtype is composed of plump atypical round cells with prominent nucleoli and definite intracytoplasmic lumina containing red blood cells (i.e., epithelioid endothelial cells).

Treatment

Radical surgery with ample margins is the treatment of choice in patients with head and neck angiosarcoma. Generally, the treatment of angiosarcoma is based on radical surgery and postoperative radiation therapy. Surgery is postulated to attain a wide excision of the tumor with histologically negative margins. Unfortunately achieving negative margins is difficult, as multifocal and extensive microscopic spread is common in this disease. Intraoperative frozen sections are often performed to assist in determining section margins (Morrison et al. 1995).

Radiation-induced angiosarcomas of the oral cavity, like non-oral primary angiosarcomas, are reported to behave poorly, with early onset of metastases and death within 2 years after treatment.

Angiosarcoma of the skin or soft tissue of the head and neck is associated with a 50% mortality rate within the first 25 months and a 12% survival rate at 5 years, compared to nasal cavity or paranasal sinus angiosarcoma, which have a 22% survival rate at 5 years according to grade of differentiation and early diagnosis. Because of this pattern of diffuse, clinically undetectable spread, the disease is very difficult to treat surgically, and long-term results using surgery alone have been very poor.

Leiomyosarcoma

Epidemiology, Etiology, and Pathology

Leiomyosarcoma is a malignant smooth muscle tumor, considered a rare lesion of the head and neck, with mostly case reports published in the literature. In the head and neck, smooth muscle is sparse and found mainly in the walls of blood vessels and in the erector pili musculature of the skin. It is presumed that these are the cells of origin of such tumors. These tumors are more likely to be found in adults ranging from third to seventh decades, with little predominance in men. Pediatric cases are described to represent the most aggressive forms.

Clinical Features

The lesion is poorly circumscribed, with firm consistency on palpation, usually measuring more

than 2.5 cm, and can sometimes present with hemorrhage and necrosis. The lesions may affect the skin, scalp, neck, nose, tongue, gingiva, maxillary sinus, and hard and soft palate. Due to the rarity of the lesion, a preferred site in the head and neck region is inconclusive (Mindell et al. 1975; Montgomery et al. 2002).

Investigations

Microscopically, typical features of leiomyosarcoma consist of perpendicularly arranged fascicles of spindle cells with eosinophilic delicately fibrillary cytoplasm, hyperchromatic blunt-ended nuclei, and scattered paranuclear vacuoles growing in interlacing cords of cells with tapered nuclei and delicate tiny nucleoli. Nuclear palisading and myofibrils could also be noticed in well-differentiated lesions, but high-grade tumors exhibit more anaplastic features such as large, bizarre, pyknotic nuclei and a large number of mitotic figures. The lesions are mostly well circumscribed, although infiltrative areas may be noted at the periphery. Leiomyosarcomas in the head and neck tend to be more inflamed than leiomyosarcomas elsewhere.

Immunohistochemistry panels for leiomyosarcoma include smooth muscle actin (+), muscle-specific actin (+), desmin (+), cytokeratin (−), S100 protein (focally), myogenin (eventually +), CD34 (−), and Ki67 (5–50% nuclear staining). The differential diagnosis of adult spindle cell tumors in this site includes primarily spindled carcinoma and melanoma, other sarcoma types, and various benign fibrous tumors and pseudotumors. Spindle cell carcinomas in the head and neck are frequently polypoid mucosal-based tumors. Adequate sampling can sometimes detect an in situ or obviously epithelial infiltrating component, if one is present, and focal cytokeratin expression. However, the surface component can be lost by ulceration, and many spindle cell carcinomas are cytokeratin-negative yet can occasionally express immunoreactivity for actin. Sarcomas that should be distinguished from leiomyosarcoma in this area include myofibrosarcoma, fibrosarcoma, malignant nerve sheath tumor, malignant fibrous histiocytoma, and rhabdomyosarcoma. The latter is of the most clinical importance. Distinction among the others is less important than assigning a histological grade.

Treatment

Radical surgical excision with clear margins is always the preferred treatment for leiomyosarcomas. These tumors are likely to recur if incompletely excised, and morbidity relates to adequacy of surgical excision. However, the majority of leiomyosarcomas in the head and neck are aggressive intermediate- or high-grade tumors with little response to adjuvant therapy.

Rhabdomyosarcoma

Epidemiology, Etiology, and Pathology

Rhabdomyosarcomas (RMS) are malignant neoplasms of skeletal striated muscle cells. The head and neck are the most common anatomic sites for rhabdomyosarcoma, with an incidence currently placed at 0.104 cases per 100,000. Rhabdomyosarcomas are the most common soft tissue sarcomas in children and adolescents, accounting for 5–8% of all childhood malignancies. In contrast, it is rare in adults, occurs more frequently in the extremities, and is not as well characterized clinically and pathologically in the head and neck region.

The WHO classification divides rhabdomyosarcomas into four clinicopathologic variants: embryonal (ERMS), alveolar (ARMS), spindle cell-sclerosing (SRMS-ScRMS) RMS, and pleomorphic RMS. ERMS is the most common variant and occurs in younger patients. ARMS is the second most common variant and has a predilection for older children and young adults. Pleomorphic RMS is a rare variant, usually diagnosed in patients over the age of 45.

Although most RMS have a sporadic presentation, in a small subset of patients, RMS is part of a genetic syndrome, such as Beckwith-Wiedemann, Von Recklinghausen disease, Costello, Noonan, Gorlin, Rubinstein-Taybi, and Li-Fraumeni syndromes.

Clinical Features

The clinical presentation of head and neck RMS is divided into three subsites based on its anatomic location and local relapse: parameningeal (PM), including the paranasal sinuses, nasopharynx, nasal cavity, middle ear, mastoid, parapharyngeal region, pterygopalatine, and infratemporal fossa; orbital; and non-PM/non-orbital site, encompassing the neck, face, oral cavity, cheek, external ear, scalp, and larynx. PM subsite is the most common presentation and is associated with the least favorable outcome compared to other locations (Chen et al. 2017).

Investigations

Head and neck rhabdomyosarcoma in adults can manifest both classic and unique histologic features for each subtype. ERMS shows a morphologic resemblance to fetal skeletal muscle. ARMS, having a histological appearance of undifferentiated small blue round cells, is arranged in a variable alveolar or solid pattern. Spindle cell RMS (SRMS) is composed of monomorphic spindle cells arranged in intersecting fascicles, lacking overt rhabdomyoblastic differentiation (Fig. 110). A subset of SRMS display areas of hyaline sclerosis suggesting a morphologic overlap with the even less common sclerosing RMS (ScRMS). ScRMS may show an undifferentiated round cell component arranged in a pseudovascular or pseudoalveolar pattern in a prominent hyalinized stroma. SRMS-ScRMS represent a rare and recently recognized standalone pathologic entity, separated from the broad spectrum of ERMS. Pleomorphic RMS has a morphologic appearance of large pleomorphic cells.

Although no genetic abnormality prevails, small subsets of ERMS harbor loss of heterozygosity (LOH) at 11p15, as well as FGFR4, P53, BCOR, ARID1A, and RAS mutations, as shown in recent large genomic studies. The genetic hallmark of ARMS is either the more common t(2;13)(q35;q14) translocation or the t(1;13)(q36;q14) resulting in the PAX3-FOXO1 or PAX7-FOXO1 fusion, respectively (Owosho et al. 2016). SRMS-ScRMS share genetic alterations, although these vary depending on the clinical presentation: recurrent NCOA2 and VGLL2 related fusions in congenital/infantile setting, which are associated with a favorable outcome, or MYOD1-mutations in older children and adults which are associated with a poor prognosis (Kohsaka et al. 2014; Szuhai et al. 2014; Rekhi et al. 2016).

Treatment

The management of head and neck RMS remains challenging due to an increased failure of local control as well as a high rate of early metastases and high stage and recurrence rates, with often limited benefit from surgical management due to its proximity to vital structures. In the last three decades, RMS outcomes have improved significantly due to evolving multidisciplinary therapy paradigms, such as improved surgical techniques, aggressive chemotherapy regimens, and more effective conformal intensity-modulated radiotherapy. In adults, RMS presents an aggressive clinical behavior regardless of subtype. The prognostic factors in head and neck RMS have been multifactorial, such as age, tumor site, overall stage, distant metastases, histologic variant, nodal status, and status of primary surgical site (Agaram et al. 2014).

In children, RMS occurring in the head and neck tends to have favorable outcomes except for tumors arising in parameningeal sites such as the nasal cavity, paranasal sinuses, infratemporal fossa, and mastoid. Poorer outcomes for tumors in these sites are due in part to difficulty in achieving complete resection from these areas. Embryonal RMS is associated with the most favorable outcome compared to other variants. Alveolar RMS is associated with a poor prognosis. The 5-year overall survival rate of childhood RMS has risen to 62%, and the 5-year relative survival rate is estimated at 63%.

Tumors of the Temporomandibular Joints

Tumors of the temporomandibular joint (TMJ) are rare but comprise a broad spectrum of lesions. Given the potential for malignancies to mimic TMJ pathology or remain asymptomatic, the oral

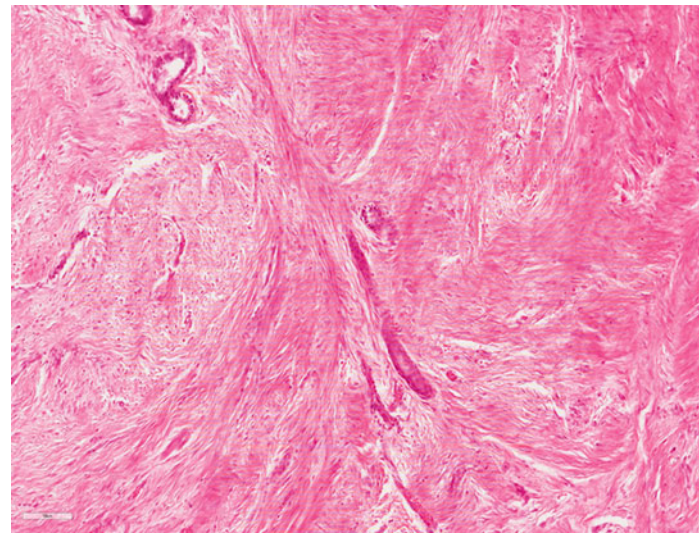

Fig. 110 Rhabdomyosarcoma. Monomorphic spindle cells are arranged in intersecting fascicles, lacking overt rhabdomyoblastic differentiation (Hematoxylin and eosin stain)

medicine clinician should be familiar with changes affecting the TMJ. Lesions discussed in this section constitute a representative sample of tumors involving the TMJ but are far from complete. Various conditions affecting the TMJ are covered in specific chapters such as ▶ "Non-odontogenic Bone Pathology," ▶ "Arthritic Conditions Affecting the Temporomandibular Joint," and ▶ "Internal Derangements of the Temporomandibular Joint." In this section, we only highlight the more common tumors and pseudotumors affecting the TMJ.

The most frequent lesions affecting the TMJ are benign (81.8%); however, the greater majority of these are pseudotumors (synovial chondromatosis (Figs. 111 and 112), pigmented villonodular synovitis (Fig. 113), eosinophilic granuloma, and osteochondroma (Fig. 114)) representing 71.6% of lesions and do not represent true benign tumors (Poveda-Roda et al. 2013). The majority of true tumors are indeed malignant, making up almost two-thirds of cases of true tumors. Of the pseudotumors, the majority present as synovial chondromatosis (61.8%), followed by osteochondroma (24%), pigmented villonodular synovitis (4.4%), and eosinophilic granuloma (4.4%). Of the true benign tumors, chondroblastoma (Fig. 115) represents the largest single entity (17.2%), followed by osteoid osteoma (Fig. 116) (13.8%) and then chondroma, osteoma (Fig. 117), and osteoblastoma (Fig. 118) (10.9% each). Malignant tumors are mostly sarcomas of various types (synovial sarcoma, chondrosarcoma, osteosarcoma) making up 53.8% of malignant disease, followed by metastatic disease (Fig. 119) (32.7%) (Poveda-Roda et al. 2013).

Tumors of the temporomandibular joint are characteristically found in young adults, and because of the scant specificity of their symptoms, many are initially diagnosed and treated as temporomandibular joint dysfunction or derangement (Poveda-Roda et al. 2013). The mean age of presentation is 42 years and 1 month ±16 years and 2 months. Tumors are more common in females. The mean time from symptom onset to consultation is 30 months and 8 days ±41 months and 9 days, and almost 19.6% of cases are initially diagnosed and treated as TMJ dysfunction. The most frequent clinical manifestations are pain, swelling, and the limitation of joint movement. Both clicks and crepitus are more common among the pseudotumors than in true tumors. No significant differences are noted between malignant and benign tumors in terms of joint sounds. Other more specific alterations such as facial asymmetry or occlusal disorders are less common. Occlusion alterations, one of the signs most suggestive of TMJ tumors together with the presence of swelling, are reported in 20.5% of patients. The most

common occlusal disorders are ipsilateral posterior open bite, contralateral cross-bite, and anterior cross-bite (Poveda-Roda et al. 2013).

Many tumors show no radiological alterations on routine panoramic imaging (Fig. 113). Radiolucencies, and especially a poorly defined tumor contour, are suggestive of malignancy (Fig. 119). The most common radiological findings in the case of benign and malignant lesions are radiopacities and radiolucencies, respectively. Radiolucencies are significantly more frequent in tumors (77.8%) than in pseudotumors (22.0%). In contrast, radiopacities are significantly more common in pseudotumors (61.0%) (Figs. 115, 116, 117, and 118) than among tumors (7.4%). No panoramic radiographic alterations are observed in 14.6% of benign tumors and in 7.7% of malignant lesions (Poveda-Roda et al. 2013).

Treatment usually involves surgery, and relapse is observed in 10% of the cases – particularly among malignant tumors. The most frequent treatment method is total or partial synovectomy, which is a commonly used approach for synovial chondromatosis which makes up a large proportion of cases requiring treatment. Arthroscopic treatment is used in 7.3% of cases, and

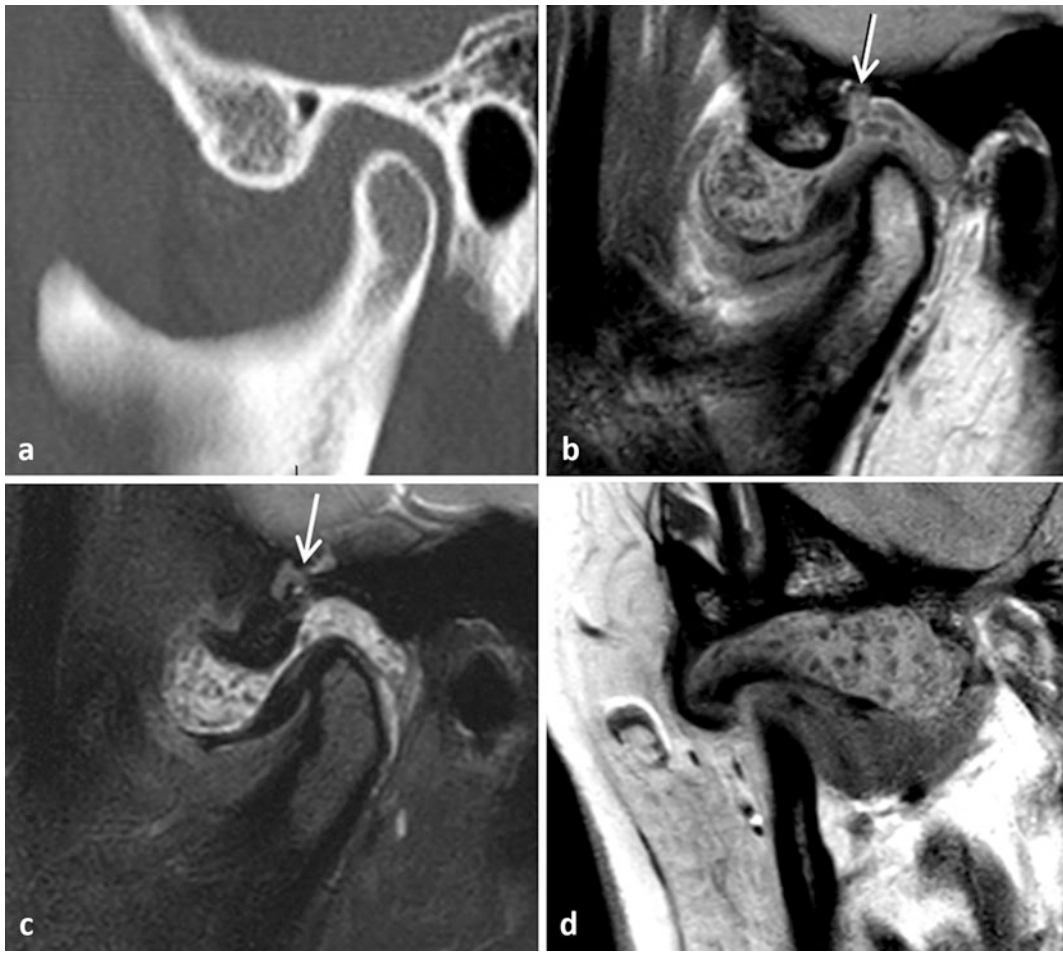

Fig. 111 Synovial chondromatosis with noncalcified bodies in the superior joint space of the right temporomandibular joint. CT sagittal (**a**), proton density sagittal (**b**), fat saturation T2 sagittal (**c**), and coronal proton density MRI (**d**). White arrows in (**b** + **c**) show erosion of the roof of the glenoid fossa. (Images courtesy of Clinical Associate Professor Andy Whyte, Perth Radiological Clinic, Perth WA, Australia)

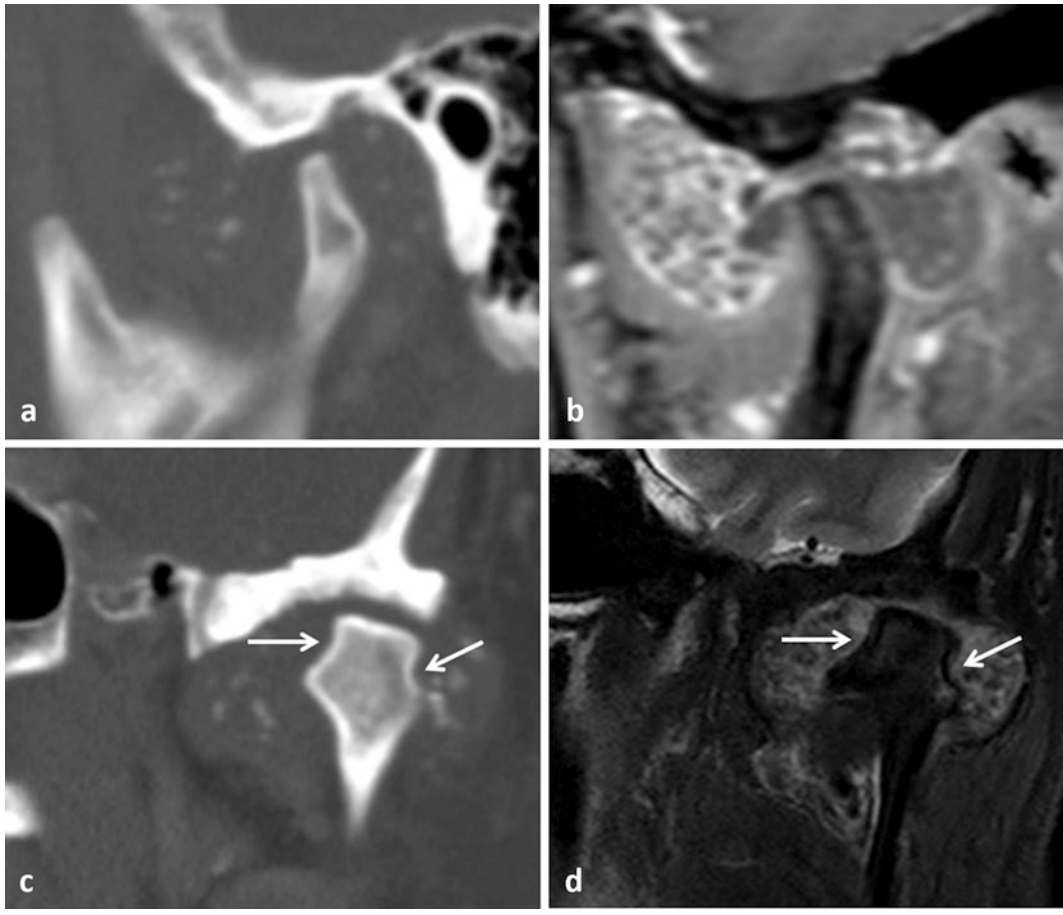

Fig. 112 Synovial chondromatosis with calcified bodies in the superior joint space of the left temporomandibular joint. CT sagittal (**a**), post-gadolinium T1 fat saturation sagittal reconstruction (**b**), CT coronal (**c**), fat saturation T2 coronal (**d**). Synovial proliferation enhances with gadolinium and is hyperintense on T2. The "bodies" are low signal on all sequences whether they are calcified or not. MRI shows many more bodies than CT for this reason. Note remodeled condyle (white arrows in **c** + **d**) probably due to pressure from the distended medial and lateral recesses of the upper joint space. (Images courtesy of Clinical Associate Professor Andy Whyte, Perth Radiological Clinic, Perth WA, Australia)

practically all of these correspond to synovial chondromatosis. The most common surgical procedure in the case of malignant disease is tumor resection with margins, followed by simple tumor resection. Sequelae are noted in 18.2% of cases, with tumor relapse in 9.1%. The most common problems are mandibular deviation, limited range of movement, facial palsy, crepitus, and pain. The 4-year survival rate in the case of malignant tumors of TMJ is 72.2%, with a mean survival of 6 years, in comparison with metastatic disease which presents with a mean survival of 11.4 months. Benign lesions respond well to treatment, with minimal postsurgical complications (Poveda-Roda et al. 2013).

Molecular Aspects of Head and Neck Squamous Cell Carcinoma

Head and neck squamous cell carcinomas (HNSCC) arising from the mucosal epithelia of the head and neck region have diverse etiologies and are managed differently depending on

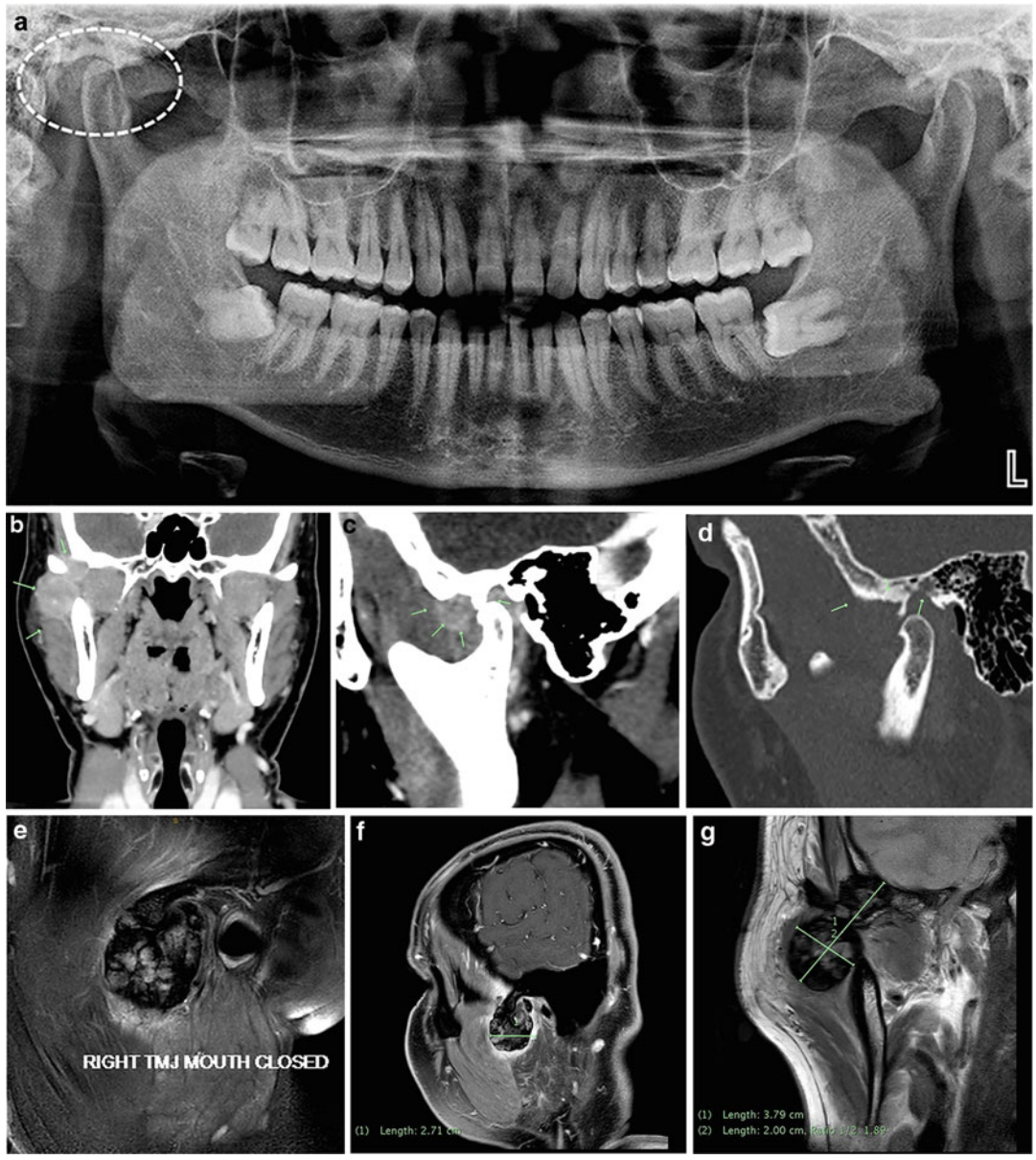

Fig. 113 Pigmented villonodular synovitis. Orthopantomogram (**a**) showing circumscribed lucency overlying the right articular eminence (white dotted oval). No temporomandibular joint arthropathy or other osseous abnormalities are seen. On CT (**b–d**) there is an avidly enhancing 27 × 24 × 27 mm right preauricular mass lesion which appears to be centered within the posterior aspect of the masseter muscle (**b**) and extends anterosuperiorly to involve the posterior aspect of both the medial and lateral pterygoid muscles (**b + c**). This component scallops the greater wing of the sphenoid bone (**d**) and the anterior aspect of the articular eminence of the right temporomandibular joint. There is only a tiny component of the soft tissue that projects into the temporomandibular joint itself. On MRI (**e–g**), there is a large multilobulate mass with dimensions of 36 × 30 × 27 mm (**e–g**) arising within the markedly distended lateral aspect of the anterior recess of the superior compartment of the right temporomandibular joint. The smaller superior lobule represents the component eroding the articular eminence as seen on the CT. The larger inferolateral lobule indents the posterosuperior fibers of masseter and the anteromedial aspect of the superficial lobe of the right parotid gland (**f + g**). On its medial margin, this larger lobule extends to the coronoid notch. The meniscus is normally positioned with an upper compartment effusion and additional small, intra-articular

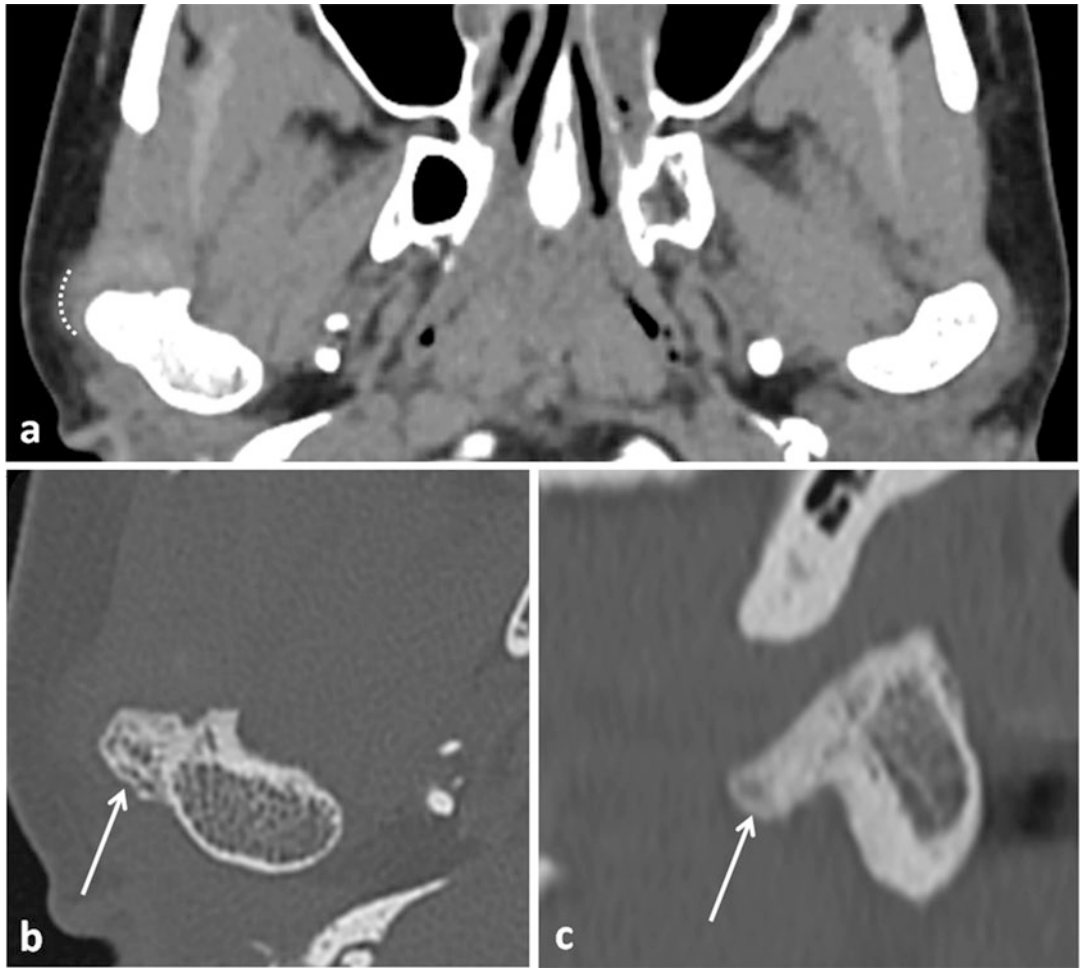

Fig. 114 Osteochondroma of the right condyle. Axial soft tissue CT reconstruction (**a**), axial bone window of the right condyle (**b**), and lateral, bone window, sagittal reconstruction of the right condyle (**c**). An exostosis of cortical and medullary bone projects anteriorly and laterally from the right condyle (white arrows in **b** and **c**). Overlying the bony component, there is a non-ossified cartilage cap (curvilinear white dotted line in **a**). (Images courtesy of Clinical Associate Professor Andy Whyte, Perth Radiological Clinic, Perth WA, Australia)

anatomical site and disease extent. While they may appear to be morphologically similar, molecular studies have underscored the heterogeneity of HNSCC demonstrating that they are instead composed of distinct diseases at the molecular level. While much work remains to demonstrate how these molecular subtypes affect patient and treatment outcomes, the development of

Fig. 113 (continued) foci, the largest of which is situated in the posterior recess and measures 6 mm in diameter. The roof of the glenoid fossa is focally eroded with adjacent synovial proliferation and opacification of overlying mastoid air cells. The enhancement of the lesion and the superior compartment synovitis, capsulitis, and pericapsular edema are consistent with pigmented villonodular synovitis. (Images courtesy of Clinical Associate Professor Andy Whyte, Dr Gavin Chapeikin, and Dr Rudolf Boeddinghaus, Perth Radiological Clinic, Perth WA, Australia)

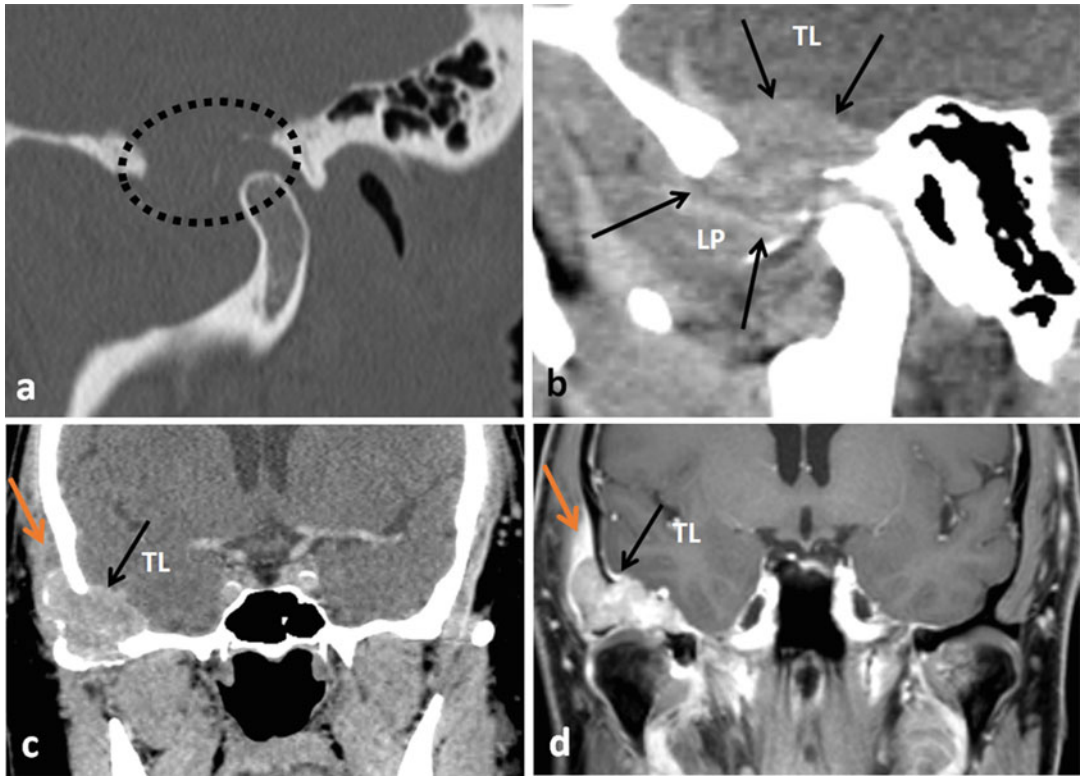

Fig. 115 Chondroblastoma of the right articular eminence, glenoid fossa, and middle cranial fossa. Sagittal bone window CT reconstruction (**a**), sagittal post-contrast CT soft tissue reconstruction (**b**), coronal CT soft tissue reconstruction (**c**), and post-gadolinium, fat saturation, coronal T1-weighted MRI (**d**). There is a large enhancing mass (black arrows) destroying the articular eminence and glenoid fossa (black dotted oval in **a**) which extends superiorly into the middle cranial fossa with mass effect on the right temporal lobe (TL in **b**–**d**). Inferior extension of the tumor into the right lateral pterygoid muscle (LP in **b**) and lateral extension into the temporalis (orange arrows in **c** and **d**) is also present; the latter is more clearly shown on MRI (**d**). (Images courtesy of Clinical Associate Professor Andy Whyte, Perth Radiological Clinic, Perth WA, Australia)

molecular targeted therapies may very well change the way we classify and treat patients with HNSCC.

Cancer is a disease that is driven by genetic alterations, and this can occur at multiple levels, either at DNA, RNA, or protein. With the advent of high-throughput technologies, initially microarrays, array comparative genomic hybridization, and then next-generation sequencing, there currently exists the capability to catalogue genetic alterations that occur in cancer cells to unprecedented detail. This section discusses recent molecular findings in HNSCC and where appropriate how these have impacted on the clinical understanding of the disease. While etiologies, management, and outcomes of HNSCC from different subsites are distinct, much of the literature in HNSCC unfortunately does not distinguish the subsites included in studies and typically include the major sites within the head and neck region such as the oral cavity, oropharynx, hypopharynx, larynx, and less commonly nasopharynx. Therefore, this section covers HNSCC in general, but data on specific subsites is provided where possible.

Genome-Wide Studies

To date, several large-scale genomic studies on the characterization of HNSCC have been completed (Agrawal et al. 2011; Stransky et al.

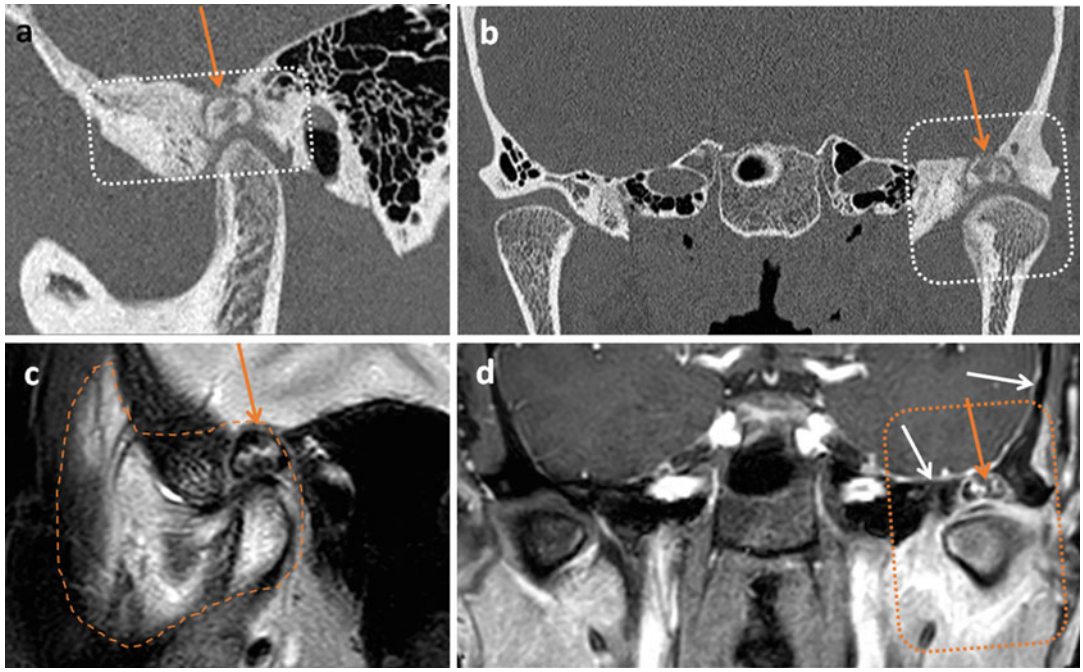

Fig. 116 Osteoid osteoma of the left glenoid fossa and articular eminence; presentation with pain and trismus in a young adult patient. Sagittal bone window CT reconstruction (**a**), coronal bone window reconstruction (**b**), fat saturation T2 sagittal MRI of the left TMJ (**c**), and post-gadolinium, fat saturation T1 coronal MRI (**d**). There is a round sclerotic nidus representing an osteoid osteoma with a lucent margin measuring 10 mm in diameter in the roof of the glenoid fossa (orange arrows). There is diffuse sclerosis of the articular eminence, root of the zygoma, remainder of the glenoid fossa, and to a lesser extent the condyle (white dotted oval in **a**, white dotted square in **b**). Extensive, hyperintense marrow and soft tissue edema is present within the nidus of osteoid osteoma, adjacent sclerotic bone, condyle, joint, and lateral pterygoid muscle (orange dashed outline in **c**). Following gadolinium contrast, the nidus and its lucent margin, joint, surrounding soft tissues, and condylar marrow show diffuse enhancement (orange dotted oval in **d**). Faint enhancement is present in marrow surrounding the nidus in the glenoid fossa with subtle meningeal thickening in the overlying left middle cranial fossa (white arrows in **d**). (Images courtesy of Clinical Associate Professor Andy Whyte, Perth Radiological Clinic, Perth WA, Australia)

2011). The largest and most comprehensive yet is **t**he **C**ancer **G**enome **A**tlas (TCGA) study where 279 head and neck cancer specimens were analyzed comprehensively (2015). This study included specimens from the oral cavity ($n = 172$), oropharynx ($n = 33$), larynx ($n = 72$), and hypopharynx ($n = 2$), and comprehensive analyses revealed chromosomal changes, mutational profiles, and gene expression signatures in HNSCC. This and previous studies unveiled the catalogue of genetic alterations in cancer and provide insights into the possible vulnerabilities within cancer cells that could be targeted for therapeutic purposes.

Copy Number Alterations

Global genetic alterations can be examined at different molecular levels; the most fundamental changes occur at the DNA level. Changes within the DNA have been reported at the chromosomal level where advancements in technology have enabled the examination of these alterations beyond the resolution of classical cytogenetics. Initially analyzed by array comparative genomic hybridization (aCGH) and more recently by single nucleotide polymorphism (SNP) arrays, chromosomal aberrations in terms of loss or gain of focal regions within chromosomes are found to

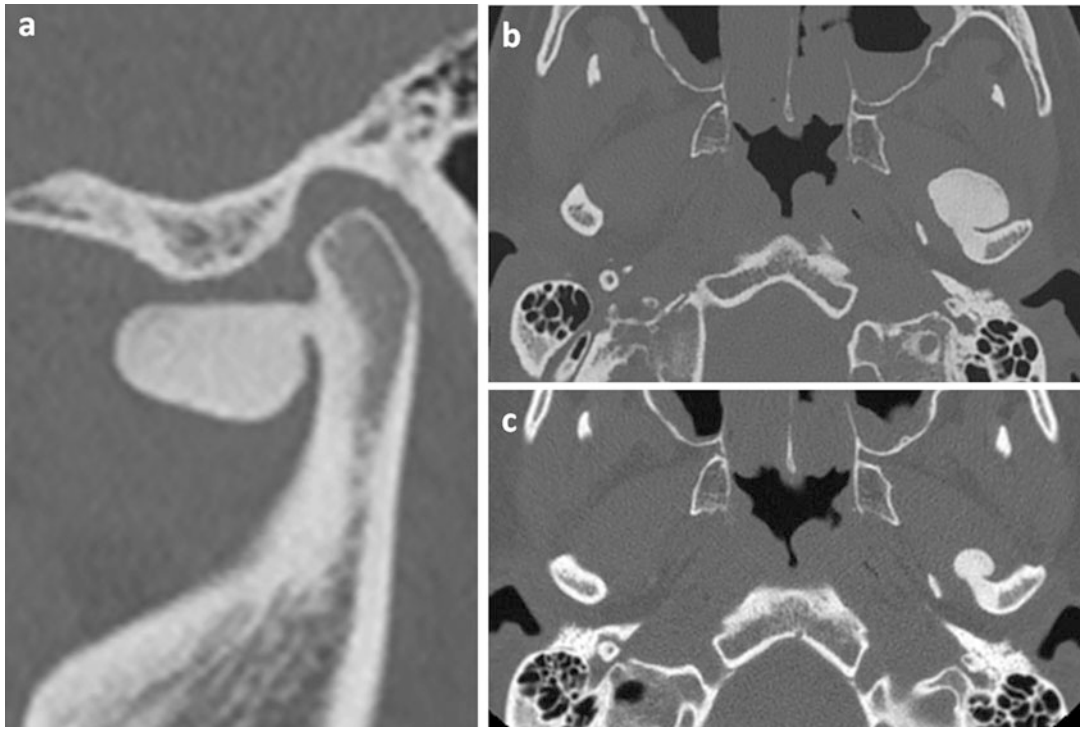

Fig. 117 Osteoma of the left condylar head and neck. CT shows a well-defined pedunculated, dense, sclerotic, ovoid lesion with a maximum length of 15 (AP) × 17 (transverse) × 9 (height) mm, projecting anteriorly from the junction of the left condylar head and neck (**a**). There is diffuse thickening of the anteromedial cortex of the junction of the condylar head and neck contiguous with the pedicle of the described lesion (**b**). This lesion had increased in size significantly as compared with a CT taken 11 years earlier (**c**). (Images courtesy of Clinical Associate Professor Andy Whyte, Perth Radiological Clinic, Perth WA, Australia)

be common in HNSCC. This is perhaps not surprising as a comprehensive analysis of more than 3000 tumors across 12 cancer types showed that HNSCC are broadly categorized as "C" class tumors, where these tumors are largely driven by chromosomal aberrations (Ciriello et al. 2013). Loss of chromosomal regions of 3p and 8p and gains of 3q, 5p, and 8q are found in the majority of HNSCC (Agrawal et al. 2011; Stransky et al. 2011; Seiwert et al. 2015), and these mimic observations in lung squamous cell carcinoma (Cancer Genome Atlas Research 2012). The copy number changes within these regions are consistent with changes in the genes that reside within these regions such as squamous lineage transcription factors TP63 and SOX2 and the oncogene PIK3CA (3q), the c-MYC oncogene (8q), and the fragile histidine triad gene (FHIT) (3p).

When comparing HPV-positive to HPV-negative tumors, differences in chromosomal aberrations are apparent. HPV-positive tumors were characterized by loss of the 11q region (containing the DNA repair gene ATM1), TNF receptor-associated factor 3 (TRAF3) implicated in innate and acquired antiviral responses (Oganesyan et al. 2006), and gain of the transcription factor E2F1. HPV-positive tumors are also less likely to have the deletion of the 9p region containing the CDKN2a gene and amplification of the 7p region which hosts the EGFR gene. By contrast, HPV-negative tumors are characterized by frequent loss of CDKN2a and co-amplification of 11q13 (CCND1, FADD, and CTTN) and 11q22 (BIRC2 and YAP1) regions. Recurrent focal amplifications in receptor tyrosine kinase (EGFR, ERBB2, and FGFR1) are also more likely to occur in HPV-negative cancers (2015).

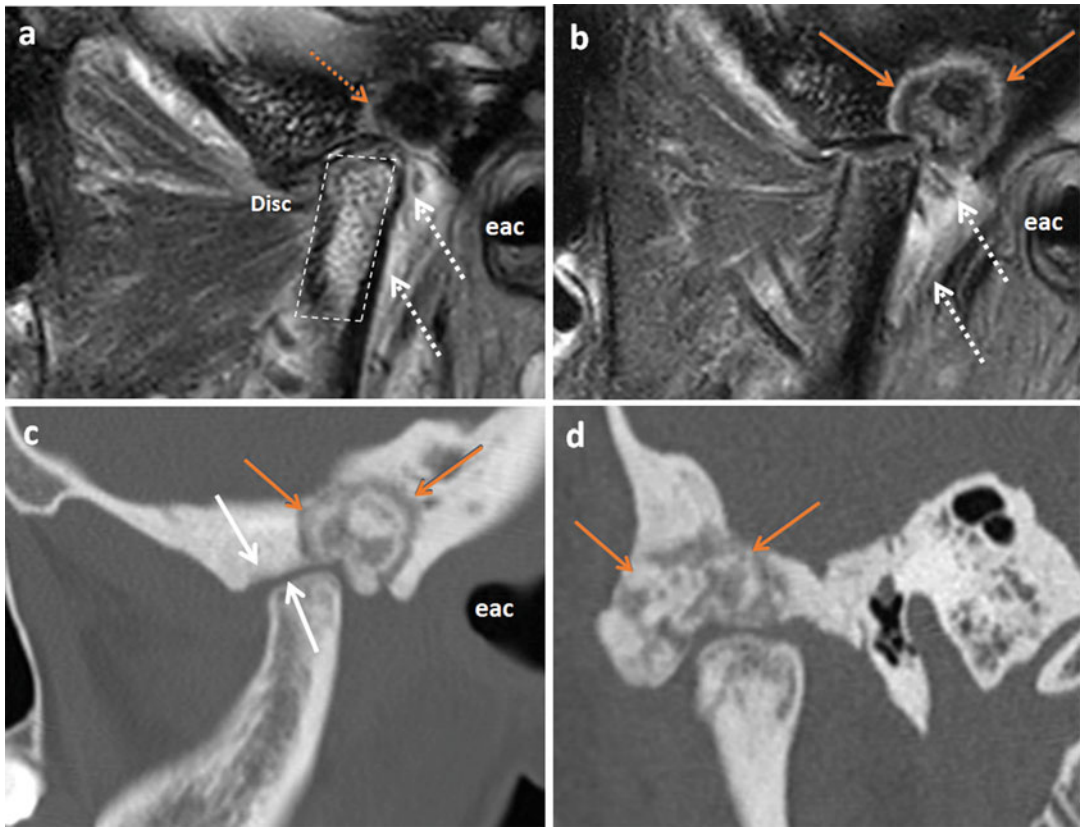

Fig. 118 Osteoblastoma of the right glenoid fossa superimposed on internal derangement, remodeling, and early arthropathy of the right TMJ in a 17-year-old female. Initial fat saturation T2 sagittal of the right TMJ demonstrates an attenuated, anteriorly displaced disc (Disc) and marrow edema in the right condylar head and neck (white dotted oval in **a**) and retro-condylar soft tissue edema (white dotted arrows). There is a subtle band of edema in the roof of the glenoid fossa (orange dotted arrow in **a**). Fourteen months later, there is now a 16 mm, edematous round nidus in the expanded posterosuperior aspect of the glenoid fossa demarcated by more marked marginal edema (orange arrows in **b**) on a similar fat saturation T2 sequence. The condylar marrow edema has resolved; the soft tissue edema posterior to the condyle (white dotted arrows in **b**) is unchanged. The external auditory canal (EAC) is indicated. Sagittal (**c**) and coronal (**d**) CT bone window reconstructions demonstrate the large, sclerotic nidus (orange arrows), an irregular thin relatively lucent margin, and marked adjacent sclerosis and thickening of the temporal bone. There is joint space narrowing, articular surface flattening, and subarticular sclerosis in the TMJ (white arrows in **c**) due to remodeling and early degenerative arthropathy. (Images courtesy of Clinical Associate Professor Andy Whyte, Perth Radiological Clinic, Perth WA, Australia)

Mutations

With the advent of Sanger sequencing in 1977 (Sanger et al. 1977), mutations at the single base level of DNA could be commonly detected. At the start of the twenty-first century, and with the advent of next-generation sequencing which enables massive parallel sequencing, it is now possible to characterize the genome of many organisms to unprecedented depth, allowing the cataloguing of mutations that are associated with diseases including cancer. In 2011, the first literature that comprehensively described the mutational landscape by whole exome sequencing of HNSCC was published, and subsequently other large studies provided further insights into the mutational profiles of HNSCC (Agrawal et al. 2011; Stransky et al. 2011; India Project Team of the International Cancer Genome 2013). These studies reported

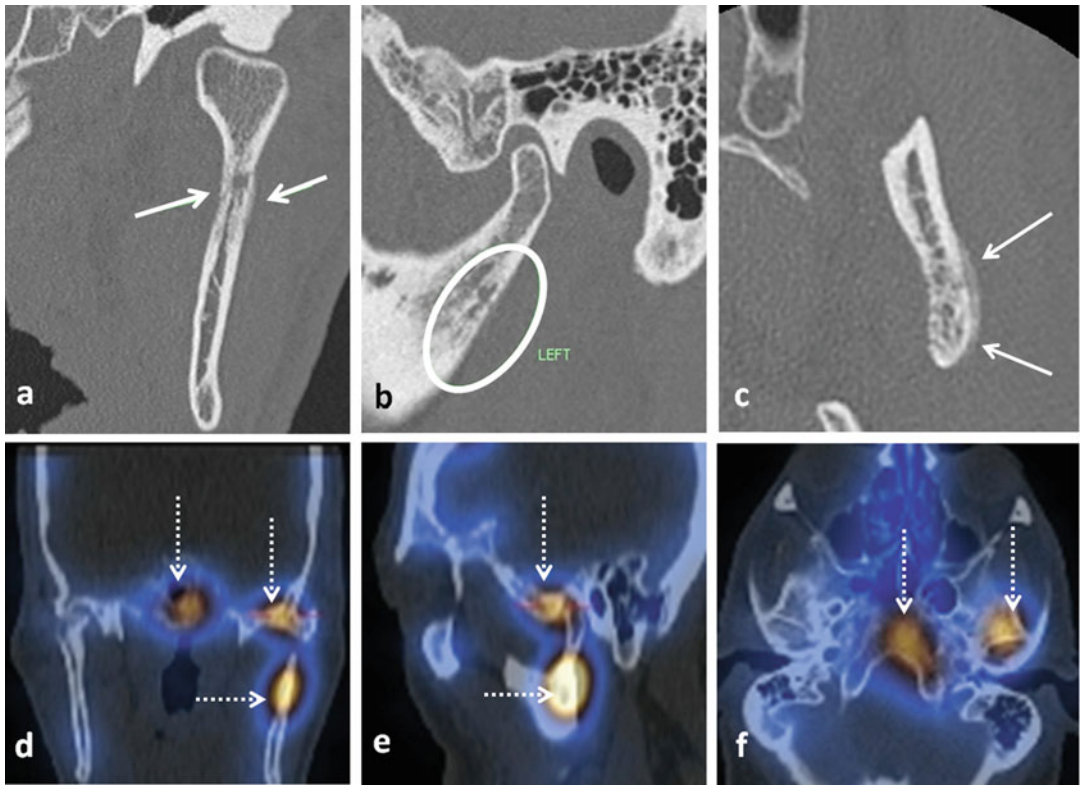

Fig. 119 Metastatic renal cell carcinoma. CT coronal (**a**), sagittal (**b**), and axial of the left condyle and ramus (**c**) demonstrate permeative radiolucency of cortical and medullary bone of the left ramus with buccal periosteal new bone formation (white arrows and white oval). Combined low-dose CT isotope bone scan coronal (**d**), sagittal (**e**), and axial (**f**) images show additional metastases (white dotted arrows) in the clivus and the left articular eminence as well as the lesion seen on CT in the left ramus. (Images courtesy of Clinical Associate Professor Andy Whyte, Perth Radiological Clinic, Perth WA, Australia)

an average of 130 coding mutations per tumor which is comparable with other smoking-related cancers such as small-cell lung cancer and lung adenocarcinomas (Lee et al. 2010b; Pleasance et al. 2010). From the largest of the sequencing studies, mutations were found to be enriched in 11 significant genes (*CDKN2A*, *FAT1*, *TP53*, *CAPS8*, *AJUBA*, *PIK3CA*, *NOTCH1*, *KMT2D*, *NSD1*, *HLA-A*, and *TGFBR2*). The majority of these genes regulate and control critical pathways such as the cell cycle (*CDKN2A*, *TP53*, *AJUBA*), squamous differentiation (*NOTCH1*), or immunosurveillance (*KMT2D*, *HLA-A*). PIK3CA is the only oncogene that achieved statistical significance in HNSCC; however, it is noteworthy that an additional 20% of tumors have PIK3CA amplified without any sign of mutations. Again, distinct differences in the mutational profiles of HPV-positive and HPV-negative tumors were obvious. *CDKN2A*, *TP53*, *AJUBA*, and *FAT1* mutations were more predominantly seen in HPV-negative tumors, and while 86% of HPV-negative tumors had *TP53* mutations, only ~3% of HPV-positive tumors had these mutations (2015). Gain-of-function mutations in *PIK3CA*, E542K, E545K, and H1047R/L are predominantly observed in HPV-positive tumors (2015, Chung et al. 2015; Seiwert et al. 2015). Patients who are HPV-positive and those who are HPV-negative with *TP53* wild-type tumors demonstrated favorable outcomes compared to *TP53* mutants and those with 11q13/CCND1-amplified tumors (2015).

Gene Expression

There are four validated gene expression subtypes of HNSCC (Chung et al. 2004; Walter et al. 2013), namely, basal, mesenchymal, atypical, and classical. More recently these subtypes have been also reported within the TCGA dataset where the largest subtype was basal (31%), followed by mesenchymal (27%), atypical (24%), and classical (18%). By integrating the genomic features with these gene expression subtypes, it is evident that these subtypes are characterized by distinct features (2015). Mutations in *TP53*, *CDKN2A*, 3q amplification, alteration of oxidative stress genes, heavy smoking history, and larynx subsite characterize the classical subtype. The basal subtype is represented by activation of EGFR and is associated with *NOTCH1* mutations, an intact oxidative stress signaling, and fewer alterations of chromosome 3q. Further, the majority of tumors with *HRAS* and *CASP8* co-mutations and with co-amplification of 11q13/q22 were of this subtype. The atypical subtype is defined by lack of chromosome 7 amplifications and enrichment of HPV-positive tumors with activating mutations in *PIK3CA*. The mesenchymal subtype has distinct immunological features, where high levels of alterations in innate immunity genes including high expression of natural killer cell marker CD56 and a low frequency of HLA class 1 mutations are observed, suggesting that this group may respond particularly well to immunotherapy.

Targeting Key Signaling Pathways

To date, the only approved molecular targeted therapy for head and neck cancers is cetuximab, which inhibits EGFR signaling, and the drug is indicated for regionally advanced and metastatic cancers (Baselga et al. 2005; Vermorken et al. 2008). While the molecular subtypes described above do not currently dictate therapeutic regimes, the ability to integrate genomic and gene expression information has given some insights into the critical pathways that could be targeted for cancer control. Among these, receptor tyrosine kinases such as EGFR continue to be targeted and to improve in efficacy; cetuximab is now being tested in combination with other targeted therapies such as those targeting ERBB2 (NCT02538627). PIK3CA is the most commonly mutated oncogene in HNSCC, and actionable mutations within PIK3CA afford an opportunity to inhibit the PI3K pathway. Indeed, PI3K inhibitors are actively being evaluated either alone or in combination with other agents in HNSCC (NCT02540928, NCT02646748, NCT01602315). Further, targeting of mTOR, which is a downstream target in the PI3K pathway, is also being actively pursued (NCT01051791, NCT01009346, NCT01195922).

It is evident that many of the genes that govern the cell cycle are altered in HNSCC suggesting that this pathway could be exploited for tumor control. Cyclin-dependent kinase (CDK) inhibitors are of much interest especially among HNSCC with amplified cyclin D (CCND1) and loss of CDKN2A. Recently, a CDK4/6 inhibitor, palbociclib, was approved for the treatment of estrogen receptor (ER)-positive and HER2-negative breast cancers in combination with letrozole (Finn et al. 2015). More recently, a Phase I trial demonstrated that palbociclib administered with cetuximab was safe in HNSCC patients (Michel et al. 2016) making way for a Phase II trial to evaluate palbociclib in combination with cetuximab in recurrent/metastatic HNSCC (NCT02499120). Other drugs targeting the cell cycle including inhibitors of WEE-1, a kinase that phosphorylates components within the cell cycle, are also currently being evaluated (NCT02508246, NCT02585973).

Several challenges remain in targeting the HNSCC genome. Firstly, biomarkers of response that could help with the identification of patients who would likely respond to a particular therapy are needed. Secondly, it is very likely that single agents may not be able to completely inhibit the many perturbed pathways in cancer cells, and innovative predictive methods on which drug combinations would work without causing prohibitive toxicity would be important moving forward. Last but not least, novel ways to target tumors with loss-of-function mutations and identification of new targets are necessary to enable

further development of novel ways to treat HNSCC. Projects such as the Genomics of Drug Sensitivity (GDSC) and Cancer Therapeutics Response Portal (CTRP) among other emerging studies are enabling the identification of plausible biomarkers of response (Barretina et al. 2012; Garnett et al. 2012; Basu et al. 2013; Seashore-Ludlow et al. 2015; Rees et al. 2016). Further, techniques such as the gene editing tool CRISPR/Cas9 (Koike-Yusa et al. 2014; Shalem et al. 2014; Wang et al. 2014) that can systematically knock down genes within the HNSCC genome may reveal genes that are critical for the survival of cancer and hence could be targeted for tumor control.

Immune Markers and Immunotherapy

Molecular characterization of tumors has enabled identification of cancers with high mutational burden, i.e., those that have a high number of mutations within the tumor. Cancers that are associated with high mutational burden are typically those that are associated with external and known carcinogens such as melanoma which is associated with UV exposure and lung cancer which is associated with tobacco use (Lawrence et al. 2013). HNSCC falls within this group of cancers of high mutational burden, and these cancers have been reported to have a high number of infiltrating lymphocytes within the tumor (called tumor-infiltrating lymphocytes, TIL). This is possibly attributed to the increase in mutated proteins that are unique and immunogenic (not been encountered by the immune system previously) that could induce the immune system to mount an immune response. In fact, HNSCC is among the top 10 cancers with the highest level of immune infiltrates (Senbabaoglu et al. 2015; Mandal et al. 2016), making this cancer a relevant model to study cancer immunotherapy.

The equilibrium between factors that promote or suppress anticancer immunity has been recently proposed and described as the concept of "cancer-immune set point" (Chen and Mellman 2017), and in order to induce a positive immune response, induction of an effect that surpasses this point is required to illicit a protective immune effect in cancer patients. For example, the presence of $CD8^+$ cytotoxic T cells and high immune infiltration has been associated with good prognosis in cancer patients, while other features including the presence of regulatory T cells (Treg) and other molecules involved in immune blockade such as CTLA-4, PD-1, and PD-L1 are indicative of immunosuppression and poor prognosis (Teng et al. 2015).

A recent bioinformatic analysis of transcriptome data from TCGA revealed the global immune repertoire of HNSCC (Mandal et al. 2016). This information provides a snapshot of the immune status of HNSCC patients, which could provide ability to subcategorize HNSCC into clinically actionable groups with important therapeutic implications, particularly in the application of cancer immunotherapy. While this analysis revealed a wide range in the level of immune infiltrates across HNSCC, overall, HNSCC are marked with high levels of immune cell infiltration which is also accompanied by a striking observation that these cancers had notable signs of immunosuppression marked by high Treg infiltration and high Treg/CD8+ ratios. Another unique immune feature of HNSCC revealed by this study was the presence of natural killer (NK) cells within the tumor where among ten most common tumor types that were examined, HNSCC was the cancer with the highest level of NK cells. With these observations, HNSCC presents as one of the most exciting and promising areas of research in immunotherapy and could be a tumor type that is highly likely to respond to immunotherapeutic strategies.

Comparing among the subsites of HNSCC, tumors of the oropharynx have the highest levels of T cell infiltration and immune activation compared to the hypopharynx, larynx, and oral cavity; however, in parallel, tumors of the oropharynx also have higher levels of immunoregulatory influence with higher Treg infiltration and low CD8+/Treg ratios. The immune repertoire is also influenced by the gene expression patterns of the tumor. Comparing the immune cell subsets across the four gene expression subgroups of HNSCC (Chung et al. 2004; Walter et al. 2013; Cancer

Genome Atlas 2015), the atypical and mesenchymal subtypes have a higher degree of immune infiltration and T cell activation, compared to the basal and classical subtypes. As explained above, the atypical subtype is highly associated with HPV positivity, while the classical subtype is associated with the use of tobacco. Consistently, mutational signatures associated with tobacco smoking (Alexandrov et al. 2013) are also inversely associated with levels of immune infiltrates. While the immunosuppressive mechanism of smoking is not well defined, a recent study suggests that smoking could have suppressive effects on specific subsets of immune cells including natural killer (NK) cells, CD8+ T cells, and dendritic cells (DC) (Stampfli and Anderson 2009).

HPV status has a significant influence on the survival of HNSCC patients, and HPV-positive patients experience higher cure rates and better overall survival (Ang et al. 2010). While this could be attributed to the differences in the genetic background of HPV-positive tumors, it is conceivable that the differences in immune infiltration may also mediate part of these survival differences as suggested in other cancers (Fridman et al. 2012). Indeed, looking at the TCGA study, patients with high immune infiltration had significantly improved survival regardless and independent of HPV status. Interestingly, Treg infiltration was associated with better prognosis, and higher levels of Treg were associated with superior overall survival – however, when examined further and taking into consideration the trafficking of other immune cells into the tumor, Treg levels did not remain an independent prognostic factor underscoring the complexity and the interaction between the cells within the immune system and those that infiltrate into the tumor. NK cells are also associated with prognosis. The presence of a subset of activated NK cells (CD56dim) within the tumor is associated with superior survival.

There are two basic requirements for the immune system to control tumor growth effectively; the immune cells must overcome interstitial pressures in order to infiltrate the tumor and recognize appropriate tumor antigens. In addition, to sustain an immune response, the immune system must be free from immune inhibitory influences from the tumor (Zitvogel et al. 2006). A critical immune checkpoint often found to be downregulated the patient's immune response is programmed cell death 1 (PD-1), an inhibitory receptor expressed on many subsets of immune cells including T cells, dendritic cells, natural killer cells, macrophages, and B cells. PD-1 function is dependent on the binding of its ligand PD-L1 or PD-L2 which are upregulated in many solid tumors including HNSCC (Cho et al. 2011; Lyford-Pike et al. 2013; Zandberg and Strome 2014). Studies have suggested a role for PD-1 in mediating T cell exhaustion in advanced solid cancers including the head and neck (Topalian et al. 2012; Lipson et al. 2015). High levels of PD-1 on T cells coupled with the presence of PD-L1 in the tumor could cause a state of anergy and an impairment in the immune system that could facilitate tumor growth (Lyford-Pike et al. 2013). Recently, two immune checkpoint inhibitors pembrolizumab and nivolumab targeting PD-1 were approved for treatment of chemotherapy refractory HNSCC. Patients treated with pembrolizumab showed an overall response rate of 18%, and the 6-month progression-free survival and overall survival rates were 23% and 59%, respectively (Chow et al. 2016; Ranee Mehra et al. 2016). On the other hand, nivolumab demonstrated an overall response rate of 13% compared to 5.8% in the standard therapy group, where the overall survival of nivolumab-treated patients was 7.5 months compared to 5.1 months in the standard therapy group (Ferris et al. 2016). These trials have now led to the approval of both pembrolizumab and nivolumab for the treatment of advanced head and neck cancers, increasing the therapeutic options for HNSCC patients with advanced disease. Several clinical trials combining anti-PD1 with standard and new agents are underway. Further, the use of monoclonal antibodies targeting the ligand of PD-1 (anti-PD-L1) as monotherapy or in combination is also in progress (Pai et al. 2016) (NCT02501096, NCT02646748, NCT02454179, NCT02586987).

The emerging understanding of the unique aspects of the immune landscape of HNSCC provides a strong rationale to use immunotherapy on these cancers, and in addition to immune

checkpoint inhibitors that have been recently approved, HNSCC could also benefit from immune agonists which could reactivate the immune system, some of which like vaccines are currently in clinical testing (Yoshitake et al. 2015). Furthermore, the presence of NK cells within HNSCC affords an opportunity to reactivate NK cells by monoclonal antibodies, and these strategies are currently in preclinical and clinical investigation (NCT02643550). Therapies such as inhibitors of indoleamine-2,3-dioxygenase (IDO) with the potential to target Treg could exhibit activity in HNSCC. These work by increasing bioavailable tryptophan within the tumor microenvironment and decreasing the proliferation and activation of Tregs (Munn 2011). Further, directly targeting molecules that are highly expressed in Tregs such as glucocorticoid-induced tumor necrosis factor-related receptor (GITR) or the inducible T cell co-stimulator (ICOS) have shown promising results (Schaer et al. 2013; Mandal and Chan 2016) but have yet to be used in HNSCC.

Conclusions and Future Directions

The head and neck region is a complex part of the human body which necessitates a thorough understanding of its anatomy and resultant pathologies. The diversity of lesions, masses, and tumors that arise in this complex structure can be challenging to any clinician and underscores the importance of a multidisciplinary team approach in diagnosis, management, and surveillance of patients with such lesions. Morbidity and mortality for many years have been poor, although in recent time, mortality and morbidity for HPV-positive oropharyngeal carcinomas have improved significantly, as too has our understanding of the molecular basis of head and neck squamous cell carcinoma. As HPV-positive tumors of the head and neck region dominate the attention of practitioners and researchers alike, an equal amount of effort is required to better understand other diseases with poor outcomes. Targeted immunotherapies, precision medicine approaches, and diagnostic and prognostic biomarkers are shaping the way patients are treated. Clinicians practicing in head and neck oncological teams must stay abreast of developments in the underlying sciences which underpin these advancements in diagnosis, stratification, and management. Primary prevention of HPV-associated tumors through HPV vaccination is an important global challenge and one that requires a concerted effort across the globe. Finally, evidence-based guidelines for follow-up, surveillance, and monitoring are urgently required to better inform our management approaches and to enhance secondary prevention measures in the long-term survivor.

Cross-References

- ▶ Arthritic Conditions Affecting the Temporomandibular Joint
- ▶ Clinical Evaluation of Oral Diseases
- ▶ Cutaneous Pathology of the Head and Neck
- ▶ Diagnostic Imaging Principles and Applications in Head and Neck Pathology
- ▶ Internal Derangements of the Temporomandibular Joint
- ▶ Laboratory Medicine and Diagnostic Pathology
- ▶ Non-Odontogenic Bone Pathology
- ▶ Normal Variation in the Anatomy, Biology, and Histology of the Maxillofacial Region
- ▶ Oral and Maxillofacial Viral Infections
- ▶ Oral Mucosal Malignancies
- ▶ Pediatric Oral Medicine
- ▶ Salivary Gland Disorders and Diseases
- ▶ Soft and Hard Tissue Operative Investigations in the Diagnosis and Treatment of Oral Disease
- ▶ White and Red Lesions of the Oral Mucosa

References

Abergel A, Cavel O, Margalit N, Fliss DM, Gil Z. Comparison of quality of life after transnasal endoscopic vs open skull base tumor resection. Arch Otolaryngol Head Neck Surg. 2012;138(2):142–7.

Abdurehim Y, Hua Z, Yasin Y, Xukurhan A, Imam I, Yuqin F. Transoral laser surgery versus radiotherapy: systematic review and meta-analysis for treatment options of T1a glottic cancer. Head Neck. 2012;34(1):23–33.

Adegboyega PA, Qiu S. Hemangioma versus vascular malformation: presence of nerve bundle is a diagnostic

clue for vascular malformation. Arch Pathol Lab Med. 2005;129(6):772–5.

Adelchi C, Mara P, Melissa L, De Stefano A, Cesare M. Ectopic thyroid tissue in the head and neck: a case series. BMC Res Notes. 2014;7:790.

Adelstein DJ, Ridge JA, Gillison ML, Chaturvedi AK, D'Souza G, Gravitt PE, Westra W, Psyrri A, Kast WM, Koutsky LA, Giuliano A, Krosnick S, Trotti A, Schuller DE, Forastiere A, Ullmann CD. Head and neck squamous cell cancer and the human papillomavirus: summary of a National Cancer Institute State of the Science Meeting, November 9–10, 2008, Washington, D.C. Head Neck. 2009;31(11):1393–422.

Adelstein D, Gillison ML, Pfister DG, Spencer S, Adkins D, Brizel DM, Burtness B, Busse PM, Caudell JJ, Cmelak AJ, Colevas AD, Eisele DW, Fenton M, Foote RL, Gilbert J, Haddad RI, Hicks WL Jr, Hitchcock YJ, Jimeno A, Leizman D, Lydiatt WM, Maghami E, Mell LK, Mittal BB, Pinto HA, Ridge JA, Rocco J, Rodriguez CP, Shah JP, Weber RS, Witek M, Worden F, Yom SS, Zhen W, Burns JL, Darlow SD. NCCN guidelines insights: head and neck cancers, version 2.2017. J Natl Compr Cancer Netw. 2017;15(6):761–70.

Agaram NP, Chen CL, Zhang L, LaQuaglia MP, Wexler L, Antonescu CR. Recurrent MYOD1 mutations in pediatric and adult sclerosing and spindle cell rhabdomyosarcomas: evidence for a common pathogenesis. Genes Chromosom Cancer. 2014;53(9):779–87.

Agrawal N, Frederick MJ, Pickering CR, Bettegowda C, Chang K, Li RJ, Fakhry C, Xie TX, Zhang J, Wang J, Zhang N, El-Naggar AK, Jasser SA, Weinstein JN, Trevino L, Drummond JA, Muzny DM, Wu Y, Wood LD, Hruban RH, Westra WH, Koch WM, Califano JA, Gibbs RA, Sidransky D, Vogelstein B, Velculescu VE, Papadopoulos N, Wheeler DA, Kinzler KW, Myers JN. Exome sequencing of head and neck squamous cell carcinoma reveals inactivating mutations in NOTCH1. Science. 2011;333(6046):1154–7.

Alexandrov LB, Nik-Zainal S, Wedge DC, Aparicio SA, Behjati S, Biankin AV, Bignell GR, Bolli N, Borg A, Borresen-Dale AL, Boyault S, Burkhardt B, Butler AP, Caldas C, Davies HR, Desmedt C, Eils R, Eyfjord JE, Foekens JA, Greaves M, Hosoda F, Hutter B, Ilicic T, Imbeaud S, Imielinski M, Jager N, Jones DT, Jones D, Knappskog S, Kool M, Lakhani SR, Lopez-Otin C, Martin S, Munshi NC, Nakamura H, Northcott PA, Pajic M, Papaemmanuil E, Paradiso A, Pearson JV, Puente XS, Raine K, Ramakrishna M, Richardson AL, Richter J, Rosenstiel P, Schlesner M, Schumacher TN, Span PN, Teague JW, Totoki Y, Tutt AN, Valdes-Mas R, van Buuren MM, Van't Veer L, Vincent-Salomon A, Waddell N, Yates LR, I. Australian Pancreatic Cancer Genome, I. B. C. Consortium, I. M.-S. Consortium, I. PedBrain, Zucman-Rossi J, Futreal PA, McDermott U, Lichter P, Meyerson M, Grimmond SM, Siebert R, Campo E, Shibata T, Pfister SM, Campbell PJ, Stratton MR. Signatures of mutational processes in human cancer. Nature. 2013;500(7463):415–21.

Ali S, Tiwari R, Snow GB, vd Waal I. Incidence of squamous cell carcinoma of the head and neck: report of 1,000 cases. J Laryngol Otol. 1986;100(3):315–27.

Ambrosch P. The role of laser microsurgery in the treatment of laryngeal cancer. Curr Opin Otolaryngol Head Neck Surg. 2007;15(2):82–8.

Ang KK, Harris J, Wheeler R, Weber R, Rosenthal DI, Nguyen-Tan PF, Westra WH, Chung CH, Jordan RC, Lu C, Kim H, Axelrod R, Silverman CC, Redmond KP, Gillison ML. Human papillomavirus and survival of patients with oropharyngeal cancer. N Engl J Med. 2010;363(1):24–35.

Anghileri M, Miceli R, Fiore M, Mariani L, Ferrari A, Mussi C, Lozza L, Collini P, Olmi P, Casali PG, Pilotti S, Gronchi A. Malignant peripheral nerve sheath tumors: prognostic factors and survival in a series of patients treated at a single institution. Cancer. 2006;107(5):1065–74.

Andersen A, Berge SR, Engeland A, Norseth T. Exposure to nickel compounds and smoking in relation to incidence of lung and nasal cancer among nickel refinery workers. Occup Environ Med. 1996;53(10):708–13.

Aoki Y, Tosato G. HIV-1 Tat enhances Kaposi sarcoma-associated herpesvirus (KSHV) infectivity. Blood. 2004;104(3):810–4.

Baert AL. Encyclopedia of diagnostic imaging. Berlin: Springer Verlag; 2008.

Barnes CM, Christison-Lagay EA, Folkman J. The placenta theory and the origin of infantile hemangioma. Lymphat Res Biol. 2007;5(4):245–55.

Barretina J, Caponigro G, Stransky N, Venkatesan K, Margolin AA, Kim S, Wilson CJ, Lehar J, Kryukov GV, Sonkin D, Reddy A, Liu M, Murray L, Berger MF, Monahan JE, Morais P, Meltzer J, Korejwa A, Jane-Valbuena J, Mapa FA, Thibault J, Bric-Furlong-E, Raman P, Shipway A, Engels IH, Cheng J, Yu GK, Yu J, Aspesi P Jr, de Silva M, Jagtap K, Jones MD, Wang L, Hatton C, Palescandolo E, Gupta S, Mahan S, Sougnez C, Onofrio RC, Liefeld T, MacConaill L, Winckler W, Reich M, Li N, Mesirov JP, Gabriel SB, Getz G, Ardlie K, Chan V, Myer VE, Weber BL, Porter J, Warmuth M, Finan P, Harris JL, Meyerson M, Golub TR, Morrissey MP, Sellers WR, Schlegel R, Garraway LA. The cancer cell line encyclopedia enables predictive modelling of anticancer drug sensitivity. Nature. 2012;483(7391):603–7.

Baselga J, Trigo JM, Bourhis J, Tortochaux J, Cortes-Funes H, Hitt R, Gascon P, Amellal N, Harstrick A, Eckardt A. Phase II multicenter study of the anti-epidermal growth factor receptor monoclonal antibody cetuximab in combination with platinum-based chemotherapy in patients with platinum-refractory metastatic and/or recurrent squamous cell carcinoma of the head and neck. J Clin Oncol. 2005;23(24):5568–77.

Baverstock K, Egloff B, Pinchera A, Ruchti C, Williams D. Thyroid cancer after Chernobyl. Nature. 1992;359(6390):21–2.

Basu A, Bodycombe NE, Cheah JH, Price EV, Liu K, Schaefer GI, Ebright RY, Stewart ML, Ito D, Wang S, Bracha AL, Liefeld T, Wawer M, Gilbert JC, Wilson AJ, Stransky N, Kryukov GV, Dancik V, Barretina J, Garraway LA, Hon CS, Munoz B, Bittker JA, Stockwell BR, Khabele D, Stern AM, Clemons PA, Shamji AF, Schreiber SL. An interactive resource to identify cancer genetic and lineage dependencies targeted by small molecules. Cell. 2013;154(5):1151–61.

Baujat B, Bourhis J, Blanchard P, Overgaard J, Ang KK, Saunders M, Le Maitre A, Bernier J, Horiot JC, Maillard E, Pajak TF, Poulsen MG, Bourredjem A, O'Sullivan B, Dobrowsky W, Andrzej H, Skladowski K, Hay JH, Pinto LH, Fu KK, Fallai C, Sylvester R, Pignon JP, M. C. Group. Hyperfractionated or accelerated radiotherapy for head and neck cancer. Cochrane Database Syst Rev. 2010; (12): CD002026.

Becker M. Larynx and hypopharynx. Radiol Clin N Am. 1998;36(5):891–920. vi

Becker M, Zbaren P, Delavelle J, Kurt AM, Egger C, Rufenacht DA, Terrier F. Neoplastic invasion of the laryngeal cartilage: reassessment of criteria for diagnosis at CT. Radiology. 1997;203(2):521–32.

Benson E, Li R, Eisele D, Fakhry C. The clinical impact of HPV tumor status upon head and neck squamous cell carcinomas. Oral Oncol. 2014;50(6):565–74.

Bhattacharyya N. Factors affecting survival in maxillary sinus cancer. J Oral Maxillofac Surg. 2003;61 (9):1016–21.

de Bondt RB, Nelemans PJ, Hofman PA, Casselman JW, Kremer B, van Engelshoven JM, Beets-Tan RG. Detection of lymph node metastases in head and neck cancer: a meta-analysis comparing US, USgFNAC, CT and MR imaging. Eur J Radiol. 2007;64(2):266–72.

Bonner JA, Harari PM, Giralt J, Azarnia N, Shin DM, Cohen RB, Jones CU, Sur R, Raben D, Jassem J, Ove R, Kies MS, Baselga J, Youssoufian H, Amellal N, Rowinsky EK, Ang KK. Radiotherapy plus cetuximab for squamous-cell carcinoma of the head and neck. N Engl J Med. 2006;354(6):567–78.

Bradley PF. A review of the use of the neodymium YAG laser in oral and maxillofacial surgery. Br J Oral Maxillofac Surg. 1997;35(1):26–35.

Bradley PJ. Primary malignant mucosal melanoma of the head and neck. Curr Opin Otolaryngol Head Neck Surg. 2006;14(2):100–4.

Bremer JW, Neel HB 3rd, DeSanto LW, Jones GC. Angiofibroma: treatment trends in 150 patients during 40 years. Laryngoscope. 1986;96(12):1321–9.

Brierley JD, Gospodarowicz MK, Wittekind C, editor. TNM Classification of Malignant Tumours, 8th Edition. Wiley-Blackwell; 2017

Buckmiller LM, Richter GT, Suen JY. Diagnosis and management of hemangiomas and vascular malformations of the head and neck. Oral Dis. 2010;16(5):405–18.

Cabanillas ME, McFadden DG, Durante C. Thyroid cancer. Lancet. 2016;388(10061):2783–95.

Califano J, Koch W, Sidransky D, Westra WH. Inverted sinonasal papilloma: a molecular genetic appraisal of its putative status as a Precursor to squamous cell carcinoma. Am J Pathol. 2000;156(1):333–7.

Cancer Genome Atlas, N. Comprehensive genomic characterization of head and neck squamous cell carcinomas. Nature. 2015;517(7536):576–82.

Cancer Genome Atlas Research, N. Comprehensive genomic characterization of squamous cell lung cancers. Nature. 2012;489(7417):519–25.

Canis M, Ihler F, Martin A, Matthias C, Steiner W. Transoral laser microsurgery for T1a glottic cancer: review of 404 cases. Head Neck. 2015;37(6):889–95.

de Carvalho FK, Pinheiro TN, da Silva RA, de Queiroz AM, da Silva LA, Nelson-Filho P. Lymphangioma of the lower lip mimicking a mucocele in children. J Dent Child (Chic). 2015;82(2):116–9.

Castellanos JL, Diaz-Guzman L. Lesions of the oral mucosa: an epidemiological study of 23785 Mexican patients. Oral Surg Oral Med Oral Pathol Oral Radiol Endod. 2008;105(1):79–85.

Castinetti F, Moley J, Mulligan LM, Waguespack SG. A comprehensive review on MEN 2B. Endocr Relat Cancer. 2018;25(2):T29–T39.

Chan JKC, Bray F, McCarron P, Foo W, Lee AWM, Yip T, Kuo TT, Pilch BZ, Wenig BM, Huang D, Lo KW, Zeng YX, Jia WH. Nasopharyngeal carcinoma. In: Barnes EL, Eveson JW, Reichart P, Sidransky D, editors. Pathology and genetics of head and neck tumours. Lyon: IARC Press; 2005. p. 85–97.

Chaturvedi AK, Engels EA, Pfeiffer RM, Hernandez BY, Xiao W, Kim E, Jiang B, Goodman MT, Sibug-Saber-M, Cozen W, Liu L, Lynch CF, Wentzensen N, Jordan RC, Altekruse S, Anderson WF, Rosenberg PS, Gillison ML. Human papillomavirus and rising oropharyngeal cancer incidence in the United States. J Clin Oncol. 2011;29(32):4294–301.

Chen H. Atlas of genetic diagnosis and counseling. New York: Springer Verlag; 2012.

Chen DS, Mellman I. Elements of cancer immunity and the cancer-immune set point. Nature. 2017;541 (7637):321–30.

Chen KH, Chen TD, Chen CW, Lee LY. Iatrogenic Kaposi's sarcoma in nasal cavity: a case report. World J Surg Oncol. 2014;12:172.

Chen E, Ricciotti R, Futran N, Oda D. Head and neck rhabdomyosarcoma: clinical and pathologic characterization of seven cases. Head Neck Pathol. 2017;11 (3):321–326.

Cho YA, Yoon HJ, Lee JI, Hong SP, Hong SD. Relationship between the expressions of PD-L1 and tumor-infiltrating lymphocytes in oral squamous cell carcinoma. Oral Oncol. 2011;47(12):1148–53.

Choussy O, Ferron C, Vedrine PO, Toussaint B, Lietin B, Marandas P, Babin E, De Raucourt D, Reyt E, Cosmidis A, Makeiff M, Dehesdin D, G. S. Group. Adenocarcinoma of ethmoid: a GETTEC retrospective multicenter study of 418 cases. Laryngoscope. 2008;118(3):437–43.

Chow LQ, Haddad R, Gupta S, Mahipal A, Mehra R, Tahara M, Berger R, Eder JP, Burtness B, Lee SH, Keam B, Kang H, Muro K, Weiss J, Geva R, Lin CC, Chung HC, Meister A, Dolled-Filhart M, Pathiraja K, Cheng JD, Seiwert TY. Antitumor activity of pembrolizumab in biomarker-unselected patients with recurrent and/or metastatic head and neck squamous cell carcinoma: results from the phase Ib KEYNOTE-012 expansion cohort. J Clin Oncol. 2016;34 (32):3838–45.

Chung CH, Parker JS, Karaca G, Wu J, Funkhouser WK, Moore D, Butterfoss D, Xiang D, Zanation A, Yin X, Shockley WW, Weissler MC, Dressler LG, Shores CG, Yarbrough WG, Perou CM. Molecular classification of head and neck squamous cell carcinomas using patterns of gene expression. Cancer Cell. 2004;5(5):489–500.

Chung CH, Guthrie VB, Masica DL, Tokheim C, Kang H, Richmon J, Agrawal N, Fakhry C, Quon H, Subramaniam RM, Zuo Z, Seiwert T, Chalmers ZR, Frampton GM, Ali SM, Yelensky R, Stephens PJ, Miller VA, Karchin R, Bishop JA. Genomic alterations in head and neck squamous cell carcinoma determined by cancer gene-targeted sequencing. Ann Oncol. 2015;26(6):1216–23.

Ciriello G, Miller ML, Aksoy BA, Senbabaoglu Y, Schultz N, Sander C. Emerging landscape of oncogenic signatures across human cancers. Nat Genet. 2013;45 (10):1127–33.

Cohen LM, Schwartz AM, Rockoff SD. Benign schwannomas: pathologic basis for CT inhomogeneities. AJR Am J Roentgenol. 1986;147(1):141–3.

Colreavy MP, Lacy PD, Hughes J, Bouchier-Hayes D, Brennan P, O'Dwyer AJ, Donnelly MJ, Gaffney R, Maguire A, O'Dwyer TP, Timon CV, Walsh MA. Head and neck schwannomas – a 10 year review. J Laryngol Otol. 2000;114(2):119–24.

Cove H. Melanosis, melanocytic hyperplasia, and primary malignant melanoma of the nasal cavity. Cancer. 1979;44(4):1424–33.

Crippa S, Mazzucchelli L, Cibas ES, Ali SZ. The Bethesda system for reporting thyroid fine-needle aspiration specimens. Am J Clin Pathol. 2010;134(2):343–4. author reply 345

D'Souza G, Kreimer AR, Viscidi R, Pawlita M, Fakhry C, Koch WM, Westra WH, Gillison ML. Case-control study of human papillomavirus and oropharyngeal cancer. N Engl J Med. 2007;356(19):1944–56.

Das Gupta TK, Brasfield RD, Strong EW, Hajdu SI. Benign solitary Schwannomas (neurilemomas). Cancer. 1969;24(2):355–66.

Dayyani F, Etzel CJ, Liu M, Ho CH, Lippman SM, Tsao AS. Meta-analysis of the impact of human papillomavirus (HPV) on cancer risk and overall survival in head and neck squamous cell carcinomas (HNSCC). Head Neck Oncol. 2010;2:15.

Department of Veterans Affairs Laryngeal Cancer Study, G, Wolf GT, Fisher SG, Hong WK, Hillman R, Spaulding M, Laramore GE, Endicott JW, McClatchey K, Henderson WG. Induction chemotherapy plus radiation compared with surgery plus radiation in patients with advanced laryngeal cancer. N Engl J Med. 1991;324(24):1685–90.

Durante C, Montesano T, Torlontano M, Attard M, Monzani F, Tumino S, Costante G, Meringolo D, Bruno R, Trulli F, Massa M, Maniglia A, D'Apollo R, Giacomelli L, Ronga G, Filetti S, P. T. C. S. Group. Papillary thyroid cancer: time course of recurrences during postsurgery surveillance. J Clin Endocrinol Metab. 2013;98(2):636–42.

Eeles RA, Fisher C, A'Hern RP, Robinson M, Rhys-Evans P, Henk JM, Archer D, Harmer CL. Head and neck sarcomas: prognostic factors and implications for treatment. Br J Cancer. 1993;68(1):201–7.

Ellis GL, Auclair PL, Gnepp DR. Surgical pathology of the salivary glands. Philadelphia: WB Saunders; 1991.

Ettl T, Kleinheinz J, Mehrotra R, Schwarz S, Reichert TE, Driemel O. Infraorbital cutaneous angiosarcoma: a diagnostic and therapeutic dilemma. Head Face Med. 2008;4:18.

Eveson JW, Cawson RA. Tumours of the minor (oropharyngeal) salivary glands: a demographic study of 336 cases. J Oral Pathol. 1985;14(6):500–9.

Fakhry C, Zhang Q, Nguyen-Tan PF. Human papillomavirus and overall survival after progression of oropharyngeal squamous cell carcinoma. J Natl Cancer Inst. 2008;100(4):261–9.

Fanburg-Smith JC, Furlong MA, Childers EL. Oral and salivary gland angiosarcoma: a clinicopathologic study of 29 cases. Mod Pathol. 2003;16(3):263–71.

Favus MJ, Schneider AB, Stachura ME, Arnold JE, Ryo UY, Pinsky SM, Colman M, Arnold MJ, Frohman LA. Thyroid cancer occurring as a late consequence of head-and-neck irradiation. Evaluation of 1056 patients. N Engl J Med. 1976;294(19):1019–25.

Ferreira JC, Oton-Leite AF, Guidi R, Mendonca EF. Granular cell tumor mimicking a squamous cell carcinoma of the tongue: a case report. BMC Res Notes. 2017;10(1):14.

Ferris RL, Blumenschein G Jr, Fayette J, Guigay J, Colevas AD, Licitra L, Harrington K, Kasper S, Vokes EE, Even C, Worden F, Saba NF, Iglesias Docampo LC, Haddad R, Rordorf T, Kiyota N, Tahara M, Monga M, Lynch M, Geese WJ, Kopit J, Shaw JW, Gillison ML. Nivolumab for recurrent squamous-cell carcinoma of the head and neck. N Engl J Med. 2016;375 (19):1856–67.

Fitzpatrick SG, Gordon SC. Benign non-neoplastic lesions of the head and neck. In: Radosevich JA, editor. Head & neck cancer: current perspectives, advances, and challenges. Netherlands: Springer; 2013. p. 199–256.

Finn RS, Crown JP, Lang I, Boer K, Bondarenko IM, Kulyk SO, Ettl J, Patel R, Pinter T, Schmidt M, Shparyk Y, Thummala AR, Voytko NL, Fowst C, Huang X, Kim ST, Randolph S, Slamon DJ. The cyclin-dependent kinase 4/6 inhibitor palbociclib in combination with letrozole versus letrozole alone as first-line treatment of oestrogen receptor-positive, HER2-negative, advanced breast cancer (PALOMA-1/

TRIO-18): a randomised phase 2 study. Lancet Oncol. 2015;16(1):25–35.
Fletcher CD. Solitary circumscribed neuroma of the skin (so-called palisaded, encapsulated neuroma). A clinicopathologic and immunohistochemical study. Am J Surg Pathol. 1989;13(7):574–80.
Forastiere AA, Goepfert H, Maor M, Pajak TF, Weber R, Morrison W, Glisson B, Trotti A, Ridge JA, Chao C, Peters G, Lee DJ, Leaf A, Ensley J, Cooper J. Concurrent chemotherapy and radiotherapy for organ preservation in advanced laryngeal cancer. N Engl J Med. 2003;349(22):2091–8.
Forastiere AA, Zhang Q, Weber RS, Maor MH, Goepfert H, Pajak TF, Morrison W, Glisson B, Trotti A, Ridge JA, Thorstad W, Wagner H, Ensley JF, Cooper JS. Long-term results of RTOG 91-11: a comparison of three nonsurgical treatment strategies to preserve the larynx in patients with locally advanced larynx cancer. J Clin Oncol. 2013;31(7):845–52.
Franchi A. Head and neck pathology. M. Volavšek. 2016. https://www.springer.com/gp/book/9783319286174.
Fregnani ER, Pires FR, Falzoni R, Lopes MA, Vargas PA. Lipomas of the oral cavity: clinical findings, histological classification and proliferative activity of 46 cases. Int J Oral Maxillofac Surg. 2003;32 (1):49–53.
Fridman WH, Pages F, Sautes-Fridman C, Galon J. The immune contexture in human tumours: impact on clinical outcome. Nat Rev Cancer. 2012;12(4):298–306.
Friedman AB, Munson PD, Richter GT. Vascular anomalies of head and neck. In: Kountakis SE, editor. Encyclopedia of otolaryngology, head and neck surgery. Berlin: Springer; 2013. p. 2975–88.
Gallo RC. The enigmas of Kaposi's sarcoma. Science. 1998;282(5395):1837–9.
Gallo WJ, Moss M, Shapiro DN, Gaul JV. Neurilemoma: review of the literature and report of five cases. J Oral Surg. 1977;35(3):235–6.
Ganly I, Patel SG, Singh B, Kraus DH, Cantu G, Fliss DM, Kowalski LP, Snyderman C, Shah JP. Craniofacial resection for malignant tumors involving the skull base in the elderly: an international collaborative study. Cancer. 2011;117(3):563–71.
Garden AS, Morrison WH, Wong PF, Tung SS, Rosenthal DI, Dong L, Mason B, Perkins GH, Ang KK. Disease-control rates following intensity-modulated radiation therapy for small primary oropharyngeal carcinoma. Int J Radiat Oncol Biol Phys. 2007;67(2):438–44.
Garland SM, Smith JS. Human papillomavirus vaccines: current status and future prospects. Drugs. 2010;70 (9):1079–98.
Garnett MJ, Edelman EJ, Heidorn SJ, Greenman CD, Dastur A, Lau KW, Greninger P, Thompson IR, Luo X, Soares J, Liu Q, Iorio F, Surdez D, Chen L, Milano RJ, Bignell GR, Tam AT, Davies H, Stevenson JA, Barthorpe S, Lutz SR, Kogera F, Lawrence K, McLaren-Douglas A, Mitropoulos X, Mironenko T, Thi H, Richardson L, Zhou W, Jewitt F, Zhang T, O'Brien P, Boisvert JL, Price S, Hur W, Yang W, Deng X, Butler A, Choi HG, Chang JW, Baselga J, Stamenkovic I, Engelman JA, Sharma SV, Delattre O, Saez-Rodriguez J, Gray NS, Settleman J, Futreal PA, Haber DA, Stratton MR, Ramaswamy S, McDermott U, Benes CH. Systematic identification of genomic markers of drug sensitivity in cancer cells. Nature. 2012;483(7391):570–5.
Gibas Z, Miettinen M. Recurrent parapharyngeal rhabdomyoma. Evidence of neoplastic nature of the tumor from cytogenetic study. Am J Surg Pathol. 1992;16(7):721–8.
Gildener-Leapman N, Lee J, Ferris RL. Tailored immunotherapy for HPV positive head and neck squamous cell cancer. Oral Oncol. 2014;50(9):780–4.
Gnepp DR. Diagnostic surgical pathology of the head and neck. Philadelphia: WB Saunders; 2001.
Golledge J, Fisher C, Rhys-Evans PH. Head and neck liposarcoma. Cancer. 1995;76(6):1051–8.
Gourin CG, Johnson JT. Incidence of unsuspected metastases in lateral cervical cysts. Laryngoscope. 2000;110 (10 Pt 1):1637–41.
Granata R, Miceli R, Orlandi E, Perrone F, Cortelazzi B, Franceschini M, Locati LD, Bossi P, Bergamini C, Mirabile A, Mariani L, Olmi P, Scaramellini G, Potepan P, Quattrone P, Ang KK, Licitra L. Tumor stage, human papillomavirus and smoking status affect the survival of patients with oropharyngeal cancer: an Italian validation study. Ann Oncol. 2012;23 (7):1832–7.
Grau C, Jakobsen MH, Harbo G, Svane-Knudsen V, Wedervang K, Larsen SK, Rytter C. Sino-nasal cancer in Denmark 1982–1991 – a nationwide survey. Acta Oncol. 2001;40(1):19–23.
Hamdoon Z, Jerjes W, Al-Delayme R, Hopper C. Solitary giant neurofibroma of the neck subjected to photodynamic therapy: case study. Head Neck Oncol. 2012;4:30.
Hanna EY. Comprehensive management of skull base tumors. New York: Informa Healthcare; 2009.
Harnsberger HR, Osborn AG. Diagnostic and surgical imaging anatomy: brain, head & neck, spine. Salt Lake City: Amirsys; 2006.
Harnsberger HR, Wiggins RH, Hudgings PA, Michel MA, Swartz J, Davidson CH, Macdonald AJ, Glastonbury CM, Cure JK, Branstetter B. Diagnostic imaging head and neck. Salt Lake City: Amirsys; 2006.
Harrison LB. Head and neck cancer, a multidisciplinary approach. Philadelphia: Lippincott, Williams & Wilkins; 2014.
Haugen BR, Alexander EK, Bible KC, Doherty GM, Mandel SJ, Nikiforov YE, Pacini F, Randolph GW, Sawka AM, Schlumberger M, Schuff KG, Sherman SI, Sosa JA, Steward DL, Tuttle RM, Wartofsky L. 2015 American Thyroid Association management guidelines for adult patients with thyroid nodules and differentiated thyroid cancer: the American Thyroid Association guidelines task force on thyroid nodules and differentiated thyroid cancer. Thyroid. 2016;26(1):1–133.

Heck JE, Berthiller J, Vaccarella S, Winn DM, Smith EM, Shan'gina O, Schwartz SM, Purdue MP, Pilarska A, Eluf-Neto J, Menezes A, McClean MD, Matos E, Koifman S, Kelsey KT, Herrero R, Hayes RB, Franceschi S, Wunsch-Filho V, Fernandez L, Daudt AW, Curado MP, Chen C, Castellsague X, Ferro G, Brennan P, Boffetta P, Hashibe M. Sexual behaviours and the risk of head and neck cancers: a pooled analysis in the International Head and Neck Cancer Epidemiology (INHANCE) consortium. Int J Epidemiol. 2010;39 (1):166–81.

Heyer GL, Dowling MM, Licht DJ, Tay SK, Morel K, Garzon MC, Meyers P. The cerebral vasculopathy of PHACES syndrome. Stroke. 2008;39(2):308–16.

Higgins KM, Shah MD, Ogaick MJ, Enepekides D. Treatment of early-stage glottic cancer: meta-analysis comparison of laser excision versus radiotherapy. J Otolaryngol Head Neck Surg. 2009;38(6):603–12.

Hirsch B, Moskowitz HS. Benign neoplasia-schwannoma-neurofibromatosis type 1, Encyclopedia of Otolaryngology, Head and Neck Surgery. Berlin: Springer; 2013.

Hofbauer GF, Boni R, Simmen D, Mihic D, Nestle FO, Burg G, Dummer R. Histological, immunological and molecular features of a nasal mucosa primary melanoma associated with nasal melanosis. Melanoma Res. 2002;12(1):77–82.

Holmstrom M, Lund VJ. Malignant melanomas of the nasal cavity after occupational exposure to formaldehyde. Br J Ind Med. 1991;48(1):9–11.

Hong A, Dobbins T, Lee CS, Jones D, Jackson E, Clark J, Armstrong B, Harnett G, Milross C, O'Brien C, Rose B. Relationships between epidermal growth factor receptor expression and human papillomavirus status as markers of prognosis in oropharyngeal cancer. Eur J Cancer. 2010;46(11):2088–96.

Horbach SE, Lokhorst MM, Saeed P, de Gouyon Matignon de Pontouraude CM, Rothova A, van der Horst CM. Sclerotherapy for low-flow vascular malformations of the head and neck: a systematic review of sclerosing agents. J Plast Reconstr Aesthet Surg. 2016;69 (3):295–304.

Hourani R, Taslakian B, Shabb NS, Nassar L, Hourani MH, Moukarbel R, Sabri A, Rizk T. Fibroblastic and myofibroblastic tumors of the head and neck: comprehensive imaging-based review with pathologic correlation. Eur J Radiol. 2015;84(2):250–60.

Howard DJ, Lund VJ, Wei WI. Craniofacial resection for tumors of the nasal cavity and paranasal sinuses: a 25-year experience. Head Neck. 2006;28 (10):867–73.

Howlader N, Noone AM, Krapcho M, Miller D, Bishop K, Altekruse SF, Kosary CL, Yu M, Ruhl J, Tatalovich Z, Mariotto A, Lewis DR, Chen HS, Feuer EJ, Cronin KA. SEER cancer statistics review, 1975–2013, National Cancer Institute. Bethesda: National Cancer Institute; 2016.

Hurtuk AM, Marcinow A, Agrawal A, Old M, Teknos TN, Ozer E. Quality-of-life outcomes in transoral robotic surgery. Otolaryngol Head Neck Surg. 2012;146 (1):68–73.

India Project Team of the International Cancer Genome, C. Mutational landscape of gingivo-buccal oral squamous cell carcinoma reveals new recurrently-mutated genes and molecular subgroups. Nat Commun. 2013;4:2873.

ISSVA Classification of Vascular Anomalies ©2018 International Society for the Study of Vascular Anomalies Available at issva.org/classification Accessed [11 July 2018]

Itakura E, Yamamoto H, Oda Y, Furue M, Tsuneyoshi M. VEGF-C and VEGFR-3 in a series of lymphangiomas: is superficial lymphangioma a true lymphangioma? Virchows Arch. 2009;454(3):317–25.

Jansen EP, Keus RB, Hilgers FJ, Haas RL, Tan IB, Bartelink H. Does the combination of radiotherapy and debulking surgery favor survival in paranasal sinus carcinoma? Int J Radiat Oncol Biol Phys. 2000;48(1):27–35.

Jemal A, Thomas A, Murray T, Thun M. Cancer statistics, 2002. CA Cancer J Clin. 2002;52(1):23–47.

Karligkiotis A, Bignami M, Terranova P, Gallo S, Meloni F, Padoan G, Lombardi D, Nicolai P, Castelnuovo P. Oncocytic Schneiderian papillomas: clinical behavior and outcomes of the endoscopic endonasal approach in 33 cases. Head Neck. 2014;36 (5):624–30.

Khan MK, Koyfman SA, Hunter GK, Reddy CA, Saxton JP. Definitive radiotherapy for early (T1-T2) glottic squamous cell carcinoma: a 20 year Cleveland Clinic experience. Radiat Oncol. 2012;7:193.

Klintenberg C, Olofsson J, Hellquist H, Sokjer H. Adenocarcinoma of the ethmoid sinuses. A review of 28 cases with special reference to wood dust exposure. Cancer. 1984;54(3):482–8.

Kluwe L, Mautner V, Heinrich B, Dezube R, Jacoby LB, Friedrich RE, MacCollin M. Molecular study of frequency of mosaicism in neurofibromatosis 2 patients with bilateral vestibular schwannomas. J Med Genet. 2003;40(2):109–14.

Kohsaka S, Shukla N, Ameur N, Ito T, Ng CK, Wang L, Lim D, Marchetti A, Viale A, Pirun M, Socci ND, Qin LX, Sciot R, Bridge J, Singer S, Meyers P, Wexler LH, Barr FG, Dogan S, Fletcher JA, Reis-Filho JS, Ladanyi M. A recurrent neomorphic mutation in MYOD1 defines a clinically aggressive subset of embryonal rhabdomyosarcoma associated with PI3K-AKT pathway mutations. Nat Genet. 2014;46(6):595–600.

Koike-Yusa H, Li Y, Tan EP, Velasco-Herrera Mdel C, Yusa K. Genome-wide recessive genetic screening in mammalian cells with a lentiviral CRISPR-guide RNA library. Nat Biotechnol. 2014;32(3):267–73.

Koujok K, Ruiz RE, Hernandez RJ. Myofibromatosis: imaging characteristics. Pediatr Radiol. 2005;35 (4):374–80.

Koutlas IG, Scheithauer BW. Palisaded encapsulated ("solitary circumscribed") neuroma of the oral cavity: a review of 55 cases. Head Neck Pathol. 2010;4(1):15–26.

Kraus DH, Dubner S, Harrison LB, Strong EW, Hajdu SI, Kher U, Begg C, Brennan MF. Prognostic factors for recurrence and survival in head and neck soft tissue sarcomas. Cancer. 1994;74(2):697–702.

La Ferla L, Pinzone MR, Nunnari G, Martellotta F, Lleshi A, Tirelli U, De Paoli P, Berretta M, Cacopardo B. Kaposi' s sarcoma in HIV-positive patients: the state of art in the HAART-era. Eur Rev Med Pharmacol Sci. 2013;17(17):2354–65.

La Vecchia C, Ron E, Franceschi S, Dal Maso L, Mark SD, Chatenoud L, Braga C, Preston-Martin S, McTiernan A, Kolonel L, Mabuchi K, Jin F, Wingren G, Galanti MR, Hallquist A, Lund E, Levi F, Linos D, Negri E. A pooled analysis of case-control studies of thyroid cancer. III. Oral contraceptives, menopausal replacement therapy and other female hormones. Cancer Causes Control. 1999;10(2):157–66.

Landis SH, Murray T, Bolden S, Wingo PA. Cancer statistics, 1999. CA Cancer J Clin. 1999;49(1):8–31. 31

Lassen P, Eriksen JG, Krogdahl A, Therkildsen MH, Ulhøi BP, Overgaard M, Specht L, Andersen E, Johansen J, Andersen LJ, Grau C, Overgaard J; Danish Head and Neck Cancer Group (DAHANCA). The influence of HPV-associated p16-expression on accelerated fractionated radiotherapy in head and neck cancer: evaluation of the randomised DAHANCA 6&7 trial. Radiother Oncol. 2011;100(1):49–55.

Lawrence MS, Stojanov P, Polak P, Kryukov GV, Cibulskis K, Sivachenko A, Carter SL, Stewart C, Mermel CH, Roberts SA, Kiezun A, Hammerman PS, McKenna A, Drier Y, Zou L, Ramos AH, Pugh TJ, Stransky N, Helman E, Kim J, Sougnez C, Ambrogio L, Nickerson E, Shefler E, Cortes ML, Auclair D, Saksena G, Voet D, Noble M, DiCara D, Lin P, Lichtenstein L, Heiman DI, Fennell T, Imielinski M, Hernandez B, Hodis E, Baca S, Dulak AM, Lohr J, Landau DA, Wu CJ, Melendez-Zajgla J, Hidalgo-Miranda A, Koren A, McCarroll SA, Mora J, Lee RS, Crompton B, Onofrio R, Parkin M, Winckler W, Ardlie K, Gabriel SB, Roberts CW, Biegel JA, Stegmaier K, Bass AJ, Garraway LA, Meyerson M, Golub TR, Gordenin DA, Sunyaev S, Lander ES, Getz G. Mutational heterogeneity in cancer and the search for new cancer-associated genes. Nature. 2013;499(7457):214–8.

Lawson W, Schlecht NF, Brandwein-Gensler M. The role of the human papillomavirus in the pathogenesis of Schneiderian inverted papillomas: an analytic overview of the evidence. Head Neck Pathol. 2008;2(2):49–59.

Layfield LJ. Fine-needle aspiration in the diagnosis of head and neck lesions: a review and discussion of problems in differential diagnosis. Diagn Cytopathol. 2007;35(12):798–805.

Leaute-Labreze C, Dumas de la Roque E, Hubiche T, Boralevi F, Thambo JB, Taieb A. Propranolol for severe hemangiomas of infancy. N Engl J Med. 2008;358(24):2649–51.

Lee MJ, Chung KH, Park JS, Chung H, Jang HC, Kim JW. Multiple endocrine neoplasia type 2B: early diagnosis by multiple mucosal neuroma and its DNA analysis. Ann Dermatol. 2010a;22(4):452–5.

Lee W, Jiang Z, Liu J, Haverty PM, Guan Y, Stinson J, Yue P, Zhang Y, Pant KP, Bhatt D, Ha C, Johnson S, Kennemer MI, Mohan S, Nazarenko I, Watanabe C, Sparks AB, Shames DS, Gentleman R, de Sauvage FJ, Stern H, Pandita A, Ballinger DG, Drmanac R, Modrusan Z, Seshagiri S, Zhang Z. The mutation spectrum revealed by paired genome sequences from a lung cancer patient. Nature. 2010b;465(7297):473–7.

Lee EY, Kim JJ, Seok H, Lee JY. Schwannoma of the tongue: a case report with review of literature. Maxillofac Plast Reconstr Surg. 2017;39(1):17.

Lefebvre JL, Chevalier D, Luboinski B, Kirkpatrick A, Collette L, Sahmoud T. Larynx preservation in pyriform sinus cancer: preliminary results of a European Organization for Research and Treatment of Cancer phase III trial. EORTC Head and Neck Cancer Cooperative Group. J Natl Cancer Inst. 1996;88(13):890–9.

Lefebvre JL, Andry G, Chevalier D, Luboinski B, Collette L, Traissac L, de Raucourt D, Langendijk JA, Head E, Neck Cancer G. Laryngeal preservation with induction chemotherapy for hypopharyngeal squamous cell carcinoma: 10-year results of EORTC trial 24891. Ann Oncol. 2012;23(10):2708–14.

Leung SF, Zee B, Ma BB, Hui EP, Mo F, Lai M, Chan KC, Chan LY, Kwan WH, Lo YM, Chan AT. Plasma Epstein-Barr viral deoxyribonucleic acid quantitation complements tumor-node-metastasis staging prognostication in nasopharyngeal carcinoma. J Clin Oncol. 2006;24(34):5414–8.

Levine PA, Cunningham MJ, Brantley S, Barnes L, Schramm VL Jr. Oncocytic Schneiderian papilloma in a young adult: a rare diagnosis. Otolaryngol Head Neck Surg. 1987;97(1):47–51.

Lipson EJ, Forde PM, Hammers HJ, Emens LA, Taube JM, Topalian SL. Antagonists of PD-1 and PD-L1 in cancer treatment. Semin Oncol. 2015;42(4):587–600.

Liu HL, Yu SY, Li GK, Wei WI. Extracranial head and neck Schwannomas: a study of the nerve of origin. Eur Arch Otorhinolaryngol. 2011;268(9):1343–7.

Lonneux M, Hamoir M, Reychler H, Maingon P, Duvillard C, Calais G, Bridji B, Digue L, Toubeau M, Gregoire V. Positron emission tomography with [18F] fluorodeoxyglucose improves staging and patient management in patients with head and neck squamous cell carcinoma: a multicenter prospective study. J Clin Oncol. 2010;28(7):1190–5.

Lu B, Kumar A, Castellsague X, Giuliano AR. Efficacy and safety of prophylactic vaccines against cervical HPV infection and diseases among women: a systematic review & meta-analysis. BMC Infect Dis. 2011;11:13.

Lu H, Liu S, Yang W, Zhang C. Unexpected extracardiac multifocal adult rhabdomyomas with 10 lesions of the head and neck: epidemiology, diagnosis, and therapy. J Oral Maxillofac Surg. 2017.

Luna MA, Pineda-Daboin K. Cysts and unknown primary and secondary tumours of the neck, and neck

dissection. In: Cardesa A, Slootweg PJ, editors. Pathology of the head and neck. Berlin: Springer; 2006. p. 262–82.

Lydiatt WM, Patel SG, O'Sullivan B, Brandwein MS, Ridge JA, Migliacci JC, Loomis AM, Shah JP. Head and neck cancers-major changes in the American Joint Committee on cancer eighth edition cancer staging manual. CA Cancer J Clin. 2017;67(2):122–37.

Lyford-Pike S, Peng S, Young GD, Taube JM, Westra WH, Akpeng B, Bruno TC, Richmon JD, Wang H, Bishop JA, Chen L, Drake CG, Topalian SL, Pardoll DM, Pai SI. Evidence for a role of the PD-1:PD-L1 pathway in immune resistance of HPV-associated head and neck squamous cell carcinoma. Cancer Res. 2013;73 (6):1733–41.

Maitra A, Baskin LB, Lee EL. Malignancies arising in oncocytic schneiderian papillomas: a report of 2 cases and review of the literature. Arch Pathol Lab Med. 2001;125(10):1365–7.

Mamelle G, Pampurik J, Luboinski B, Lancar R, Lusinchi A, Bosq J. Lymph node prognostic factors in head and neck squamous cell carcinomas. Am J Surg. 1994;168(5):494–8.

Mancuso AA, Mukherji SK, Schmalfuss I, Mendenhall W, Parsons J, Pameijer F, Hermans R, Kubilis P. Preradiotherapy computed tomography as a predictor of local control in supraglottic carcinoma. J Clin Oncol. 1999;17(2):631–7.

Mandal R, Chan TA. Personalized oncology meets immunology: the path toward precision immunotherapy. Cancer Discov. 2016;6(7):703–13.

Mandal R, Senbabaoglu Y, Desrichard A, Havel JJ, Dalin MG, Riaz N, Lee KW, Ganly I, Hakimi AA, Chan TA, Morris LG. The head and neck cancer immune landscape and its immunotherapeutic implications. JCI Insight. 2016;1(17):e89829.

Mannone F, De Giorgi V, Cattaneo A, Massi D, De Magnis A, Carli P. Dermoscopic features of mucosal melanosis. Dermatol Surg. 2004;30(8):1118–23.

Marks JE, Phillips JL, Menck HR. The National Cancer Data Base report on the relationship of race and national origin to the histology of nasopharyngeal carcinoma. Cancer. 1998;83(3):582–8.

Marocchio LS, Oliveira DT, Pereira MC, Soares CT, Fleury RN. Sporadic and multiple neurofibromas in the head and neck region: a retrospective study of 33 years. Clin Oral Investig. 2007;11(2):165–9.

Marur S, D'Souza G, Westra WH, Forastiere AA. HPV-associated head and neck cancer: a virus-related cancer epidemic. Lancet Oncol. 2010;11 (8):781–9.

Meccariello G, Deganello A, Choussy O, Gallo O, Vitali D, De Raucourt D, Georgalas C. Endoscopic nasal versus open approach for the management of sinonasal adenocarcinoma: a pooled-analysis of 1826 patients. Head Neck. 2016;38(Suppl 1):E2267–74.

Michel L, Ley J, Wildes TM, Schaffer A, Robinson A, Chun SE, Lee W, Lewis J Jr, Trinkaus K, Adkins D. Phase I trial of palbociclib, a selective cyclin dependent kinase 4/6 inhibitor, in combination with cetuximab in patients with recurrent/metastatic head and neck squamous cell carcinoma. Oral Oncol. 2016;58:41–8.

Mindell RS, Calcaterra TC, Ward PH. Leiomyosarcoma of the head and neck: a review of the literature and report of two cases. Laryngoscope. 1975;85(5):904–10.

Montgomery E, Goldblum JR, Fisher C. Leiomyosarcoma of the head and neck: a clinicopathological study. Histopathology. 2002;40(6):518–25.

Moore PS, Chang Y. Detection of herpesvirus-like DNA sequences in Kaposi's sarcoma in patients with and those without HIV infection. N Engl J Med. 1995;332 (18):1181–5.

Morrison PJ, Nevin NC. Multiple endocrine neoplasia type 2B (mucosal neuroma syndrome, Wagenmann-Froboese syndrome). J Med Genet. 1996;33 (9):779–82.

Morrison WH, Byers RM, Garden AS, Evans HL, Ang KK, Peters LJ. Cutaneous angiosarcoma of the head and neck. A therapeutic dilemma. Cancer. 1995;76 (2):319–27.

Minovi A, Basten O, Hunter B, Draf W, Bockmuhl U. Malignant peripheral nerve sheath tumors of the head and neck: management of 10 cases and literature review. Head Neck. 2007;29(5):439–45.

Mukherji SK, Bradford CR. Controversies: is there a role for positron-emission tomographic CT in the initial staging of head and neck squamous cell carcinoma? AJNR Am J Neuroradiol. 2006;27(2):243–5.

Munn DH. Indoleamine 2,3-dioxygenase, Tregs and cancer. Curr Med Chem. 2011;18(15):2240–6.

Myers LL, Nussenbaum B, Bradford CR, Teknos TN, Esclamado RM, Wolf GT. Paranasal sinus malignancies: an 18-year single institution experience. Laryngoscope. 2002;112(11):1964–9.

Nabavizadeh SA, Zimmerman RA, Mattei P, Liu GT. Infantile myofibroma of the carotid space presenting as Horner syndrome. J Neuroophthalmol. 2017;37(4):459–60.

Nagornaya N, Bhatia RG. Imaging for parapharyngeal space tumors, LIPOMA, Encyclopedia of Otolaryngology, Head and Neck Surgery. Berlin: Springer; 2013.

Neel HB 3rd, Whicker JH, Devine KD, Weiland LH. Juvenile angiofibroma. Review of 120 cases. Am J Surg. 1973;126(4):547–56.

Negri E, Dal Maso L, Ron E, La Vecchia C, Mark SD, Preston-Martin S, McTiernan A, Kolonel L, Yoshimoto Y, Jin F, Wingren G, Rosaria Galanti M, Hardell L, Glattre E, Lund E, Levi F, Linos D, Braga C, Franceschi S. A pooled analysis of case-control studies of thyroid cancer. II. Menstrual and reproductive factors. Cancer Causes Control. 1999;10(2):143–55.

Nutting CM, Morden JP, Harrington KJ, Urbano TG, Bhide SA, Clark C, Miles EA, Miah AB, Newbold K, Tanay M, Adab F, Jefferies SJ, Scrase C, Yap BK, A'Hern RP, Sydenham MA, Emson M, Hall E, P. t. m. group. Parotid-sparing intensity modulated versus conventional radiotherapy in head and neck cancer (PARSPORT): a phase 3 multicentre randomised controlled trial. Lancet Oncol. 2011;12(2):127–36.

O'Sullivan B, Huang SH, Siu LL, Waldron J, Zhao H, Perez-Ordonez B, Weinreb I, Kim J, Ringash J, Bayley A, Dawson LA, Hope A, Cho J, Irish J, Gilbert R, Gullane P, Hui A, Liu FF, Chen E, Xu W. Deintensification candidate subgroups in human papillomavirus-related oropharyngeal cancer according to minimal risk of distant metastasis. J Clin Oncol. 2013;31(5):543–50.

Oganesyan G, Saha SK, Guo B, He JQ, Shahangian A, Zarnegar B, Perry A, Cheng G. Critical role of TRAF3 in the Toll-like receptor-dependent and -independent antiviral response. Nature. 2006;439 (7073):208–11.

Oguejiofor KK, Hall JS, Mani N, Douglas C, Slevin NJ, Homer J, Hall G, West CM. The prognostic significance of the biomarker p16 in oropharyngeal squamous cell carcinoma. Clin Oncol (R Coll Radiol). 2013;25 (11):630–8.

Osguthorpe JD. Sinus neoplasia. Arch Otolaryngol Head Neck Surg. 1994;120(1):19–25.

Owosho AABCD, Huang SCM, Chen SM, Kashikar SD, Estilo CLD, Wolden SLM, Wexler LHM, Huryn JMD, Antonescu CRM. A clinicopathologic study of head and neck rhabdomyosarcomas showing FOXO1 fusion-positive alveolar and MYOD1-mutant sclerosing are associated with unfavorable outcome. Oral Oncol. 2016;61:89–97.

Pai SI, Zandberg DP, Strome SE. The role of antagonists of the PD-1:PD-L1/PD-L2 axis in head and neck cancer treatment. Oral Oncol. 2016;61:152–8.

Pleasance ED, Stephens PJ, O'Meara S, McBride DJ, Meynert A, Jones D, Lin ML, Beare D, Lau KW, Greenman C, Varela I, Nik-Zainal S, Davies HR, Ordonez GR, Mudie LJ, Latimer C, Edkins S, Stebbings L, Chen L, Jia M, Leroy C, Marshall J, Menzies A, Butler A, Teague JW, Mangion J, Sun YA, McLaughlin SF, Peckham HE, Tsung EF, Costa GL, Lee CC, Minna JD, Gazdar A, Birney E, Rhodes MD, McKernan KJ, Stratton MR, Futreal PA, Campbell PJ. A small-cell lung cancer genome with complex signatures of tobacco exposure. Nature. 2010;463 (7278):184–90.

Pavlov KA, Dubova EA, Shchyogolev AI, Mishnyov OD. Expression of growth factors in endotheliocytes in vascular malformations. Bull Exp Biol Med. 2009;147(3):366–70.

Pignon JP, le Maitre A, Maillard E, Bourhis J, M.-N. C. Group. Meta-analysis of chemotherapy in head and neck cancer (MACH-NC): an update on 93 randomised trials and 17,346 patients. Radiother Oncol. 2009;92 (1):4–14.

Pisharodi LR. False-negative diagnosis in fine-needle aspirations of squamous-cell carcinoma of head and neck. Diagn Cytopathol. 1997;17(1):70–3.

Pellitteri PK, Ferlito A, Bradley PJ, Shaha AR, Rinaldo A. Management of sarcomas of the head and neck in adults. Oral Oncol. 2003;39(1):2–12.

Pointreau Y, Garaud P, Chapet S, Sire C, Tuchais C, Tortochaux J, Faivre S, Guerrif S, Alfonsi M, Calais G. Randomized trial of induction chemotherapy with cisplatin and 5-fluorouracil with or without docetaxel for larynx preservation. J Natl Cancer Inst. 2009;101 (7):498–506.

Posner MR, Lorch JH, Goloubeva O, Tan M, Schumaker LM, Sarlis NJ, Haddad RI, Cullen KJ. Survival and human papillomavirus in oropharynx cancer in TAX 324: a subset analysis from an international phase III trial. Ann Oncol. 2011;22(5):1071–7.

Poveda-Roda R, Bagan JV, Sanchis JM, Margaix M. Pseudotumors and tumors of the temporomandibular joint. A review. Med Oral Patol Oral Cir Bucal. 2013;18(3):e392–402.

Ranee Mehra TYS, Mahipal A, Weiss J, Berger R, Eder JP, Burtness B, Tahara M, Keam B, Le DT, Muro K, Geva R, Chung HC, Lin C-C, Meister A, Hille D, Cheng JD, Chow LQM, Haddad RI, Fox Chase Cancer Center, Philadelphia, PA; University of Chicago, Chicago, IL; H. Lee Moffitt Cancer Center & Research Institute, Tampa, FL; Lineberger Comprehensive Cancer Center at the University of North Carolina, Chapel Hill, NC; Sheba Medical Center, Tel Hashomer, Israel; Yale Cancer Center, New Haven, CT; National Cancer Center Hospital East, Chiba, Japan; Seoul National University Hospital, Seoul, Korea, The Republic of; Johns Hopkins University, Baltimore, MD; Aichi Cancer Center Hospital, Nagoya, Japan; Sourasky Medical Center, Tel Aviv, Israel; Yonsei Cancer Center, Yonsei University College of Medicine, Seoul, Korea, The Republic of; National Taiwan University Hospital, Taipei, Taiwan; Merck & Co., Inc., Kenilworth, NJ; Seattle Cancer Care Alliance, Seattle, WA; Dana-Farber Cancer Institute, Boston, MA. Efficacy and safety of pembrolizumab in recurrent/metastatic head and neck squamous cell carcinoma (R/M HNSCC): pooled analyses after long-term follow-up in KEYNOTE-012. J Clin Oncol. 2016;34:6012–2.

Rasmussen SA, Yang Q, Friedman JM. Mortality in neurofibromatosis 1: an analysis using U.S. death certificates. Am J Hum Genet. 2001;68(5):1110–8.

Reed RJ, Fine RM, Meltzer HD. Palisaded, encapsulated neuromas of the skin. Arch Dermatol. 1972;106 (6):865–70.

Reiners C, Wegscheider K, Schicha H, Theissen P, Vaupel R, Wrbitzky R, Schumm-Draeger PM. Prevalence of thyroid disorders in the working population of Germany: ultrasonography screening in 96,278 unselected employees. Thyroid. 2004;14(11):926–32.

Rees MG, Seashore-Ludlow B, Cheah JH, Adams DJ, Price EV, Gill S, Javaid S, Coletti ME, Jones VL, Bodycombe NE, Soule CK, Alexander B, Li A, Montgomery P, Kotz JD, Hon CS, Munoz B, Liefeld T, Dancik V, Haber DA, Clish CB, Bittker JA, Palmer M, Wagner BK, Clemons PA, Shamji AF, Schreiber SL. Correlating chemical sensitivity and basal gene expression reveals mechanism of action. Nat Chem Biol. 2016;12(2):109–16.

Rekhi B, Upadhyay P, Ramteke MP, Dutt A. MYOD1 (L122R) mutations are associated with spindle cell

and sclerosing rhabdomyosarcomas with aggressive clinical outcomes. Mod Pathol. 2016;29(12):1532–40.
Remmelts AJ, Hoebers FJ, Klop WM, Balm AJ, Hamming-Vrieze O, van den Brekel MW. Evaluation of lasersurgery and radiotherapy as treatment modalities in early stage laryngeal carcinoma: tumour outcome and quality of voice. Eur Arch Otorhinolaryngol. 2013;270(7):2079–87.
Richards ML. Familial syndromes associated with thyroid cancer in the era of personalized medicine. Thyroid. 2010;20(7):707–13.
Rischin D, Young RJ, Fisher R, Fox SB, Le QT, Peters LJ, Solomon B, Choi J, O'Sullivan B, Kenny LM, McArthur GA. Prognostic significance of p16INK4A and human papillomavirus in patients with oropharyngeal cancer treated on TROG 02.02 phase III trial. J Clin Oncol. 2010;28(27):4142–8.
Robin PE, Powell DJ, Stansbie JM. Carcinoma of the nasal cavity and paranasal sinuses: incidence and presentation of different histological types. Clin Otolaryngol Allied Sci. 1979;4(6):431–56.
Robinson M, Sloan P, Shaw R. Refining the diagnosis of oropharyngeal squamous cell carcinoma using human papillomavirus testing. Oral Oncol. 2010;46(7):492–6.
Roush GC. Epidemiology of cancer of the nose and paranasal sinuses: current concepts. Head Neck Surg. 1979;2(1):3–11.
Rumboldt Z. Imaging the neck in children. Pediatr Neuroradiol. 2015. https://link.springer.com/referenceworkentry/10.1007%2F978-3-662-46258-4_65-1
Sakata K, Hareyama M, Tamakawa M, Oouchi A, Sido M, Nagakura H, Akiba H, Koito K, Himi T, Asakura K. Prognostic factors of nasopharynx tumors investigated by MR imaging and the value of MR imaging in the newly published TNM staging. Int J Radiat Oncol Biol Phys. 1999;43(2):273–8.
Sanger F, Nicklen S, Coulson AR. DNA sequencing with chain-terminating inhibitors. Proc Natl Acad Sci U S A. 1977;74(12):5463–7.
Schaer DA, Budhu S, Liu C, Bryson C, Malandro N, Cohen A, Zhong H, Yang X, Houghton AN, Merghoub T, Wolchok JD. GITR pathway activation abrogates tumor immune suppression through loss of regulatory T cell lineage stability. Cancer Immunol Res. 2013;1(5):320–31.
Scudellari M. HPV: sex, cancer and a virus. Nature. 2013;503(7476):330–2.
Seashore-Ludlow B, Rees MG, Cheah JH, Cokol M, Price EV, Coletti ME, Jones V, Bodycombe NE, Soule CK, Gould J, Alexander B, Li A, Montgomery P, Wawer MJ, Kuru N, Kotz JD, Hon CS, Munoz B, Liefeld T, Dancik V, Bittker JA, Palmer M, Bradner JE, Shamji AF, Clemons PA, Schreiber SL. Harnessing connectivity in a large-scale small-molecule sensitivity dataset. Cancer Discov. 2015;5(11):1210–23.
Seiwert TY, Zuo Z, Keck MK, Khattri A, Pedamallu CS, Stricker T, Brown C, Pugh TJ, Stojanov P, Cho J, Lawrence MS, Getz G, Bragelmann J, DeBoer R, Weichselbaum RR, Langerman A, Portugal L, Blair E, Stenson K, Lingen MW, Cohen EE, Vokes EE, White KP, Hammerman PS. Integrative and comparative genomic analysis of HPV-positive and HPV-negative head and neck squamous cell carcinomas. Clin Cancer Res. 2015;21(3):632–41.
Senbabaoglu Y, Winer AG, Gejman RS, Liu M, Luna A, Ostrovnaya I, Weinhold N, Lee W, Kaffenberger SD, Chen YB, Voss MH, Coleman JA, Russo P, Reuter VE, Chan TA, Cheng EH, Scheinberg DA, Li MO, Hsieh JJ, Sander C, Hakimi A. The landscape of T cell infiltration in human cancer and its association with antigen presenting gene expression. bioRxiv. 2015. https://www.biorxiv.org/content/early/2015/09/01/025908.
Shalem O, Sanjana NE, Hartenian E, Shi X, Scott DA, Mikkelsen TS, Heckl D, Ebert BL, Root DE, Doench JG, Zhang F. Genome-scale CRISPR-Cas9 knockout screening in human cells. Science. 2014;343(6166):84–7.
Steigman SA, Nemes L, Barnewolt CE, Estroff JA, Valim C, Jennings RW, Fauza DO. Differential risk for neonatal surgical airway intervention in prenatally diagnosed neck masses. J Pediatr Surg. 2009;44(1):76–9.
Soares AB, Lins LH, Macedo AP, Pereira-Neto JS, Vargas PA. Fibrosarcoma originating in the mandible. Med Oral Patol Oral Cir Bucal. 2006;11(3):E243–6.
Society, A. C. Cancer facts & figures, 2015. Atlanta: American Cancer Society; 2015.
Spiro RH, Koss LG, Hajdu SI, Strong EW. Tumors of minor salivary origin. A clinicopathologic study of 492 cases. Cancer. 1973;31(1):117–29.
Spitz MR. Epidemiology and risk factors for head and neck cancer. Semin Oncol. 1994;21(3):281–8.
Stampfli MR, Anderson GP. How cigarette smoke skews immune responses to promote infection, lung disease and cancer. Nat Rev Immunol. 2009;9(5):377–84.
Stransky N, Egloff AM, Tward AD, Kostic AD, Cibulskis K, Sivachenko A, Kryukov GV, Lawrence MS, Sougnez C, McKenna A, Shefler E, Ramos AH, Stojanov P, Carter SL, Voet D, Cortes ML, Auclair D, Berger MF, Saksena G, Guiducci C, Onofrio RC, Parkin M, Romkes M, Weissfeld JL, Seethala RR, Wang L, Rangel-Escareno C, Fernandez-Lopez JC, Hidalgo-Miranda A, Melendez-Zajgla J, Winckler W, Ardlie K, Gabriel SB, Meyerson M, Lander ES, Getz G, Golub TR, Garraway LA, Grandis JR. The mutational landscape of head and neck squamous cell carcinoma. Science. 2011;333(6046):1157–60.
Szabo G. The number of melanocytes in human epidermis. Br Med J. 1954;1(4869):1016–7.
Szuhai K, de Jong D, Leung WY, Fletcher CD, Hogendoorn PC. Transactivating mutation of the MYOD1 gene is a frequent event in adult spindle cell rhabdomyosarcoma. J Pathol. 2014;232(3):300–7.
Teng MW, Galon J, Fridman WH, Smyth MJ. From mice to humans: developments in cancer immunoediting. J Clin Invest. 2015;125(9):3338–46.

Topalian SL, Drake CG, Pardoll DM. Targeting the PD-1/B7-H1(PD-L1) pathway to activate anti-tumor immunity. Curr Opin Immunol. 2012;24(2):207–12.

Trevino-Gonzalez JL, Santos-Lartigue R, Gonzalez-Andrade B, Villagomez-Ortiz VJ, Villegas M, Venegas-Garcia EM. Angiosarcoma of the nasal cavity: a case report. Cases J. 2009;2(1):104.

de Trey LA, Schmid S, Huber GF. Multifocal adult rhabdomyoma of the head and neck manifestation in 7 locations and review of the literature. Case Rep Otolaryngol. 2013;2013:758416.

Tucker T, Wolkenstein P, Revuz J, Zeller J, Friedman JM. Association between benign and malignant peripheral nerve sheath tumors in NF1. Neurology. 2005;65(2):205–11.

van der Wal JE. Granular cell tumor, dental and oral, Encyclopedia of Pathology. Switzerland: Springer International Publishing; 2016. p. 202–4.

van der Waal I. Diseases of the oral mucosa and soft tissues: general aspects, Atlas of Oral Diseases. Berlin: Springer; 2016. p. 7–66.

Vermorken JB, Mesia R, Rivera F, Remenar E, Kawecki A, Rottey S, Erfan J, Zabolotnyy D, Kienzer HR, Cupissol D, Peyrade F, Benasso M, Vynnychenko I, De Raucourt D, Bokemeyer C, Schueler A, Amellal N, Hitt R. Platinum-based chemotherapy plus cetuximab in head and neck cancer. N Engl J Med. 2008;359(11):1116–27.

Vikram B, Mishra UB, Strong EW, Manolatos S. Patterns of failure in carcinoma of the nasopharynx: I. Failure at the primary site. Int J Radiat Oncol Biol Phys. 1985;11(8):1455–9.

Villa A, Nordio F, Strohmenger L, Abati S. Clinical–pathologic agreement for oral lesions in an oral medicine setting. Am J Oral Med. 2016;2(1):1–10.

Wang T, Wei JJ, Sabatini DM, Lander ES. Genetic screens in human cells using the CRISPR-Cas9 system. Science. 2014;343(6166):80–4.

Ward MJ, Thirdborough SM, Mellows T, Riley C, Harris S, Suchak K, Webb A, Hampton C, Patel NN, Randall CJ, Cox HJ, Jogai S, Primrose J, Piper K, Ottensmeier CH, King EV, Thomas GJ. Tumour-infiltrating lymphocytes predict for outcome in HPV-positive oropharyngeal cancer. Br J Cancer. 2014;110(2):489–500.

Waldron CA, El-Mofty SK, Gnepp DR. Tumors of the intraoral minor salivary glands: a demographic and histologic study of 426 cases. Oral Surg Oral Med Oral Pathol. 1988;66(3):323–33.

Weber RS, Benjamin RS, Peters LJ, Ro JY, Achon O, Goepfert H. Soft tissue sarcomas of the head and neck in adolescents and adults. Am J Surg. 1986;152(4):386–92.

Wenig BM. Nasopharyngeal carcinoma. Ann Diagn Pathol. 1999;3(6):374–85.

Westra WH. The changing face of head and neck cancer in the 21st century: the impact of HPV on the epidemiology and pathology of oral cancer. Head Neck Pathol. 2009;3(1):78–81.

Westra WH, Taube JM, Poeta ML, Begum S, Sidransky D, Koch WM. Inverse relationship between human papillomavirus-16 infection and disruptive p53 gene mutations in squamous cell carcinoma of the head and neck. Clin Cancer Res. 2008;14(2):366–9.

Wingo PA, Ries LA, Rosenberg HM, Miller DS, Edwards BK. Cancer incidence and mortality, 1973–1995: a report card for the U.S. Cancer. 1998;82(6):1197–207.

WHO Classification of Head and Neck Tumours. WHO Classification of Tumours, 4th Edition, Volume 9. Edited by El-Naggar AK, Chan JKC, Grandis JR, Takata T, Slootweg PJ. IARC Publications. 2017. http://publications.iarc.fr/Book-And-Report-Series/Who-Iarc-Classification-Of-Tumours/Who-Classification-Of-Head-And-Neck-Tumours-2017

Wall J, Sylvester K, Albanese C. Lymphatic malformations in children. In: Puri P, editor. Pediatric surgery. Germany: Verlag GmbH Springer; 2016.

Walter V, Yin X, Wilkerson MD, Cabanski CR, Zhao N, Du Y, Ang MK, Hayward MC, Salazar AH, Hoadley KA, Fritchie K, Sailey CJ, Weissler MC, Shockley WW, Zanation AM, Hackman T, Thorne LB, Funkhouser WD, Muldrew KL, Olshan AF, Randell SH, Wright FA, Shores CG, Hayes DN. Molecular subtypes in head and neck cancer exhibit distinct patterns of chromosomal gain and loss of canonical cancer genes. PLoS One. 2013;8(2):e56823.

Woodruff JM. The pathology and treatment of peripheral nerve tumors and tumor-like conditions. CA Cancer J Clin. 1993;43(5):290–308.

Yoshitake Y, Fukuma D, Yuno A, Hirayama M, Nakayama H, Tanaka T, Nagata M, Takamune Y, Kawahara K, Nakagawa Y, Yoshida R, Hirosue A, Ogi H, Hiraki A, Jono H, Hamada A, Yoshida K, Nishimura Y, Nakamura Y, Shinohara M. Phase II clinical trial of multiple peptide vaccination for advanced head and neck cancer patients revealed induction of immune responses and improved OS. Clin Cancer Res. 2015;21(2):312–21.

Yu Y, Flint AF, Mulliken JB, Wu JK, Bischoff J. Endothelial progenitor cells in infantile hemangioma. Blood. 2004;103(4):1373–5.

Zak FG, Lawson W. The presence of melanocytes in the nasal cavity. Ann Otol Rhinol Laryngol. 1974;83(4):515–9.

Zandberg DP, Strome SE. The role of the PD-L1:PD-1 pathway in squamous cell carcinoma of the head and neck. Oral Oncol. 2014;50(7):627–32.

Zhang L, Wu HW, Yuan W, Zheng JW. Propranolol therapy for infantile hemangioma: our experience. Drug Des Dev Ther. 2017;11:1401–8.

Zheng JW, Zhou Q, Yang XJ, Wang YA, Fan XD, Zhou GY, Zhang ZY, Suen JY. Treatment guideline for hemangiomas and vascular malformations of the head and neck. Head Neck. 2010;32(8):1088–98.

Zidar N. Branchial cyst in head and neck pathology. In: Volavšek M, editor. Encyclopedia of pathology. Switzerland: Springer International Publishing; 2016. p. 43–6.

Zitvogel L, Tesniere A, Kroemer G. Cancer despite immunosurveillance: immunoselection and immunosubversion. Nat Rev Immunol. 2006;6 (10):715–27.

Ziyeh S, Strecker R, Berlis A, Weber J, Klisch J, Mader I. Dynamic 3D MR angiography of intra- and extracranial vascular malformations at 3T: a technical note. AJNR Am J Neuroradiol. 2005;26(3):630–4.